HEU CONVERTER CHARACTERIZATION STUDY

F. Di Gasbarro, A. Proietti
Sogin S.p.A. Italy
B. Bianchilli, E. Mauro, E. Gorello
Nucleco S.p.A. Italy

1. Introduction

Sogin, the state company in charge of the decommissioning of the Italian NPPs and Nuclear Research Centers, is completing the management of the closure of the fuel cycle in the nuclear sites. The strategies implemented are the reprocessing abroad for spent nuclear fuel and elimination for not irradiated nuclear materials.
Since 2008, Sogin has been starting to participate to the Global Threat Reduction Initiative (GTRI) program of the National Nuclear Security Administration (NNSA) of the United States Department of Energy (DOE) for the repatriation to US of American origin nuclear materials.
After the conclusion of three GTRI projects, in the framework of the M^3 (Material Management and Minimization) program, Sogin signed a contract with Consolidated Nuclear Security (CNS) of the US DOE for the characterization of an HEU converter, hosted and operated by a third party. Scope of this work is the description of the characterization activities performed and the classification of the converter according to the transport regulations.

2. HEU Converter

The HEU converter is a neutron source designed primarily for experiments on models of radiation shielding. It consists of a disc made by six trapezoidal highly enriched U-Al alloy plates, developing a nearly circular source with a theoretical diameter of about 80 cm. The fuel plates are positioned into an aluminum cooling chamber confined inside a steel shielding. The HEU converter was designed and constructed to study neutron propagation in large homogeneous models. The converter was placed in front of the thermal column of the reactor producing a plane fission source of high intensity.
This converter, conceived mainly to perform experiments on shielding models, has been irradiated for experimental purposes during the ‘70s and early ‘80s. After that, it has been maintained inside a 10 cm thick steel shielding. Information about irradiation cycles of the converter are now difficult to retrieve: moreover, not all the construction details (in particular the exact geometry of the fuel converter) and previous irradiation data are available. For these reasons, it was not possible to determine if the device could be classified as “not irradiated” according to the transport standards of IAEA Regulations for the Safe Transport of Radioactive Material.
To overcome this situation, the converter has been subject in the past to a preliminary characterization activity via gamma spectrometry. However, the study carried out, because based on a geometric model of the converter derived by an incomplete knowledge of its construction details, did not give satisfying results as a definitive conclusion.

Therefore, a new in-situ characterization activities have been performed, removing the outer steel shielding.

Figure 1 – HEU converter inside the steel shielding

3. On-site activities

The activities consist of three phases:

- preliminary phase for the working area preparation, the converter positioning and the radiation protection measurements;
- characterization phase for the detector setup and the data acquisition;
- inspection phase via the x rays and the endoscope.

The time schedule can be summarized as follow:

- Day 1: positioning of the converter into the characterization area inside the dynamic confinement tent through the use of crane and handling pulley;
- Day 2: partial lifting of the screen using the handling pulley connected to the four tons hook of the crane and its positioning on appropriate supports.
  First radiometric checks (dose and removable contamination) and inspections;
- Day 3: surveys results analysis:
  - the smear tests showed traces of activation products (^{60}Co and ^{152}Eu) compatible with the specific history of irradiation of the converter and the absence of fission products;
  - the MOCF technique analysis, on the air filter sampled inside the tent in the area adjacent to the converter, showed asbestos values largely below the limits established by the law;
- Days 4, 5, 6, 7, 8: full lifting of the screen and characterization measurements;
- Day 9: acquisition of the results of the radiographies taken on different angles for defining the internal construction details;

- Day 10: visual inspection inside the aluminum-cooling chamber of the converter by endoscope, inclining the converter few degrees to permit its entrance through the open base of the converter.

a. Preliminary phase

The working area was encapsulated into a confinement tent with dimensions of 3,46 x 7,68 x 4,00 meters. Moreover, to create an additional separation environment on the entering side to the tent, a Safety Access System (SAS) has been installed sized 3,46 x 1,14 meters.
The entire tent was wrapped with low-density polythene sheets, transparent and fireproof, of 20 mm thickness of. This type of covering has been chosen for both to confine the working area and to follow from outside the operations performed inside the tent.
To guarantee a depression of 5 Pa (up to a maximum of 30 Pa), an aspirator equipped with pre-filter and absolute filter was installed. The aspiration from the cap has been released into the main ventilation system by means of a pipe inserted in a nozzle of the ventilation system itself.
On the top of the confinement tent there was an access for the handling of the converter through the crane and the handling pulley. In order to perform the first radiation protection measurements (dose and removable contamination), the converter shielding was partially lifted using the four tons hook.

b. Characterization phase

In this phase, the converter was left unshielded, in order to permit direct assay via gamma spectrometry in good geometry conditions. The measurements were performed using a BEGE type High Purity Germanium detector (HPGe) with 30% relative efficiency, equipped with ISOCS software for geometric efficiency estimation. Multiple assays were performed trying to determine the optimal measurement condition in terms of dead time and efficiency, taking into account various factors like distance, dose rate and collimation.
The key parameter for this kind of measurements is the geometric simulation for efficiency estimation. In order to simulate correctly the emission of the converter is mandatory to know (at the best) the emitting mass, the distance and the relative position of the system: detector – converter, together with the correct shield sequence (aluminum, PVC and any other).
Different measurement setup were tested, varying the relative distance (from 2.5 up to 5.5 m at the center of the converter) and the shielding systems (from 0.3 cm Al foil to 10 cm of steel).
The main outputs of the characterization were the quantification of the ^{235}U mass (for ^{238}U only an MDA estimation was been possible) and the activities of ^{137}Cs and ^{60}Co (whose presence were expected given the plant process). Taking into account all the possible uncertainty sources, the ^{235}U mass is in agreement with the historical information, validating therefore the model used for the analysis and the results obtained (i.e. ^{137}Cs and ^{60}Co estimation).
Obviously, during the irradiation phases, apart from ^{137}Cs and ^{60}Co, a whole set of radionuclides was created (fission and activation products, nuclear materials), most of them were practically impossible to determine using the gamma spectrometry. In order to fully calculate the radiological content of the converter (i.e. the materials response to the irradiation of a neutron flux), numerical

simulations have been performed using EASY-2001, combination of codes, data and historical documentation.
The definition of EASY_2001 program inputs requires a collection of a wide range data such as:

- the characteristics of the reactor in terms of flux and neutron spectrum;
- the composition of the irradiated material;
- the irradiation profile in terms of irradiation and cooling time.

In order to validate the results obtained with EASY-2001 code, the activities measured fof^{137}Cs and ^{60}Co have been utilized as markers: knowing that the gamma spectrometry results are validated through the U^{235} mass, it is possible to compare the activities simulated with those experimentalones. The results are in good agreement with the gamma spectroscopy: therefore, it is possible to consider the EASY-2001 output as the radiological spectrum of the converter.

c. Radiographs

To plan a safe and correct way to dismantle the converter it is necessary to have a precise idea of its structural composition and the status of the HEU trapezoidal plates; it is also crucial to identify the exact location of possible fracture, bolts or welding.
Due to high activity and dose rate into the working area, the characterization phase was essential to provide a starting point to correctly evaluate the hot areas on the converter and to study a shielding system to avoid the blinding of the photographic plate. After a first acquisition test, the optimal shielding solution founded was a thin copper foil placed in front of the radiograph head.
The RX investigation has been performed on the entire converter (with the shielding lifted up) by dividing it into different sectors on both sides. Many radiographs have been taken, showing the plates condition state, their relative interconnection and also how the converter active region was put in place into the shielding and cooling system.

Figure 2 - The X-rays equipment and the positioning of the system

Figure 3 – Converter disk reconstruction with six radiographs

d. Visual inspection (inside and outside) via microcamera

Due to the narrowness of the spaces inside the aluminum-cooling chamber of the converter and the reflection of the light on the internal surface of aluminum, it was possible to visually inspect only the internal part of the base of the converter. During the inspection, a sample was collected at the base.

At the end of this last phase, the converter steel shielding was reassembled and the converter returned into the storage area.

The subsequent analysis of the sample taken from the base of the converter confirmed the presence of asbestos (chrysotile type) with a percentage in the material of 90.4%.

4. Conclusions

The converter characterization activities have been carried out by Sogin and Nucleco, without incidents, in compliance with time schedule agreed between Sogin and CNS/DOE and authorized by the Safety Authority.
Safety Authority inspectors and DOE/NNSA representatives participated to specific phases of the operational activities.

Relating to the physical integrity and condition, the converter apparently does not show any significant aging effect on the external structure (e.g. aluminum oxidation).
Both RX and visual inspections seems to confirm a good structural status of the converter, without cracking and major scratches, allowing a better definition of the internal structure of the converter.
Relating to the radiological part, the characterization campaign confirmed the historical data, in terms of ^{235}U mass.
A numerical simulation, with EASY-2001 code, was performed for the final quantification of the radiological content of the converter. The results are shown below:

- The dominant fission products with the estimation of respective activities are: ^{137}Cs (9.16 GBq), ^{90}Sr (8.18 GBq), ^{151}Sm (0.41 GBq), ^{85}Kr (0.22 GBq), ^{3}H (9.16 MBq), ^{147}Pm (2.85 MBq), ^{155}Eu (3.02 MBq) and ^{99}Tc (3.26 MBq);
- The total fission products activity is roughly equal to 17.9 GBq, a value well below the limit of fission products for irradiated uranium (38.6 GBq for 4.29 kg of ^{235}U);
- The mass of ^{236}U can be estimated in 41.2 mg, a value well below the limit of ^{236}U for the definition of irradiated uranium (21.45 g of ^{236}U for 4.29 kg of ^{235}U);
- The total activity of plutonium is around a value of 0.27 MBq, well below the limit of Pu for the definition of irradiated uranium (9.58 MBq of Pu for 4.29 kg of ^{235}U);
- The activity of ^{60}Co can be estimated as 0.70 MBq.

The presence of asbestos spacers inside the aluminum-cooling chamber of the converter has been detected.
Referring to the IAEA and ADR definition for not irradiated uranium: *"Uranium containing not more than 2×10^3 Bq of plutonium per gram of uranium-235, not more than 9×10^6 Bq of fission products per gram of uranium-235 and not more than 5×10^{-3} g uranium-236 per gram of uranium-235"* , the converter can be classified as not irradiated for the transport.
The analyses performed has highlighted a dose rate distribution comprised between 280 µSv/h (at the lateral bottom parts of the aluminum box) and 15 mSv/h (at the center of the converter disk on aluminum box surface).
For the purpose of a possible repatriation of the converter to US, the following technical activities have to be defined, together with a transport activities time schedule:

- Installation of an asbestos proof tent
- Opening of the aluminum-cooling chamber of the converter
- Asbestos removal
- Recovery of the HEU fuel plates from the converter and repackaging
- Loading of the cask and shipment.

All in all, the future potential dismantling activities of the converter, finalized to recover the HEU fuel, shall have to take into account both radiological risks connected to the high dose rates and the conventional risks due to the presence of asbestos which will require additional safety measures.

LICENSING OF UKRAINE NEUTRON SOURCE FACILITY: CHALLENGES AND BREAKTHROUGHS

O.V. KUKHOTSKYI, O. M.DYBACH
State Enterprise "State Scientific and Technical Center for Nuclear and Radiation Safety"
35-37V.Stusa st., 03142, P.O. Box 124 - Kyiv, Ukraine

A.V. SHEPITCHAK, S.A. NEMTSOVA
State Nuclear Regulatory Inspectorate of Ukraine
3 Verkhovna Rada av., 02100 – Kyiv, Ukraine

An experimental nuclear facility the Neutron Source Based on the Subcritical Assembly Driven by a Linear Electron Accelerator (Neutron Source) is under design and construction in the National Scientific Center "Kharkov Institute of Physics and Technology" (NSC KIPT), Ukraine as an international collaborative project of NSC KIPT and Argone National Laboratory (ANL), USA. The construction of a state-of-art nuclear research facility – Neutron Source – is a challenge for both the operating organization (NSC KIPT) and the regulatory authority (SNRIU). NSC KIPT faced the technical challenges caused by the unique design features of the facility. SNRIU faced the two major challenges. This paper discusses aspects related to the challenges and its breakthroughs in licensing of Neutron Source, including development of the regulatory and legal framework on nuclear and radiation safety, and review of the safety justification documents for the new nuclear subcritical facility.

1. Introduction

The National Scientific Center "Kharkov Institute of Physics and Technology" (NSC KIPT), with support of the Argonne National Laboratory (USA), is constructing the nuclear subcritical facility "Neutron Source Based on the Subcritical Assembly Driven by the Linear Electron Accelerator". According to Article 1 of the Law of Ukraine "On Nuclear Energy Use and Radiation Safety" [1], the Neutron Source is the nuclear facility that requires all measures on its safety assessment and licensing. Under the realization of the Neutron Source project in accordance with the Law of Ukraine "On Authorizing Activity in Nuclear Energy Use", the following separate stages of the life cycle of a nuclear installation are subject to be licensed:

- construction and commissioning;
- operation;
- decommissioning.

The licensing activities are carried out by the State Nuclear Regulatory Inspectorate of Ukraine (SNRIU) with the technical support of the State Scientific and Technical Center for Nuclear and Radiation Safety (SSTC NRS).

2. Design features of the Neutron Source

The Neutron Source is an entirely new type of nuclear facilities where the rate of 235U isotope fission in the core is driven by an electron accelerator. The IAEA classifies such facilities as ADS (Accelerator Driven Systems) [2]. In nuclear subcritical facilities, neutrons are generated through the multiplication of primary neutrons from an external source in the environment of heavy elements (tungsten or natural uranium). The geometry of the medium and the mass of fissionable material are chosen so that the effective neutron multiplication factor k_{eff} remains lower than 0.98 ($k_{eff}<1$) under any initiating events. This solution ensures nuclear safety of such research facilities. This is the fundamental difference and advantage of the nuclear subcritical facility from nuclear research reactors which are operated through self-sustaining fission chain reaction (SFCR).

The Neutron Source consists of the following components (Fig. 1) [3- 5]: subcritical assembly (SA) on thermal neutrons with shielding; neutron-generating target (NGT) to produce primary neutrons, located inside the subcritical assembly core; linear electron accelerator with a channel for beam transport; cold neutron source (CNS); facility control panel; general engineering systems; test neutron channels for nuclear and physical surveys; engineering systems for the facility.

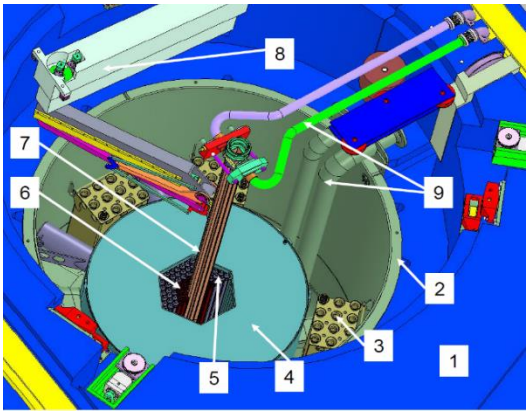

1 - biological shielding; 2 - tank SCC; 3 - fuel containers; 4 - graphite reflector; 5 - beryllium reflector; 6 - core; 7 - target; 8 - refueling machine; 9 - cooling system

Fig. 1 The layout of "Neutron Source"

The NGT made of metal tungsten or natural uranium located in the SA core center between fuel assemblies is a source of external neutrons. The mechanism of neutron emission from the target is based on (γ, n)-reaction which occurs after its irradiation by hard γ-radiation with energy of γ-quantum, exceeding neutron-binding energy in target nuclei (8…10 MeV). Such F-radiation (deceleration, γ-radiation) is generated during deceleration of high-energy neutrons (over 10 MeV) in material from heavy chemical elements. The linear electron accelerator is used to produce electrons with energy of 100 MeV, average current 1 mA and beam power 100 kW. A vacuum electron transportation channel with magnetic optics elements intended to focus the electron beam, change its direction and form necessary dimensions of the target irradiation area is used to transfer the beam from LEA to SA, which are spatially separated. The SA core consists of 37 fuel assemblies in case of a uranium target and 38 in case of a tungsten target, and is located in the subcritical assembly tank. The core is surrounded by a compound radial reflector consisting of beryllium units and an annular graphite reflector. The SA core uses nuclear fuel in fuel assemblies of VVR-M2 type with low enriched uranium with 19.7 % of 235U isotope. The layout and geometry of the SA core ensure that the effective neutron multiplication factor is not higher than 0.98 (K_{eff}<0.98). Therefore, the self-sustaining chain fission reaction of 235U must not occur in the Neutron Source SA core [4], [5].

Normal operation of the main process equipment to receive and use neutrons is maintained by auxiliary control and support systems. The design envisages an automated control system (ACS) of the Neutron Source. ACS controls the state of facility systems, operating modes, diagnoses equipment malfunctions and failures and incompliance of parameters with setpoints, provides relevant information to the operator, performs necessary tripping in accordance with the set algorithm and interlocking. There is also an automated radiation monitoring system (ARMS) as an integral part of ACS. ARMS functions independently of other systems both during facility operation and in shutdown states (scheduled outage, maintenance, etc.). For removal of heat generated in the process equipment during the nuclear facility operation, several two-loop systems are used for cooling of: the subcritical assembly (260 kW), the target (100 kW), the transportation channel (50 kW) and the LEA (985 kW). The LEA cooling system includes three subsystems of water cooling. Ventilation cooling towers of secondary cooling system ensure heat dissipation in the environment [3- 5]. The Neutron Source design is peculiar in the use of a relativistic energy electron accelerator to generate neutrons through photonuclear reactions in the neutron generation target and in significant

thermal power in comparison with other operational subcritical systems - so-called zero power subcritical systems.
The Neutron Source is oriented towards scientific investigations of subcritical assemblies, generation of neutrons and their applications in nuclear physics, solid state physics, biology, generation of medical isotopes, radionuclide transmutations and training of experts in the sphere of nuclear energy.

3. Licensing of Neutron Source Facility

The construction of a state-of-art nuclear research facility – Neutron Source – is a challenge for both the operating organization (NSC KIPT) and the regulatory authority (SNRIU). NSC KIPT faced the technical challenges caused by the unique design features of the facility. SNRIU faced the two major challenges. First, there were no regulations to govern nuclear and radiation safety of such type of facilities. Second, there was no experience in regulating the nuclear and radiation safety of such type of facilities.

3.1 Development of regulatory framework on nuclear and radiation safety for the Neutron Source.

Availability of the regulatory framework is the necessary condition of licensing process. At the beginning of the Neutron Source's construction, the Ukrainian regulatory framework included only two valid former USSR's regulations with regard to SA:

- Nuclear safety rules for subcritical benches (PBYa-01-75) that was put into force in 1975;
- General safety provisions for research reactors during design, construction and operation (OPB IR) that was put into force in 1988.

Taking into account the above mentioned regulatory requirements had to be revised considering state-of-the-art IAEA standards and international experience, SNRIU in cooperation with SSTC NRS developed and brought into action the regulation "General Safety Provisions for Nuclear Subcritical Assembly" (GSP) [6].
The basis for the development of the GSP [6] was: accumulated national experience in research facilities, current regulatory requirements for nuclear power plants which was used applying the graded approach, as well as accumulated international experience, in particular the IAEA's developments in terms of research facilities and subcritical systems, which were elaborated and published as SSR -3 "Safety of research reactors" [7] by the IAEA later.
The new regulation establishes the criteria and principles for safety of the nuclear subcritical facility, the requirements and conditions for ensuring nuclear and radiation safety at all stages of the life cycle of the nuclear subcritical facility, the main technical means and organizational measures aimed to protecting personnel, the population and the environment from possible radiation exposure. According to IAEA standard, GSP [6] states that the main safety objective of the nuclear facility is to ensure protection of personnel, population and the environment against negative radiation impact of this facility during commissioning, operation and decommissioning. The nuclear facility will comply with the safety requirements if its radiation impact on personnel, the public and the environment under normal operation, operational occurrences and design-basis accidents is below the dose limits for personnel, the public, and the levels of permissible environmental releases. Safety criteria at all stages of the nuclear subcritical facility lifecycle are as follows [6]:

- the probability of beyond design-basis accidents that lead to exceeding the levels to make decisions on evacuation of population, set by radiation safety standards in Ukraine [8] (NRBU-97), is not higher than 10-7 per year;
- $K_{eff\ max}$ 0.98 is not exceeded in normal operation, operational occurrences and design-basis accidents;
- $K_{eff\ max}$ 0.95 is not exceeded in normal operation, operational occurrences and design-basis accidents for storage systems and fresh and spent fuel management systems;
- subcriticality of the nuclear facility in all shutdown states is not lower than 5%.

The GSP [6] defines and specifies principles for ensuring safety of the Neutron Source: *fundamental* – safety culture; responsibility of the operating organization; state safety regulation; defense-in-depth strategy; *general organizational and technical* – proven engineering and technical practices; implementation of management systems; safety assessment of the Neutron Source; human factor; operating experience feedback; internal oversight; nuclear safety; radiation safety; security.
Peculiar attention is paid to Neutron Source's nuclear safety. The main nuclear safety principles at all stages of the Neutron Source lifecycle includes: principle for prevention of self-sustaining chain reaction through compliance with conditions that eliminate its occurrence; principle for preservation of efficiency of safety barriers through preventing damage of fuel rods, SA casing, cooling loops and experimental devices and elimination of radioactive releases beyond the established safety barriers; principle for prevention of unauthorized access to nuclear fuel, radioactive materials and their unauthorized use through preservation and prevention of unauthorized access.
Nuclear safety of the Neutron Source is ensured by a series of technical features and organizational measures through:

- use of inherent self-protection features of the Neutron Source;
- use of defense-in-depth strategy;
- use of safety systems designed on the principles of single failure, diversity, redundancy and physical separation;
- impossibility of the self-sustaining chain fission reaction both under normal operation and any initiating events that may lead to accidents;
- compliance with regulations, rules and standards on nuclear and radiation safety, and requirements incorporated in the Neutron Source design;
- compliance with conditions and limits for safe operation, requirements of nuclear safety regulated by design and technical documentation, regulatory documents;
- compliance with safety culture principles;
- use of the management system at all stages of the Neutron Source lifecycle;
- relevant personnel qualification;
- availability of operational and technical documentation;
- use of a conservative approach to nuclear safety justification.

The preliminary list of initiating events for the Neutron Source design and for safety justification in the safety analysis report presented in Annex for GSP [6] and includes the following groups of initiating events: initiating events that lead to insertion of positive reactivity, initiating events that lead to heat removal failure, initiating events related to failures during treatment of nuclear materials, natural and man-made events, accidents with unauthorized insertion of positive reactivity when several failures or personnel errors are combined, accidents with total loss of external power supply, accidents with increased heat generation in NGT.
The GSP [6] defines general requirements for all stages of the Neutron Source lifecycle. Some requirements should be specified in other lower level regulations (for example, safety requirements during tests at the Neutron Source). If foreign regulations are used, it is necessary to ensure harmonization of their requirements with Ukrainian law in the sphere of nuclear and radiation safety. International regulations and rules may be used, if: a) their requirements are more conservative; b) the aspects that are not reflected in national regulations need to be addressed. Comparative analysis of regulatory documents (analysis of compliance) should be submitted to the SNRIU for consideration.

3.2 Expert review of the Neutron Source documents

In the Neutron Source's licensing process SNRIU with the involvement of the technical support organization - SSTC NRS performs an expert review of the licensing and operational documentation. The purpose of the nuclear and radiation safety expert review is to assess the compliance of the submitted materials with the requirements of nuclear and radiation safety norms, rules and standards, as well as the assessment of the completeness, correctness, sufficiency and justification of the information provided. To date, SSTC NRS has evaluated the

Safety Analysis Report (SAR), design and the operational documentation of the Neutron Source. The following main conclusions were made as a result of the expert review.
The defense-in-depth strategy has been implemented in the Neutron Source. This strategy is based on a system of safety barriers to prevent releases of ionizing radiation and radioactive substances into the environment and a system of technical features and organizational measures to protect the safety barriers and preserve their efficiency. The safety barriers include the fuel rod and NGT claddings, primary system, confinement system.
The Neutron Source is designed to fulfill the principles of ensuring nuclear safety at all stages of the life cycle of the Neutron Source in accordance with the GSP [6]. The results of the calculations of subcriticality presented in PSAR [5] of the Neutron Source indicate that safety criteria are not exceeded during normal operation, operational occurrences and design-basis accidents.
The experience of the Fukushima-1 NPP's accident was taken into account in the design of the Neutron Source (in the design, the maximum design earthquake (MDE) is 7 points according to the seismic scale of Medvedev-Sponheuer-Karnik (MSK-64), which provides an adequate supply of seismicity with respect to the seismicity of the site which is 6 points according to MSK-64 scale. As a part of the accident analysis, an analysis was carried out and the safety of the Neutron Source was proved in case of loss-of-heat-sink accident and complete blackout. The Neutron Source cooling systems are designed as two-loop and one-channel. The redundancy of equipment is provided, and passive flooding of SA during failure of operating and backup cooling pumps will be ensured. Coolant pressure in the primary system is lower than operating pressure of cooling water in the secondary system, which eliminates the possibility of radioactive coolant penetration into the secondary system in case of heat exchanging pipe leakage.
The cooling systems are systems of normal operation that are important for safety. The safety analysis of the subcritical assembly cooling systems failure indicates that the temperature of the nuclear fuel element cladding is not exceeded the acceptance criteria.
In order to confirm the analysis provided in PSAR [5] the verification calculations of chosen scenarios were done. On 26 September 2013, the SNRIU Board made a decision to issue a license for construction and commissioning of the Neutron Source to the NSC KIPT, which was then granted on 10 October 2013 (License Series EO 001018).

3.3 Verification calculations

Licensing of new nuclear installations is impossible without using of various types of analytical tools for the verification safety analysis. Besides, IAEA recommends developing and using of independent expert models for regulatory safety assessment of nuclear installations. In the Neutron Source's licensing process SSTC NRS with the support of European experts (in frame of INSC projects [10]), developed the independent models of key nuclear facility elements and performed calculations for verification safety studies using non-identical analytical tools. The models of key nuclear facility elements were developed in the directions of neutron-physics calculations, thermal hydraulics safety analysis and radiation protection calculations.
Neutron-physics calculations. In order to confirm the calculations of subcriticality provided in PSAR [5] of the Neutron Source the calculation models were developed. Neutron-physics verification calculations were performed with the SCALE code. Neutron-physics calculations covered the VVR-M2 fuel assembly, the subcritical assembly, the transport casks for fresh fuel and spent fuel storage facility. The calculations used standard 38-group library of the SCALE program package based on the ENDF/B-VI data files. Configuration of the subcritical assembly with 38 fuel assemblies was calculated for using of the NGT. The target itself was not modeled at this stage since its removal increases the multiplication properties of the SA.
Using the average design fuel parameters, a good compliance of the results of the verification calculation and the result given in PSAR was obtained. At the same time, according to expert estimates, with the conservative consideration of changes in the parameters of fuel assemblies within the technological tolerances for their manufacture, $K_{eff\ max}$ may exceed the permissible value of 0.98. To resolve this issue, the number of the nuclear fuel assemblies which are permitted to load into the core was limited to 35 nuclear fuel assemblies (instead of 38), with the subsequent justification of the possibility of increasing this number to 38 not exceeding the

$K_{eff\ max}$. The criticality of the spent fuel storage pool was calculated with variation in the density of cooling fluid (water or water-air mixture). The obtained results are consistent with the results of the calculations in PSAR [5] and confirm a significant margin to achieve the safety criteria for the spent fuel storage pool in all operational modes.

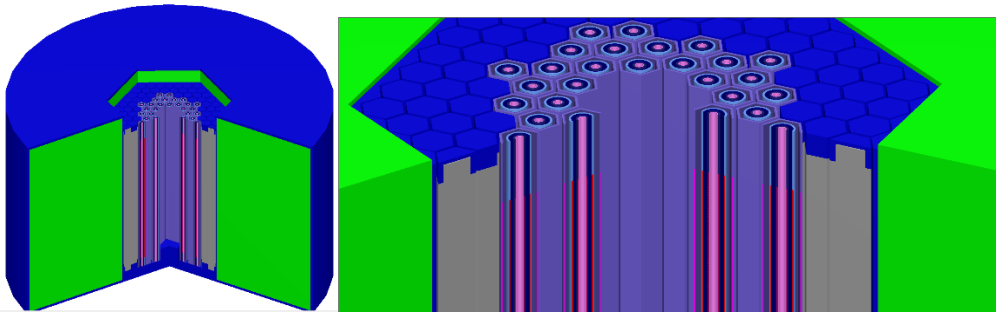

Fig. 2 Horizontal and Vertical Cross Section of the Neutron Source SA

Thermal hydraulics safety analysis According to GSP [6] the Neutron Source safety is ensured by consistent implementation of defense-in-depth strategy based on the use of physical barrier system on the way of radiation and radioactive substance spreading to the environment, and system of technical means and organizational measures on protection of physical barriers and maintaining of their efficiency. Neutron Source physical barrier system on the way of radioactive substances and radiation spreading includes: fuel and NGT cladding, equipment of primary cooling circuits of the subcritical assembly and the NGT, confining system of leaktight compartments. The integrity criterion for the mentioned physical barriers are established and justified in Neutron Source PSAR [5]. Non-exceeding of the established criteria justified for all operating modes of the Neutron Source, emergencies and accidents. Accident management Guides and their justifying documents developed based on purposes not to reach or exceed criteria of physical barriers integrity. As it is shown by the integrity criteria, the following components of the Neutron Source are the key components affecting safety: NGT and the fuel assembly with claddings of aluminum alloy with the lowest melting temperature in the system. In order to perform independent verification calculations the technical support organization SSTC NRS are working to develop independent models of key “Neurons Source” components using other analytical tools [11]. Related to the verification of the safety criteria, two types of calculations are performed with the CFD code ANSYS CFX. The first one describes the NGT and the second one - the fuel assembly. Geometries, meshing, boundary conditions are summarized and calculations are carried out for steady state normal operation and few accidental transient. Comparison of the results with the PSAR shows comparable temperatures of the neutron generating target plates and fuel assembly for steady state normal operation [11]. According to the results of the analysis of the accidents, it was confirmed that the established safety criteria were not exceeded, however, recommendations were given for the actions of personnel which will be included to the Accident Management Guidance.

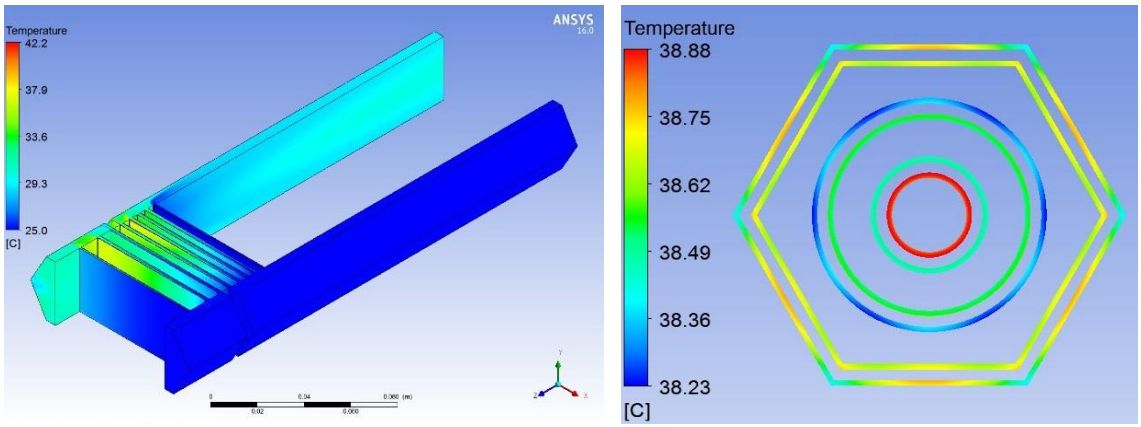

Fig. 3 The results of the thermal hydraulics calculations of the neutron generation target and nuclear fuel assembly

Radiation protection calculations. In the framework of review of the technical solutions for establishing biological shielding for the Neutron Source, calculations of biological shielding for the radial part of the SA core were performed. Biological shielding of SA is a system of concrete structures consisting of a radial shield for the core and two sections of upper shield for the electron beam and nuclear subcritical assembly. The basis for the radiation protection calculations (radiation is generated directly by linear accelerator and SA) is energy characteristics and ionizing radiation intensity, geometry of the Neutron source and protective structures. The radiation protection is calculated using the MCNPX code. The analysis showed the adequacy and correctness of the calculations performed in the PSAR [5] on the one hand, and, on the other hand, the fulfillment of the basic requirements for the safety of the personnel that will be located in the experimental room.

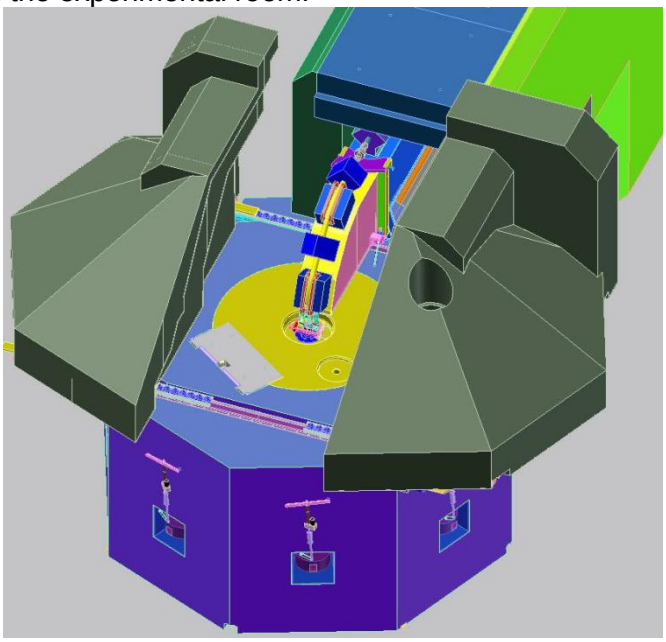

Fig. 4 Neutron Source biological shielding

4. Conclusions

Construction of a fundamentally new nuclear research facility – Neutron Source – is a challenge for both operating organization (NSC KIPT) and regulatory authority (SNRIU). In the world practice, significant experience has been accumulated on safe operation of ADS. Nevertheless, each subcritical system is unique by its design and technical features. The Neutron Source design is peculiar in the use of a relativistic energy electron accelerator to generate neutrons through photonuclear reactions in the neutron generation target and in significant thermal power in comparison with other subcritical systems.

The regulatory authority SNRIU with SSTC NRS technical support has created all the necessary conditions for licensing of the Neutron Source. The regulation “General Safety Provisions for the Nuclear Subcritical Facility” was created based on IAEA standards and international experience. Review of the Neutron Source safety justification documents has been performed with high quality level. Independent thermohydraulic, neutron-physics and radiation shielding models of key nuclear facility elements were developed with assistance of the EC experts with further performing of the calculations for verification safety studies using non-identical analytical tools. Currently, all construction activities on the NSC KIPT site, installation and functional tests of equipment and systems important to safety have been completed. At the end 2018 KIPT conducted the integral test successfully. A package of documentation has been preparing by the operating organization to obtain the separate permits for the first nuclear fuel delivery to the NSC KIPT site and for the physical start-up of the Neutron Source. The tentative period for commissioning of the Neutron Source is the end of 2020.

5. References

1. Law of Ukraine “On Nuclear Energy Use and Radiation Safety” No. 39/95-VRdated 08 February 1995 — 1995.
2. Status of accelerator driven systems research and technology development. — Vienna: International Atomic Energy Agency. IAEA TECDOC-1766, 2015.
3. M.Kh. Gashev, O.V. Grigorash, A.V. Dolotov, A.V. Nosovsky, O.M. Dybach, A.I. Berezhnoi, O.V. Kukhotsky. Licensing of the Neutron Source Based on the Subcritical Assembly Driven by a Linear Electron Accelerator // Nuclear and Radiation Safety. 2013, Issue 4, p. 3-9.
4. Nuclear Subcritical Facility “Neutron Source Based on the Subcritical Assembly Driven by a Linear Electron Accelerator”. The Design. — NSC KIPT, 2012.
5. Nuclear Subcritical Facility “Neutron Source Based on the Subcritical Assembly Driven by a Linear Electron Accelerator”. Preliminary Safety Analysis Report. PSAR — NSC KIPT, 2012.
6. General Safety Provisions for Nuclear Subcritical Assemblies: NP 306.2.183-2012, SNRIU. — 2012.
7. Safety of research reactors. IAEA safety standards series no. SSR-3 / International Atomic Energy Agency. Vienna: International Atomic Energy Agency, 2016.
8. Radiation Safety Standards of Ukraine, NRBU-97. DHN 6.6.1.-6.5.001-98. — Ministry of Health, 1998.
9. License EA 001018 for Construction and Commissioning of Nuclear Subcritical Facility “Neutron Source Based on the Subcritical Assembly Driven by a Linear Electron Accelerator”. — SNRIU, 2013.
10. INSC U3.01/12 “Support to the Ukrainian Regulatory Authorities”, component UK/TS/49 "Licensing of new nuclear subcritical facility - neutron source based on an electron accelerator-driven subcritical assembly".
11. Development of thermohydraulic models of core elements of “Neutron source” / O.V. Kukhotsky, A.V. Nosovsky, O.M. Dybach // Problems of Atomic Science and Technology. — 2017. — № 2. — p. 131-137.

COMPARISON OF SLOWPOKE-2 BURNUP SIMULATIONS AGAINST REACTOR PERIOD MEASUREMENTS

J.E. ATFIELD, C. JEWETT
Applied Physics, Canadian Nuclear Laboratories
286 Plant Road, K0J 1J0 – Canada

ABSTRACT

The inherent safety of the SLOWPOKE-2 (Safe Low Power Kritical Experiment) reactor design relies on maintaining a low core excess reactivity limit of <400 pcm at all times. This restriction places high importance on reactivity shimming, accomplished by the periodic addition of beryllium plates to the top of the core. These additions are required every few years throughout the ~20 calendar-year life of the core, nominally providing the reactor with two effective full-power years of operation before the entire core must be replaced with fresh fuel. The regular measurement of excess reactivity conducted with each reactor shim provides a useful dataset for code comparison. Detailed reactor core simulations were constructed in MCNP6.1 based on actual operating/core shim records from both Highly-Enriched Uranium (HEU) fuelled and Low-Enriched Uranium (LEU) fuelled SLOWPOKE-2 reactors. The predicted excess reactivity values were compared to actual reactor period measurements, providing the first validation of a SLOWPOKE-2 burnup simulation. This validation supports the use of such high fidelity models to predict the impact of reactor modifications such as addition of neutron beam tubes or irradiation sites, some of which have been included in select SLOWPOKE-2 reactors already. This work also aims to provide a better understanding of the observed deviation of shim worth from the initial commissioning curve taken from measurements on a fresh HEU fuelled core, which translates into a small reduction in core lifespan from initial predictions. Excess reactivity validation results are presented and discussed.

1. Introduction

The SLOWPOKE (Safe Low Power Kritical Experiment) is a pool-type reactor first built in the early 1970s by Atomic Energy of Canada Limited (AECL) as a safe, inexpensive source of neutrons, available for purchase by universities, hospitals, and laboratories [1]. The 20 kW SLOWPOKE-2 design aimed to provide neutron activation and isotope production capabilities to organizations that are otherwise unable to afford the significant investment required by most reactor technologies. Typical barriers to reactor construction from high capital cost and licensing burden were reduced by minimizing the fuel mass of the core, and including a high degree of operational simplicity and inherent safety. The core features a very low excess reactivity limit coupled with large negative temperature reactivity feedback, ensuring an automatic, passive reactor shutdown in the event of a positive power/reactivity transient. The resulting design has been licensed for unattended operation (with remote monitoring), and staffed by licensed personnel of non-nuclear-technology organizations. Nine SLOWPOKE-1 and -2's have been built (including the initial prototype), four of which are still in operation today.

The initial design of the SLOWPOKE-2 reactor core incorporated fuel rods of Highly-Enriched Uranium (HEU, 93 wt% ^{235}U/U) in U-Al metal alloy, clad in aluminum. The later design replaced these elements with Low-Enriched Uranium (LEU, 19.75 wt% ^{235}U/U) in UO_2 ceramic fuel pellets clad in Zircaloy-4 [2]. Two HEU fuelled SLOWPOKE-2 reactors were later refuelled with LEU, and one began with an initial core loading of LEU fuel. The core is formed by a pattern of approximately 200 (LEU) to 350 (HEU) 350 fuel elements (~0.8-1.2 kg ^{235}U), locked into a hexagonal lattice by a ~22 cm diameter by ~22 cm tall spool-shaped fuel cage (See Figure 1).

Reactivity control is achieved using a cadmium control rod which passes through the centre of the central tube of the fuel cage spindle.

The core is light water moderated and cooled, and is surrounded on the bottom and sides by a thick beryllium metal reflector. The top of the core is covered by a tray which holds thin beryllium shim plates that are added as required to compensate for burnup reactivity loss. A previous simulation study modelling the reactivity changes from core burnup and shim plate addition showed good agreement with the expected behaviour of an idealized SLOWPOKE-2 reactor [2]. Here, we simulated the core modifications, fuel loadings, and actual shim history of an HEU fuelled SLOWPOKE-2, and a different LEU fuelled SLOWPOKE-2 using MCNP6.1 [3]. The excess reactivity at the end of each burnup stage of the simulation, both before and after shim plate addition, was compared to measurements at the corresponding reactors. The operating records are summarized in Section 2, details of the simulation approach provided in Section 3, and the results discussed in Section 5. Conclusions and future work are presented in Section 5.

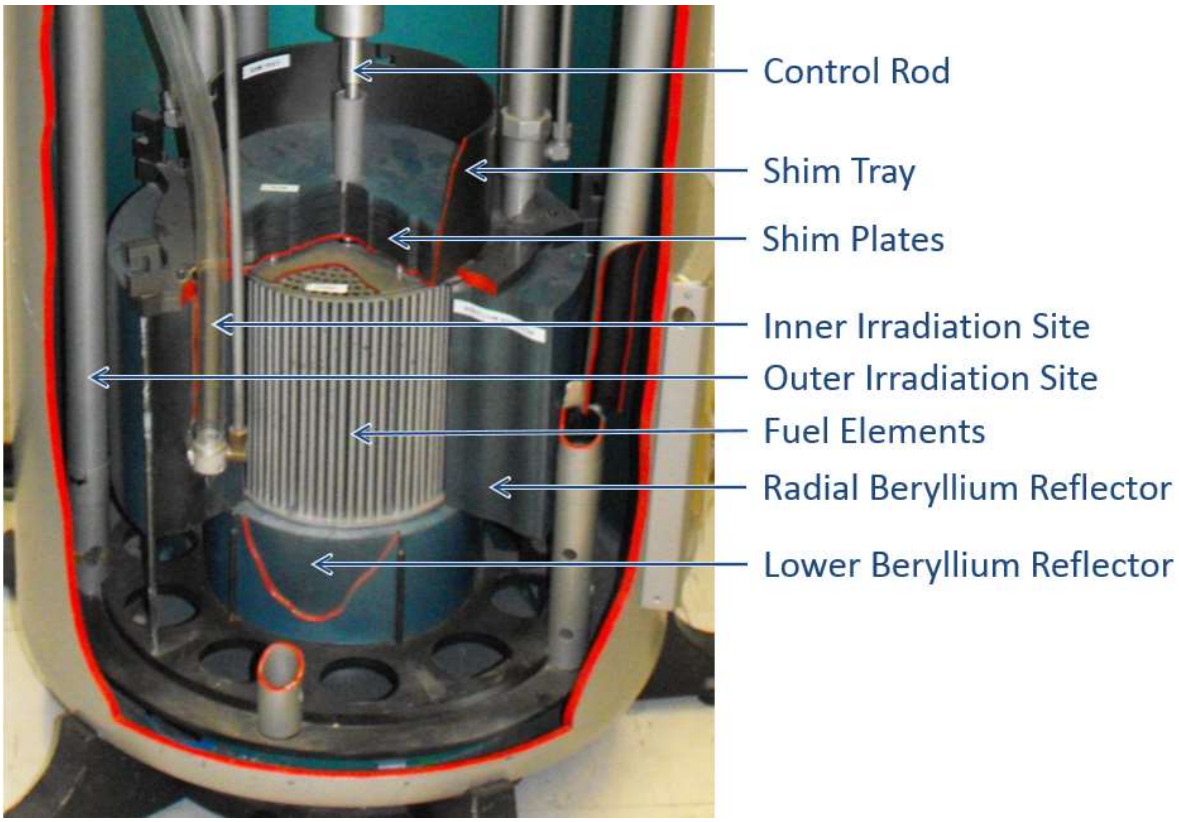

Figure 1 – Photograph of Cut-away model of SLOWPOKE-2 Reactor depicting fuel cage surrounded by beryllium reflectors, including beryllium shim tray. Used with permission of SLOWPOKE-2 staff of Royal Military College of Canada.

2. Operating Records

SLOWPOKE-2 reactor operators keep detailed reactor logs, recording total neutron fluence at the irradiation sites (located in the radial beryllium reflector), and integrated energy output from the reactor. Because reactor power is monitored by neutron flux level using a self-powered flux detector in the beryllium annulus, both of these records depend on commissioning calibrations. The calibration for neutron flux at the irradiation sites was measured by cobalt wire activation. Calibration for reactor power is based on careful heat balance measurements conducted on the 2 kW prototype SLOWPOKE-1 reactor at Chalk River Laboratories. The calibrated current signal from an ion chamber positioned out-of-core during the heat balance measurement was

used to derive the "effective power" of a neutron source placed at the centre of the defuelled core. This neutron source of known effective power was then used for the power calibration at all subsequent SLOWPOKE-2 reactors[1].

Reactivity shim procedures are carried out by a specialized maintenance team, authorized by the nuclear regulator to access the core and perform the adjustment. Reactor period measurements are conducted both before and after shim plate addition to ensure that the excess reactivity is maintained below the 400 pcm limit at all times[2]. The reactivity change is predicted prior to the addition of any shim plate based on measurements conducted in 1971-72 during commissioning of the first 20 kW SLOWPOKE-2 reactor, located in Ottawa, Canada. The measured cumulative shim worth from both the HEU and LEU cores being studied are compared to the commissioning measurements in Figure 2 below. The measured cumulative shim worth from the operating HEU reactor shows reasonable agreement with the commissioning curve, but the LEU core appears to gain less reactivity for a given addition to the plate stack. The shim tray is 4 in. (~10 cm) thick, and therefore, by extrapolation, the total available reactivity shim for the LEU core may be reduced from ~2000 pcm to ~1700 pcm, corresponding to a reduction in core lifespan of ~15%.

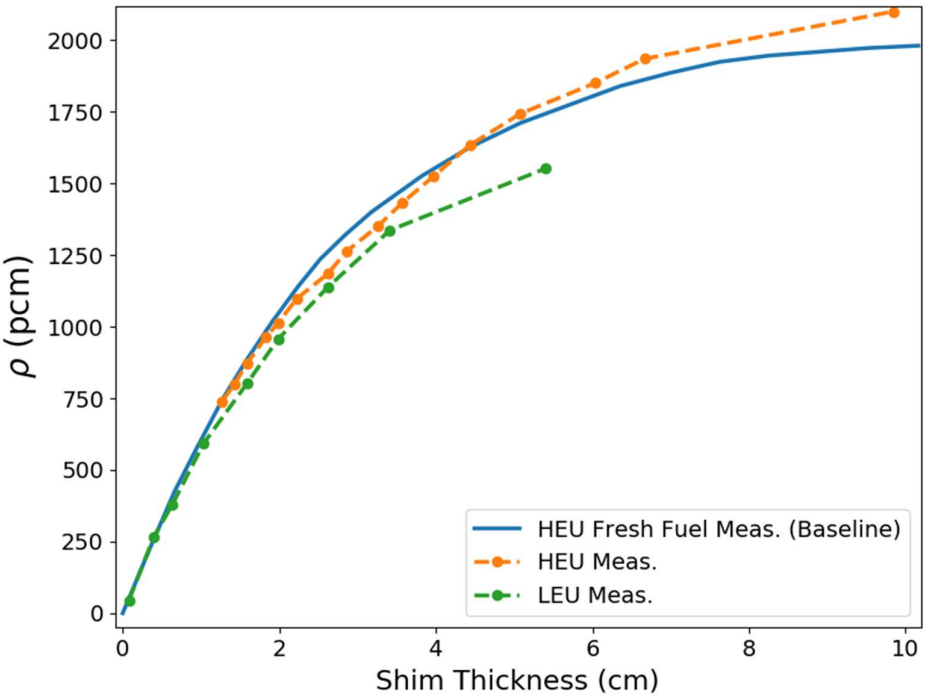

Figure 2 – Measured variation in reactivity worth of beryllium top reflector with thickness.

The core depletion-and-shim process was simulated to assist with predicting timelines for future core replacement. Modifications to existing SLOWPOKE-2 reactors will also benefit from better predictions of the perturbations they have on the core. Past modifications to SLOWPOKE-2 reactors have included flooding of irradiation sites, core life-extension by the addition of a second radial beryllium reflector above the first (surrounding the shim tray), and the addition of a beam tube for neutron radiography.

3. Full-Reactor Simulations using MCNP6.1

[1] In reality, this Am:Be source was used to calibrate the first SLOWPOKE-2, and to calibrate a secondary Ac:Be source. This secondary source was used for all subsequent SLOWPOKE-2 power calibrations.
[2] Of note is the total worth of the cadmium control rod is less than 600 pcm, resulting in a shutdown margin of less than 200 pcm without the manual addition of cadmium capsules to the irradiation sites.

Full-reactor simulations of both an HEU and an LEU fuelled SLOWPOKE-2 were conducted in MCNP6 Version 1.0 [3] with a multi-temperature nuclear data library based on ENDF/B-VII.0 [4]. The input files were based on those described in [2], where it was shown that the overall reactivity behaviour with burnup and shimming a nominal SLOWPOKE-2 reactor was consistent with expectations and the results from other physics codes. For the current study, the input models were modified to reflect minor variations in the specific operating reactors being studied (e.g., specific fuel arrangement, flux detector location(s), appropriate number and state of irradiation sites). The reactor logs list all reactivity values corrected to the reference operating temperature of the reactor, and therefore the simulation temperature corresponded to this value as well. The simulations tracked shim addition and depletion based on the operating records.

MCNP6 coordinates the linking of MCNP6 steady-state transport to built-in CINDER90 depletion calculations [5]. A single depletion 'step' was applied between successive SLOWPOKE-2 shim adjustments, wherein the initial steady-state MCNP6 calculation is used to determine reaction-rates for the "predictor" depletion calculation in CINDER90. The half-time-step nuclide inventories are then used for revised MCNP6 calculation. Finally, the revised reaction-rates are subsequently used in the "corrector" CINDER90 depletion calculation, which implements the fuel depletion from beginning to end of the time step. Only the fuel was depleted in this calculation, with no changes or activation of other materials. Each fuel pin was divided axially into thirteen independent depletion zones, but pins irradiated in similar flux levels were grouped together. The irradiation history in SLOWPOKE-2 reactors is not feasible to simulate explicitly due to the complicated power cycling arising from the demands of neutron activation and small scale isotope production. Instead, depletion is calculated based on operating at steady power for one year to achieve the same total energy output at the time of the shim operation. This results in lower equilibrium poison concentrations compared to what can be achieved at full power operation, but is assumed to be a reasonable first approximation of the non-equilibrium fission product concentrations achieved by the short duration power cycling at low burnup. Additionally, in practice the short lived fission products are allowed to decay before the period measurements are taken for a shim addition. Therefore, a decay calculation would need to be applied to determine core reactivity if a more realistic power level were selected for the depletion simulation (where decay is ignored here).

The MCNP6 depletion simulations each used a total of 200 cycles, with the first 30 discarded. Each cycle contained 100,000 histories, so the total number of active neutron histories used in each of the three transport stages of the calculation was 1.7×10^7. Static MCNP6 transport calculations with improved statistics were conducted at the conclusion of each depletion simulation, with and without including the next shim addition, each with a total of 10^8 active neutron histories. The resulting reactivity vs. burnup profiles for the HEU and LEU cores are shown in Figure 3, where the simulation results were adjusted to remove the reactivity bias for the initial core state. The results show reasonable agreement for the LEU simulation relative to experiment, but a clear increasing trend in the bias of the HEU simulations. The figures also show some inconsistencies between the reactivity loss rates with energy output between the different burnup steps. Repeat simulations with adjusted random number seeds and better statistics shows that this variation can be likely attributed to Monte-Carlo uncertainties. These results prompted further study of the commissioning and shim records for all of the SLOWPOKE-2 reactors, the findings of which are discussed in the following section.

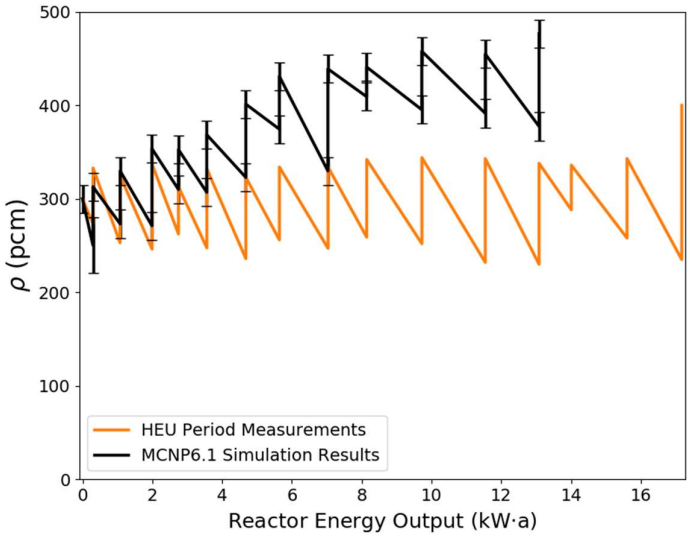

(a) HEU Core

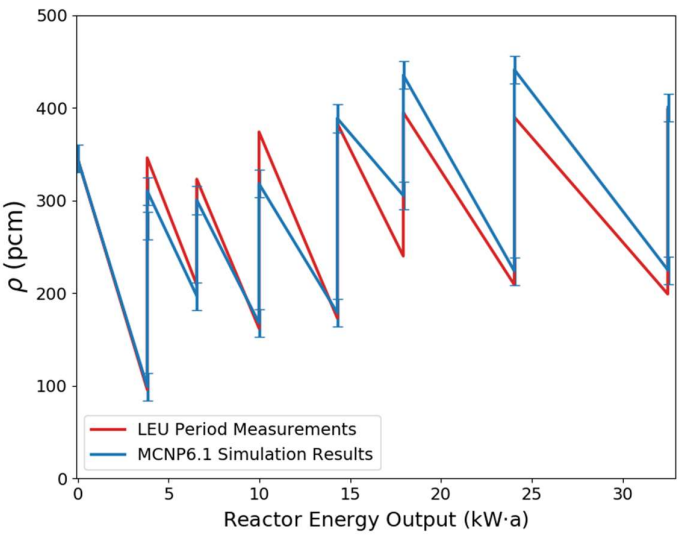

(b) LEU Core

Figure 3 – Core Reactivity with fuel burnup and shimming. Error bars account for Monte-Carlo statistical uncertainty only.

4. Discussion

4.1 Depletion Calculations

A comparison between shim records of different SLOWPOKE-2 reactors revealed that the power calibration factor varied significantly between nominally identical reactors, resulting in large differences in the reactivity loss with burnup between cores, as shown in Figure 4. It's clear that the HEU core that was used as the basis of simulation is an outlier, which explains much of the trend shown in Figure 3 (a). Commissioning records of the later SLOWPOKE-2 reactors remarked that the power calibration method (see Section 2) has significant uncertainty from the assignment of an "effective power" to the commissioning neutron source, which is sensitive to positioning of the source and ion chambers being calibrated for power. This is compounded by the fact that the calibration source experienced several physical changes during the decades of initial reactor construction and commissioning (e.g., transition from Am:Be to Ac:Be, then a step change in strength from a geometric change). Furthermore, the calibration against the known source occurs with the ion chambers operating near their lower limit of sensitivity. The variation in zero current readings at this low range produced an uncertainty of ~10%. Lastly, the "effective power" of the neutron source was not re-derived for LEU fuel, although it was calculated that the power output of an LEU core is ~13% larger than the HEU core for the same flux at the irradiation sites. This may explain the increased reactivity loss of the LEU core measurements relative to simulation shown in Figure 4 (b). To better understand these measurement issues, the depletion curves shown in Figure 4 were re-derived by applying the average[3] calibration factor to all of the cores. The calibration factor of the LEU core was then adjusted to increase the energy output of each data point by 13%. The results are shown in Figure 5. As expected, the spread in results decreases significantly, while the agreement between measurement and simulation has improved.

[3] Excluding the outlier shown in Figure 3(a)

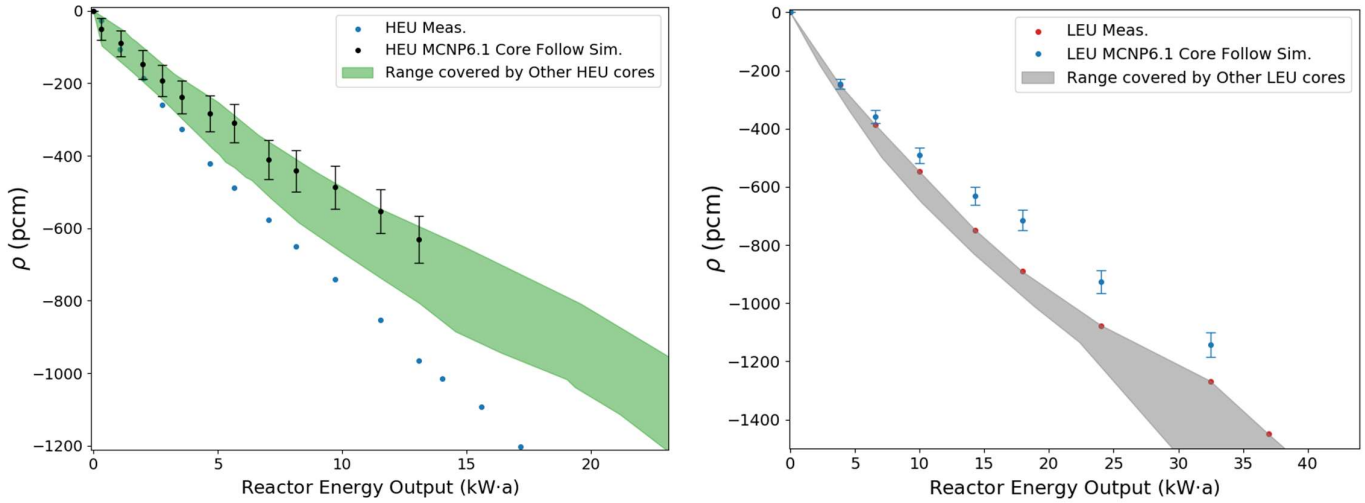

(a) HEU Core (b) LEU Core

Figure 4 – Comparison of core reactivity loss from fuel depletion between different SLOWPOKE-2 reactors. The HEU core compared against simulation in Figure 3 is shown to be a clear outlier relative to the other HEU reactors, which show better agreement with the simulation results. Error bars account for Monte-Carlo statistical uncertainties only. These errors increase with burnup due to the increasing number of simulations used to determine the reactivity value.

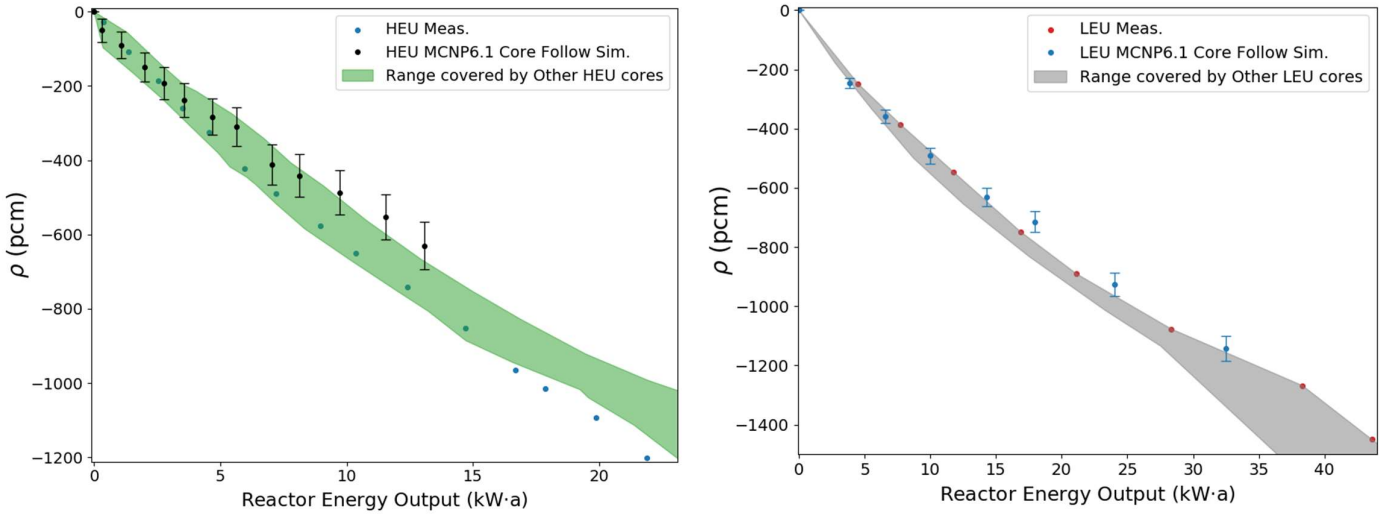

(a) HEU Core (b) LEU Core

Figure 5 – Re-derived core reactivity loss from fuel depletion. The measured results have been adjusted to correspond to a unified power calibration, and to account for the difference in calibration between HEU and LEU cores. Error bars account for Monte-Carlo statistical uncertainties only. These errors increase with burnup due to the increasing number of simulations used to determine the reactivity value.

The measurement issues discussed above account for much of the observed variations between different nominally identical SLOWPOKE-2 reactors, but can also cause significant systematic errors applicable to the results from all cores. Aside from the difference between LEU and HEU cores, these systematic errors are largely undetermined, but could be quantified by comparing simulation to foil activation measurements. Such an approach has been applied in safety analyses of the ZED-2 research reactor for the last decade [6], and was also applied during commissioning of a reactor similar to the SLOWPOKE-2 in the 1980s. The commissioning records of this reactor list the method outlined in Section 2 to derive an initial

power calibration with a target accuracy of a factor of 2. This target reflects the difficulties recognized in the approach. To improve the calibration, experimenters then placed gold foils in several neutron activation sites to determine the absolute flux in these locations. These flux values were then used to normalize the ratio of core-power-to-flux calculated with a historical reactor physics code. The results showed that the initial calibration underestimated the reactor power by a factor of 1.9 ± 0.4. This technique could be used to explore the power calibrations of the SLOWPOKE-2 fleet in the future, as the required flux measurements were routinely conducted during commissioning for each SLOWPOKE-2 reactor. These measurements could also be repeated during any future SLOWPOKE-2 commissioning, such as would occur during a core change.

4.2 Shim Addition Calculations

Records from the other HEU fuelled SLOWPOKE-2s showed fairly consistent agreement in shim worth as a function of top reflector thickness compared to the initial calibration curve (to within $\pm$~100 pcm with the shim tray full). However, both LEU core measurements show a consistent departure from this curve, where, by extrapolation, the worth of a full shim tray is reduced by approximately 300 pcm compared to the calibration curve. These results are compared to the MCNP6.1 core following simulations in Figure 6. Also shown are additional MCNP6.1 simulations quantifying the upper reflector worth with fresh cores of LEU and HEU, which is directly applicable to the calibration curve. The results show that the difference in behaviour between the HEU and LEU cores is not predicted by simulation. Furthermore, the simulations under-predict the reactivity worth of the beryllium upper reflector for both. However, the simulation results do show agreement between the shim worth calculated from simulations incorporating fuel depletion and the fresh fuel simulations. This illustrates it is not necessary to simulate the exact burnup-and-shimming process for the low burnups seen in the SLOWPOKE-2 reactors to predict the reactivity changes.

It should be noted that the baseline shim worth curve from commissioning is a useful reference, but may not correspond exactly to the ideal fresh fuel configuration. The core lattice used fuel arranged in rings, instead of the hexagonal configuration deployed in all subsequent reactors. Further, cadmium capsules were used during the period measurement to reduce the core reactivity to reasonable levels; combined with a partially inserted control rod, the flux distribution may have been altered enough to cause some of the observed discrepancy. The curves for all of the HEU cores also depend somewhat on this baseline curve, as the worth of the initial shim tray loading, typically ~0.5 in. (~1.3 cm) for HEU, is always determined directly from the baseline (rather than from period measurements before and after reactivity changes). Some of the difference between the results of the LEU and HEU shim worth measurements may be due to the fact that the LEU cores started life with nearly empty shim trays.

Further study is required to resolve the discrepancies observed for upper reflector worth. Based on the success in [7] for predicting initial excess reactivity for both the HEU and LEU cores, further refinement of the MCNP models, for example to include nominal reflector impurities, may prove useful.

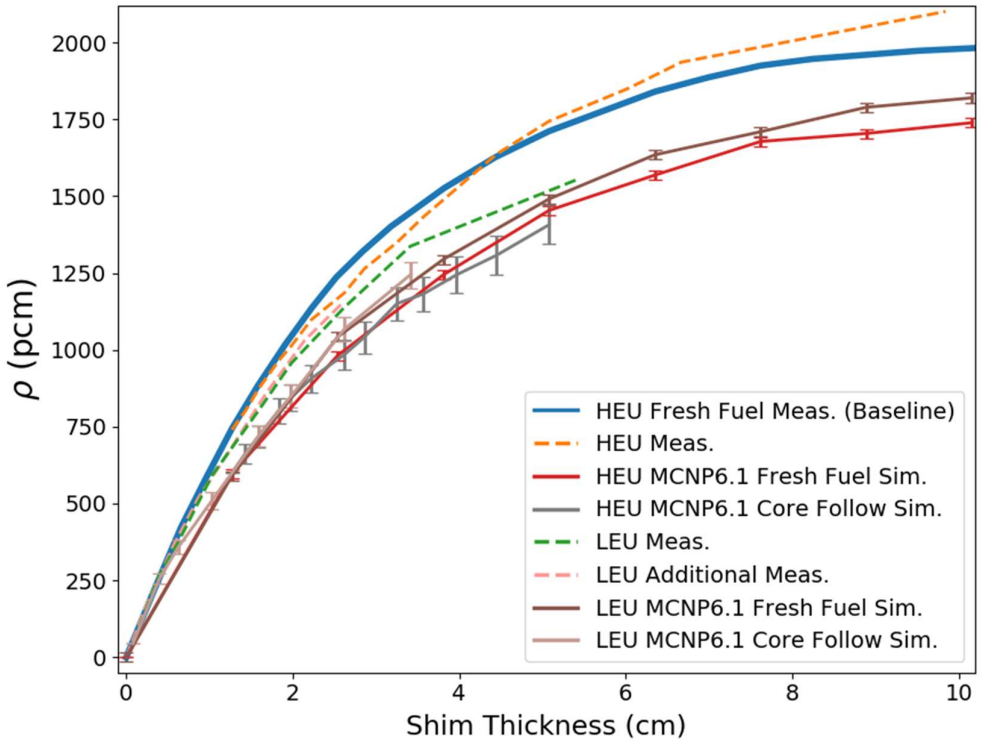

Figure 6 – Comparison of simulation to measurement for upper reflector worth. Error bars account for Monte-Carlo statistical uncertainty only.

5. Conclusions and Recommendations

The core burnup and reactivity shimming of SLOWPOKE reactors was modelled using the burnup and Monte-Carlo based neutron transport capabilities of MCNP6.1. After attempting to correct for deficiencies in the measured data, the simulation results show reasonable agreement in the reactivity behaviour of core depletion, but some disagreement for predictions of reactivity shim. It is suggested that foil activation measurements used to determine the absolute flux in SLOWPOKE irradiation sites could normalize reactor simulations relating flux to reactor power, to improve confidence in the power calibration. Further refinement of the SLOWPOKE model, beginning with inclusion of nominal impurities in the beryllium reflector, is recommended to better predict axial beryllium reflector worth.

6. Acknowledgements

This study was funded by Atomic Energy of Canada Limited, under the auspices of the Federal Nuclear Science and Technology Program. The authors would like to acknowledge the guidance and assistance provided by Dr. Steve Livingstone, Justin Spencer, and Dr. Geoffrey Edwards.

7. References

[1] R.E. Kay, P.D. Stevens-Guille, J.W. Hilborn, and R.E. Jervis, 1973, “SLOWPOKE: A New Low Cost Laboratory Reactor,” Int. J. Appl. Radiation and Isotopes, 24, p. 509.
[2] T.S. Nguyen, G.B. Wolkin, J.E. Atfield, 2012, “Monte Carlo Calculations Applied to SLOWPOKE Full-Reactor Analysis,” AECL Nuclear Review, 1(2), p. 43.
[3] T. Goorley et al., 2012, "MCNP6 Initial Release," Nuclear Technology,” 180, pp. 298-315.

[4] D. Altiparmakov, “ENDF/B-VII.0 Versus ENDF/B-VI.8 in CANDU® Calculations,” PHYSOR 2010 – Advances in Reactor Physics to Power the Nuclear Renaissance, May 9–14, 2010, Pittsburgh, Pennsylvania, USA. Library generated using: R.E. MacFarlane and D.W. Muir, 1994, “The NJOY Nuclear Data Processing System, Version 91,” LA-12470-M, Los Alamos National Laboratory.

[5] W. B. Wilson, et al., 2008, “A Manual for CINDER’90 Version 07.4 Codes and Data,” LAUR-07-8412, Los Alamos National Laboratory, USA.

[6] G. B. Wilkin & K. R. Kumar, 2011, “Overcoming challenges in the ZED-2 reactor safety analysis”, Technical Meeting on Low-Power Critical Facilities and Small Reactors, November 1-3, 2010, Ottawa, Canada.

[7] D. Haile and F. Puig, 2014, “Analysis of the Jamaican SLOWPOKE-2 research reactor for the conversion from HEU to LEU fuel”, RETR 2014 – 35th International Meeting on Reduced Enrichment for Research and Test Reactors, October 12-16, 2014, Vienna, Austria.

A REPORT: 'HIGH-DENSITY U-MO/AL AND U_3SI_2/AL DISPERSION FUELS FOR HIGH-POWER RESEARCH REACTORS'

YEON SOO KIM, L.M. JAMISON, B. YE, W. MOHAMED, Z. MEI,
Y. MIAO, A. OAKS, K. MO, G.L. HOFMAN, A.M. YACOUT

Nuclear Engineering Division, Argonne National Laboratory (ANL)
9700 S. Cass Ave, Argonne, IL 60439 – USA

ABSTRACT

An introduction to a new report on high-density U-Mo/Al and U_3Si_2/Al dispersion fuels for high power research reactors that ANL is drafting is given in this paper. The main objective of this report is to produce a stand-alone data compilation that can be used by fuel designers, fuel performance analyzers, and fuel safety evaluators, as well as reactor operators. It is also intended to build a foundation for an eventual U-Mo/Al dispersion fuel qualification report that supports the licensing of this fuel for high-power research reactors. U-silicide dispersion fuel is also included in the report for potential applications beyond the ranges of the fuel licensed in NUREG-1313 (Safety Evaluation Report for U_3Si_2/Al). The contents and framework of the dispersion fuel report is described. A gap analysis provides a summary of the areas where sufficient data and information are not currently available.

1. INTRODUCTION

This report is composed of three parts. The first part is a general introduction to units, fundamental unit conversions, and operation conditions of research and test reactors (RTR) for which this report is concerned with. The second part is devoted to U-Mo dispersion fuel and the third part is for U_3Si_2 dispersion fuel.

For U-Mo alloy dispersion fuel, designated as U-Mo/Al hereafter, there is no publication that compiles data in an integral manner including thermo-physical properties, irradiation behavior, and performance prediction methods and models. ANL, with collaboration with INL, published a U-Mo Fuels Handbook [1] in 2009 consisting of primarily U-Mo property data, but topics relevant to dispersion fuel were largely excluded. A need has risen to collect all available information of U-Mo/Al fuel in one place, particularly covering the topics of coated U-Mo dispersion fuel. This report will be a living document, able to incorporate new data from on-going tests, and is expected to facilitate easy identification of gaps regarding this fuel type. This publication is also expected to be used as a map clarifying the PIE focuses for the on-going and currently planned tests such as the SEMPER FIDELIS and EMPIRE tests.

An IAEA-lead international collaboration is in progress to pursue a publication of a U-Mo book, the scope of which is, however, limited to un-modified U-Mo fuel dispersion, so the performance of coated U-Mo dispersion fuel and heat-treated U-Mo dispersion fuel are not included. Coated U-Mo dispersion fuel is regarded as the most advanced, so it is a major focus in current tests. Therefore, the thermophysical data and performance behavior of this fuel are also required to be collected, which are in large parts unknown.

INL, with collaboration with ANL, prepared a report on U-Mo monolithic fuel [2], which focused

predominantly on U-Mo fuel itself, so the performance of matrix Al were outside of the scope. U-Mo itself should behave similarly regardless of the fuel form, so U-Mo data available from the INL report are somewhat useful. However, some differences between the U-Mo in a foil form and in a U-Mo powder in view of fuel performance have also been identified, primarily due to the different heat processes during fabrication.

U_3Si_2 dispersion in an Al matrix, U_3Si_2/Al, will be included to a similar extent as the U-Mo/Al in this report because this fuel is considered as a substitute for U-Mo/Al. The silicide dispersion fuel is the densest fuel qualified for the use for research reactors to date. The safety evaluation report (SER) issued by the US NRC (NUREG-1313 [3]) includes PIE data from the qualification test of this fuel. Since then more test data, particularly at high powers, have been collected. An extension to NUREG-1313, or re-qualification of this fuel, for higher power applications may be necessary.

In this paper, a brief introduction of this report is given. In Section 2, a brief summary of U-Mo/Al and U_3Si_2/Al dispersion fuel development is given. In Section 3, the report framework is introduced. In Section 4, gap analysis of the available data is given.

2. Summary of high-density dispersion fuel development

2.1 U-Mo/Al dispersion fuel

Conversion of HEU-using high-performance research reactors in the U.S. and abroad to the use of LEU requires substantial increases in uranium density in the fuel meat. U-Mo alloy fuel was selected to meet this end. Since 1997, U-Mo dispersion fuels in an aluminum matrix have been extensively studied through both in-pile irradiation tests and out of pile tests. Irradiation tests showed that the U-Mo fuel kernel itself with a Mo content ranging 6 – 10 wt% performed well, showing stable irradiation behavior.

However, the overall performance of U-Mo/Al was not acceptable when irradiated under very high power and burnup conditions. The major problem was due to high porosity formation in the meat, which leads to breakaway swelling. The root cause of the problem was found to be due to the reaction between the U-Mo and the Al matrix. Therefore, a remedy that suppresses the reaction between the U-Mo and the Al was sought. One of the methods that received the most study was adding a small amount of silicon to the Al matrix. Irradiation tests of this method showed promising results, but it was insufficient to meet the desired goal that was needed to qualify the fuel for high power research reactors, particularly for European high power research reactors (EUHPRR).

To further improve fuel performance, a direct coating of Si or ZrN on U-Mo particles was proposed and tested. A positive test result was observed from the SELENIUM test at BR2, which warranted a more systematic test of the coating method. The EMPIRE test at ATR was designed to further examine the effectiveness of ZrN coating. The EMPIRE test was also designed to test the viability with other performance improvement concepts such as the use of larger U-Mo particles, annealed U-Mo particles, and U-Mo particles with higher Mo content (10wt% instead of 7wt%). The PIE results of the EMPIRE test will be included in this report.

2.2 U_3Si_2/Al dispersion fuel

U_3Si_2/Al has the highest uranium density among qualified research reactor fuels. U_3Si_2/Al was one of the outcomes of the RERTR program in the period of 1978 – 1988, by which LEU-core conversion of approximately 60% of the worldwide research and test reactors has been possible. This fuel was qualified with a U-density of 4.8 g/cm^3 in the fuel meat [3]. This fuel

showed excellent stability during irradiation. Fission gas bubble swelling is of no concern at typical research and test reactor applications except for high power applications.

However, U_3Si_2/Al was tested predominantly at low temperatures for the qualification [3]. There have been several high temperature tests since then. These new data collected from a higher temperature-regime have kindled hope for possible applications of this fuel o high power research reactors. However, a hint of accelerated fuel swelling was observed in the higher temperature tests. PIE analyses of these tests are to be discussed in the report.

3. Report structure

3.1 Table of contents and brief description for the report

The report is composed of three parts (see Table 1). PART 1 discusses general information commonly used for the entire report. The first section of this part is an introduction to the report. The second section contains definitions including terms and acronyms and the method for burnup-to-fission density conversion.

PART 2 describes U-Mo/Al dispersion fuel. The first two sections of this part are to describe fabrication methods and characterization of as-fabricated fuel. Section 5 will describe fuel irradiation performance topics, in which fuel meat swelling and cladding oxide growth are the two most important performance topics. The next two sections are to include material properties of U-Mo, ZrN coating, matrix, and cladding. Section 6 describes un-irradiated properties and Section 7 discusses irradiated material properties. Section 8 discusses off-normal performance and behavior, in which blister threshold temperatures, fuel failure modes, and fuel behavior during heating by reactivity insertion accidents will be discussed. Section 9 outlines the plate fabrication specifications for the fuel to be qualified, once the exact fabrication methods have been down-selected..

PART 3 is devoted to U_3Si_2/Al dispersion fuel. A similar format to that of the U-Mo/Al section is adopted. However, although U_3Si_2/Al has been qualified, fewer amounts of data exist than those for U-Mo/Al in the regimes of interest. In addition, compared to U-Mo/Al, U_3Si_2/Al does not include a coating process. Information for the Al matrix and cladding given in the U-Mo/Al part is also applicable for U_3Si_2/Al, so these sections will not be repeated. The major emphasis is given to performance behavior of this fuel in higher power applications compared to the earlier qualification.

Table 1 Table of Contents of the report

Table 2 Table of Contents of the report (continued)

3. Gap analysis as of February 2019

There are numerous areas for which information and data are not available. In particular, the concept of coating U-Mo particles is new, so the topics relying on irradiation data and properties of the coated U-Mo are listed as gap items in Table 3.

Table 3 Gap analysis for U-Mo/Al and U_3Si_2/Al dispersion fuels for HPRR

Report section	U-Mo/Al topic	Reason and status	Data sources	Resolution method
3.2	**Coated** U-Mo/Al plate fabrication method	- Final fabrication technique not decided upon (rolling schedule, etc). Write-up to be based on EMPIRE fabrication as a placeholder.	- CERCA	Info from CERCA to be pursued
4.1	As-fabricated fuel meat microstructure analysis	- Particle distribution, porosity, IL during fabrication, alpha-phase transformation	- ANL - INL data from open literature - CEA publications	Data collection and analysis
5.1.2	Fuel meat swelling correlation development	- Fuel meat swelling is the ultimate metric to evaluate fuel performance. - Using meat swelling data and immersion density data, an empirical correlation can be developed.	- ANL - EMPIRE PIE data	Correlation development
5.1.2.1.2	U-7Mo swelling correlation	- A correlation for U-10Mo monolithic fuel available - SCK-CEN found U-10Mo monolithic fuel correlation and U-7Mo/Al dispersion fuel data were consistent - Fuel fabrication analysis for alpha-phase transformation may be needed. - A correlation for U-7Mo swelling is preferable.	- ANL - EMPIRE PIE data	Correlation development
5.1.2.3	IL growth in **coated**-U-Mo/Al	- An update for coated fuel from the current IL growth model may be necessary.	- SCK-CEN for SELENIUM - ANL for EMPIRE	- Correlation development - EMPIRE PIE becomes available
5.3	Cladding oxide model for EU reactors	- Existing models are for AA 6061 alloy - EU reactors use AG3NE or AlFeNi claddings - EU reactors have different coolant conditions (e.g. higher pH) - Reactor-dependent correlations need to be developed with input from the EU reactors - DART update is also aimed	- Test data of BR2 and other EU reactors from open literature	- Correlation development - Correlation for BR2 as an example case
6.3	Un-irradiated properties of ZrN coating	- Bulk material property data are available. Need to examine differences for thin coating. - Effect of thin (< 2 μm) coating may be negligible. - This approach needs justification. - Impact of fabrication technique on material properties to be assessed based on bulk material	- Open literature	Data collection and analysis
6.4.5	Un-irradiated **meat** mechanical properties	- Mainly for elastic range (E, ν, YS, etc) - Measured data are scarce. - Have to rely on modeling (homogenization).	- Other report sections (6.1, 6.2, 6.3)	Using data from other report sections, FEM modeling
6.5	Un-irradiated materials properties of cladding	- AA 6061 cladding property data are mostly available. - Data for AG3NE and AlFeNi are generally unknown.	- EU - Open literature for similar alloys	- EU collaboration - Data collection and analysis
7.1.1	Fuel meat density change by irradiation	- Meat density decreases by fuel particle swelling and porosity formation in IL. - Meat swelling data and immersion density data are to be collected. - This item uses results from subsect. 5.1.2.	- ANL - EU	- EU collaboration - Data collection and analysis
7.1.2	Fuel meat thermal conductivity degradation by irradiation	- Meat thermal conductivity decreases by fission gas bubble swelling and fission product accumulation in fuel particles and porosity growth in IL - Two data points (AFIP-1) are available.	- Open literature	Data collection and analysis
7.1.4	Meat mechanical properties during irradiation	- Data not available	- None	- Low scale modeling - Sensitivity studies via FEA
8.1 8.1.2	- Blister threshold temperature	- Measured data for U-Mo dispersion fuel are fewer than U-Mo monolithic fuel data. - The effect of ZrN-coating may be needed.	- ANL - INL - EU	- EU collaboration - Data collection and analysis

	data - Effect of ZrN coating	- Collaboration with CERCA may be needed if they have data.		
8.2	Thermal modeling for AOO states	- FEM modeling to be pursued		Lower priority
8.3	Mechanical modeling for AOO states	- FEM modeling to be pursued		Lower priority
8.6	Fission gas release during fuel melting	- Literature data for other fuel types are available, but they need to be examined to apply for U-Mo dispersion fuel.	- No data for U-Mo dispersion fuel	Data collection for other types of fuel and analysis
7	Fabrication specification	- This whole chapter is identified as gap currently because the fuel form and relevant fabrication method are not determined.		Lower priority

Report section	U_3Si_2/Al topic	Reason and status	Data sources	Resolution method
13.1	Fuel meat swelling	- NUREG-1313 data were for low temperatures (< 120 ºC). - Recent high Temp and hi burnup data showed potentially higher swelling (much larger FGB size). - Need to collect data to correlate as a function of Temp, FR, or FD or a combination of these.	Legacy data, RERTR-8 test data, SCK-CEN data	Collect data and analyze

4. SUMMARY

A report on U-Mo/Al and U_3Si_2/Al dispersion fuels is currently under preparation. The report will be filled with all aspects of fuel development information. For U-Mo/Al, coated U-Mo together with other performance improvement concepts has been tested in the EMPIRE test and more tests are possisble in the future, so more data will be included in the report. For U_3Si_2/Al, although this fuel was qualified previously, application to higher power, i.e., higher temperatures, may require PIE analyses from recent high power tests. These new data will be included in the report.

ACKNOWLEDGMENTS

This study was sponsored by the U.S. Department of Energy, National Nuclear Safety Administration (NNSA), Office of Material Management and Minimization (NA-23) Reactor Conversion Program under Contract No. DE-AC-02-06CH11357 between UChicago Argonne, LLC and the US Department of Energy.

REFERENCES

[1] J. Rest et al., U-Mo fuels handbook, ANL-09/31, ANL, 2009.
[2] M Meyer et al., Preliminary report on U-Mo monolithic fuel for research reactors, INL/EXT-17-40975, Sept. 2018.
[3] Safety Evaluation Report, NUREG-1313, US NRC, July 1988.

OVERVIEW OF ALUMINUM CLADDING OXIDE PREDICTION MODELS FOR EUROPEAN HIGH POWER RESEARCH REACTORS

YEON SOO KIM, A.M. YACOUT
Nuclear Engineering Division, Argonne National Laboratory (ANL)
9700 S. Cass Ave, Argonne, IL 60439 – USA

H.T. CHAE
Korea Atomic Energy Research Institute (KAERI)
989-111 Daedeok-daero, Yuseong-gu, Daejeon 305-353 – Republic of Korea

S. VAN DEN BERGHE, A. LEENAERS, V. KUZMINOV
Nuclear Materials Science Institute, SCK.CEN, Boeretang 200, 2400 Mol - Belgium

ABSTRACT

UMo/Al dispersion fuel clad with aluminum alloy is a primary candidate fuel form that is being developed for the European high power research reactors (EUHPRR). In BR2 tests, water oxidation of cladding grew thick due to high powers. Excessive cladding oxidation is a cause for serious fuel performance degradation in a test while fuel performance itself may be sound. It is necessary for a fuel designer to have a reliable model to predict cladding oxidation for fuel licensing activities. Using oxide data from BR2 tests, this study reviews the prominent oxide prediction models and cladding-to-coolant heat transfer correlations. Because the oxide growth models were based upon different coolant flow conditions from those of the EUHPRR, the effect of the heat transfer correlations at the cladding-to-coolant interface on the oxide thickness prediction were also examined. The best combination of the oxide prediction model and the heat transfer correlation applicable for the EUHPRR is recommended. Since the existing oxide models were all developed for aluminum alloy types different from those currently considered for the EUHPRR, the effect of cladding alloy type is also discussed.

1. INTRODUCTION

For the conversion of the European high power research reactors (EUHPRR) such as BR2, RHF, and JHR from highly enriched uranium (HEU) to low enriched uranium (LEU), a high uranium-density fuel is being developed. The primary candidate is UMo alloy fuel kernel dispersion in an Aluminum matrix (UMo/Al) with a meat uranium-density of up to 8.5 g-U/cm^3. In order for this fuel to be qualified, stable and predictable fuel behavior, and mechanical integrity and dimensional stability of the fuel plate must be demonstrated over the range of anticipated normal and off-normal operating conditions. In this regard, two traditionally used metrics to assess fuel performance are fuel meat swelling (or fuel plate thickness expansion) and cladding oxidation. The former performance topic has received extensive studies including experiment and modeling. The latter has had relatively less attention because no further development for cladding has been pursued from previously qualified fuels.

Aluminum alloy has well served as research reactor fuel cladding since its first use for the MTR in 1950s. When fuel temperatures were relatively low, cladding oxidation was not a concern. However, when LEU fuel is considered for high power applications, cladding

oxidation becomes a critical factor that elevates fuel temperature because its oxide, typically a Boehmite, has a thermal conductivity that is about two orders of magnitude lower than aluminum. Therefore, excessive oxidation can potentially degrade fuel performance that may be otherwise sound. In this sense, providing a reliable prediction model for cladding oxidation is crucial to help fuel design and improve modeling fuel performance behavior.

Because the existing oxide growth models were mostly developed based on the measured data obtained at lower temperatures and powers than the EUHPRR, a review of the existing models became necessary before applied to the EUHPRR. The frequently used oxide prediction models available in the literature were investigated in this study by comparing with the measured data from the tests at bounding power and burnup conditions in the BR2.

The accurate prediction of cladding surface temperature relies on an accurate model for the heat transfer coefficient at the cladding surface. The most frequently used models predicting the heat transfer coefficient at the cladding surface were also examined, incorporating detailed thermal-hydraulic properties.

In addition, the effect of alloy types on oxidation growth kinetics was examined between AG3NE and AlFeNi.

2. Basic data for oxide thickness prediction

2.1 Irradiation tests

The oxide data of the irradiation tests E-FUTURE [1] and SELENIUM [2], irradiated in the BR2 at SCK.CEN, were examined in this study. Three full-sized plates out of four of the E-FUTURE test (see Figure 1) and one plate from the SELENIUM test were picked. Two different cladding types, AG3NET and AlFeNi, were studied. Plate dimensions are shown in Figure 2.

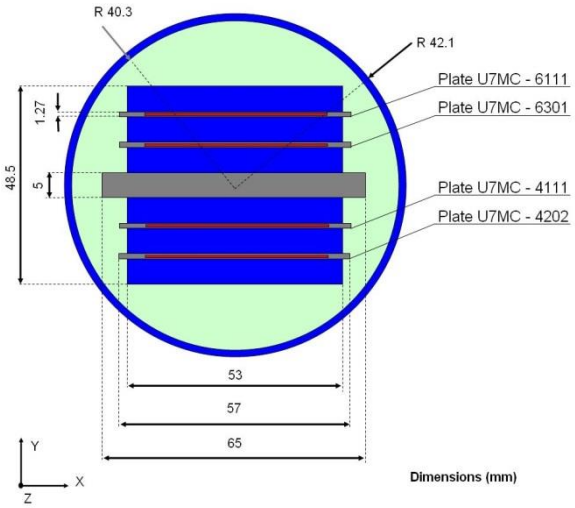

Figure 1 Schematic of the cross section of the E-FUTURE basket with four fuel plates. The same basket was used for the SELENIUM test, with the fuel plates loaded in the bottom half of the basket.

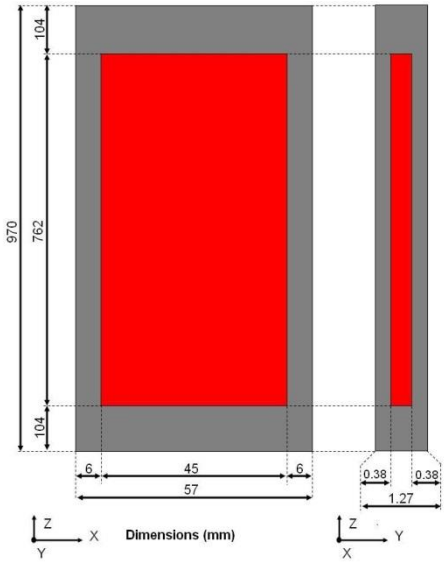

Figure 2 Schematic of a fuel plate and meat used for E-FUTURE and SELENIUM.

Both tests had the same coolant speed of 12 m/s (downward flow), the coolant pH of 6.1, and the coolant inlet temperature of 38 °C, and the same test basket having the coolant channel gap of 6.4 mm.

Power histories of the plates are shown in Figure 3 [3][4]. Heat flux data along the axial line 41 mm from the lower-power plate-edge are given because the peak oxide thicknesses were measured along this line. Although the power was lower there than at the meat edge, the highest cladding surface temperature was predicted along this line due to lower cooling.

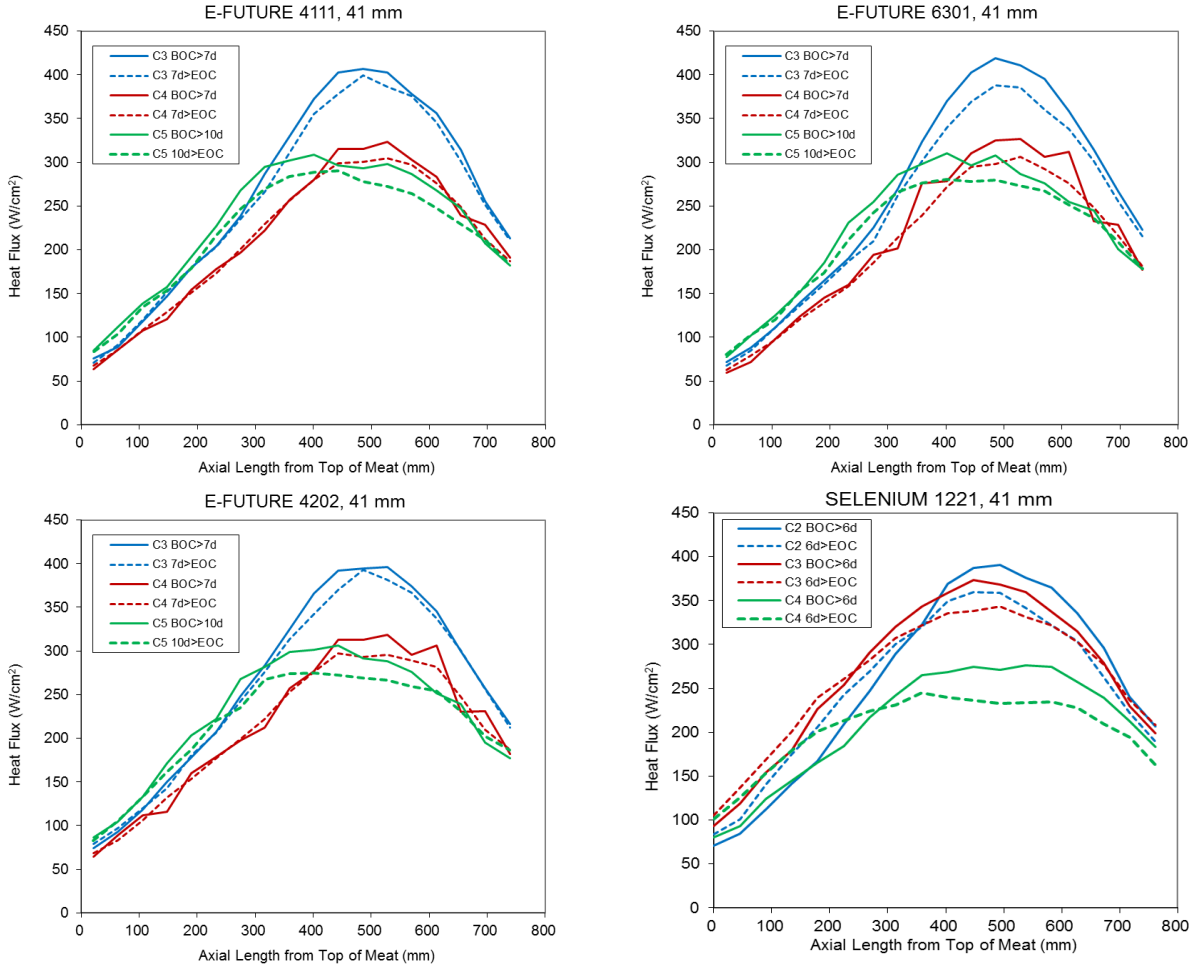

Figure 3 Power histories of E-FUTURE plates and SELENIUM plate along the line 41 mm from the lower-power plate-edge

2.2 Heat transfer coefficient at cladding surface

Due to the high coolant speed, the coolant flow condition of the experiments in this study was in the turbulent flow regime. Convection is, therefore, the dominant mode of heat transfer. Applying Newton's law of cooling, the cladding surface temperature can be calculated by

$$T_w = T_b + \frac{q''}{h_a} \quad (1)$$

where T_b is the bulk fluid temperature, q" is the heat flux, and h_a is the heat transfer coefficient (HTC).

Four HTC correlations applicable to plate type geometry, including the Dittus-Boelter

correlation [5], the Sieder-Tate correlation [6], the Colburn correlation [7], and the recently developed KAERI correlation [8], were selected for the study. The Dittus-Boelter correlation is recommended specifically for a situation in which the difference between cladding surface temperature and fluid temperature is small. On the other hand, the Sieder-Tate correlation is known to be more accurate for a condition that has a large temperature difference between cladding surface and fluid because it is capable of explicitly incorporating the viscosities of the fluid at the bulk fluid temperature and the cladding surface temperature. The Colburn correlation is similar to the Dittus-Boelter correlation while it is different in that it considers the fluid properties at the film temperature defined by the average of the bulk coolant temperature and cladding surface temperature. The KAERI correlation was recently developed based on experimental data measured for rectangular channels, simulating coolant channels set by fuel plates.

2.3 Cladding surface temperature

In order to compare the four HTC correlations discussed in subsect. 2.2, the calculated Nusselt number and the cladding surface temperature versus axial length for the E-FUTURE 6301 plate are plotted in Figure 4. Because the HTC is proportional to the Nusselt number, a higher Nusselt number yields a lower cladding surface temperature (see Eq.(1)).

The Dittus-Boelter correlation gave the highest cladding surface temperature, which may be attributed to the model's inability to differentiate the coolant viscosity at the cladding surface and that of the bulk coolant. The difference in the cladding surface temperature between the predictions by the Dittus-Boelter and KAERI correlations was ~30 °C at axial length ~500 mm. The axial surface temperature was calculated using a program developed at KAERI (Thermal Hydraulic Margin Calculator for Plate-type Fueled Reactor Core for Windows) [9].

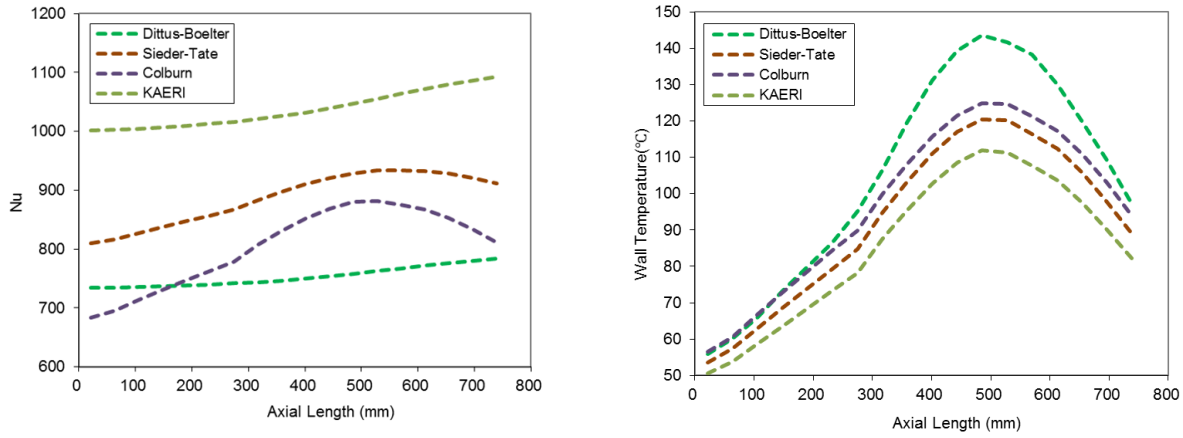

(a) Nusselt number (b) Cladding surface temperature

Figure 4 Nusselt number and cladding surface temperature for E-FUTURE 6301 plate

3. Oxide thickness prediction models

3.1 ANL model

Oxide growth on cladding surface follows the following equation [10]:

$$x = \left[x_o^{p+1} + (p+1) k t \right]^{p+1} \quad (2)$$

where x_0 is the oxide thickness at time zero, p is the rate law power, k is the rate function and t is the time.

The rate law power p is given by:

$$p = 0.12 + 9.22 \exp\left(-\frac{C_s}{6.82\times10^{-9}}\right) \quad (3)$$

Here C_s considers oxide dissolution in coolant and is expressed by:

$$C_s = \exp\left[-\left(-13.79 - \frac{1211.16}{T_{x/w}}\right)\left(0.041H^2 - 0.41H - 0.07\right)\right] \quad (4)$$

where $T_{x/w}$ is the temperature at the oxide-water interface in K and H is pH of the coolant. The applicable temperature range is 25 ≤ T ≤ 300 °C and pH not greater than 7.0.

The rate function k is expressed by an empirical formula:

$$k = 3.9\times10^{5}\, exp\left(\frac{-6071}{T_{x/w} + AB\frac{q'' x}{k_T}}\right) \quad (5)$$

where $T_{x/w}$ is the oxide-water interface temperature in K, q" is the surface heat flux in MW/m^2, x is the oxide thickness in μm, k_T is the thermal conductivity of the oxide in W/m-K, A is the augmentation factor as described below.

A is added to the equation as a multiplier to take into account the effect of coolant velocity. The augmentation factor increases as the coolant velocity increases because of the water ingress through the defective oxide. A is correlated with the coolant velocity using the following sigmoidal function:

$$A = 0.43 + \frac{3.21}{1 + \exp\left(-\frac{v_c - 13.39}{3.60}\right)} \quad (6)$$

where v_c is the coolant velocity in m/s. The applicable range of coolant velocity for this correlation is 3 - 28 m/s.

A correction constant, B, is needed to account for the reduction in the 'oxide thickness' caused by oxidant migration. B = 0.37 for AA 6061 and the ATR data. Since x is included in Eq.(5), the time interval was set equal to the reactor cycle length.

The oxide thermal conductivity decreases as the oxide thickens. The oxide thermal conductivity was formulated as a function of the oxide thickness as follows:

k_T = 2.25, for x ≤ 25, (7)

k_T = 2.25 - 0.016 (x - 25), for 25 ≤ x ≤ 100 (8)

where k_T is in W/m-K and x is the oxide thickness in μm.

3.2 Griess Model

The Griess model uses the following correlations for two pH regimes [11]:

$$x = \begin{cases} 11{,}252\, exp\left(-\frac{4{,}600}{T}\right) t^{0.778}, & \text{for pH = 5.0} \\ 30{,}480\, exp\left(-\frac{4{,}600}{T}\right) t^{0.778}, & \text{for } 5.7 \le pH \le 7.0 \end{cases} \quad (10)$$

where x is the oxide layer thickness in μm, t is the time in h, and T is the cladding surface

temperature in K. The uniqueness of the Griess model is its ignorance of the effect of heat flux.

3.3 KAERI Model (Modified-Griess model)

The KAERI model is the product of an experimental study on the effect of the heat flux on oxide growth to modify the Griess model. The experiment study found that the Griess model over-predicted when the heat flux was below 3.18 MW/m^2. A modification factor was added to the Griess model as follows [9]:

$$x = \begin{cases} 11{,}252\exp\left(-\dfrac{4{,}600}{T}\right)t^{0.778} f_q, & \text{for pH} = 5.0 \\ 30{,}480\exp\left(-\dfrac{4{,}600}{T}\right)t^{0.778} f_q, & \text{for } 5.7 \le \text{pH} \le 7.0 \end{cases} \tag{9}$$

Here the factor f_q is a function of the heat flux given by

$$f_q = \begin{cases} 0.2, & \text{for } q < 2.16 \text{ MW/m}^2 \\ -0.20836 + 0.18915\,q, & \text{for } 2.16 \text{ MW/m}^2 < q \end{cases} \tag{10}$$

where q is the heat flux in MW/m^2.

4. Oxide thickness prediction

The three oxide prediction models described in sect. 3 were employed to calculate oxide thickness for the test conditions at BR2. The details of this section can be found elsewhere [12].

The oxide thickness data measured along the axial line 41 mm from the cooler side of plate edge are compared with the predictions made by the models for four HTC correlations for E-FUTURE 6301 plate(Figure 5) and for SELENIUM 1221 (Figure 6). When coupled with the Colburn correlation or the Sieder-Tate correlation, the ANL model (Kim model) was consistent with the measured data.

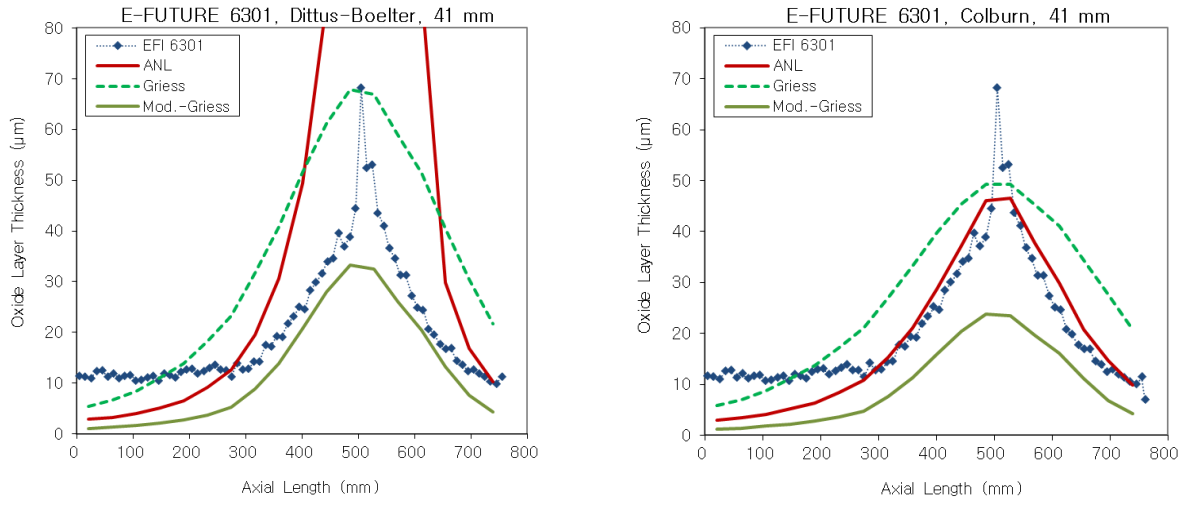

(a) Dittus-Boelter (b) Colburn

Figure 5 Comparison of HTC correlations for oxide thickness data of E-FUTURE 6301

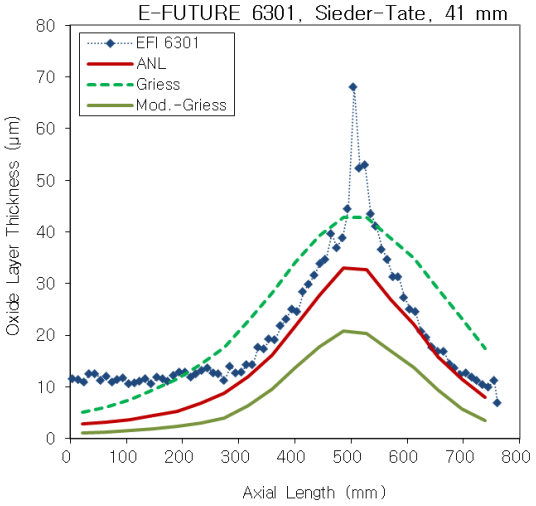

(c) Sieder-Tate

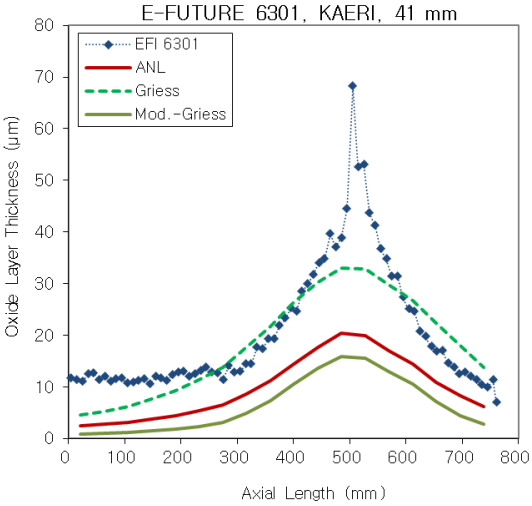

(d) KAERI

Figure 5 Comparison of HTC correlations for oxide data of E-FUTURE 6301(cont'd)

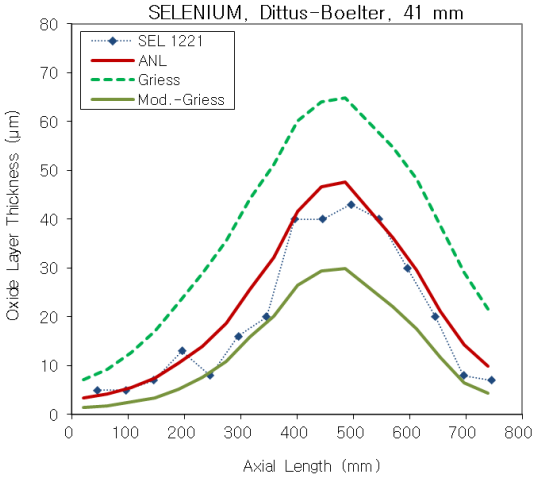

(a) Dittus-Boelter

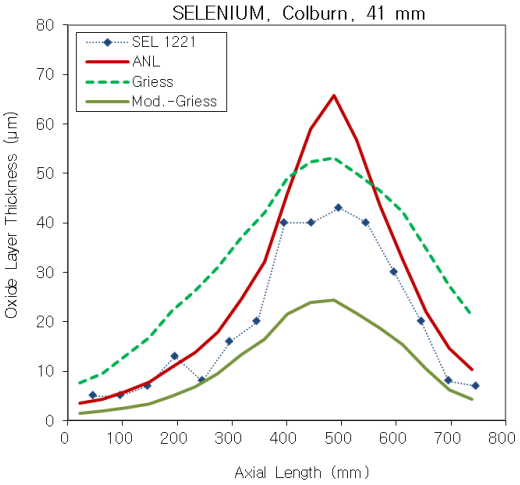

(b) Colburn

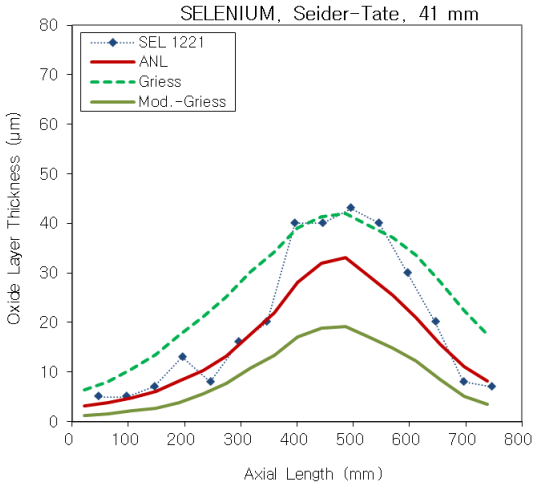

(c) Sieder-Tate

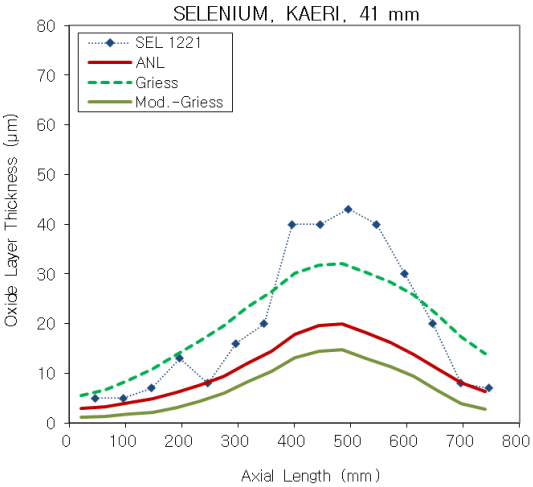

(d) KAERI

Figure 6 Comparison of HTC correlations for oxide data of SELENIUM 1221

5. Effect of cladding type

Because the cladding materials of the BR2 test plates were AG3NE (close to AA5754) and AlFeNi, different from AA6061 that the models were based upon, one might expect an effect of cladding type on the oxide growth (see Table 1 of Ref. [13] for the nominal compositions of the cladding types).

The E-FUTURE test results with different cladding types were compared in Figure 7. The E-FUTURE 4111 plate made with AlFeNi showed, in general, lower oxide thickness than those of the E-FUTURE 4202 and 6301 plates made with AG3NE, implying that AlFeNi cladding appears to be slightly advantageous over AG3NE. This result is an outlier compared to the findings in the literature [14], in which no discernable effect was found. The possible reason may be attributed to the higher temperatures for the present test than those in the literature. Like a magnifying glass, the high temperature test magnifies the difference that was not obvious in the previous low temperature tests.

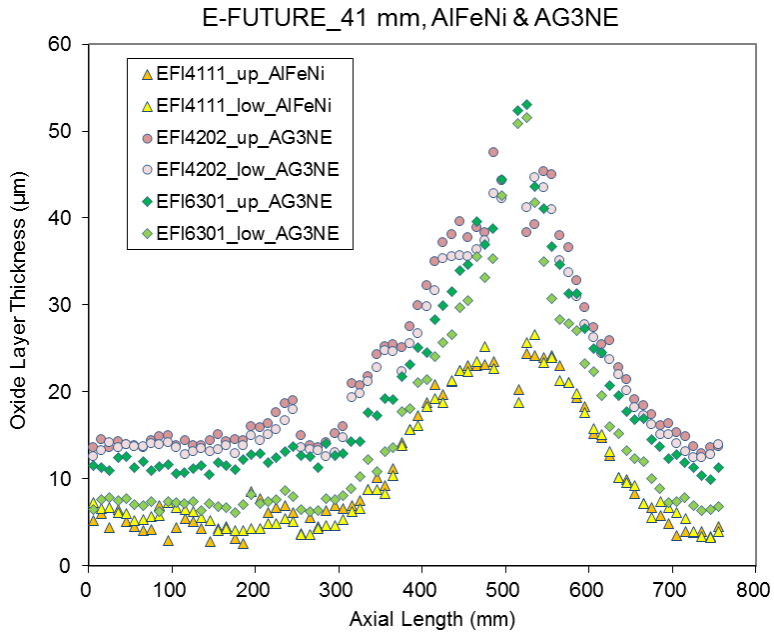

Figure 7 Examination of the effect of cladding type on oxidation kinetics by using E-FUTURE test plates.

4. Conclusions

The Griess model generally overpredicted for all heat transfer correlations. The ANL model was also found inapplicable to the EUHPRR test conditions at peak power locations when it is coupled with the Dittus-Boelter correlation because the Dittus-Boelter correlation resulted in high cladding temperatures. The ANL model, coupled with the Colburn correlation or the Sieder-Tate correlation, gave most consistent results with the measured oxide data.

The examination of the E-FUTURE test plates revealed that a noticeable difference, albeit small, exists between AG3NE and AlFeNi. AlFeNi appears to result in a slightly thinner oxide layer. However, it was thought that this difference only became significant because the high power test enhanced the oxide growth. For lower power test cases, however, the difference in alloy type was believed to have only a secondary effect, hard to differentiate from other uncertainties.

ACKNOWLEDGMENTS

This study was sponsored by the U.S. Department of Energy, National Nuclear Safety Administration (NNSA), Office of Material Management and Minimization (NA-23) Reactor Conversion Program under Contract No. DE-AC-02-06CH11357 between UChicago Argonne, LLC and the US Department of Energy.

The submitted manuscript has been created by the UChicago Argonne, LCC as Operator of Argonne National Laboratory under contract No. DE-AC-02-06CH11357 between the UChicago Argonne, LLC and the Department of Energy. The U.S. Government retains for itself, and others acting on its behalf, a paid-up, nonexclusive, irrevocable worldwide license in said article to reproduce, prepare derivative works, distribute copies to the public, and perform publicly and display publicly, by or on behalf of the Government.

REFERENCES

[1] F. Frery et al., “LEONIDAS UMo Dispersion Fuel Qualification Program: Progress and Prospects,” Proceedings of the 32nd International Meeting on Reduced Enrichment for Research and Test Reactors, Lisbon, Portugal, October 10-14, 2010.
[2] S. Van den Berghe, Y. Parthoens, G. Cornelis, A. Leenaers, E. Koonen, V. Kuzminov, C. Detavernier, J. Nucl. Mater. Vol.442, 60-68, 2013.
[3] V. Kuzminov, E. Koonen, “Qualification irradiation of new high density UMo LEU fuel plates and operating conditions during irradiation at the BR2 high flux materials testing reactor,” Proceedings of the International Conference on Research Reactor Fuel Management (RRFM), Rome, Italy, 2011.
[4] V. Kuzminov, “SELENIUM Test Irradiation. Evaluation of Irradiation Conditions for Two UMo LEU ‘SELENIUM’ Fuel Plates during the BR2 Cycles 02/2012 – 04/2012,” Report, SCK·CEN-R-5639. Revision 1, SCK·CEN, January 2013.
[5] F.W. Dittus, L.M.K. Boelter, “Heat transfer in automobile radiator of the tubular type,” University of California at Berkley Publ. Eng. 2, 443-461, 1930.
[6] E.N. Sieder, G.E. Tate, Industrial and Engineering Chemistry 28, 1429-1435, 1936.
[7] A.P. Colburn, Trans. AIChE J. 29, 174-210, 1933.
[8] D. Jo, et al., Nucl. Engin. Technol. Vol.46 No.2, 195-206, 2014.
[9] H.M. Sohn, “User manual of TH_Calc Win 1.0a,” Report in Korean, KAERI Report, 2017.
[10] Y.S. Kim, G.L Hofman, A.B. Robinson, J.L. Snelgrove, N. Hanan, J. Nucl. Mater. Vol.378, 220-228, 2008.
[11] J.C. Griess, H.C. Savage, J.L. English, “Effect of heat flux on the corrosion of aluminum by water. Part IV. Tests relative to the Advanced Test Reactor and correlation with previous results,” Report, ORNL-3541, February 1964. Also see J.C. Griess et al., ORNL-3230, 1961.
[12] H.T. Chae, Y.S. Kim, A.M. Yacout, ANL report, ANL/RTR/TM-18/10 (2018).
[13] B. Kapusta, J. Garnier, B. Maugard, L. Allais, P. Lemoine, “Irradiation effects on 6061-T6 aluminum alloy used for JHR internal structures,” 12th IGORR meeting, Beijing, China, 2009.
[14] K. Farrell, Performance of Aluminum in Research Reactors. In: R.J.M. Konings, (ed.) Comprehensive Nuclear Materials, volume 5, pp. 143-175 Amsterdam: Elsevier, 2012.

THE IMPACT OF FUEL SHUFFLING STRATEGY ON THE NEUTRONIC PARAMETERS OF MATERIAL TEST RESEARCH REACTOR CORE

R.O. ABDALAZIZ,
Department of Nuclear Safety, Radiation and Nuclear Safety Institute
Sudan Atomic Energy Commission
Aljamaa Street, 3001 Khartoum – SUDAN

ABSTRACT

In the present paper, the fuel shuffling strategy used in the Material Test Research Reactor has been investigated to determine its impact on the neutronic parameters of the core. The neutronic analysis has been done using the deterministic approach. The computer code CITVAP has been used to determine the neutronic parameter of the core and the WIMSD code has been used to build the cross section library needed for the diffusion calculation. A computer program has been developed to search for the optimum shuffling strategy that has the maximum Keff and the best power density and burnup distribution. A comparison between an exist strategy and the strategy determined by the program has been done. The comparison shows the high ability of the developed program to estimate the optimum shuffling strategy. Also the result reflect that there is no clear impact on the keff and the reactivity of the core while it has clear impact on the power density and burnup distribution.

1. Introduction

Nuclear fuel management is the processes that involve the formulation of policies or decisions for the fuel cycle that lead to a decrease in the cost or to a more effective utilization of the fuel. Specifically, the core management includes the schemes for loading (and unloading) of fuel and the techniques of utilizing control elements. It has two main objectives: to increase the burn-up of the fuel, thereby improving its utilization, and to achieve a more uniform thermal power distribution in the core, thereby facilitating heat removal and thus safety. The principles of fuel management are the same in general for research and power reactors, but they differ in goals. In power reactors the main goal is to produce energy thus decisions will follow the energy demands. While in research reactors the main task is to obtain a neutron flux with a desired amount at certain time, thus decisions are made based on neutron flux demands. The processes of nuclear fuel management can be subdivided into two topics; out of core and in core nuclear fuel management. In each one there are many tasks that should be followed to achieve the desired goals of management. (Turinsky and Parks 2002). The Out-of-core fuel management concerns the decisions that will impact future reload cycles, and aims to answering the questions “What to purchase?” and “What to reinsert?”. On the other hand, The In-core fuel management is done on fuel utilization, in order to reduce the fuel costs, reduce the volume of nuclear waste, and satisfying required operational and safety limits (Safarzadeh et al. 2014). It concerns processes which characterize the core loading pattern and control rod location. The core loading pattern determination is a complex problem due to economic, operation constrains and safety margins aspects. Thus the optimization of loading pattern has been responsible for neutronics characteristics of core such as neutron flux, radial power peaking factor, burn-up, cycle length and moderator temperature coefficient (Safarzadeh et al. 2011)(Turinsky et al. 2005).

The major design objectives related to the selection of the core loading pattern are; the minimization of the power peaking by making the cores power distribution as flat as possible and the maximization of the cycle energy production/neutron flux for fuel to be loaded into the core.

The power-peaking factor minimization results in reduction of thermal stress on fuel leading to reduction of fuel-failure rates and consequently enhancing plant availability and operational safety. While the cycle length/neutron flux maximization leads to improving fuel utilization and consequently leads to better economy (Zameer, Mirza, and Mirza 2014).

Recognizing that cores utilize multiple fuel regions for improved economics, advantage can be taken of this by locating the most reactive and lesser reactivity region then draw the suitable movement or strategy that satisfying the desired objective. As example the Out-In loading strategy that will counteract the neutron leakage from the core radial periphery. Another example is the In-Out loading strategy that positioned the most reactive fuel in the core center spatial zone and lesser and lesser reactive fuel in placed further and further out from the core center. There are other strategies that were evolved to improve the objectives in the previously mentioned strategies. One of them is, In-Out-In strategy that would seem to be a compromise between an Out-In and In-Out loading strategy. Another is a more complicated loading pattern strategy referred to as a Low Leakage Loading Pattern (L3p) with a Ring of Fire. (Turinsky 2010).

2. Description of the Reactor and Core under Study

The reactor used in this study is the Pakistan Research Reactor-1 (PARR-1) which is a swimming pool, Material Test Research (MTR) reactor type located in the Pakistan Institute of Nuclear Science and Technology (PINSTECH). It was originally designed to utilize Highly Enriched Uranium (HEU) fuel, 93% enriched in U-235, at a power level of 5MW. The reactor was made critical on December 21, 1965 and attained its full power on June 22, 1966. It was converted to utilize Low Enriched Uranium (LEU) fuel ~20% enriched in U-235 in October, 1991. It's power upgraded initially from 5 to 9 and then to 10MW(Ali Khan et al. 2000). Light water is used as coolant and moderator. The shielding is provided by water and regular or high density concrete. The reactor core is immersed in either of the two sections of the concrete pool filled with water which acts as reflector. One of the sections of the pool is an open area for bulk irradiation and is called open pool end. The other section where beam tubes and other experimental facilities surround the core is called the stall pool. When operating in stall end, one side of the reactor core is reflected by a graphite thermal column. (R. Ahmed 2006) (S.-U.-I. Ahmed 2005) (Ali Khan et al. 2000). The core of PARR-1 consists of an assembly of standard fuel elements (SFE) and control fuel elements (CFE) mounted on a 127mm thick aluminum grid plate. The grid plate has 54 circular holes in 9× 6 pattern with (81.00× 77.11) mm2 lattice spacing to accommodate end fittings of the fuel elements. The fuel elements can be assembled in different ways on grid plate to obtain desired core configuration. In between these holes, there are 40 smaller holes each with radius of 11 mm for water to pass through the sides of fuel plates. The core is immersed in demineralized light water, which acts as coolant, moderator and reflector. However, specially designed reflector elements, sometimes, replace light water on any one or more sides. The reflectors include graphite and beryllium blocks, or canned heavy water etc (S. U. I. Ahmad, Ahmad, and Aslam 2004).

The First Equilibrium Core of PARR-1 selected as the basic reference core configuration for this work. which is one of the cores designed by the PARR-1 operating organization (PINSTEC). It has been studied in details to determine the essential parameters needed as, effective multiplication factors, reactivity, neutron flux, burn-up, and power density distripution, beside some safety parameters like Maximum Power Peaking Factor, Control rod worth, and shutdown margin. The configuration of the core has been shown in Figure 1. It contains 24 standard fuel elements and 5 control fuel elements. Graphite and light water has been used as reflector. As seen from the figure, in two sides only water reflector is used, on one side there is a thermal column, while on the other side there is a graphite blocks and water. Also there is two in-core irradiation positions,

at location C7 which is the central irradiation position, and at location C4 which is the side irradiation position.

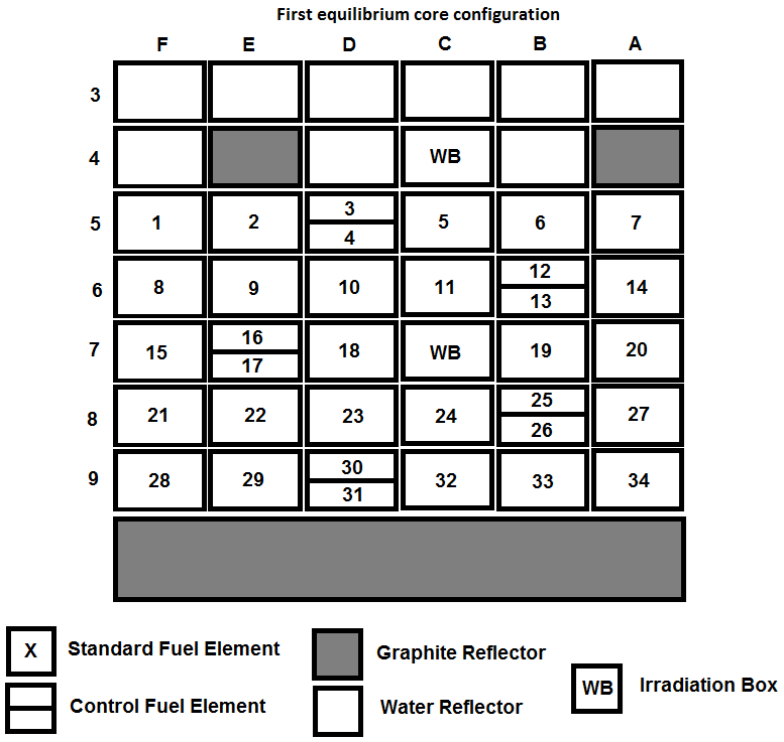

Figure 1: The First Equilibrium core configuration of PARR-1

3. Calculation Methodology and Models

The Neutronic calculation method used in this work was done in three steps summarized in a calculation line shown in figure 2, with the following items:

(a) Working Library Generation: This step was done using the evaluated nuclear data files as input. * The output is the working library, which was used as input for the next step.

(b) Cell Calculation: This step was done by WIMSD-5 code to generate homogenized macroscopic X-Sections for every component of the core. These X-Sections were used as input for the next step.

(c) Global Core Calculation: In this step the whole core calculation was done by using CITVAP code. The outputs of this step are the neutronic parameters needed, e.g. neutron flux, burn-up, power densities, etc.

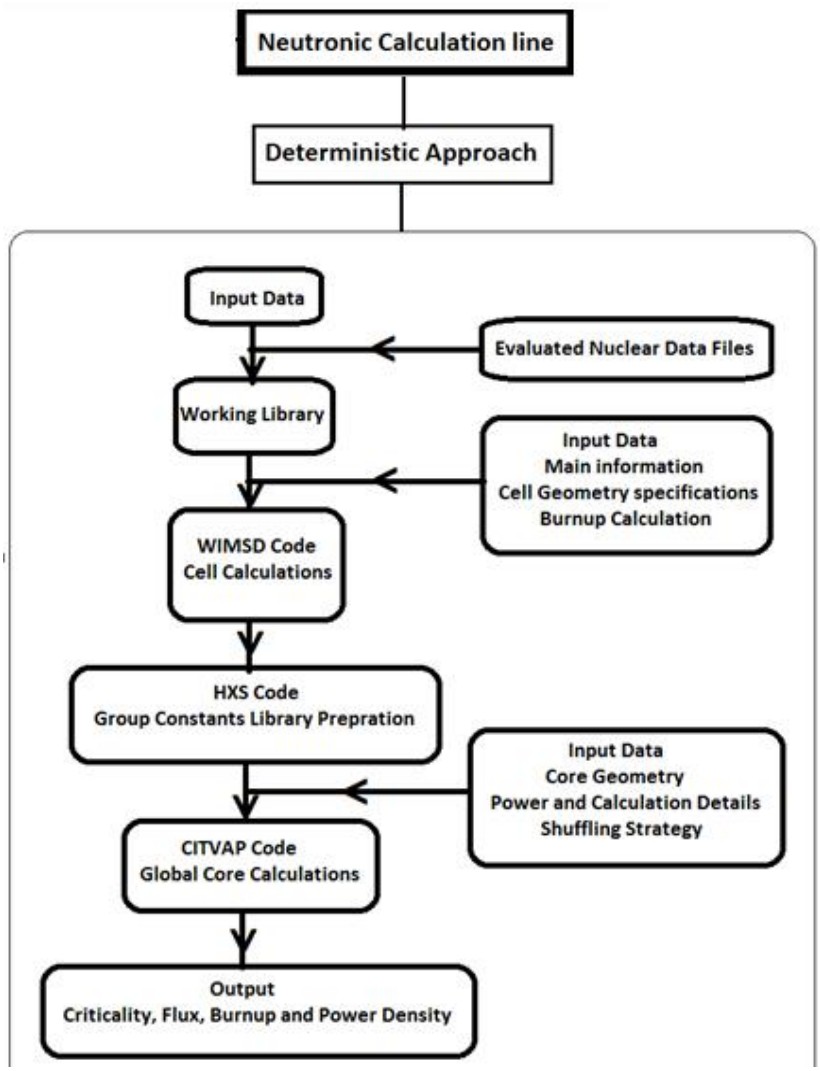

Figure2: Neutronic Calculation Line

4. The proposed Shuffling Strategies models

The proposed shuffling strategies were presented in Figure 3, 4, 5 and 6. They were used in transition from the fresh core to the succeeding burned cores. The original shuffling strategy that proposed by PARR-1 designer was shown in Figure 3a, while on Figure 3b the modified shuffling strategy was presented. The arrows indicate the path of movements from insertion as a fresh fuel element to extraction as a burned fuel element. The proposed modification was done in the two zones with brown and pink colors. The modification applied on the original strategy is just a rearrangement of movements to be more organized in order to satisfy the criteria of out-to-in method.

In figure 4 the proposed shuffling strategy that developed by using the first resorting method (direct movement) was shown. Also the proposed shuffling strategy that determined by the second resorting method (scattering shuffling) was presented in figure 5. Finally in figure 6 the proposed shuffling strategy with the third resorting method (scattering shuffling) was illustrated.

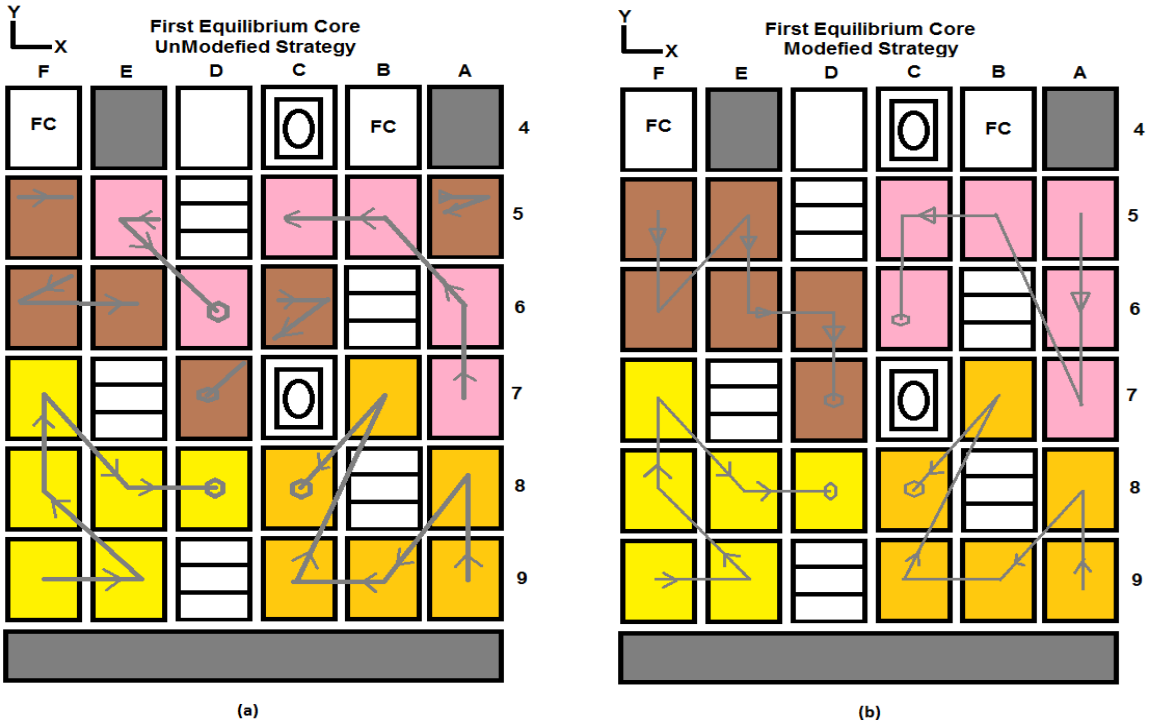

Figure 3: The Original Unmodified Strategy and Modified One

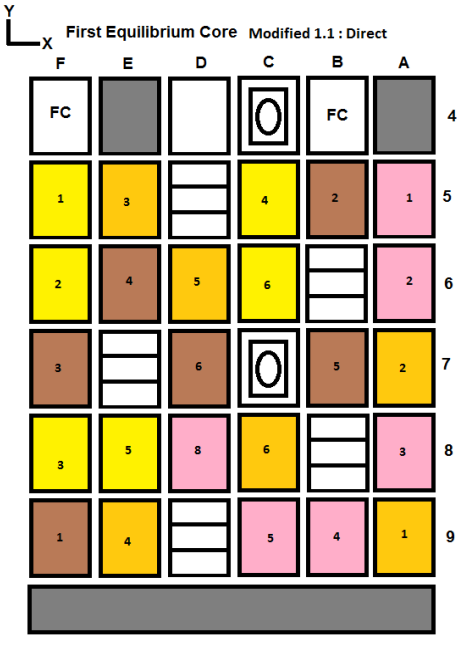

Figure 4: The Modified Strategy 1.1

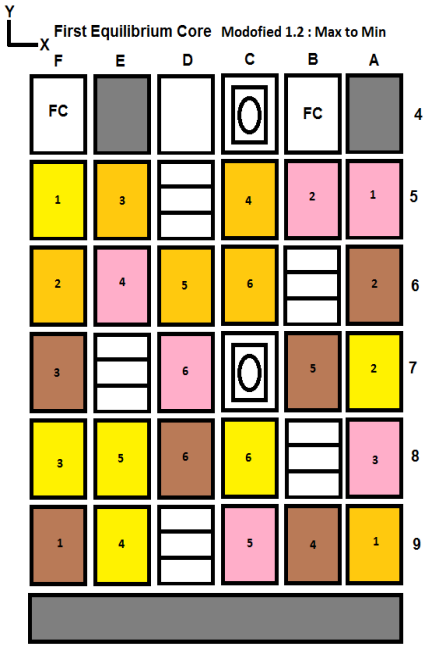

Figure 5: The Modified Strategy 1.2

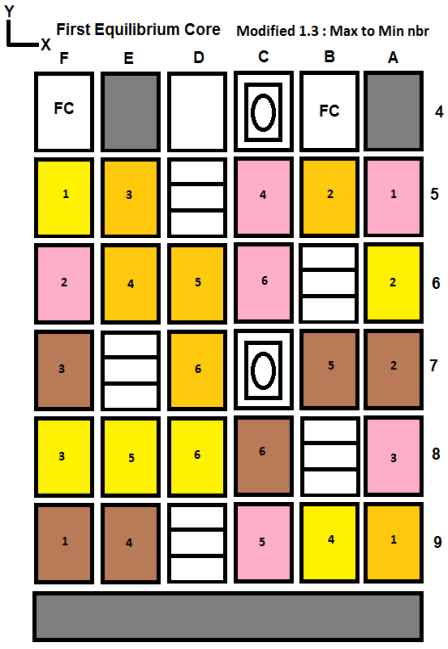

Figure 6: The Modified Strategy 1.3

5. Result and Discussion

The following paragraphs present the neutronic analysis results for the first equilibrium core that used the proposed modified shuffling strategies. First the criticality characteristics and neutron flux was shown, then the burnup distribution was illustrated, and finally the power density distribution was presented.

The results obtained were demonstrated in Figure 7. It illustrates the calculated effective multiplication factor for the first equilibrium core of PARR-1 based on the shuffling strategies that proposed. It show values at BOC and EOC for 10 full power day cycles, with cycle length of 40 days. The results reflect; by using the different proposed shuffling strategies the equilibrium cycle appear at the same cycle number 6, which is begins after 200 days and ends at 240 days. Also it show that there is no significant change in the K_{eff} value.

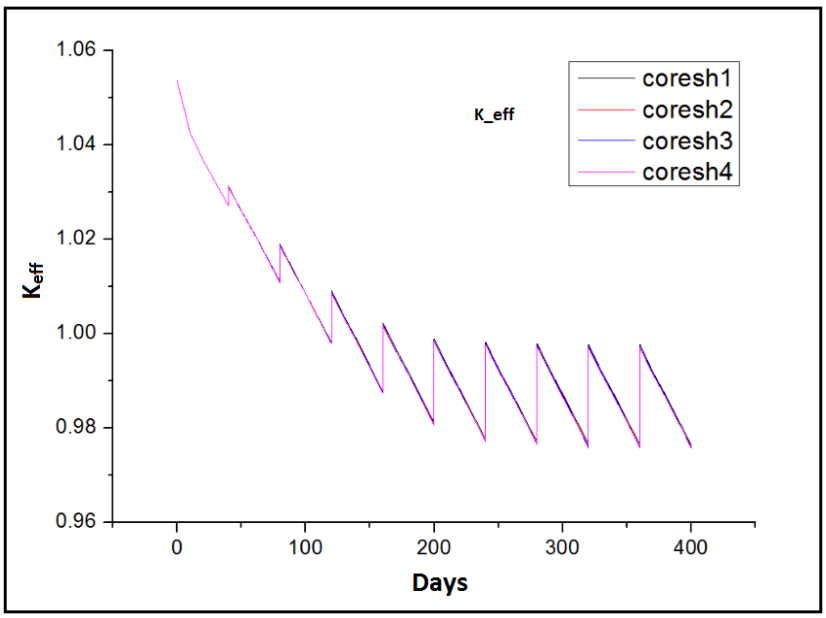

Figure 7: The Effective Multiplication Factor for 10 Cycles

The neutron flux calculated was shown in Table 1 a, b, c and d. The tables show the values for the four cores, in the two in-core irradiation positions C7 (Zone 498) and C4 (Zone-499). The values at BOC and EOC of the cycle was showed. The different columns represented the values for the five groups used in the whole core calculations. It showed that, the neutron flux in the irradiation positions will slightly change by using different shuffling strategies.

Table 1: Neutron Flux at Irradiation Positions C7 and C4

Coresh1					
BOC					
	Group1	**Group2**	**Group3**	**Group4**	**Group5**
Zone 498	5.05818E+13	5.54337E+13	5.76904E+13	1.40877E+13	1.33794E+14
Zone 499	1.34128E+13	1.43319E+13	1.61903E+13	5.20074E+12	6.55909E+13
EOC					
	Group1	Group2	Group3	Group4	Group5
Zone 498	5.14221E+13	5.63707E+13	5.87235E+13	1.44108E+13	1.37816E+14
Zone 499	1.37439E+13	1.46845E+13	1.65889E+13	5.34098E+12	6.74925E+13

(a)

Coresh2					
BOC					
	Group1	**Group2**	**Group3**	**Group4**	**Group5**
Zone 498	5.02769E+13	5.51182E+13	5.73996E+13	1.40298E+13	1.33428E+14
Zone 499	1.36058E+13	1.45319E+13	1.64100E+13	5.27205E+12	6.64985E+13
EOC					
	Group1	Group2	Group3	Group4	Group5
Zone 498	5.10771E+13	5.60157E+13	5.83995E+13	1.43478E+13	1.37441E+14
Zone 499	1.39254E+13	1.48722E+13	1.67950E+13	5.40815E+12	6.83501E+13

(b)

Coresh3					
BOC					
	Group1	Group2	Group3	Group4	Group5
Zone 498	5.03424E+13	5.51832E+13	5.74513E+13	1.40371E+13	1.33431E+14
Zone 499	1.36102E+13	1.45371E+13	1.64182E+13	5.27557E+12	6.65528E+13
EOC					
	Group1	Group2	Group3	Group4	Group5
Zone 498	5.11432E+13	5.60810E+13	5.84510E+13	1.43547E+13	1.37434E+14
Zone 499	1.39375E+13	1.48857E+13	1.68129E+13	5.41502E+12	6.84485E+13

(c)

Coresh4					
BOC					
	Group1	Group2	Group3	Group4	Group5
Zone 498	5.02838E+13	5.51241E+13	5.74016E+13	1.40286E+13	1.33397E+14
Zone 499	1.36453E+13	1.45733E+13	1.64539E+13	5.28510E+12	6.66519E+13
EOC					
	Group1	Group2	Group3	Group4	Group5
Zone 498	5.11084E+13	5.60461E+13	5.84225E+13	1.43502E+13	1.37422E+14
Zone 499	1.39665E+13	1.49155E+13	1.68409E+13	5.42160E+12	6.85066E+13

(d)

Burn-up Distribution: figure 8 represents the distribution of fuel burn-up among the core in the four cases when using the proposed shuffling strategies. It showed values for the equilibrium cycle, at BOC in figure 8a and at EOC in figure 8b. The results were presented in the unit of U235 burn-up percentage. In each box there is four values for each fuel element. The first one belongs to the core using the original shuffling strategy, the second, third and fourth for the cores using the proposed strategies. All these results were calculated under the criteria that no power change will be applied nor any change in the core design. Only the shuffling strategy are changed. Found that all the cores were consumed the same amount of fuel with a value of 2251 gram per equilibrium

cycle. The difference between the four cores were found to be in the fuel burn-up distribution. The percentage difference in burn-up between the cores with the modified shuffling and that with the original shuffling, for each fuel element was illustrated in figure 9. The black column indicates the difference for coresh2, and the red column indicates the difference for coresh3, and the blue column indicates the difference for coresh4. The change has taken the same form at BOC and EOC of the equilibrium cycle. As seen from the result, the burn-up distribution has been as flat as possible in the cores with the modified shuffling, than the core with the original shuffling strategy.

F	E	D	C	B	A	
0	19.45		14.39	9.8995	4.7206	
0	9.588		13.785	5.2676	0	5
0	9.4886		14.342	4.4235	0	
0	9.7728		13.256	5.0083	0	
8.0306	12.289	23.751	17.887		5.6806	
4.7982	14.964	19.695	24.679		4.4223	6
5.0001	13.546	19.466	25.48		5.2636	
4.4251	14.623	20.172	24.065		4.8051	
15.553		24.724		20.847	0	
9.9819		26.714		20.502	5.0181	7
9.4801		24.725		19.379	4.8128	
9.7934		26.126		20.035	5.2659	
10.982	20.251	25.969	27.137		5.0815	
9.2105	18.931	23.727	25.717		8.6572	8
9.3147	19.171	25.698	24.929		9.159	
9.0026	18.523	24.325	26.317		8.8747	
0	5.2922		14.961	9.7431	0	
0	14.472		18.059	13.085	0	9
0	13.934		19.186	14.504	0	
0	14.82		18.463	13.616	0	

(a)

F	E	D	C	B	A	
4.7471	24.11		19.721	14.568	8.1209	
4.8374	14.586		19.183	10.064	4.4505	5
4.8474	14.499		19.731	9.2414	4.4513	
4.8454	14.775		18.676	9.8183	4.4548	
12.411	18.11	29.905	25.032		9.9825	
9.3262	20.78	26.046	31.575		8.7372	6
9.5341	19.416	25.832	32.353		9.5613	
8.9693	20.458	26.513	30.993		9.1141	
20.495		32.277		27.463	5.72	
15.115		34.186		27.079	9.6298	7
14.633		32.291		25.994	9.425	
14.938		33.627		26.626	9.8692	
15.694	26.298	32.663	34.55		9.811	
13.972	25.022	30.479	33.13		13.237	8
14.073	25.253	32.364	32.367		13.718	
13.771	24.627	31.046	33.695		13.442	
5.3159	11.053		21.07	15.09	5.1096	
5.2932	19.941		23.996	18.265	5.0379	9
5.2872	19.407		25.068	19.631	5.0235	
5.2902	20.272		24.372	18.768	5.0264	

(b)

Figure 8: Burn-up Distribution for the Four Cores using *different Shuffling Strategies*

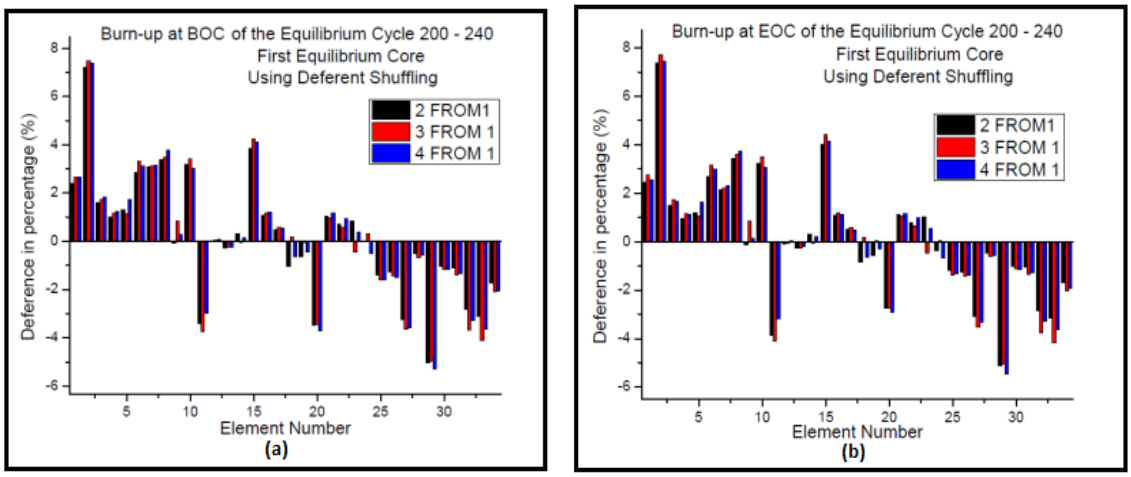

Figure 9: Difference in Burn-up between core using *the original strategy and the modified strategies.*

Power Density Distribution: The power density distribution of the equilibrium cycle for the four cores with the proposed shuffling strategies was illustrated in figure10. All cores were used the same cycle length of 40 days and the same power of 9MW. The power density distribution at BOC of the equilibrium cycle was illustrated in figure10a, while at EOC was showed in figure 10b. The maximum total power peaking factor calculated for the core with the different proposed shuffling strategies has the same value around 2.88, which mean that, using the proposed shuffling strategy will not affect the MPPF of the selected core.

F	E	D	C	B	A	
74.15654	91.2909		104.4434	91.18475	66.25771	
75.94313	97.88804		105.7897	93.79246	68.2951	
76.12411	98.11993		105.6213	94.20795	68.32235	5
76.13602	98.02419		106.2554	94.03671	68.35239	
85.5967	114.0114	120.8596	140.4822		84.02537	
88.48815	113.9188	124.7009	135.6812		84.29654	
88.59326	114.9617	124.9845	135.2341		83.98348	6
88.83556	114.3335	124.5324	136.2906		84.14565	
96.66038		148.733		129.9356	93.34118	
100.3926		147.1708		129.1134	90.09677	
100.7626		148.9939		129.8662	90.13053	7
100.6325		147.7566		129.3558	89.88809	
92.17402	118.5861	131.5509	146.0503		92.55078	
93.13375	119.4472	132.6544	146.0252		89.55882	
93.06888	119.2682	130.987	146.5073		89.17194	8
93.26648	119.7128	132.06	145.3107		89.25343	
85.4073	112.8811		119.8382	104.7093	81.32758	
84.96503	107.2097		116.4705	101.4508	79.90615	
84.84288	107.2798		115.4131	100.4157	79.63827	9
84.91546	106.8829		115.919	100.8737	79.65108	

(a)

F	E	D	C	B	A	
74.97157	91.88052		105.0418	92.6051	67.89526	
76.80242	98.66946		106.2998	95.08875	69.35565	
77.03972	98.96606		106.1607	95.53555	69.39359	5
76.8972	98.70566		106.7711	95.379	69.4567	
86.7653	114.6093	120.4482	139.4144		85.55032	
89.75363	114.4642	124.3542	134.0192		85.80643	
89.89777	115.5728	124.6748	133.716		85.49326	6
89.99596	114.7832	124.1222	134.9882		85.71729	
97.49807		146.4088		129.6119	94.21757	
101.396		145.1654		128.8742	91.62003	
101.7975		146.6467		129.6562	91.64719	7
101.5333		145.4631		129.2086	91.48025	
93.05532	118.5418	130.4277	144.1718		93.78506	
94.09411	119.4873	131.7498	143.6272		90.89176	
94.03576	119.2995	129.8387	144.2462		90.47947	8
94.15102	119.6926	131.1228	143.2008		90.65179	
85.90226	113.3042		119.8581	105.513	82.19261	
85.49899	107.4959		116.45	102.2052	80.80827	
85.37979	107.5705		115.3499	101.1278	80.52435	9
85.39874	107.1227		115.921	101.676	80.60699	

(b)

Figure 10: Power Density Distribution of the Equilibrium Cycle for the four cores

6. Conclusion

The impact of some modifications applied to the exist fuel shuffling strategy of the first equilibrium core of Pakistan Research Reactor 1 (PARR-1) was investigated, as a process of optimization to find the optimum neutron flux and fuel consumption while ensuring the satisfying of the safety limits criteria. The modifications was achieved by directly searching for the optimum fuel shuffling strategies that satisfying the criteria of “burnup and power distribution as flat as possible”, while conserving the multiplication factor and neutron flux, beside the lower consumption rate. From this study we conclude that; by using the proposed fuel shuffling strategy, there is no significant change observed on the neutron flux and the total consumption rate. While On the other hand the burnup distribution changed to be “as flat as possible” with using the proposed shuffling strategies. Also there is no significant changes observed on the Maximum Power Peaking Factor (MPPF).

Reference

Turinsky, Paul J., and Geoffrey T. Parks. 2002. “Advances in Nuclear Fuel Management for Light Water Reactors.” In *Advances in Science and Technology*, eds. Jeffery Lewins and Martina Becker. New York: Kluwer Academic Publishers.

Safarzadeh, O., a. Zolfaghari, M. Zangian, and O. Noori-kalkhoran. 2014. “Pattern Optimization of PWR Reactor Using Hybrid Parallel Artificial Bee Colony.” *Annals of Nuclear Energy* 63: 295–301. http://linkinghub.elsevier.com/retrieve/pii/S0306454913004192 (October 18, 2014).

Safarzadeh, O., a. Zolfaghari, a. Norouzi, and H. Minuchehr. 2011. “Loading Pattern Optimization of PWR Reactors Using Artificial Bee Colony.” *Annals of Nuclear Energy* 38(10): 2218–26. http://linkinghub.elsevier.com/retrieve/pii/S0306454911002192 (October 18, 2014)

Turinsky et al. 2005. “EVOLUTION OF NUCLEAR FUEL MANAGEMENT AND REACTOR OPERATIONAL AID TOOLS.” *Nuclear Engineering and Technology* Volume 37(Issue 1): pp.79–90.

Zameer, Aneela, Sikander M. Mirza, and Nasir M. Mirza. 2014. "Core Loading Pattern Optimization of a Typical Two-Loop 300MWe PWR Using Simulated Annealing (SA), Novel Crossover Genetic Algorithms (GA) and Hybrid GA(SA) Schemes." *Annals of Nuclear Energy* 65: 122–31. http://linkinghub.elsevier.com/retrieve/pii/S0306454913005549 (October 18, 2014)

Turinsky, Paul J. 2010. "Core Isotopic Depletion and Fuel Management." In *Handbook of Nuclear Engineering*, ed. Dan Gabriel Cacuci.

Ali Khan, Liaquat, Nasir Ahmad, M.S Zafar, and Ayaz Ahmad. 2000. "Reactor Physics Calculations and Their Experimental Validation for Conversion and Upgrading of a Typical Swimming Pool Type Research Reactor." *Annals of Nuclear Energy* 27(10): 873–85. http://linkinghub.elsevier.com/retrieve/pii/S0306454999000973.

Ahmed, Rizwan. 2006. "A Core Conversion Study by Using Higher Density Low Enriched Uranium Fuels."

Ahmed, Siraj-Ul-Islam. 2005. "Effect of New Cross-Section Evaluations on Criticality and Neutron Energy Spectrum of A Typical Material Test Research Reactor."

Ali Khan, Liaquat, Nasir Ahmad, M.S Zafar, and Ayaz Ahmad. 2000. "Reactor Physics Calculations and Their Experimental Validation for Conversion and Upgrading of a Typical Swimming Pool Type Research Reactor." *Annals of Nuclear Energy* 27(10): 873–85. http://linkinghub.elsevier.com/retrieve/pii/S0306454999000973

Ahmad, Siraj Ul Islam, Nasir Ahmad, and Aslam. 2004. "Effect of New Cross-Section Evaluations on Criticality and Neutron Energy Spectrum of a Typical Material Test Research Reactor." *Annals of Nuclear Energy* 31: 1867–81.

Determination of NUR research reactor fuel burnup using SCALE code system

N. SELLAOUI
Nuclear Research Centre of Draria, Algeria
B.P. 43 Sebala- El Achour–Draria, Algiers, Algeria

T. ZIDI
Commissariat of Atomic Energy
02 bd Frantz Fanon Street, BP 399, 1600, Algiers, Algeria

M. BELGAID
University of Sciences and Technology, Houari Boumediene
BP 32 El Alia 16111 Bab Ezzouar, Algiers, Algeria

T. ZERGOIUG
Nuclear Research Centre of Draria, Algeria
B.P. 43 Sebala- El Achour–Draria, Algiers, Algeria

Abstract

Nuclear research reactors require some physical parameters to carry out in-core fuel management such as average burnup spent fuel elements and the distribution of power and flux in the reactor during its life. These parameters give information about the evolution of nuclear isotopes inside the reactor core as depletion of fissile materials, transmutation of fertile materials into fissile materials and accumulation of fission products.

The motivation to undertake such study for the Algerian NUR nuclear research reactor is to follow the burnup data of nuclear fuel of IV.N core configuration and therefore have knowledge about the behavior of both of the fissile elements and fission products. The TRITON code of the SCALE 6.1 package was used for the first time to model the NUR configuration to determine the combustion rate of fuel elements and control rods. The results of this study were compared to a previous study carried out with the well-known CITVAP neutronic code (derived from CITATION code) on the same NUR configuration and there is a good agreement in particular for the fuel elements burnup and power.

1. Introduction

The determination of fuel burnup over the evolution calculation is an essential step in any in-core fuel management strategy to improve the economic, safety and performance aspect of nuclear research reactor. That gives an information about how long the reactor life is, which assemblage must be extracted and if the fuel element must be transported to other site what the amount of u235 contained there to get adequate precaution for safety and so on.

The evolution calculation concerns the prediction of the long-term changes in the isotopic composition of the core, average burnup spent fuel elements and the distribution of power and

flux in the reactor during its life. The fission process reduces fissile element and causes the emergence of new isotopes (fission products).

Several works [1, 2, 3] have dealt with the evolution calculation for NUR research reactor. All of them were used the two deterministic code: WIMS-D4 (Winfrith Improved Multigroup Scheme version-D4) [4] and CITVAP (derived from CITATION code) [5] to study the fuel burnup and radioactive inventory of the main isotopes in the core.

The procedure consisted of doing local calculation with WIMS-D4 at the cell level and a global calculation with CITVAP code at the core level to solve transport equation then diffusion equation in order to obtain physical parameters such as the burnup, power and flux.

Present work differing to other, probabilistic (Monte Carlo) procedure was chosen to calculate and follow the fuel element burnup of IV. N core configuration and therefore know the behavior of both of the fissile element and fission product. This configuration was modeled for the first time using the TRITON code [6] (a multipurpose SCALE control module for transport, depletion, and sensitivity and uncertainty analysis) of the SCALE 6.1 package [6] via T5-DEPL depletion sequence to determine the combustion rate of fuel elements and control rods. This study were compared to previous study carried out -on the same configuration- with the well-known neutronic code; CITVAP and there is a good agreement.

2. CODE AND METHODE

The TRITON [6] computer code is a SCALE module for transport, depletion, and sensitivity and uncertainty analysis. TRITON like other code systems for Monte Carlo burnup calculation have three general distinct parts : The neutronics solver, which makes the cross-section processing followed by multigroup transport calculations for one-, two-, and three dimensional (XSDRNPM[6] module for 1D, NEWT[6] module for 2D, and KENOV.a /KENOVI module[6] for 3D) configurations; a depletion solver, the ORIGEN [6] depletion module which calculates material changes over the time; and a coupling scheme, which combines sequential neutronics and depletion solutions to do a burnup calculation.

In this work, KENOV.a (Monte Carlo criticality transport code) [6] were used to do transport calculation; KENO V.a solves the k-effective (keff) eigenvalue problem in three dimensions using the Monte Carlo method.

The TRITON depletion sequences -in this work T5-DEPL sequence- build upon the transport sequences by automating depletion/decay calculations after the transport calculations for each material designated for depletion [6]. The depletion performed by ORIGEN (Oak Ridge Isotope Generation code) that applies a matrix exponential expansion model to calculate time-dependent concentrations. Each designated material is depleted using region-averaged reaction rates, accounting for all regions in the model associated with a given depletion material [6].

The figure 1 shows the global TRITON flowchart calculation [6]; the various computational processes—cross-section processing, transport, and depletion—over a series of depletion and decay intervals.

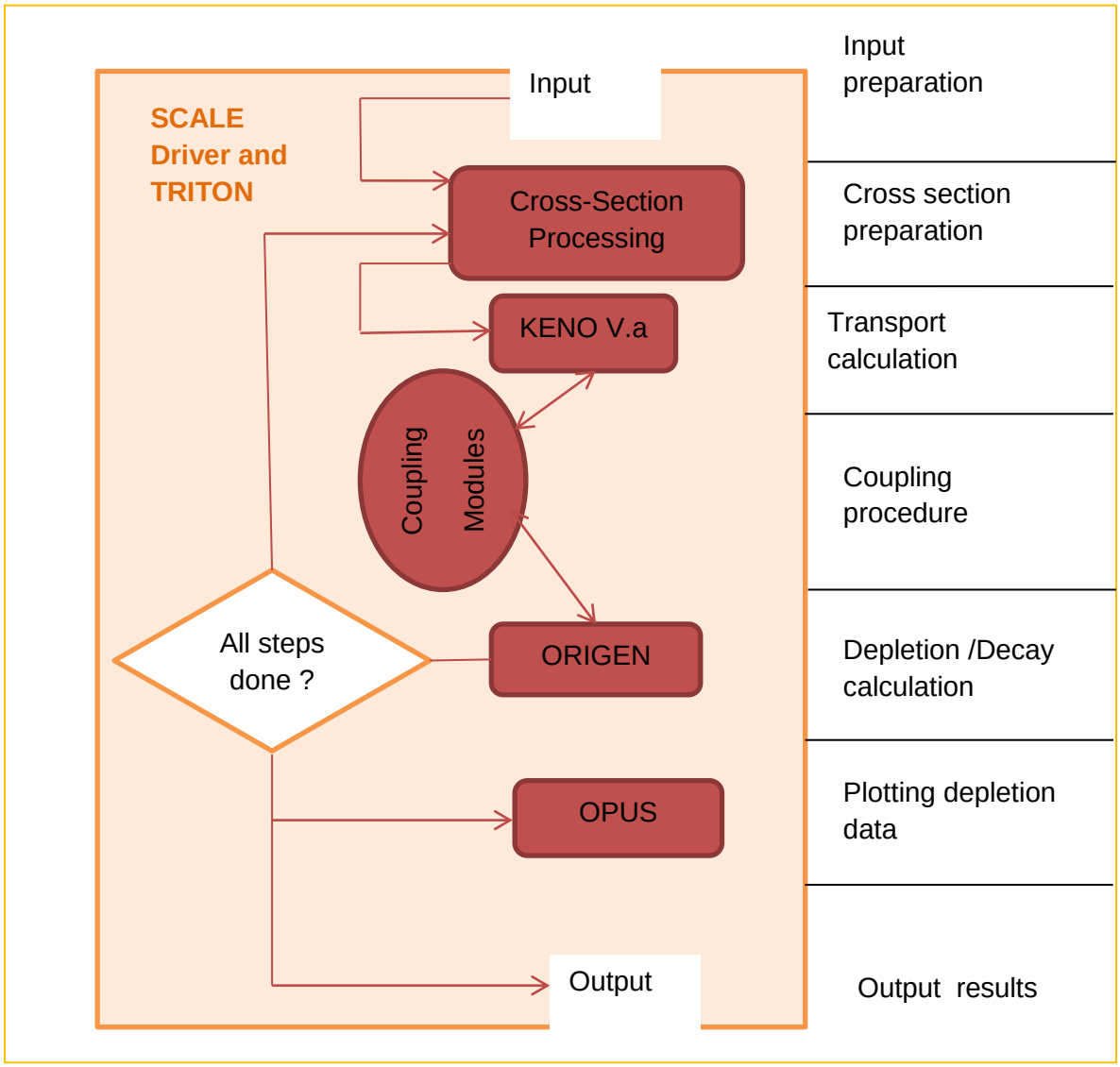

Fig 1. TRITON flow chart calculation (T5-DEPL sequence)

3. NUR reactor description and modeling

NUR is an Algerian nuclear research reactor. It was built by Argentina INVAP. It was put into operation in 1989.The reactor is installed at the Draria Nuclear Research Center (CRND). It is a pool type reactor, with great experimental flexibility that reaches a nominal power of 1 MW. The core consists of approximately 19.7% enriched MTR plate fuel elements, each plate contains U3O8-Al as fuel and aluminum as cladding cooled and moderated with light water. The reactivity control system of the reactor is made of five Ag–In–Cd absorbing rods: (C1, C2, C3, and C4) and one fine regulating rod (F) [1, 2, 3].

IV-N configuration of the core of NUR reactor with standard and control fuel elements, the graphic reflector; the water around and all other elements mentioned in Fig. 2 was modeled by KENO V.a in 238 energy groups using ENDF/B-VII.0 cross-section data and the model is validated in previous work [7].

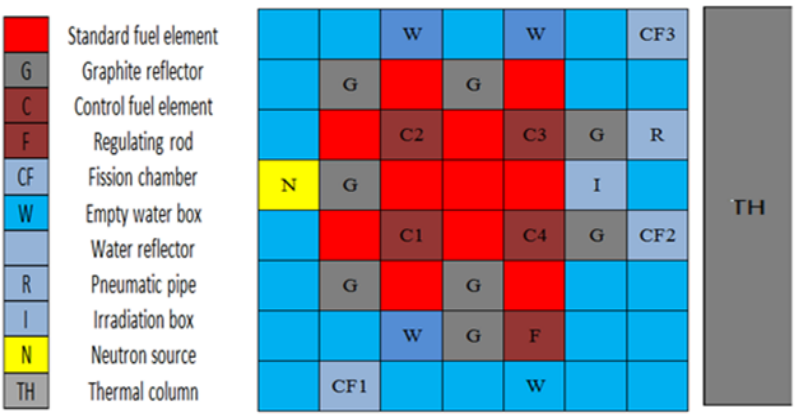

Fig2. Core configuration IV-N of the NUR

The TRITON code of the SCALE package [6] has been applied to the IV-N configuration of the NUR reactor core using T5-DEPL depletion sequence. Via this sequence -like mentioned in the section before- the code uses alternatively the transport code KENOV.a and the evolution code ORIGEN. The IV-N configuration was modeled using the following conditions: the maximum power; 1megawatt;all fuel elements were fresh in the beginning of the cycle, and control rod withdrawn.

IV-N configuration of the core of NUR reactor -studied in present work- contains eleven standard fuel element and five control fuel element. The following figure (fig 3) shows fuel elements and control bars numbered according to their layout in the IV.N configuration. Theses element are numerated from one to sixteen to make result presentation easy (fair green for standard fuel elements and dark green for control fuel elements).

	5		10
2	13	7	14
	4	11	9
1	12	6	15
	3		8
			16

Fig 3. The arrangement of fuel elements and control fuel elements

4. Result

TRITON code via T5-DEPL depletion sequence was executed for the IV-N configuration of the NUR reactor core. The process was generated for one Million neutron population; the burnup rate is calculated for 45.53 day given in megawatt day per ton of uranium (MW.d/Tu) for all fuel element and control fuel element.

Those results were compared to a previous study [2, 3] carried out with the CITVAP neutronic code (derived by CITATION code) calculated in the same conditions on the same configuration.

The figure 4 present the combustion rates (burnup) calculated by TRITON and CITVAP for fuel elements and control rods according to their position number.

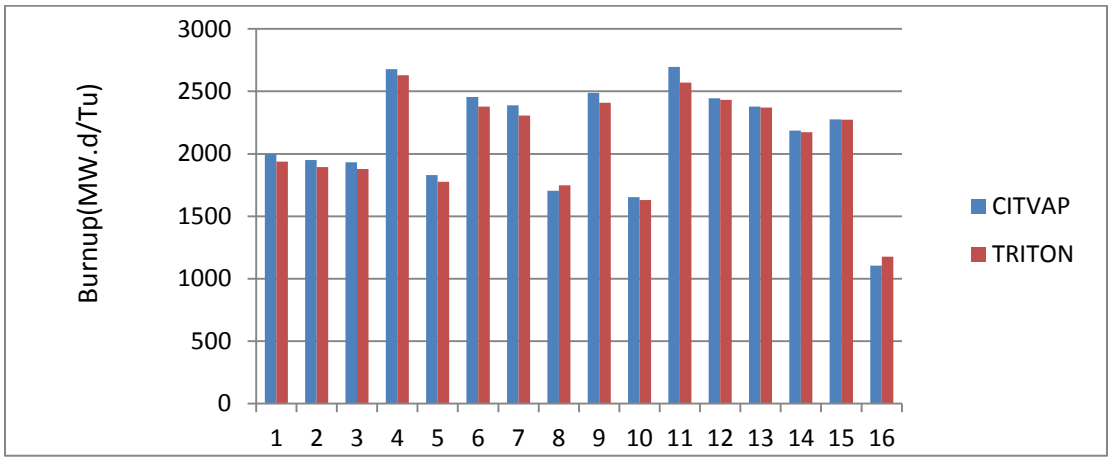

Fig 4. The combustion rates for fuel and control elements (MW.d/Tu).

A simple inspecting of fuel elements burn up values shows that the high value of burnup is for center elements with fuel elements number: 4, 6, 7, 9, 11 and control fuel elements number 12, 13, 14, 15 by the burnup band of 2270-2700 MW.d/Tu. The relative error of the burnup values between the two codes is calculated by doing a percentage of the difference between the two burnup linked to the two codes and dividing by one of them. The result is presented on the table Tab1 below.

Tab 1: The relative error of burnup calculation

N° of element	1	2	3	4	5	6	7	8	9	10	11	12	13	14	15	16
Relative Error (%)	3	3	3	2	3	3	3	3	3	1	5	1	0	1	0	6

The relative error of the two burnup values for fuel elements and control fuel elements has the maximum of 6% witch shows that the two results are close even the two models and the two method of resolving transport and evolution equations are different.

Power and total flux are also calculated using the same model, the figures: 5 and 6 present the power in kwatts and the total flux in n/ (cm².s).The power quantity was obtained through integration of the power density over the volume of the element (fuel or control elements).

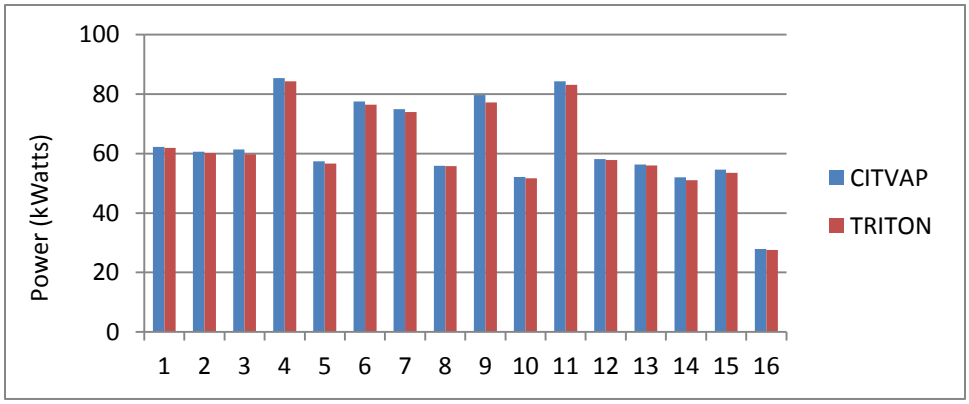

Fig 5. The power for fuel elements and control fuel element

It is completely justified that that the fuel elements characterized by the highest power are those having thehighest burnup rate as well. The soma of all fuel and control elements powers is equal to the total full reactor power (1 megawatts).The relative error of the power value for each element between the two codes is calculated and presented on the table Tab 2 below.

Tab 2: The relative error of power calculation

N° of element	1	2	3	4	5	6	7	8	9	10	11	12	13	14	15	16
Relative Error (%)	1	1	3	1	1	1	1	0	3	1	2	1	1	2	2	1

The relative error of the two burnup value for fuel elements and control fuel elements has the maximum of 1% witch shows that the two results are perfectly close.

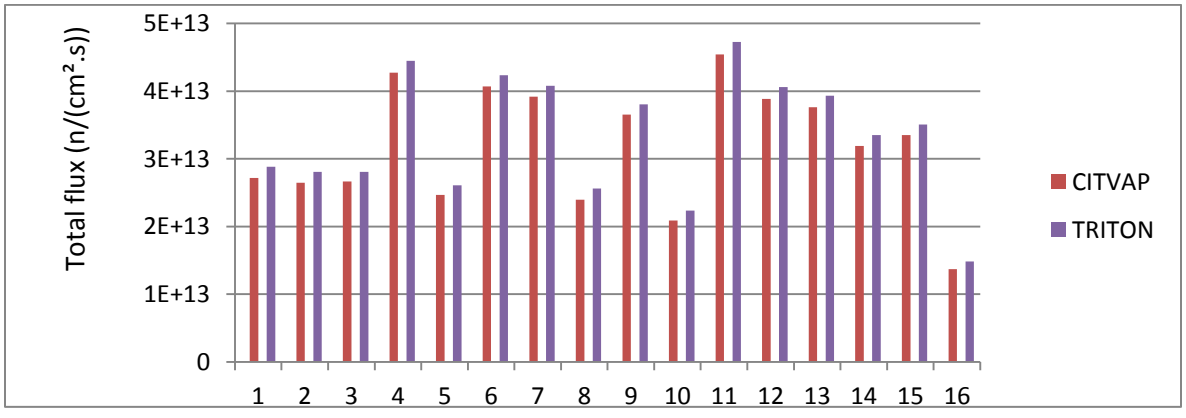

Fig 6. The total flux for fuel elements and control fuel element

The maximum total flux of fuel elements in this configuration is about 4.7 10^{13} n/cm^2.s then the minimum is about 1.5 10^{13} n/cm^2.s, the maximum relative error between value linked the two codes is about 7 %.

5. Conclusion

Burnup calculation were carried out to the IV-N configuration of the NUR reactor core using The TRITON code of the SCALE package which uses alternatively the transport solver ;Monte Carlo code KENO V.a and the evolution solver; ORIGEN code by an automatic process via T5-DEPL depletion sequence. Burnup, power and total flux were calculated for 45.53 days of functioning in full power of NUR reactor. The results were compared to previous calculation has been performed in the same condition and the same configuration using CITVAP code. There is a good agreement in particular for the fuel elements and control rods burnup and power. Also close results for total flux.

The present work opens the door for many studies attending doing burnup calculation, for global estimation or specified burnup credit using historic consumption of burnup or comparing with experimental u235 amount measurement.

Reference

[1] B. Meftah et al. “BURNUR.SYS: A 2-D code system for NUR research reactor burn up analysis”, Annals of Nuclear Energy 35 (2008) 591–600.

[2] F. Zeggar, et al. “Fuel depletion calculation MTR-LEU NUR reactor” Nuclear Technology & Radiation Protection –1/2008BIBLID: 1451-3994, 23 (2008), 1, pp. 11-18.

[3] S. Mazidi. " Systeme Expert De Suivi En Temps Reel Des Parametres Neutroniques Et Thrmohydrauliques Dans Un Reacteur De Recherche”, thesis of master in nuclear sciences, USTHB university, Alegria 2009.

[4] Askew, et al., 1967. A general Description of the Lattice Code WIMS.UKAEA.

[5] Villarino, E.A., Lecot, C.ACITVAP V3.1. A Reactor Calculation Code.NuclearEngineering Division, INVAP SE, San Carlos de Bariloche, Argentina.1995.

[6] Scale: “A Comprehensive Modeling and Simulation Suite for Nuclear Safety Analysis and Design”, ORNL/TM-2005/39, Version 6.1, Oak Ridge National Laboratory, Oak Ridge, Tennessee, June 2011. Available from Radiation Safety Information Computational Center at Oak Ridge National Laboratory as CCC-785.

[7] N. SELLAOUI, et al. "Utilisation du système de code SCALE pour la modélisation du coeur d’un réacteur nucléaire de recherche”, 11th National Congress of Physics and its Applications (CNPA'2014). University of Blida, Algeria 21 - 23 December 2014.

Irradiation Testing at HANARO after Reoperation due to Safety Reinforcement Project

K.N. CHOO, M.S. CHO, S.W. YANG, Y.T. Shin, S.J. Park, M.S. Kim
Korea Atomic Energy Research Institute 111 Daedeok-daero, Yuseong-gu, Daejeon 34057, Korea

ABSTRACT

The High Flux Advanced Neutron Application Reactor (HANARO) has been operating as a platform for basic nuclear research in Korea. Various irradiation facilities have been actively utilized for irradiation tests requested by numerous users to support national research and development programs on nuclear reactors and nuclear fuel cycle technology. HANARO was temporarily shut down during the last four years for safety reinforcement, which was completed on April, 2017. During the reactor stop, a number of user requests for neutron irradiation testing have been accumulated at HANARO. Although several preferential irradiation tests have been performed under normal HANARO operation from May of last year, the irradiation test holes (CT, OR) in the reactor were already scheduled for more than 3 years. To scope out the increasing necessity and sophisticated requirements of users from domestic and foreign countries for neutron irradiation testing at HANARO due to the recent decision of shutting down foreign research reactors, several possible methods have been considered at HANARO. The development of advanced irradiation technologies, and the provisioning of an additional test hole by removing the FTL system, have been considered as a long-term possibility.

1. Introduction

The High Flux Advanced Neutron Application Reactor (HANARO), located at the Korea Atomic Energy Research Institute (KAERI), has been operating as a platform for basic nuclear research in Korea, and the functions of its systems have been improved continuously since its first criticality in February 1995. To support the national research and development programs on nuclear reactors and nuclear fuel cycle technology in Korea, irradiation facilities have been developed and utilized for irradiation tests requested by numerous users [1-3]. Most irradiation tests have been related to national R&D relevant to present nuclear power reactors such as ageing management and evaluating the safety of the components. HANARO has recently supported national R&D projects relevant to new nuclear systems including future nuclear systems, the System-integrated Modular Advanced Reactor (SMART) and new research reactors [2,4].

After the Fukushima nuclear accident in Japan, special safety inspections by the Nuclear Safety and Security Commission (NSSC) on HANARO were conducted. A part of the reactor building did not meet the seismic performance assessment standard. HANARO has been temporarily shut down since July, 2014 for safety reinforcement construction and was completed in April, 2017. After a series of start-up tests to guarantee that every system was working safely, the reactor started its normal operation from May of last year. During the reactor stoppage, a number of user requests for neutron irradiation testing were accumulated, and a schedule for preferential testing after the reoperation of the reactor was determined at HANARO.

In this paper, the status of the HANARO irradiation testing, and an on-going effort for the active utilization of HANARO in the future, are described.

2. Irradiation Testing at HANARO

2.1 HANARO and irradiation facilities

HANARO, a 30 MW open-pool type multipurpose research reactor, has been operated as a platform for nuclear research in Korea since its first criticality in February 1995 [1]. Both the general design features and detailed information about this reactor are available on the HANARO home page (http://hanaro.kaeri.re.kr). Various neutron irradiation facilities, such as rabbit irradiation facilities, capsule irradiation facilities, loop facilities, and neutron transmutation doping (NTD) facilities, have been developed [2,3]. Figure 1 shows the HANARO complex and the reactor core of HANARO with the irradiation facilities installed in the reactor core.

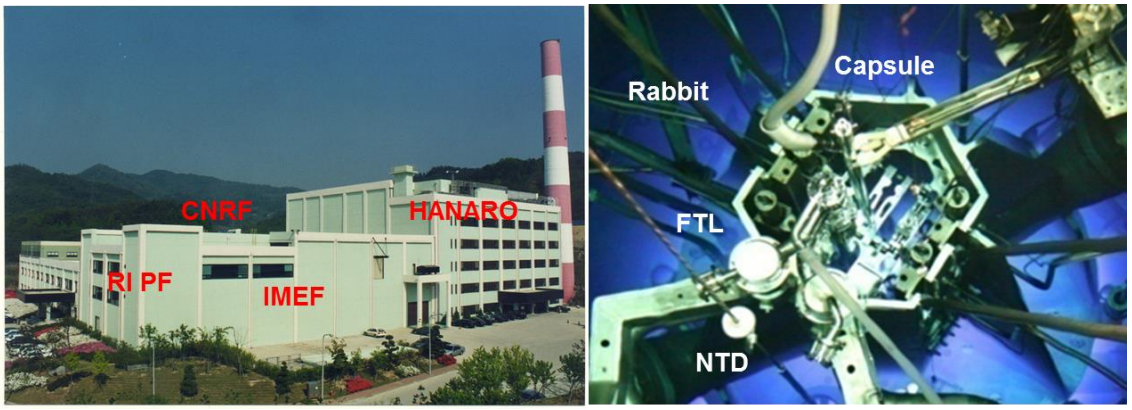

Figure 1. HANARO and reactor core with irradiation facilities

The rabbit was originally designed for isotope production, but it can also be used for the irradiation testing of fuels and materials. Figure 2 shows a typical rabbit (20 mm in diameter and 30 mm in length). It is very useful for numerous irradiation tests of small specimens at a low temperature (below 200 °C) and neutron flux conditions. The instrumented and non-instrumented capsules have been developed at HANARO for new alloy and fuel developments and the lifetime estimation of nuclear power plants (NPPs). For the development of an instrumented capsule system, capsule related systems were also developed, such as a supporting, connecting and controlling systems. HANARO has two irradiation holes for neutron transmutation doping to manufacture high-quality n-type semiconductors.

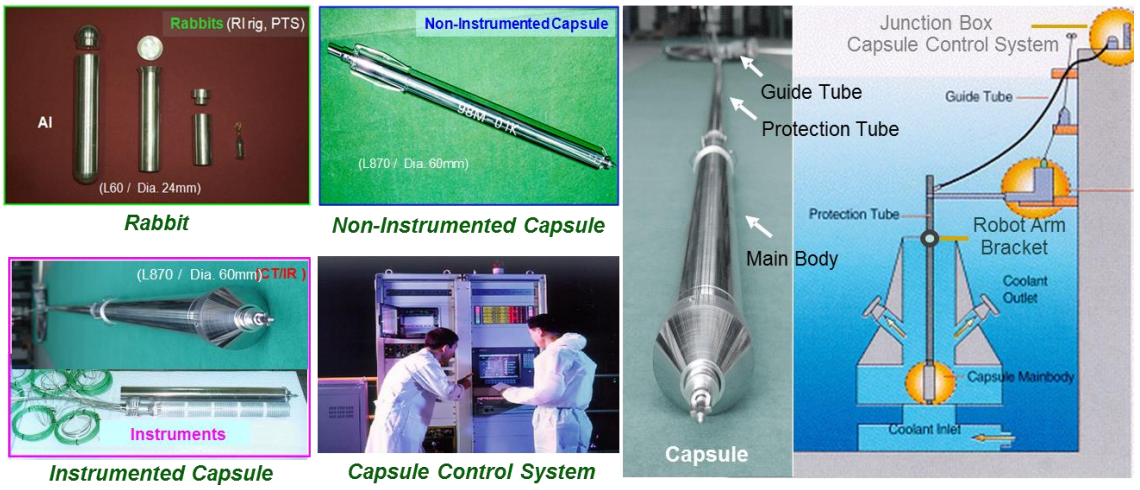

Figure 2. HANARO irradiation facilities and capsule systems

Irradiation technology at HANARO was basically developed for irradiation testing in a commercial reactor operation environment. Table 1 summarizes the current status of irradiation technology at HANARO compared with advanced technology around the world.

Fields	KAERI	Worldwide	R&D Target	Remarks
Temp. (℃)	30～700	30～1000	30～1000	Irradiation
	±10	±3	±5	Accuracy
Fluence Accuracy	-	±20%	±20%	Thermal
	±20%	±10%	±10%	Fast
Flux ($n/cm^2.sec$)	$6x10^{12}$～$1.4x10^{14}$	No limit	$1.5x10^{9}$～$1.4x10^{14}$	E>1 MeV
Cycle (n/cm^2) Fluence (n/cm^2)	8 cycles (200 days)	No limit	20 cycles (500 days)	
	$<1x10^{21}$	No limit	$<5x10^{21}$	E>1MeV

Table 1. Status of irradiation technology of HANARO

The NSCC conducted special safety inspections on HANARO after the nuclear meltdown in Fukushima, Japan. A part of the reactor building did not meet the seismic performance assessment standard of a magnitude 6.5 earthquake on the Richter scale (ground acceleration of 0.2 g). HANARO was temporarily shut down for safety reinforcement construction and which was completed by April, 2017. Reoperation of HANARO was approved after a safety assessment by the NSSC and the reactor started its normal operation from May of last year. Figure 3 shows the HANARO during and after the safety reinforcement construction.

Figure 3. HANARO during and after seismic reinforcement construction

2.2 Utilization of HANARO irradiation facilities

As a platform for nuclear research in Korea, the irradiation facilities have been actively utilized for irradiation tests requested by numerous users from research institutes, universities, and industries to support national research and development programs on

nuclear reactors and nuclear fuel cycle technology in Korea [2]. Among the irradiation facilities, the capsule is the most useful device for coping with the various test requirements at HANARO. Therefore, it has played an important role in the integrity evaluation of reactor core materials and the development of new materials through precise irradiation tests of specimens. These materials include a reactor pressure vessel, reactor core structural materials, fuel assembly parts, and high technology materials at HANARO.

Most irradiation tests were related to national R&D relevant to present nuclear power reactors such as ageing management and safety evaluation of the components. HANARO has also supported national R&D projects relevant to the System-integrated Modular Advanced Reactor (SMART) and advanced research reactors. Based on the accumulated experience as well as the sophisticated requirements of users, HANARO has recently supported national R&D projects relevant to future nuclear systems such as the Generation IV (GEN-IV) and Fusion reactor programs. Among the six GEN-IV systems, Korea has participated in the VHTR (Very-High-Temperature Reactor System) and SFR (Sodium-Cooled Fast Reactor System) R&D programs. Figure 4 shows the typical contribution of neutron irradiation at HANARO for National Nuclear R&D Programs.

Figure 4. Typical contribution of neutron irradiation at HANARO for the National Nuclear R&D Programs

Because the reactor has not been in operation for more than three years due to the safety reinforcement construction, a number of irradiation testing requests from various users have been accumulated. Because of the limited test holes in the core of HANARO (CT, IR, OR, IP), there are currently two or three users waiting for neutron irradiation testing per test hole. Based on the importance and urgency of irradiation testing, an irradiation testing schedule at HANARO was determined and performed, as shown in Figure 5. Although the IP test holes (having low neutron flux and temperature limit) are available for irradiation testing after reactor reoperation, the CT/OR test holes in the reactor core are already scheduled for over three years. The operation of the reactor was limited last year due to a formal inspection schedule and a technical problem with the CNS (Cold Neutron Scattering) system.

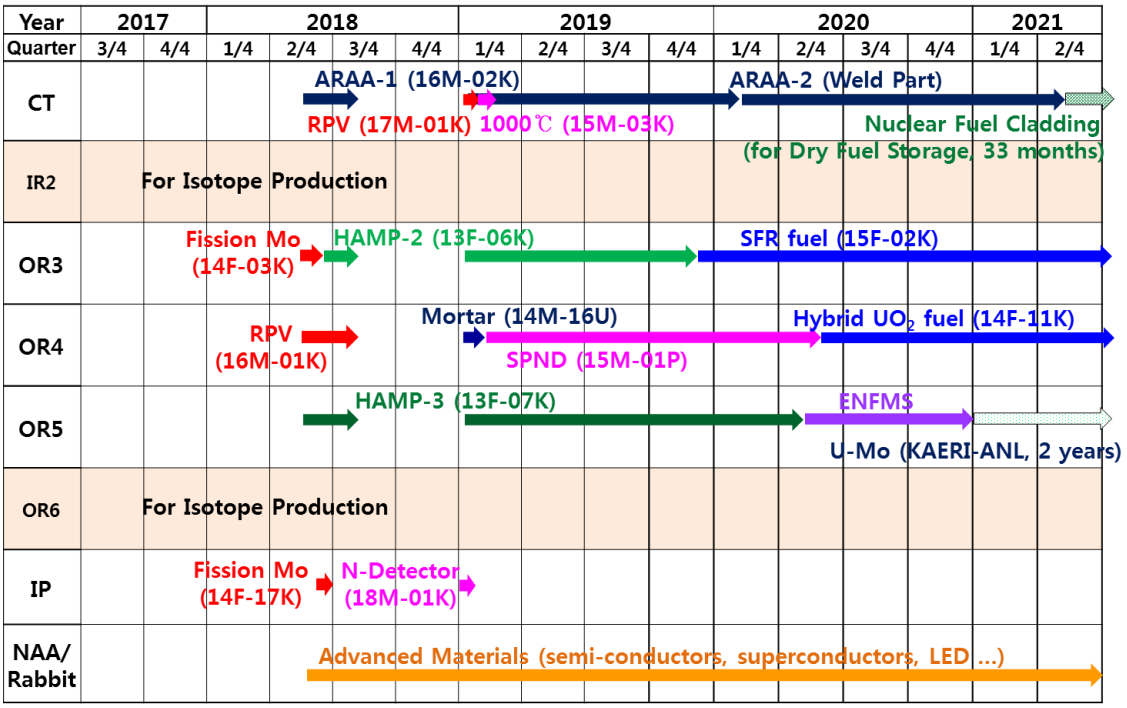

Figure 5. Irradiation testing schedule after reoperation of HANARO

3. Effort for an active utilization of HANARO

3.1 User requirement for irradiation testing

During the reactor stoppage, a number of user requests for neutron irradiation testing have accumulated, and there are increasing requests from future nuclear systems. The development of future nuclear systems such as VHTR, SFR, and Fusion reactors is one of the most important projects planned by the Korean government. The environmental conditions for these reactors are generally beyond the present reactor irradiation technology, especially regarding higher temperature and neutron fluence. Table 2 summarizes the requested irradiation testing from HANARO users up to February of this year. There is an increasing necessity and more sophisticated requirements of users from domestic and foreign countries for neutron irradiation testing at HANARO due to the recent decision to shut down outside research reactors.

	Specimen	Irradiation Temperature	Test Hole	Irradiation Cycle(dpa)	Year	User
1	Fusion Structural Mats (ARAA) (Fe-9Cr alloy)	300~350℃	CT	>8 (>5)	2018~	KAERI
2	Fusion Structural Mats ARAA Welds	320℃	CT	>8 (>5)	2019	KAERI
3	Accident-Resistant Nuclear Fuel Cladding	300℃	CT	4~6	2019	KAERI
4	Cladding Alloys for PWRs	350~400℃	CT	2~4	2019	University

5	VHTR Reactor Core Mats	300~1,000℃	CT	8~24 (5~15)	2020	KAERI
6	Long Life SPND	300℃	OR	8~24	2019	KHNP
7	U-Mo Nuclear Fuel	-	OR	8	2018~	KAERI
8	Epoxy, SiC Epoxy	~200℃	OR	8	2019	KAERI
9	Fission Mo Target	-	OR/IP	1	2018~	KAERI
10	Th-based Nuclear Fuel	-	OR	8~24	2019	KAERI
11	SiC Composite	900~1,600℃	OR	>8	2020	KAERI
12	ENFMS (Instruments)	-	IP	1	2020	USERS Co.
13	SFR Structural Mat.s (ODS)	300～500℃	CT	>8 (>5)	2019	KAERI
14	SFR Fuel	-	OR	>16	2019	KAERI
15	Low Alloy RPV Mat.s	300℃	OR	2	2018	KAERI
16	Fuel Cladding	RT	CT	33 (17)	2019	KAERI
17	Mortar	RT	OR	1	2018	University
18	U-Mo Fuel	-	OR	>16	2018~	KAERI-ANL
19	VHTR Fuel	800~1300	OR	~40	2020	KAERI-JAEA
20	Fuel Assembly (including 3-D Printing)	300℃	CT	~8(3)	2019	KAERI-NF
21	Power Rx. Control Rod/Fuel	275~310℃	CT	25	2019	KAERI
22	Research Reactor Core Mats. (Be coated)	RT	CT, IP	4/8	2018	KAERI
23	Li Oxide, Be alloy (DEMO R&D)	300~1000℃	OR/CT	<8	2020	QST(Japan)
24	LiF-ThF-Actinide Fuel in LiF/KF/NaF (MSR)	-	OR	<8	2020	SEABORG (Denmark)
25	Fusion Blanket Materials (ARAA)	-	CT	<8	2020	KIMS
26	Long-Term Fission ^{14}C Target (Ki-Jang)	RT	-	<24	2021	KAERI
27	ATF(Accident Tolerant Fuels) UN	-	-	-	2020	RITS (Sweden)
28	U_3Si_2 Plate Fuel	RT	OR		2019	KAERI-ANSTO
29	Piezoelectric sensor (Ca/Na/Nb-O)	RT	IP/OR	$10^{16}n/cm^2$	2019	KAERI
30	Advanced Materials (semi-conductors, superconductors, LED materials …)	RT	NAA/ Rabbit	<1	2018~	Universities KAERI

Table 2. Current user requirements for irradiation testing at HANARO

3.2 Development of improved irradiation technology

The development of advanced irradiation technologies, and the provisioning of an additional test hole by removing the FTL system have been considered as a long-term solution. As an effort for active utilization of HANARO, several improved irradiation technologies have been developed at HANARO. High dpa and high temperature irradiation technologies were preferentially required for R&D of future nuclear systems. New capsule technologies such as power ramping, neutron screening, and advanced instrumentation have been preliminarily evaluated and flux-boosting, re-irradiation, and re-instrumentation are planned at HANARO. The schedule of these development programs is closely connected to the national research and development program in Korea on nuclear reactors and nuclear fuel cycle technology.

The development of a high temperature irradiation technology up to 1000℃ is under development by introducing a double thermal media structure. A new capsule with a double thermal media structure such as Al-Ti, Fe-Ti, and Al-graphite was tested, and the temperature of the specimens successfully reached 700℃. Precise instrumentation and welding technologies for a higher irradiation temperature are also under development. Figure 6 shows a schematic view of the double thermal media structure capsule and the thermal media that has 4 holes to contain the specimens.

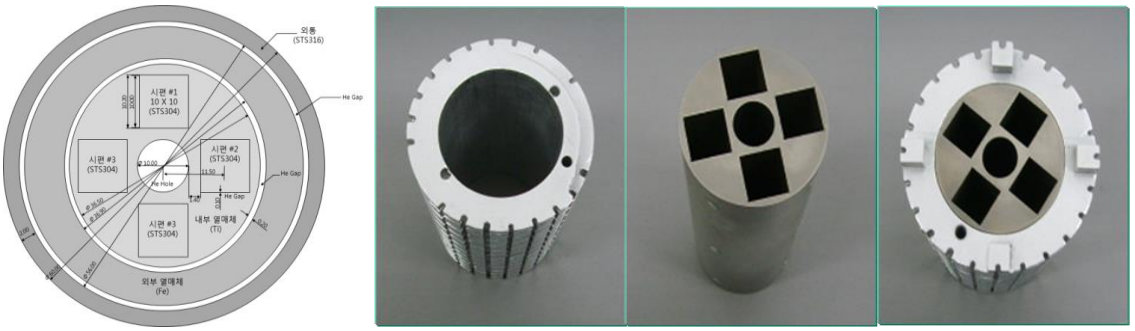

Figure 6. Schematic view of double thermal media capsule having 4 specimen holes

As future nuclear systems are demanding higher neutron fluence irradiation than present nuclear power plants [5], it is necessary to verify the integrity of the irradiation capsule for longer irradiation testing at HANARO. However, as the irradiation capsule is exposed to a very high pressure coolant flow during irradiation testing, it is suspected to be vulnerable to vibration-induced fatigue cracking. Therefore, HANARO instrumented capsules have been limited to irradiation of four reactor operation cycles equivalent to 1.5 dpa. Several design improvements of the capsules were suggested and successfully applied for irradiation at HANARO at up to eight reactor operation cycles equivalent to 3 dpa [4]. The material of the weak part of the capsule was changed from STS 304 to STS316L and the welding method was changed from TIG welding to electron beam (EB) welding to strengthen the fatigue property of the part.

Based on the stress analysis of the part during the irradiation testing, another optimized design of the rod tip of the capsule was made for 5 dpa irradiation, as shown in Figure 7 [6]. To decrease the applied stress on the rod tip, the diameter of the rod tip was increased from 8.0 mm to 9.0mm and the height of the tapered part of the rod tip was decreased from 0.5 mm to 0.2 mm. It resulted in a decrease of 22.6% of the applied stress in the same condition. To suppress the applied stress by constraining the vibration of the rod tip, the gap between the rod tip and the bottom end guide, and the gap (gap 2) between the rod tip fixture guide and the bottom end guide were

decreased from 0.05 to 0.025 mm and from 0.15 mm to 0.05 mm, respectively. The length of the rod tip was increased by 7mm to position the weld part of the rod tip above the stressing position. This will fundamentally eliminate the effect of residual stress by welding. The safety of the new capsule should be fully checked before irradiation testing. Out-pile performance and endurance testing were performed before HANARO irradiation testing. The new rod tip of the capsule was out-pile tested safely up to 450 days equivalent to 5 dpa irradiation in the reactor.

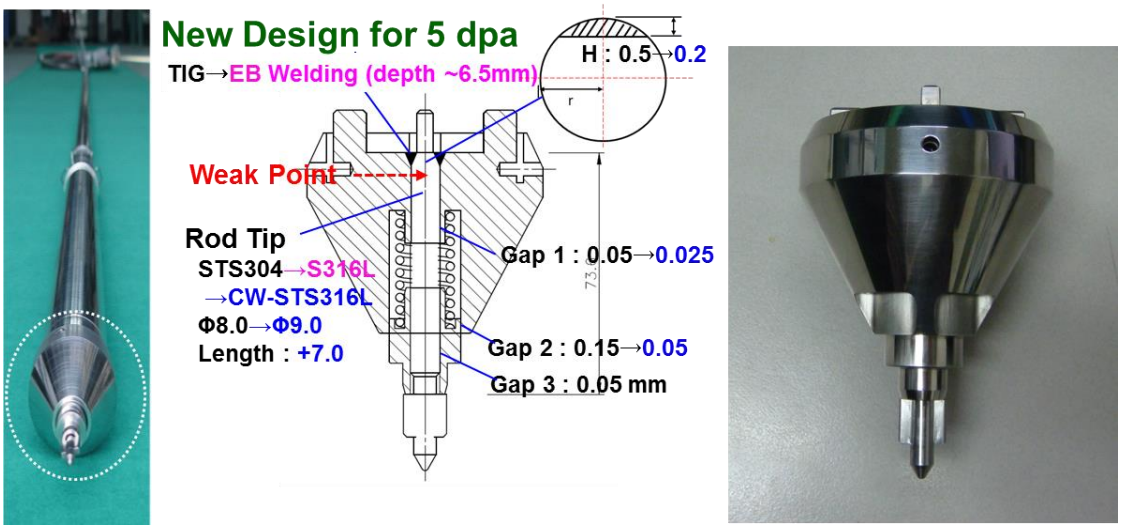

Figure 7. The optimized design of the capsule bottom part for 5 dpa irradiation

For up to 5 dpa irradiation, improvements of the capsule technology have been performed based on a design optimization of the irradiation capsule. The optimized design is under testing up to 10 dpa.
In addition, for future active utilization of HANARO irradiation facilities, new capsule technologies including a new concept capsule, flux-boosting, re-irradiation, re-instrumentation, new instrumentation, and power ramping are under plan as the next R&D project at HANARO, as shown in Figure 8. It will scope the user requirements for the National R&D on the next generation of nuclear power plants.

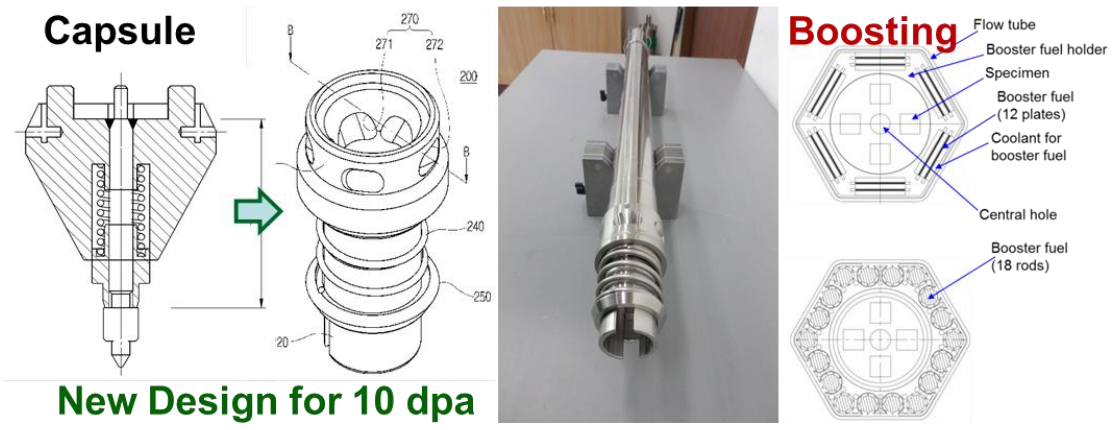

Figure 8. The design improvement of the capsule for a higher neutron fluence

4. Conclusions

HANARO was temporarily shut down during the last 4 years for a safety reinforcement, which was completed on April, 2017. During the reactor stop, a number of user requests for neutron irradiation testing have accumulated at HANARO. Although several preferential irradiation tests have been performed under normal HANARO operation from May of last year, the irradiation testing plan was already booked for more than three years. To scope out the increasing necessity and sophisticated requirements of users from domestic and foreign countries for neutron irradiation testing at HANARO, especially due to recent decisions to shut down other research reactors, several possible methods have been considered at HANARO. The development of advanced irradiation technologies, and the provisioning of an additional test hole by removing the FTL system, have been considered as a long-term plan. As an effort for an active utilization of HANARO, high dpa (up to 5 dpa) and high temperature (up to 1000 ℃) irradiation technologies have been preferentially developed at HANARO that are closely connected to the national research and development program in Korea on nuclear reactors and nuclear fuel cycle technology. New capsule technologies such as power ramping, neutron screening, and advanced instrumentation have been preliminarily evaluated and flux-boosting, re-irradiation, and re-instrumentation are being planned at HANARO.

Acknowledgements

This work was supported by the National Research Foundation of Korea (NRF) grant funded by the Korea government (MSIP) (NRF-2013M2A8A1035822).

References

1. K.N. Choo, et. al., “Material Irradiation at HANARO, Korea,” Research Reactor Application for Materials under High Neutron Fluence, IAEA-TECDOC-1659, 2011, IAEA.
2. K.N. Choo, et. al., "Contribution of HANARO Irradiation Technologies to National Nuclear R&D," *Nuclear Engineering and Technology*, **46**, 4, 501 (2014).
3. M.S. Cho, et al., “Material Irradiation by Capsules at HANARO,” *Nucl. Technol.*, **193**, 330 (2016).
4. K.N. Choo, B.G. Kim, M.S. Cho, Y.K. Kim, and J.J. Ha, "Development of a Low-Temperature Irradiation Capsule for Research Reactor Materials at HANARO," Nucl. Technol., 195, 213 (2016).
5. K. L.Murty and I. Charit, “Structural materials for Gen-IV nuclear reactors: Challenges and opportunities,” Journal of Nuclear Materials, vol. 383, no. 1-2, pp. 189-195, 2008.
6. K.N. Choo, M.S. Cho, S.Y. Yang, B.J. Jun, and M.S. Kim, "Design Optimization of HANARO Irradiation Capsule for Long-Term Irradiation Testing," Science and Technology of Nuclear Installations, Volume 2018, Article ID 3908610, (2018).

OPTIMISING ASSET MAINTENANCE STRATEGIES FOR OPAL REACTOR USING PLANT CONDITION MONITORING DATA

L.EESON[1]
1) ANSTO, New Illawarra Road, Lucas Heights, NSW, 2234, Australia

Corresponding author: lucinda.eeson@ansto.gov.au

ABSTRACT

An Asset Management Plan (AMP) demonstrates responsive management of assets, compliance with regulatory requirements, and to communicate funding needed to provide the required levels of service. The key objectives of an AMP include the documenting of services/service levels to be provided and the costs of providing the service, communicating the consequences for service levels and risk, where desired funding is not available, and provides information to assist decision makers in trading off service levels, costs and risks to provide services in a financially sustainable manner.

An aspects of the AMP is the Life Cycle Management Plan for plant and equipment which defines routine maintenance, upgrades, acquire/replacement of equipment. The focus of this paper will be on the routine maintenance component. Examples from the Australian OPAL Multipurpose Research Reactor will be presented demonstrating operating experience gained in optimising maintenance to achieve the desired level of reliability and availability.

The benefits of a condition based maintenance approach, includes managing risks associated with plant failure, and sustainable use of the assets. Data collection methods becoming more cutting edge and supported by online continuous monitoring systems, allow for more accurate maintenance forecasting, provides alerts for plant variables that feed into decision making with asset operation and maintenance. Healthier assets translates to a safer facility for reactor personnel and more cost effective life cycle of assets through better management strategies.

1. Introduction

This paper discusses the continuous improvement strategy for the OPAL Multipurpose Research Reactor. This strategy is required to meet the ANSTO business objective of operating a safe reactor with high availability and reliability greater than 98%. This is implemented through an Asset Management Plan (AMP) using the strategies of intuitive data gathering for monitoring and trending to ascertain plant health and maintenance requirements.

With the achievement of a high availability and reliability reactor strategies to further bolster this performance led by a strong drive for continuous improvement was sought. Although an AMP already existed the foundation was further strengthened by broadening and deepening the scope of the existing plan.

An AMP in essence is the responsive management of assets (and services provided from assets), compliance with regulatory requirements, and to communicate funding needed to provide the required levels of service. An aspects of the AMP is the Life Cycle Management Plan for plant and equipment that defines routine maintenance, upgrades, and the acquisition/replacement of equipment. The main focus of this paper will be on the routine maintenance component and service provided by the assets.

2. Condition-Based Maintenance Approach to Asset Management

Since 2013 OPAL has been transitioning maintenance activities from an Original Equipment Manufacturer (OEM) recommended time-based approach to an intuitive condition-based maintenance (CBM) approach. Adjusting the maintenance and operation approach on critical plant and equipment from a classical time based parts replacement and maintenance schedule to conducting periodic data collection from plant and equipment to trend and monitor specific components performance as a predictor of wear and/or impending failures of equipment that through an asset/s outage could negatively impact the reactor availability and reliability.

A condition monitoring framework for research reactors was implemented in OPAL on critical plant and equipment as part of the routine maintenance activities. This is the subject of IAEA Coordinated Research Project (CRP) T34003 due to be published in 2019, with a focus on rotating equipment. This entailed the in-house Condition Monitoring Specialist gathering data from the assets in the field using a specialised data collection unit, with the collected data uploaded into specialised software. The asset data is then stored, compared, monitored, analysed and a report on the assets health generated. This report is then distributed to the asset operators, maintainers and engineers for planned monitoring, predictive and/or preventative maintenance works.

Condition monitoring is performed on reactor plant to monitor asset health and predict failures before they occur. The following forms of condition monitoring have been used: vibration, oil analysis, thermography, process variable changes (flow, pressure, temperature etc.), chemical analysis, helium leak testing and other NDE techniques such as dye penetrant examination, magnetic particle testing and ultrasonic examination.

From the data collected, the Specialist is able to provide predictability on plant health and provide alerts in regard to early indicators of wear/faults in equipment components before wear/faults propagate and become a total failure and/or asset outage. Predictability allows for intervention actions to be conducted, such as, taking equipment offline in a planned manner, planning and conducting preventative maintenance activities and as information gathering as part of troubleshooting plant issues. These all positively contribute to minimising unplanned outages in equipment and the reactor.

As an example, during routine condition monitoring data analysis the Specialist noted a change in the vibration spectrum of a cooling water pump, with the increase in the spectrum indicative of wear and/or damage to the pump coupling. A collection of the cooling pump data acquired over time is illustrated in Figure 1. The spectrum shows an increase in the amplitude of the data signature corresponding to the coupling component showing progressive and predictable degradation of the coupling over time. The more recent data is shown in red and the yellow line indicates the alarm limits manually set in the analysis software that generates an alert if the value is above a certain level.

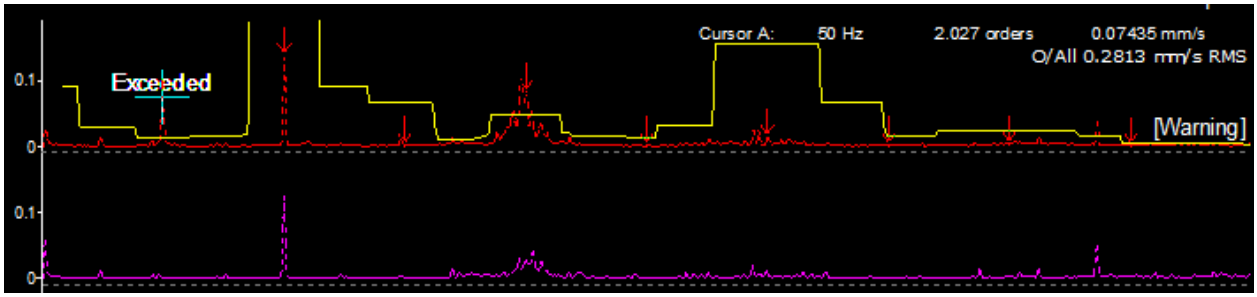

Fig 1. - Cooling Water Pump Condition Monitoring Signature

On generation of the alert, the Specialist informed the Maintenance, Operation and Engineering teams of the suspected coupling wear. Following discussions within the team the decision was

made to take the pump offline and to plan for a coupling inspection and possible replacement, if required. The pump coupling was subsequently inspected and a tear in the coupling elastomer was identified, see Figure 2 for image.

Fig 2. Cooling Pump Coupling Tear

3. Accessibility of Assets for Routine Condition Monitoring

As part of the routine maintenance it was noted that not all equipment was accessible for data gathering during equipment operation due to various factors, such as, measuring points being in the vicinity of moving parts or higher hazard or high radiation areas. OPAL has an annual radiation worker dose objective of limiting worker exposure to less than 2 mSv. It was noted that the Condition Monitoring Specialist had one of the higher annual effective doses received within OPAL. Management saw this as an ALARA opportunity and began looking into alternate methods to maintain the integrity of the data gathered during asset operation whilst also improving the safe working conditions of the Specialist. This was one of the main drivers that triggered the installation of junction boxes for the accelerometers in locations that have a lower hazard and/or radiation level and subsequently reducing the annual effective dose received by the Specialist.

Fig 3. Data Collection Manifold

3.1 Approach in Higher Hazard Areas

An example of rotating equipment with a higher hazard level that made the operating equipment inaccessible for data gathering is a set of two independent ventilation fans each housed in an air handling unit. During fan operation the air handling unit is not accessible due to hazards such as rotating machinery. As a result, the accelerometers was installed on the fan and motor and the junction box installed in an accessible location with a lower hazard level on the outside of the air handling unit wall panel, see Figure 4.

Fig 4. Manifold On Ventilation Fan Wall Panel

During normal operational plant surveillances it was noticed that one of the two fans had a reduced plant performance. As part of the fault finding investigation the Specialist was tasked with conducting a vibration analysis. The analysis found that the ventilation fan with the reduced air flowrate was running at a slightly lower speed, 38 rpm slower, than it had been running a few weeks prior, see Figure 5 for more details.

Fig 5. Ventilation Fan RPM

The more recent data in yellow indicated that the fan was running at 1290 RPM whilst the same fan was running at 1328 RPM a few weeks prior. Further investigate into the root cause of the problem was done and the fan belts we found to be slightly loose with the fan pulley also

showing signs of wear. In the interim, the belt tension was corrected until the maintenance to replace the fan pulley could be conducted. On completion of these tasks, the fan RPM and air flowrate increased.

3.2 Approach in Higher Radiation Areas

Some of the Safety Category 2 equipment located in high radiation areas within the reactor have accelerometers installed for online monitoring and are used mainly for surveillance rather than condition monitoring. The critical pumps are those that cool fissile material, namely the core and plate type uranium targets used for Mo-99 production, these have online monitoring on the flywheel with alarms limits set such that if triggered stop the pump from operating if high vibration is detected, to perform the safety function as highlighted in the OPAL safety case of 'trip pump before equipment damage'.

For a more comprehensive health check of these pumps, additional data gathering points were added to the routine condition-base maintenance schedule. This required the Specialist to enter the higher radiation area to conduct data gathering from the pump and motor. This activity was contributing to increasing the higher annual effective dose received by the Specialist. To assist in minimising this exposure the frequency of data collection was kept to a minimum.

The installed accelerometers on the flywheel were some years old and due to obsolescence were becoming harder to source parts and OPAL was experiencing reliability issues with the original supplier. A project to replace the obsolete accelerometers was initiated and an additional opportunity to implement upgrades to the data gathering system for these pumps to better reflect the current plant needs was identified. Some of the additional benefits implemented include not just the replacement of old accelerometers but the installation of accelerometers on all currently measured points including on the pump, flywheel and motor, increasing the accelerometers from four points per pump to six points, the online monitoring of the accelerometer reading with alarm limits set was maintained and expanded to include the additional points, and the location of the junction box housing the transmitters was moved to a lower radiation area as a ALARA opportunity.

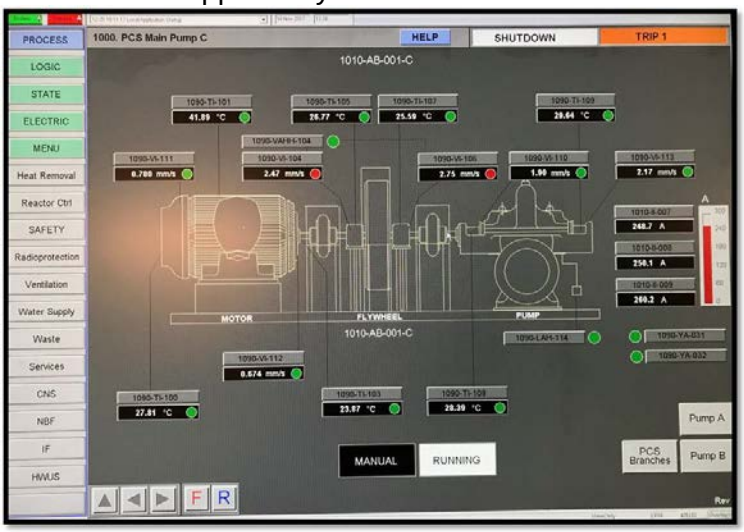

Fig 6. - Reactor Control Monitoring System Screen of Cooling Water Pump

There was some uncertainty around the new digital transmitters as the obsolete ones were analogue. OPAL has experience and knowledge around radiation effects on analogue equipment but the new supplier was unable to provide data on the effects of background radiation on the commercial grade digital transmitters. Engineering conducted their own operational exposure testing by the installation of a temporarily powered setup of the proposed equipment to expose the equipment to the same radiation conditions as the installation location. The equipment remained in this location for a reactor operating cycle (nominally 35 days) and

the equipment monitored for any effects. It was found that the equipment had experienced no adverse effects from the operational exposure and the installation on the pumps proceeded.

Fig 7. - Bank of Cooling Water Pump Transmitters

4. Conclusion

The continuous improvement strategy of the OPAL Multipurpose Research Reactor to meet its ANSTO business objective of maintaining a safe high availability and high reliability facility through the broadening of the AMP base with the implementation of CBM has had an overall positive impact on operational and maintenance activities. Condition monitoring has allowed OPAL to have more planned maintenance, less unplanned maintenance, provided improvements with preventative and predictive maintenance whilst avoiding functional failures and their consequences. Condition monitoring has a unique benefit of avoiding the consequence of functional failure while ensuring that maintenance is only undertaken when necessary i.e. a failure is imminent, this reduces cost increases availability and prevents maintenance induced failures. Knowing the health of the reactor assets has aided in minimising emergent maintenance work through breakdowns and/or complete failures that could result in an asset and/or reactor outage.

5. References

[1] INTERNATIONAL ATOMIC ENERGY AGENCY, Implementation Strategies and Tools for Condition Based Maintenance at Nuclear Power Plants, TECDOC No. 1551, 2007.
[2] ANSTO, ANSTO Asset Management Policy, AB-0116, 2018.
[3] ANSTO, ANSTO Strategic Asset Management Plan, AG-6659, 2016.
[4] ANSTO, OPAL Reactor Facility Asset Management Plan, OM 12, 2017.
[5] ANSTO, OPAL Reactor Condition Monitoring Framework, OMP 0000-001, 2018.

OPAL SPENT FUEL MANAGEMENT: STATUS IN 2019

R. FINLAY, M. HEALY, P. NAIDOO-AMEGLIO
Australian Nuclear Science and Technology Organisation (ANSTO)
New Illawarra Road, Lucas Heights, NSW 2234 - Australia

J. VALERY, L. HALLE
Orano
1 place Jean Millier, 92400, Courbevoie – France

ABSTRACT

Since the late 1950's, ANSTO has successfully operated three research reactors in Australia: HIFAR (1958-2007), MOATA (1961-1995) and OPAL (2006-present). ANSTO has demonstrated the safe and secure management of the spent fuel from those reactors. MOATA and HIFAR spent fuel was either reprocessed offshore in the UK or France and the vitrified waste returned to Australia or returned to the USA under the FRRSNFA Program.

A strategy for the management of OPAL spent fuel was developed before construction started and has evolved since then. The strategy of spent fuel disposition is now established as offshore reprocessing and management of the returned vitrified wastes.

To manage the large inventory of spent OPAL fuel generated, ANSTO has entered into a long term contract with Orano for the transportation and reprocessing of the OPAL spent fuel, with provisions included for the return of vitrified waste. The first transport of OPAL SNF to La Hague in France was performed in July 2018. Further transports are scheduled to be conducted at intervals of 6-7 years.

This paper will provide an overview of the management of spent fuel in Australia and cover the preparation that facilitated the first transport of OPAL SNF to La Hague in 2018. It will address aspects such as processing considerations, regulatory and governmental approvals, operational planning and execution.

1 Introduction

The Australian Nuclear Science and Technology Organisation (ANSTO) is the home of Australia's nuclear science expertise and landmark scientific infrastructure, including a synchrotron, accelerators, cyclotrons, the Open Pool Australian Light-water (OPAL) research reactor, and associated neutron beam instruments. ANSTO is an Australian Government agency that has been operating research reactors since the late 1950s. ANSTO is responsible for the safe, secure and sustainable management of its spent fuel.

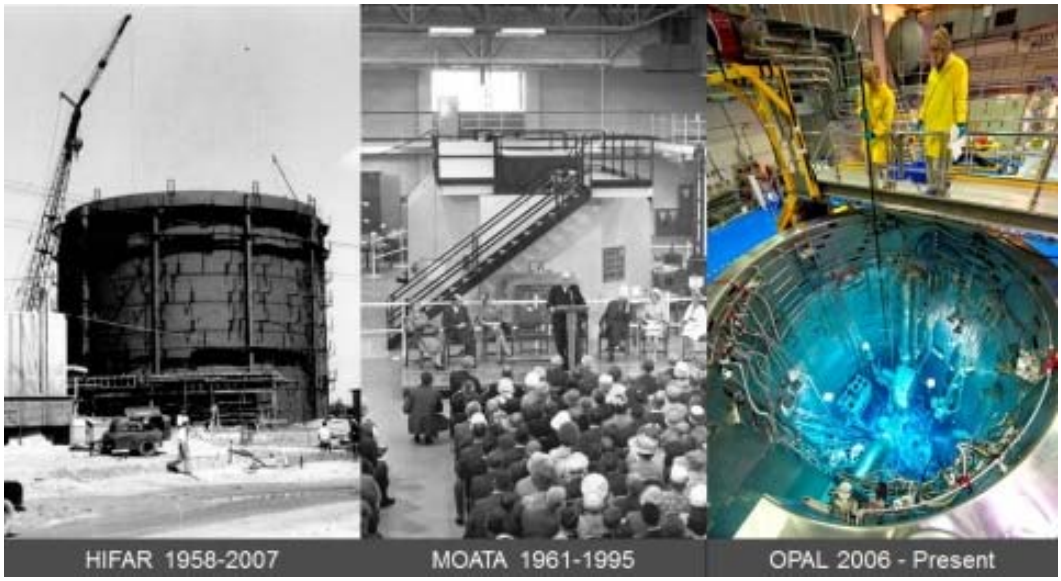

Figure 1. Australian research reactors

Research reactor spent fuel presents challenges because the aluminium cladding degrades and renders the fuel unsuitable for very long term storage or ultimate disposal. Over the past decades ANSTO has gained valuable experience in the management of research reactor spent fuel, including its storage, transportation and reprocessing.

For the HIFAR and MOATA reactors, ANSTO has previously implemented management strategies in conjunction with international service providers including France (Orano, previously AREVA NC), USA (US-DOE), and the UK (UKAEA). Details of the disposition arrangements are reported in a previous paper [1]. After assessing available options for the management of OPAL spent fuel ANSTO entered into a contract with Orano in 2016 to provide an integrated solution for the management of OPAL spent fuel. This includes packaging, transport, reprocessing and conditioning of waste suitable for disposition.

2 Previous Spent Fuel Management

2.1 Shipment Summary

Table 1 below shows all ANSTO spent fuel and intermediate level waste (ILW) return shipments, including the planned ILW return in approximately 2021. In total, 9 transports of HIFAR and MOATA spent fuel (2281 fuel assemblies) were conducted between 1963 and 2009. The experienced gained in managing HIFAR and MOATA spent fuel helped ANSTO to establish a safe, secure and sustainable management plan for OPAL spent fuel. The 10th shipment was the first transport of 236 OPAL spent fuel assemblies in 2018.

1963	UKAEA*	150 FA
1996	UKAEA*	114 FA
1998	US SRS`	240 FA
1999	ORANO^	308 FA
2001	ORANO^	360 FA
2003	ORANO^	344 FA
2004	ORANO^	276 FA
2006	US SRS`	330 FA
2009	US SRS`	159 FA
2018	ORANO^	236 FA
2015	ORANO^	ILW Return
~ 2021	UKAEA*	ILW Return

Table 1. Australian spent fuel and ILW shipments. *Dounreay, `Savannah River, ^ La Hague.

3 OPAL Spent Fuel Management Strategy

3.1 OPAL Reactor Background

The OPAL reactor is a 20 MW open pool type research reactor. It is light water cooled and moderated and has a heavy water reflector. OPAL is primarily used for the production of nuclear medicine, neutron beam science and for the production of neutron transmutation doped (NTD) silicon which is used in high power electronics.

OPAL fuel assemblies are 1045 mm long and 80.5 mm square in cross section. OPAL uses low enriched uranium silicide (U_3Si_2) dispersed in aluminium. The cladding is aluminium 6061. The fuel was initially manufactured by INVAP (Argentina), but since the resolution of a fuel fault in 2008 it has been manufactured by CERCA (France). CERCA is now an operating division within Framatome. ANSTO discharges 27-30 spent fuel assemblies per year.

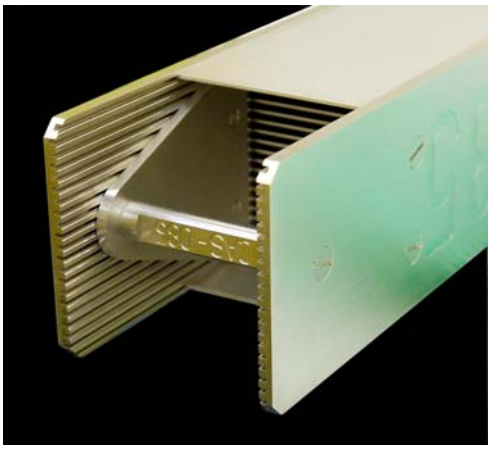

Figure 2. OPAL fuel assembly

3.2 US-DOE Spent Fuel Management Option

In the first years of OPAL operation, ANSTO investigated various options for the management of OPAL spent fuel. In accordance with operating licenses the indefinite storage of spent fuel in Australia is not acceptable.

ANSTO initially intended to ship OPAL spent fuel to the US under the US-DOE FRRSNFA program. The completion of the FRRSNFA program meant that this option would only cover spent fuel removed from the reactor core before May 2016 and ANSTO would have to develop a second disposition route for all spent fuel removed from the reactor core subsequently. Although the return of OPAL spent fuel to the US excluded waste return to Australia and was thus attractive, the completion of the FRRSNFA program meant that it would only be an interim solution.

3.3 France- Orano Spent Fuel Management Option

Due to the complexities and inefficiencies associated with having to plan for two disposition routes, ANSTO looked for an alternative solution and initiated discussions with Orano. The reprocessing of uranium silicide fuels has previously presented technical challenges because high concentrations of silicon are not compatible with the PUREX process. A dedicated R&D program conducted by the CEA and qualification programs conducted by Orano have overcome these challenges as shown in Figure 3 and reported by Valery et al [2].

After uranium silicide spent fuel is dissolved in nitric acid, and before the solvent extraction process starts, the solid silicon and fines are separated from the aqueous solution by centrifugation. The silicon and fines are set aside and later incorporated into the final vitrified ILW waste-form.

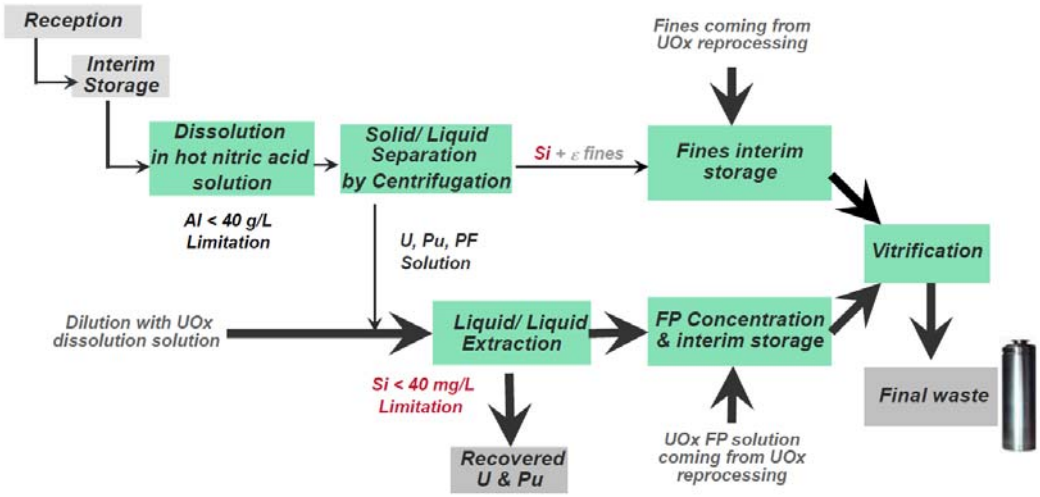

Figure 3. Process schematic for reprocessing of OPAL spent fuel at Orano La Hague

In addition to reprocessing, Orano offered ANSTO transportation services covering the transportation of spent fuel to France using the TN®MTR cask. The Orano solution was attractive because it offered a simple, integrated solution for the life of OPAL. It also offered cost savings and one less spent fuel shipment when compared to a solution incorporating shipments to the US under the FRRSNFA program.

The Orano solution was also beneficial because ILW would be returned as a vitrified waste-form, which is highly stable, compact and readily stored over long periods of time. Furthermore, the return of ILW waste related to past HIFAR spent fuel reprocessing in La Hague was successfully performed in 2015 and the residues are currently stored at ANSTO. Such proven route and tools can be then reused in the future.

Orano guaranteed the long-term availability of its transportation services and La Hague facilities. After careful consideration ANSTO accepted the Orano offer and a contract was executed mid-2016.

The first OPAL spent fuel shipment to France was completed in July 2018. Shipments will occur every 6-7 years thereafter. The first return of ILW resulting from the reprocessing of OPAL spent fuel is scheduled to occur between 2035 and 2040. In total, it is expected there will be 2 returns of ILW for the design life of OPAL.

3.4 Authorisation for U_3Si_2 Reprocessing

A submission made on the basis of the development reported above resulted in the French Safety Authority (ASN) approving the reprocessing of uranium silicide fuel from SILOE and OSIRIS stored at the Orano La Hague plant in May 2017 [3]. A subsequent submission was made to the ASN providing the detailed information on the OPAL fuel design and spent fuel characteristics including the presence of cadmium wires as a burnable poison. After detailed review the ASN approved the addition of OPAL spent fuel to the list of approved silicide fuels for reprocessing at La Hague in February 2018 [4].

4 International Agreements

4.1 Inter-Governmental Agreement

According to a European Directive and French Law, the introduction of spent fuel to France has to be framed by an Inter-Governmental Agreement (IGA) between the French and Australian Governments. The IGA was signed in November 2017 and entered into force after it was ratified in the Australian Parliament in June 2018. Work on the IGA commenced in 2015 and required approximately 3 years to complete. It was the longest single task in the preparation of the transport.

It outlines a schedule for the receipt and reprocessing of OPAL spent fuel in France and shipment of the conditioned waste to Australia resulting from reprocessing. It also defines the management and use of the separated uranium and plutonium resulting from reprocessing. Article L542-1 of the French Environment Code provides that; “Spent fuels may be brought into the national territory only for the purposes of reprocessing, research or transfer between foreign States”. Article L542-2 states “The storage in France of imported radioactive waste and of radioactive waste resulting from the processing of imported spent fuel and radioactive waste is prohibited”.

4.2 Uranium and Plutonium Transfer of Title

The reprocessing of OPAL spent fuel by Orano is subject to the conditions of a transfer of title agreement signed between ANSTO and Orano. At the completion of dissolution the title of the plutonium and uranium in the spent fuel will pass from ANSTO to Orano,

with the concurrence of the Euratom Supply Agency. The safeguards provisions in the agreement stipulate that the uranium and plutonium can only be used for peaceful purposes. The uranium and plutonium extracted from OPAL spent fuel will be used by Orano to fabricate mixed oxide (MOX) and enriched reprocessed uranium (ERU) fuel, which will be used in the civil nuclear power program.

4.3 TN®MTR Procurement

OPAL spent fuel was transported to Orano, La Hague using Orano TN®MTR type spent fuel transportation casks. A TN®MTR cask can hold up to 68 OPAL spent fuel assemblies. The casks meet the requirements of the IAEA Regulations for the Safe Transport of Radioactive Material. The Australian Radiation Protection and Nuclear Safety Agency (ARPANSA) has also validated the use of the TN®MTR in Australia.

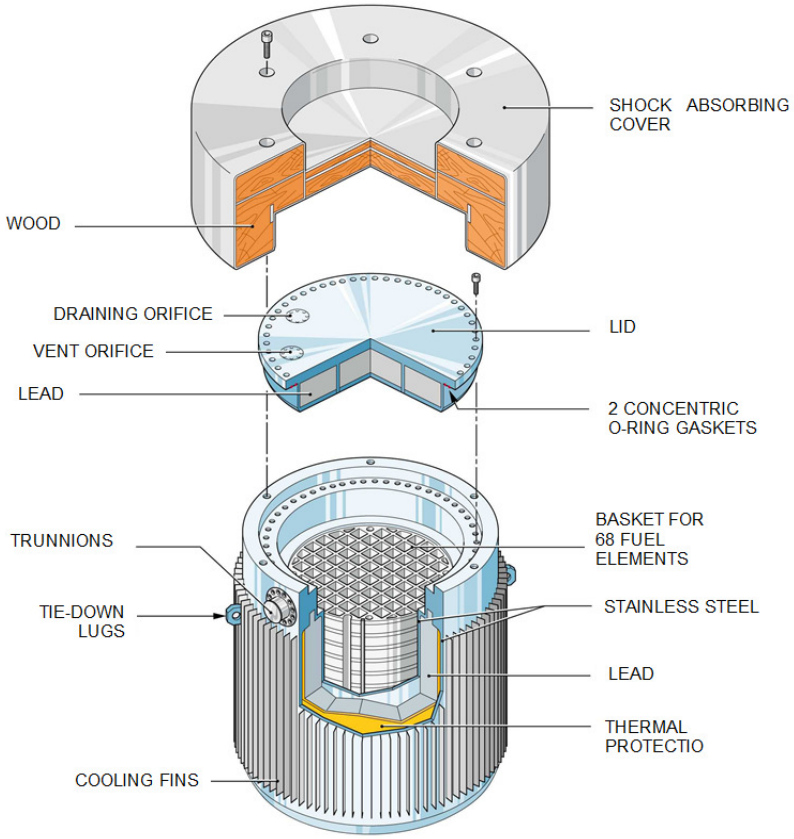

Figure 4. Orano TN®MTR spent fuel transportation cask

The first OPAL spent fuel shipment to La Hague utilised four TN®MTR casks. Three of the casks were provided by Orano and the fourth is owned by ANSTO having purchased it from Orano. ANSTO decided to purchase its own TN®MTR for risk mitigation purposes and to facilitate the transport of larger quantities of spent fuel if desired. The continued operation of OPAL is vital for the production and supply of nuclear medicine. Great importance is also placed on high reactor availability for neutron beam science and the production of NTD silicon. In the event that a spent fuel shipment is delayed the TN®MTR could be used for interim storage thus effectively increasing the capacity of spent fuel storage permitting the continued operation of OPAL, subject to regulatory approval. The fabrication of ANSTO's TN-MTR was completed in 2017. Between the first transport in 2018 and the second transport proposed for ~ 2025 the TN®MTR will be stored. It is available to support transport

projects of other RR operators, including the assistance of Orano TN for associated operations services.

5 Operations at ANSTO

The campaign to load 236 spent fuel assemblies into four TN-MTR transportation casks commenced at the beginning of April 2018 and was completed by mid-July 2018. Two “spent fuel operations teams” were formed, each including an OPAL Shift Manager, four operators, with a mixture of practical skills to cover all loading operations, and a health physics surveyor. The teams were well supported by an Orano specialist.

Prior to the campaign the two teams participated in theoretical and practical training sessions. This included the movement of a cask into and out of the reactor hall, the loading process including submersion in the service pool, and loading with dummy fuel assemblies. Some team members witnessed loading campaigns at OSIRIS and HFR. The early formation and training of the teams proved valuable because it allowed team members to be involved in the refinement of the cask loading instructions, and the design of new equipment and tooling required for the work.

The loading of each cask involved the following key steps:

- Cask transfer into reactor building within shipping container
- Cask lift from shipping container and into the reactor hall (containment)
- Cask set down adjacent to the service pool and preparation for submersion
- Cask submersion and placement on support platform at the bottom of the pool
- Underwater transfer of spent fuel assemblies from fuel storage rack into cask
- Lowering of shielded lid onto cask
- Cask lift from the pool and poolside preparation for transportation (draining, drying, decontamination and leak testing)
- Cask transfer out of reactor hall (containment) and back into shipping container for transport to France.

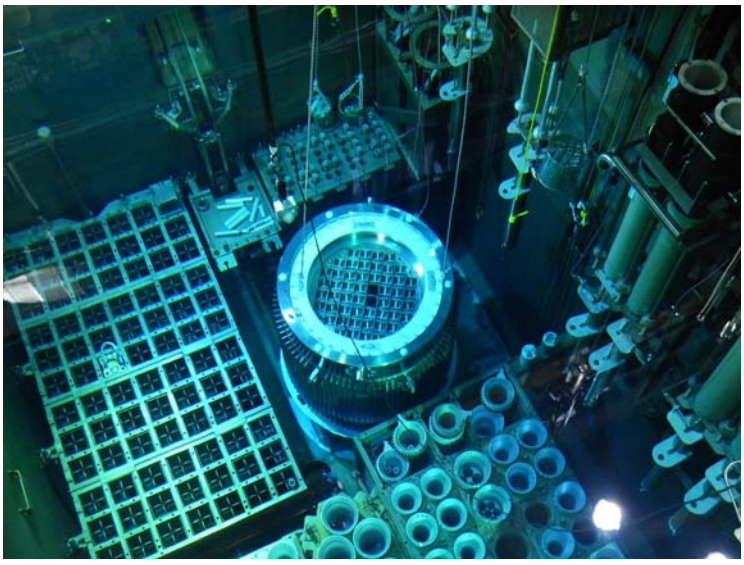

Figure 5. Loaded cask in the service pool with fuel storage rack on the left

During the loading campaign it was important to minimise disruption to the production of nuclear medicine, doped silicon and neutrons for scientific research. The movement of the casks in and out of the reactor hall required the breaking of containment, with the reactor having to be in the shutdown state (i.e. no production possible). To minimise loss of production, cask movements in and out of the reactor hall were carefully scheduled to align with periodic shutdowns for maintenance and refuelling.

All loading operations were performed in-between the periodic shutdowns with the reactor at power and production maintained. A significant amount of assessment work was completed to demonstrate that simultaneous cask loading and production operations would not create unacceptable safety risks or congestion. Assessment work was also completed to demonstrate that loading operations in the service pool would not adversely affect the core and irradiation facilities in the reactor pool.

Late July 2018 all four loaded casks were transported from ANSTO to Port Kembla (60 km south of ANSTO) in a single, secure road convoy with the assistance of Toll Transport, Australian Police and various other Australian Government Agencies. The transportation was carried out at night to minimise disruption to road users. At Port Kembla the casks were loaded onto a dedicated ship complying with the requirements of the Irradiated Nuclear Fuel (INF) Code. The ship sailed for France and arrived at Cherbourg Port in September 2018.

On the same day of arrival at Cherbourg Port the casks were loaded onto trucks and transported by road to the nearby Orano reprocessing facility at La Hague. Unloading of the four casks into interim storage ponds at La Hague was completed in January 2019. Orano will soon commence the reprocessing campaign for the 236 spent fuel assemblies.

Figure 6. Loaded casks inside shipping containers prior to departure from ANSTO

Figure 7. INF vessel and loaded truck at Cherbourg Port

6 Return of Intermediate Level Waste (ILW)

Pending continued operation of OPAL, it is expected there will be two returns of ILW resulting from the reprocessing of all OPAL spent fuel. A return of ILW resulting from the reprocessing of HIFAR spent fuel was completed in 2015. Figure 8 below shows a schematic for the 2015 ILW return. The CSD-U vitrified waste was set in stainless steel canisters, which were then packed into an Orano TN-81 cask. The TN-81 is an attractive cask design because it is dual purpose; it can be used for both transporation and long term storage with minimal maintenance.

The TN-81 arrived in Australia in December 2015. Australia has not yet established a national radioactive waste management facility and so the TN-81 was transferred to a dedicated storage building at ANSTO for interim storage. The return of the ILW has been an excellent exercise in demonstrating to the Australian public that the waste arising from the long term operation of a research reactor can be managed in a safe, secure and sustainable manner. ANSTO has also selected the TN-81 cask for the return of the ILW resulting from the reprocessing of HIFAR spent fuel in the UK, scheduled in 2021.

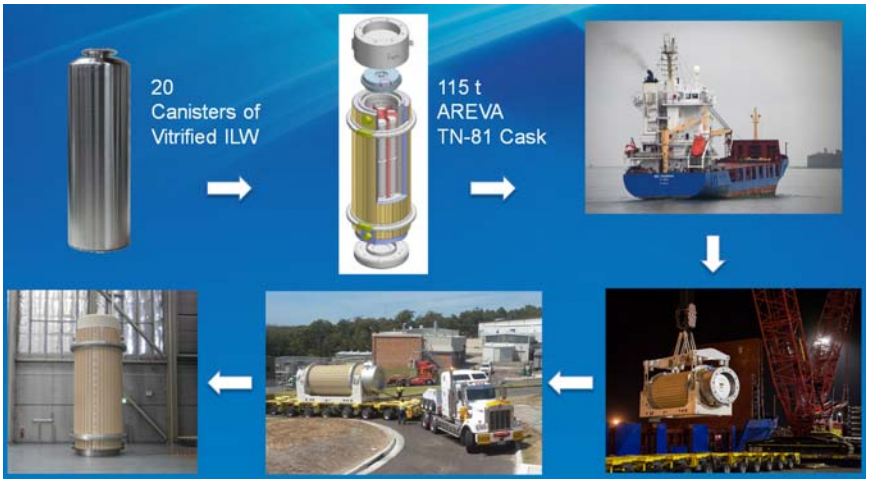

Figure 8. 2015 ILW return for reprocessed HIFAR spent fuel

A similar approach is planned for the eventual return of ILW resulting from the reprocessing of OPAL spent fuel. However, by the time the OPAL ILW is returned it is expected that Australia will have an operational national radioactive waste management facility for the long term storage of all ILW produced at ANSTO.

The Australian Government is in the final stages of selecting the site for the National Radioactive Waste Management Facility. Additional information is available at http://www.radioactivewaste.gov.au/.

7 Conclusion

ANSTO has more than 50 years of experience in the management of research reactor spent fuel. ANSTO has used this experience, together with Orano's expertise in spent fuel transportation and reprocessing, to design and implement an effective long term plan for the management of OPAL spent fuel.

ANSTO and Orano have completed the first transport of OPAL spent fuel to La Hague. It was performed with no impact on OPAL's operating schedule and minimal impact on pool top operations thus maintaining its reputation as one of the best research reactors in the world. ANSTO and Orano have now commenced working on the second shipment of OPAL spent fuel, which is scheduled for 2025.

8 References

1. R. Finlay, M. Healy, L. Dimitrovski, L. Halle, X. Domingo, P. Jacot, M. Kalifa, "Sustainable management of Australian research reactor spent fuel", RRFM2017, May 2017

2. J.F. Valery, V. Vo Van, A Talbi, C. Lavalette, L. Halle, C. Pechard and X. Renault, "Research Reactor Silicide Fuel Reprocessing at Orano La Hague", RRFM2018, March 2018.

3. Décision n°2017-DC-050: U_3Si_2 Reprocessing Authorization in Orano La Hague plant, ASN, May 2017.

4. Décision n°2018-DC-0626: U_3Si_2 Reprocessing Authorization in Orano La Hague plant, ASN, February 2018.

ROLE OF AE(ARCHITECT ENGINEER) IN THE DESIGN AND CONSTRUCTION OF RESEARCH REACTOR IN KOREA

CHOONG SANG LEE

Nuclear Project Engineering Division, DK&KOCEN Co. Ltd.

Seungnam City, Gyunggi Province, Korea

ABSTRACT

Architect Engineering company is responsible, as an independent organization, for design and engineering for all phases of a project, such as, feasibility study, basic and detail engineering, procurement, construction and commissioning. For the successful performance of a research reactor design and construction project, it is crucial to manage and coordinate the interfaces and interferences between all the project participants, that is, the owner, equipment suppliers, installation/ construction company and commissioning organization, if any. For the effective management of all the project activities to be executed by each participant, we, in Korea, are using a Project Work Breakdown Structure (PWBS) to be developed by AE for the project. The typical PWBS is introduced in this contribution. The other major role of AE company is to produce engineering documents and drawings taking into consideration of the right design information and right timing for ensuring the best quality, cost and schedule of the project. The engineering/ design evolution flow of research reactor is presented.

1. Introduction

Depending on the capability and policy of the owner, the contract for design and construction of a plant could be either Turnkey Base or Non-Turnkey Base, and in the Non-Turnkey Base contract there are two (2) types of contract, that is, Island Approach and Component Approach. The JRTR project was a Turnkey Base contract, however the contractor's work was performed as mixing of island approach and component approach types. In Korea, for nuclear power plant construction, the component base contract is being adopted and, for research reactor construction project, the owner makes two contract package such as design/engineering package and procurement/construction package. The role of AE company varies in accordance with the contract type and the capacity of the owner. However, in any type of contract, the basic functions of AE are to provide the owner with the overall project management and control system and to perform conceptual, basic, detail engineering and produce all the drawings to be used for construction. Although there are other roles to be performed on behalf of the owner as a centripetal organization between the participants in a construction project, the two major functions are introduced.

2. Project management and control system

"Project Management" is defined in PMI as "The art of directing and coordinating human and material resources throughout the life of a project by using modern management technics to achieve predetermined objectives of scope, cost, time, quality and participants satisfaction." To realize the effective project management. It is compulsory to define clearly all the project activities to be done by each participants in a project and all documents to be used for the project at the very early stage of project. We can control those things by assigning a unique

number to each drawing/document, code of account, activity and component & material. The following is a typical project numbering system being used for a research reactor construction project.

2.1 Project Work Breakdown Structure (PWBS)

The PWBS consists of PBS (Physical Breakdown Structure), OBS (Organizational Breakdown Structure and FBS (Functional Breakdown Structure). PBS, having three (3) digits numerical numbers, categorizes and defines the engineering, installation/construction, commissioning, operation, project management and administration of SSC (Structure, System and Component) of the facility. The example of PBS is as followings; 0xx: Project General, 1xx: Multi-System, 2xx: Site, Bldg.& Structure, 3xx: Reactor & Connected Items, 4xx: Experimental Facilities, 5xx: Electrical Systems, 6xx: I&C Systems, 7xx: Common Process & Services, 8xx: Radiation Protection, 9xx: Indirect Costs. OBS, having two (2) or three (3) digits numbers, defines the project entities and disciplines. FBS, having three (3) digits numbers, defines the categorization of products and related activities. The example of FBS is as follows; 1xx: Drawing, 2xx: Design Specification, 3xx: Calculation, 4xx: Report/Document, 5xx: Tasks.

2.2 Project Numbering Structure and types of numbering systems

2.2.1 The basic numbering structure is X (project code)-PBS No.- OBS No.- FBS No.- Serial No.

2.2.2 The types of numbering system are; **aa.** Drawing/Document Numbering System (Primary System drawing and document, AE drawing document, Main Component Supplier drawing and document, Auxiliary Equipment Supplier drawing and document, Constructor/Commissioner drawing and document). **bb.** Component Numbering System (Equipment Number, Valve Number, Pipe Line Number, Pipe Spool Number, Pipe Hanger & Support Number, Cable Tray & Conduit Number, Instrument Line Number, Instrument Number, HVAC Damper Number, Penetration Number, etc.). **cc.** Activity Numbering System (Engineering Activity & Interface Activity Number, Procurement Activity Number, Construction Package Specification Number, Construction Activity Number, Start-up Activity Number). **dd**. Code of Account Numbering System. **ee**. Specific Numbering System (Purchase Order Number, Purchase Order Item (Tagged and Bulk Material) Number, Main Component Number, Construction Package Number, Room Number and Area Code Number).

3. The Scope of Work performed by AE company

3.1 The full scope of AE works as per project phase

Project Management	Design Engineering	Procurement	Construction Management	Start-up
Cost Control	Soil & Environment Investigation	Localization Study	Contract Administration	Start-up Planning
Schedule Control	Licensing Support	Establish Procurement Plan	Construction Schedule Control	Prepare Procedures
Procurement Control	Conceptual Design	Tech. Bid Evaluation	Construction Material Control	Start-up Surveillance
Drawing & Document Control	Basic Design	Procurement Follow-up	Site Quality Surveillance	
Quality Assurance	Detail Design	Supplier Quality Control		

3.2 Disciplinary design works per design stage

Stage / Discipline	Conceptual Design	Basic Design	Detail Design
Electrical	-Deploy switchyard -System & component capacity design	-Prepare single line diagram -Electrical equip. arrangement -Prepare electrical equip. specification	-Technical bid evaluation -Prepare control circuit diagram, cable tray & conduit layout DWG., connection diagram, cable schedule, lighting panel & fixture schedule
I&C	-Decide computer package -Control type design -Study on control room layout	-Arrange control room & control board -Prepare I&C equip. specification	-Technical bid evaluation -Prepare instrument location DWG., control logic diagram, loop diagram, final control room layout DWG. and instrument installation DWG.
Mechanical	-Prepare Design Criteria	-Prepare preliminary P&ID -Preliminary system calculation -Prepare preliminary HVAC equip. layout DWG. -Prepare mechanical equip. specification	-Technical bid evaluation -Prepare final P&ID, system description and HVAC duct plan DWG. -Perform final system calculation
Nuclear	-Study on reactor, fuel & licensing req't	-Preliminary safety analysis -Preliminary shielding analysis	-Technical bid evaluation -Final safety analysis -Final shielding analysis

Piping	-Study on piping plan	-Prepare piping arrangement DWG. -Prepare piping specification	-Technical bid evaluation -Perform Piping stress analysis -Prepare piping isometric DWG.
Civil	-Study on seismic, soil, meteorology & hydrology	-Seismic analysis -Prepare floor response spectra -Structure analysis -Prepare structural DWG. and specification	-Technical bid evaluation -Perform final seismic analysis and structural analysis -Prepare final civil DWG.
Architecture	-Building/Structure Arrangement	-Prepare architecture DWG. and specification	-Technical bid evaluation -Prepare fire protection DWG., final architectural DWG. and penetration & door schedule
Cost/Schedule	-Study on cost/schedule control	-Prepare project milestone schedule and project summary schedule -Review project budget	-Prepare detail engineering, procurement, construction and start-up schedules -Control cost
Procurement	-Survey potential vendors	-Prepare vendor list and invitation to bid	-Prepare bid evaluation report
Quality Assurance	-Establish QA Plan	-Perform QA audit	-Perform supplier and constructor QA audit
Construction Management		-Review construction drawing & document	-Prepare field drawings
Start-up Support		-Prepare test requirements & procedures	-Prepare test list, pre-operational start-up procedures and pre-operation procedures

3.3 Engineering/Design Work Flow for Construction Drawings

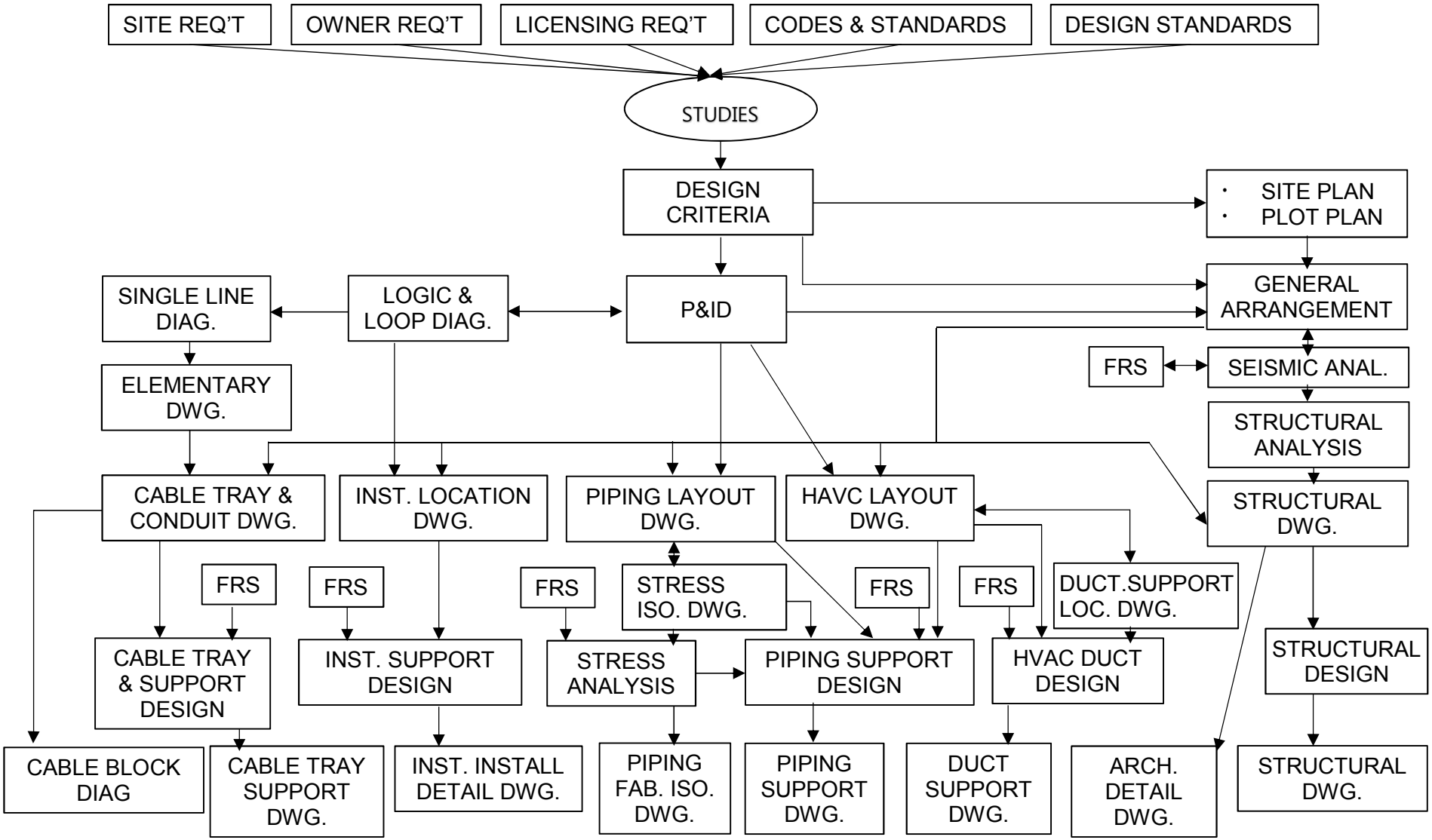

EFFECT OF ION IRRADIATION ON ALUMINIUM HYDROXIDE IN AN AL-MG-SI ALLOY

S. L'HARIDON-QUAIREAU, K. COLAS, B. KAPUSTA, B. VERHAEGHE, V. CLOUTE-CAZALAA
DEN-Service d'Etude des Matériaux Irradiés, CEA, Université Paris-Sud
F-91191, Gif-sur-Yvette - France

S. DELPECH
IPNO, Paris-Sud University
Paris - France

G. GUTIERREZ, M. LOYER-PROST
DEN-Service de Recherche de Métallurgie Physique, CEA, Université Paris-Sud
F-91191, Gif-sur-Yvette - France

D. GOSSET
DEN-Service de Recherche de Métallurgies Appliquées, CEA, Université Paris-Sud
F-91191, Gif-sur-Yvette - France

ABSTRACT

In the core of a nuclear reactor, irradiation defects created by the fast neutron flux can have a detrimental effect on the corrosion of aluminium alloys. In order to better understand the effect of irradiation on aluminium corrosion, a hydroxide obtained by corrosion of an Al-Mg-Si alloy is irradiated with Al ions. The damage created is 2.5 dpa (displacement per atom) on average in the aluminium hydroxide (Stopping and Range of Ions in Matter (SRIM) calculation). The ion irradiation seems to cause an amorphization of the hydroxide. Voids and nano-crystallites can also be observed.
After re-corrosion of the irradiated hydroxide, an increase of the thickness of the oxide layer can be observed compared to the non-irradiated oxide.

1. Introduction

Aluminium alloys are used in many fields, in particular for nuclear research reactors (NRRs). Due to a low activation, neutron transparency and good mechanical properties, aluminium alloys are used in nuclear cores of NRRs for the core components or for the fuel cladding [1]. However, these aluminium alloys are corroded in the nuclear core: an aluminium hydroxide covers their surface. The thermal conduction of this hydroxide is low (~2 W/m/K [2]): the hydroxide degrades heat exchanges between the components and the water of the primary circuit. It could therefore lead to an overheating of the components. As a result, the study of aluminium alloys corrosion is important for the safe and efficient operation of NRRs.
In this context, some authors studied the corrosion of aluminium alloys in nuclear research reactors or in corrosion loops.
Pawel et al. [3]–[5] and Griess et al. [6]–[9] studied the corrosion of aluminium alloys in corrosion loops with conditions representative of NRRs. Their corrosion tests allowed creating a model. This model was used to estimate the hydroxide thickness on aluminium alloys used in NRRs. However, this model misestimated the hydroxide thickness: the thicknesses measured on aluminium alloys corroded in nuclear core were not close to the one predicted [10]. Indeed, during their corrosion tests, the irradiation was not taken into account and corrosion tests conducted in nuclear reactor by Kim et al. [10] revealed an effect of the damage in the aluminium hydroxide created by the neutron irradiation. As a result, the model of Pawel and Griess was reassessed by Kim to take into account the effect of the irradiation. However,

the impact of the irradiation damage on aluminium hydroxide is not well known. As a result, new studies about the effect of the irradiation on aluminium hydroxide are required. In this study, in order to analyse the effect of the irradiation on aluminium corrosion without dealing with radioactive samples, ion irradiation is used to simulate the irradiation damage.

2. Experiments

The samples are in AA6061-T6 aluminium alloy. This alloy is mainly composed by Al (balance), Fe (0.7%mass), Si (0.4-0.8 %mass), Cu (0.15-0.4%mass) and Mg (0.8-1.2%mass) [11].
Before corrosion test, the samples are polished down to a 1µm finish with diamond paste.
In order to obtain an aluminium hydroxide film on the aluminium samples, corrosion experiment is performed in autoclave (V=5.5L, 316L steel, inside covered with Teflon) on aluminium alloy samples (10 x 10 x 1 mm). The samples are corroded at 70°C, for 7 days and in 2.8L of pure water. This corrosion test allows obtaining an aluminium hydroxide film on the samples surface. The thickness of this film is about 4 µm. The crystal phase of this hydroxide is studied by low-incidence X-ray diffraction (XRD, diffractometer with Cu-Kα radiation in asymmetric configuration, the incident angle of the X-ray beam is 2°) and µ-Raman spectroscopy (P=100 mW and λ=532 nm).

After the corrosion test, the samples are irradiated with ions. The ions are Al ions with successive energies of 1.2 MeV and 5 MeV in order to have a nearly homogenous damage profile in the hydroxide layer. A SRIM calculation (using the Stopping and Range of Ions in Matter software) indicates the damage is at most 4.5 dpa (displacement per atom) and 2.5 dpa on average in the aluminium hydroxide. The Al ions implantation peaks are located at a depth of 1.4 µm for the ions with an energy of 1.2 MeV and of 3.1 µm with an energy of 5 MeV. For the SRIM calculation, the threshold displacement energies used are 20 eV and 50 eV for the aluminium and oxygen sublattice, respectively [12].

After the ion irradiation, some irradiated samples are corroded a second time in order to study the impact of ion irradiation on the corrosion kinetics. For this corrosion experiment, the conditions are 4 days, 70°C and 2.8 L of pure water.

Before and after the ion irradiation, the aluminium hydroxide is examined using Scattering Electron Microscopy (SEM), Transmission Electron Microscopy (TEM, with an acceleration voltage of 300 kV and a length camera of 865 mm), XRD analyses and µ-Raman spectroscopy.
In order to examine the cross section of the hydroxide using a SEM, some samples are embedded in conductive resin and polished down to a 1 µm finish with diamond pastes.
TEM samples of the corroded materials are prepared with conventional Focused Ion Beam (FIB) methods. A Pt deposit is added on the samples surface to protect the hydroxide during the manufacturing of the TEM samples.

3. Results

The effect of the ion irradiation on aluminium hydroxide is evaluated by examining the hydroxide layer before and after irradiation. The results of these examinations are presented in the following paragraphs.
Also in order to evaluate the impact of irradiation on hydroxide growth, the irradiated samples are re-corroded. The results of this corrosion test are described in the last part.

3.1 Aluminium hydroxide before irradiation

Before ion irradiation, the aluminium hydroxide film is composed of two layers: an inner and an outer layer, as seen in Fig 1.b. The outer layer, in contact with the aqueous media, is a crystalline hydroxide: micro-crystals of aluminium hydroxide are observed on the samples surface as seen in Fig 1.a. The µ-Raman spectrum of this outer layer indicates it is composed of bayerite (α-$Al(OH)_3$, Fig 1.c, Raman peaks of bayerite : [13]).
Between the bayerite layer and the aluminium matrix, the inner layer is composed of a non-fully crystallised phase. The peaks of the µ-Raman signal obtained on this inner layer can be

attributed to boehmite (γ-AlOOH, Fig 1.c, Raman peaks of boehmite : [13], [14]); however, the peaks are poorly defined. From this Raman spectrum, it can be concluded the inner layer is pseudo-boehmite (a nanocrystalline boehmite phase). This hydroxide is often found on surface of aluminium alloys during aqueous corrosion tests at all temperature [15].

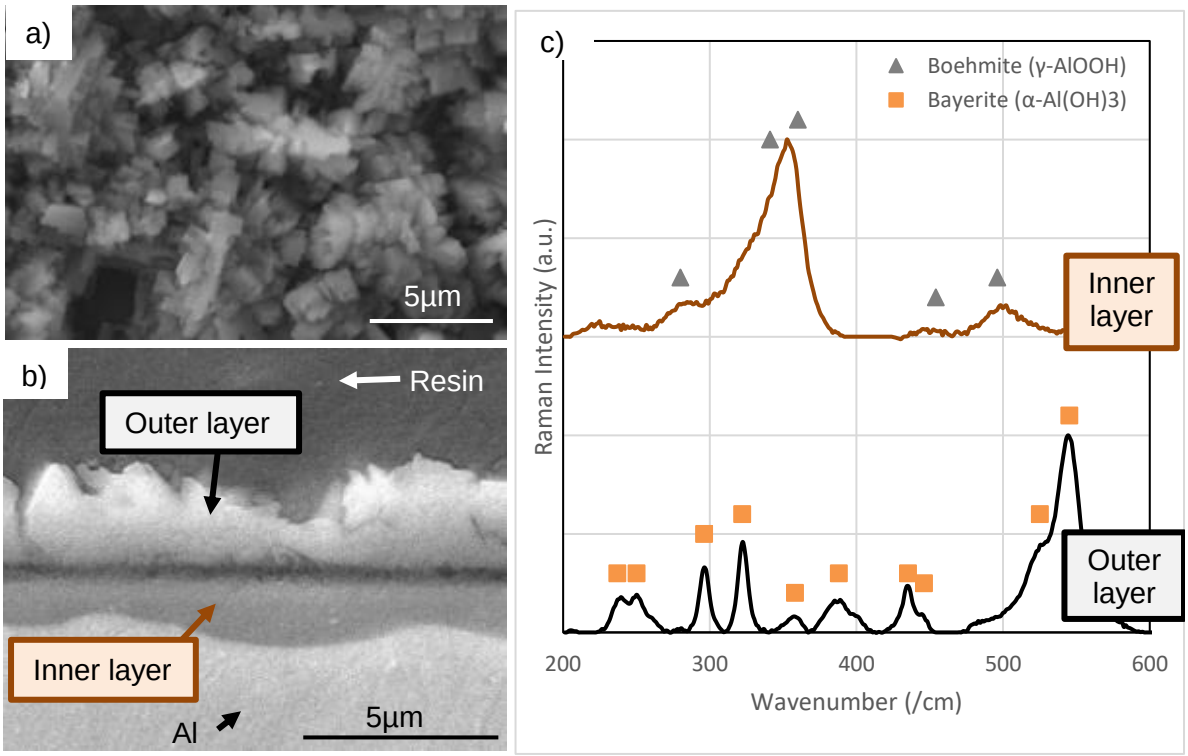

Fig 1. (a) Aluminium hydroxide crystals of the outer layer at the surface of the samples (top view, SEM, secondary electron mode), (b) cross section of the aluminium hydroxide found on the samples (SEM, secondary electron mode); (c) µ-Raman spectra obtained on the inner and outer layers.

A low incidence X-ray diffraction on the corrosion products confirms the results of µ-Raman analyses (Fig. 3): bayerite is the main crystalline phase formed during the corrosion experiments; traces of boehmite are also present. This composition of the hydroxide is common at 70°C, the temperature of the corrosion test, according to the literature [1], [15].

3.2 Irradiated aluminium hydroxide

The Fig. 2.a presents a cross section of the irradiated oxide observed by TEM. The irradiated oxide is between the Pt deposit and the aluminium matrix. After ion irradiation, the distinction between the two former layers (inner and outer layers) is difficult as seen in Fig. 2.a. The outer layer is amorphized: the former micro-crystals of bayerite could not be observed. In addition, voids are present in the irradiated oxide, in the two layers. A line of voids is observed in the middle of the former inner layer. This line corresponds to the peak of damage made by the Al ions in the inner layer (i.e. at 4.5 dpa).
Additionally, an electron diffraction observation is performed on the irradiated oxide (Fig. 2.b). The rings obtained from this electron diffraction indicate the presence of nano-crystallites. A dark field performed on the ring of 1.39 Ă is presented in Fig 2.c: the nano-crystallites that have diffracted to form this ring are in white in the oxide matrix in black.

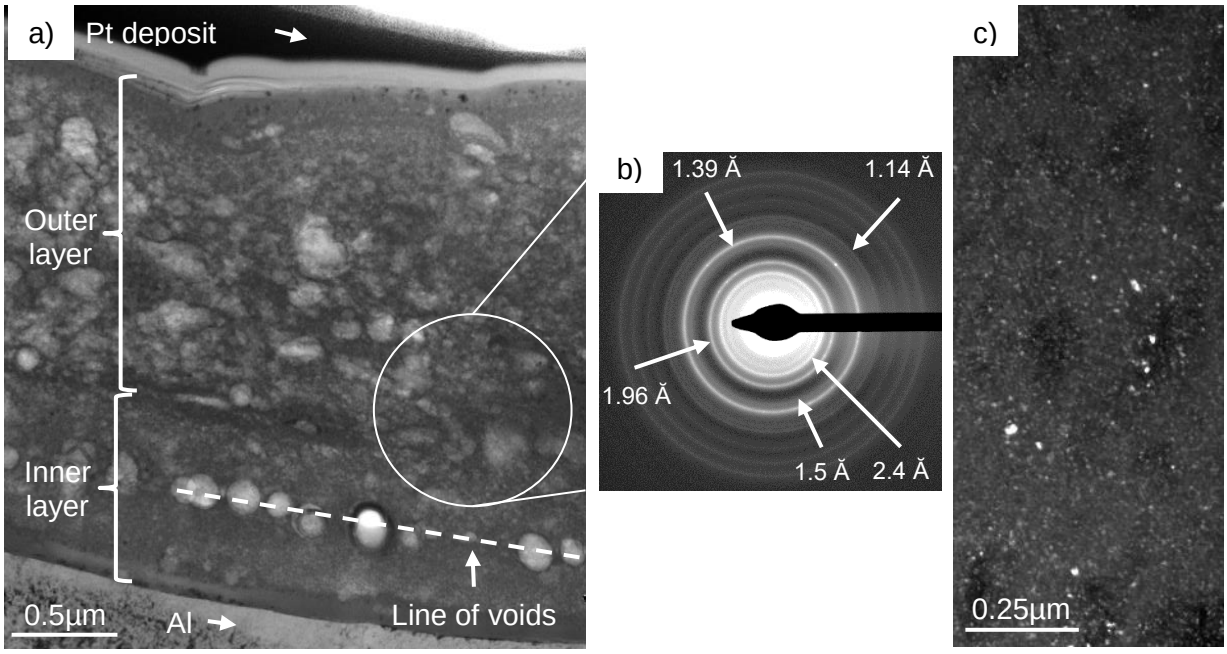

Fig 2. (a) Cross section of irradiated oxide (TEM), (b) electron diffraction pattern obtained from the irradiated oxide, attributed to η-Al_2O_3, and (c) Dark Field of the crystallites (in white) in the oxide (in black) that have diffracted to form the ring at 1.39Ă.

The electron diffraction pattern on Fig 2.b can be attributed to a nanometric η-Al_2O_3 phase: the d-spacing measured at 1.14Ă, 1.39Ă, 1.50Ă, 1.96Ă and 2.40Ă are very close to those measured by Tilley for the nanometric η-Al_2O_3 phase in bauxite [16].
In the literature [15], this oxide phase comes from the thermal decomposition of bayerite and pseudo-boehmite at 250-650°C. However, during the irradiation, the maximal temperature of the irradiated hydroxide is 20°C (a thermocouple is placed in contact with the oxide during the irradiation). As a result, the presence of η-Al_2O_3 cannot be attributed to a temperature but could be due to the ion irradiation.
In addition, when the irradiation starts, the pressure of the vacuum in the accelerator increases from 10^{-8} Pa to 10^{-7} Pa: due to the ion beam, the former aluminium hydroxide could be decomposed into η-Al_2O_3 by releasing water.
Unfortunately, the presence of η-Al_2O_3 could not be confirmed by a Raman analysis: after irradiation, the laser light is strongly diffused by the oxide, which makes impossible to realize a measurement of sufficient quality of the oxide. This type of problem is common with this aluminium oxide [17].

Additionnally, the η-Al_2O_3 phase could not be observed in the X-ray diffraction diagram of the irradiated hydroxide (Fig 3): it can be due to the small size of the crystallites (>10nm, Fig 2.c) and the insufficient resolution of the diffractometer. In addition, the main peaks of η-Al_2O_3 at 37.80° [16] is very close to the peaks of aluminium at 38.4° [18], a distinction between the two phases is impossible. However, the peaks of bayerite are still present in this spectrum but a decrease in intensity of the peaks is observed. This result can be attributed to an important amorphization of the bayerite.

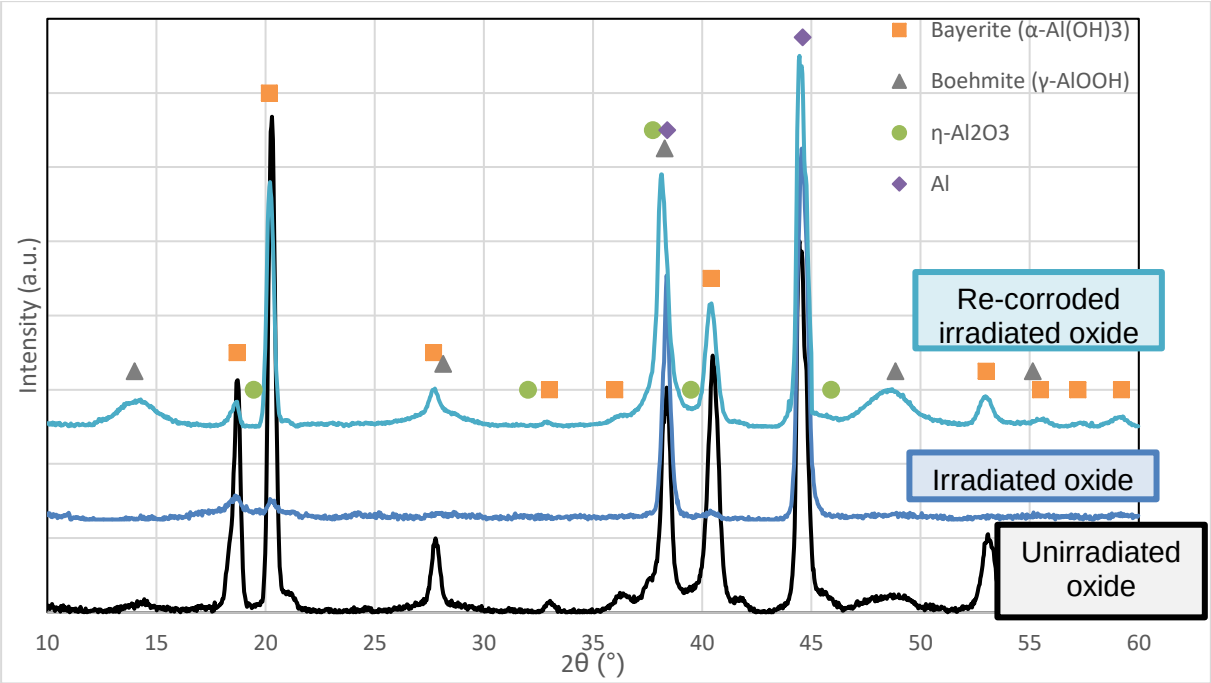

Fig 3. X-rays diffraction spectra of the aluminium hydroxide in different conditions (before and after irradiation and after re-corrosion of the irradiated oxide)

3.3 Effect of ion irradiation on corrosion kinetics

After ion irradiation, the samples are re-corroded in order to evaluate the effect of the irradiation on hydroxide growth.

After the re-corrosion of the irradiated oxide, two layers of aluminium hydroxide are present at the samples surface as seen on the picture of re-corroded irradiated oxide in Fig. 4. The inner layer, near the aluminium matrix, is pseudo-boehmite and the outer layer is bayerite (µ-Raman analyses, confirmed by XRD analysis on Fig 3). The thickness of these two layers is measured on a cross section of the hydroxide embedded in resin and observed with SEM (Fig 4).

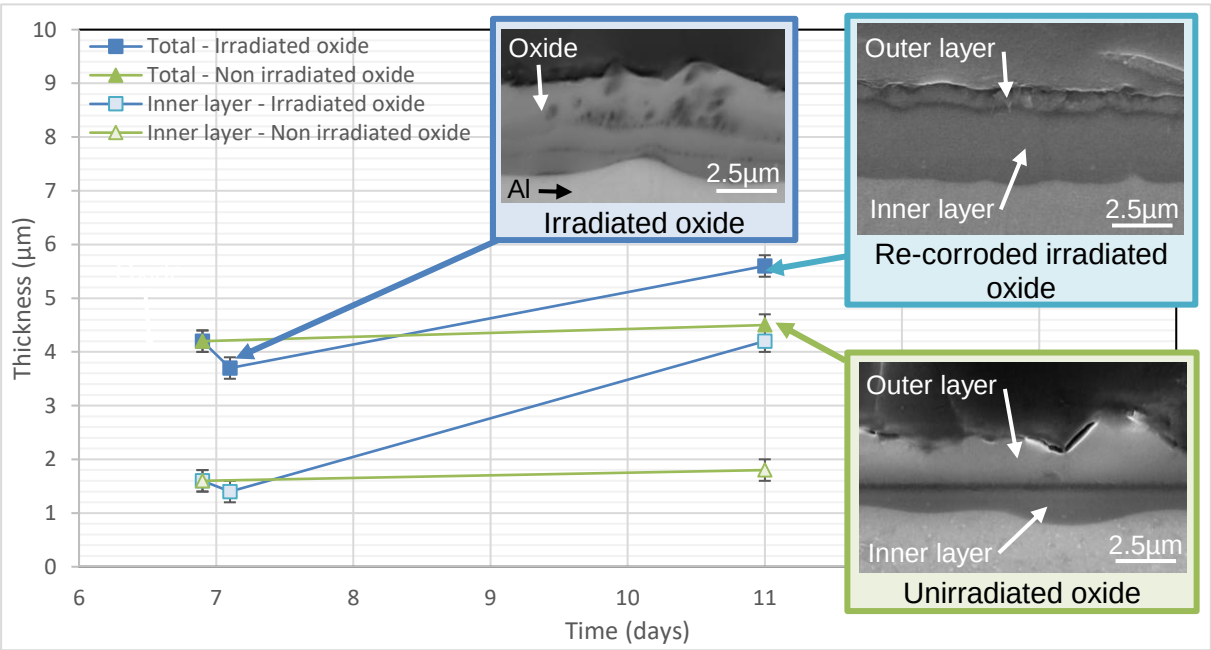

Fig 4. Evolution of the thickness of irradiated and unirradiated hydroxides and micrographs (SEM, secondary electron mode) of the aluminium hydroxide in different conditions: irradiated (in the middle), re-corroded irradiated (on the top right) and unirradiated (on the bottom right)

As illustrated by Fig. 4, after re-corrosion, at 11 days, the hydroxide thickness is larger for irradiated samples than for the unirradiated ones. The increase of the inner layer thickness in particular is very important after ion irradiation and re-corrosion. This inner layer seems to contain the former layers of bayerite and pseudo-boehmite of the hydroxide before the irradiation.

In addition, the ion irradiation seems to increase the kinetics oxidation of aluminium matrix (Fig 4): the ion irradiation degrades the hydroxide film by creating voids, by dehydrating and by amorphizing it. The irradiated film does not protect the matrix. As a result, the oxidation of the aluminium matrix is more important after irradiation compared to the unirradiated samples and it causes the observed increase of hydroxide thickness for 11 days of corrosion in Fig. 4.

4. Discussion

In the literature [1], [19] , without irradiation, the mechanism of aluminium corrosion is the following:

1. The aluminium of the matrix is oxidised at the interface oxide-metal, this oxidation is accompanied by the reduction of water and dioxygen, and the production of OH hydroxide groups. A part of this oxidised aluminium reacts with the OH hydroxide groups to form pseudo-boehmite, the inner layer, at the oxide-metal interface. As a result, the inner layer grows by replacing the oxidised aluminium.
2. The rest of the oxidised aluminium is released in solution in the form of ions in the corroding solution. This released material then precipitates at the samples surface to form bayerite, the outer layer.

With the observations made in this study, the following mechanism associated with ion irradiation can be proposed:

1. Before ion irradiation, due to the corrosion test, an hydroxide layer covers the aluminium matrix according to the mechanism described above. These are two pre-existing layers of hydroxide on the surface of the sample.
2. During ion irradiation, the former hydroxide is dehydrated and amorphized. The water of the hydroxide is released because of the vacuum and the ion irradiation. Voids and crystallites of η-Al_2O_3 can be produced in the hydroxide.
3. After irradiation, during the corrosion test, the irradiated film forms a new inner layer. Due to a bad quality of this irradiated film, the matrix is oxidised and aluminium is released in solution. A new outer layer is formed by the precipitation of aluminium in solution.

However, in this study, we can observe some limitations to the use of ion irradiation to simulate the damage created by the fast neutron flux in reactor.
During the ion irradiation, the hydroxide is irradiated in vacuum. The vacuum and the ion beam led to a dehydration of the hydroxide. The damage due to this dehydration (voids and crystallites of η-Al_2O_3) may not be observed in aluminium hydroxide irradiated in a nuclear core.
In addition, to irradiate the hydroxide, the corrosion tests are interrupted, the samples are exposed to air during the break of corrosion tests. Wintergerst observed an effect of breaks during corrosion test: the hydroxide thickness is less important during corrosion tests with breaks than without break [20]. It means the thickness measured in this study may be underestimated because of the break to irradiate the hydroxide.

In addition, we can observe some similarities between ion and neutron irradiation.
On the one hand, AlFeNi samples (composition of the alloy: Fe (0.9 %mass), Ni (0.9 %mass), Cr (0.35 %mass), Mg (1.05 %mass), Al (balance)) were corroded in the BR2 nuclear reactor during 70 days [1]. A XRD analysis performed on the irradiated hydroxide indicates the main crystalline phase is boehmite and traces of bayerite are present. This crystalline composition is the same than that of the re-corroded irradiated hydroxide obtained in this study.
On the other hand, during one year, aluminium samples were corroded in the Osiris nuclear reactor at 45°C and in a corrosion loop at 50°C with similar corrosion conditions. The thickness

of the irradiated hydroxide is about 15µm, and the thickness of the unirradiated hydroxide is about 3µm. At low temperature, the neutron irradiation leads to an increase of the hydroxide thickness. In this study, the same observation is made with ion irradiation: irradiation causes an increase of the hydroxide thickness. This increase could be due to the damage in the hydroxide.
To finish, the hydroxide irradiated in nuclear reactor needs more examinations to compared neutron and ion irradiation.

5. Conclusion

In this study, Al-Mg-Si alloy samples are corroded at 70°C, in pure water, for 7 days, in order to obtain an aluminium hydroxide film on the samples surface. This hydroxide is composed of two layers: an outer layer in contact with the solution and an inner layer between the outer layer and the aluminium matrix. Micro-crystals of bayerite (α-$Al(OH)_3$) can be observed in the outer layer. The inner layer is pseudo-boehmite, a nano-crystalline boehmite (γ-AlOOH).

The obtained aluminium hydroxide is irradiated with Al ions with successive energies of 1.2 MeV and 5 MeV. The damage created is 2.5 dpa (displacement per atom) on average (SRIM calculation). Ion irradiation induces important changes in the hydroxide: the micro-crystals of bayerite are amorphized. Bubbles and crystallites of η-Al_2O_3 are produced in the hydroxide.

After ion irradiation, the irradiated oxide is re-corroded in order to evaluate the effect of ion irradiation on the corrosion kinetics. As a result, the hydroxide thickness is larger for the irradiated samples than for the unirradiated ones. The increase of the inner layer thickness in particular is very important after ion irradiation and re-corrosion. Indeed, the ion irradiation degrades the hydroxide film by creating voids, by dehydrating it and by amorphizing it. The irradiated film does not protect the matrix. As a result, the oxidation of the aluminium matrix is more important after irradiation compared to the unirradiated samples.

To finish, during corrosion test in nuclear reactor, a Si-enrichment of the hydroxide is observed [20]. This silicon comes from the aluminium transmuted in silicon because of the thermal neutron flux. In this study, the hydroxide is irradiated with Al ions; it is not enriched with silicon. As a result, a further study will be done with an aluminium hydroxide irradiated with Si ions to simulate the Si-enrichment in order to better understand the role of the silicon in the corrosion process.

References

[1] M. Wintergerst, « Etude des mécanismes et des cinétiques de corrosion aqueuse de l'alliage d'aluminium AlFeNi utilisé comme gainage du combustible nucléaire de réacteurs expérimentaux. », Thèse de doctorat, Université Paris XI, U.F.R Scientifique d'orsay, Saclay, 2010.

[2] C. Vargel, *Corrosion de l'aluminium*. Dunod, 1999.

[3] S. J. Pawel, D. K. Felde, et R. E. Pawel, « Influence of coolant pH on corrosion of 6061 aluminium under reactor heat transfer conditions », Oak Ridge, TN, USA, 1995.

[4] S. J. Pawel, G. L. Yoder, D. K. Felde, B. H. Montgomery, et M. T. McFee, « The corrosion of 6061 aluminium under heat transfer conditions in the ANS corrosion test loop », *Oxidation of Metals*, vol. 36, nº 1/2, p. 175-194, 1991.

[5] S. J. Pawel, G. L. Yoder, C. D. West, et B. H. Montgomery, « The development of a preliminary correlation of data on oxide groth on 6061 aluminium under ANS thermal-hydraulic conditions », *ORNL/TM-11517*, 1990.

[6] J. C. Griess, H. C. Savage, T. H. Mauney, et J. L. English, « Effect of heat flux on the corrosion of aluminium by water. Part I : Experimental equipment and preliminary results », Oak Ridge, TN, USA, 1960.

[7] J. C. Griess, H. C. Savage, T. H. Mauney, J. L. English, et J. G. Rainwater, « Effect of heat flux on the corrosion of aluminium by water. Part II : Influence of water temperature, velocity and pH on corrosion-product formation », Oak Ridge, TN, USA, 1961.

[8] J. C. Griess, H. C. Savage, T. H. Mauney, J. L. English, et J. G. Rainwater, « Effect of heat flux on the corrosion of aluminium by water. Part III : Final report on tests relative ot the high-flux isotop reactor », Oak Ridge, TN, USA, 1961.
[9] J. C. Griess, H. C. Savage, et J. L. English, « Effect of heat flux on the corrosion of alumnium by water. Part IV : Tests relative to the advanced test reactor and correlation with previous results », Oak Ridge, TN, USA, 1964.
[10] Y. S. Kim, G. L. Hofman, A. B. Robinson, J. L. Snelgrove, et N. Hanan, « Oxidation of aluminum alloy cladding for research and test reactor fuel », *J. Nucl. Mater.*, vol. 378, nº 2, p. 220-228, août 2008.
[11] Y. Shen, « Comportement et endommagement des alliages d'aluminium 6061-T6 : approche micrométrique », Thèse de doctorat, Ecole Nationale Supérieure des Mines de Paris, 2012.
[12] S. . Zinkle et G. . Pells, « Microstructure of Al2O3 and MgAl2O4 irradiated at low temperatures », *J. Nucl. Mater.*, vol. 253, nº 1, p. 120-132, mars 1998.
[13] H. D. Ruan, R. L. Frost, et J. T. Kloprogge, « Comparison of Raman spectra in characterizing gibbsite, bayerite, diaspore and boehmite », *J. Raman Spectrosc.*, vol. 32, nº 9, p. 745-750, sept. 2001.
[14] C. J. Doss et R. Zallen, « Raman studies of sol-gel alumina: Finite-size effects in nanocrystalliine AlO(OH) », *Phys Rev B*, vol. 48, p. 626-637, 1993.
[15] K. Wefers et C. Misra, *Oxides and hydroxides of aluminium*. ALCOA Laboratories, 1987.
[16] D. B. Tilley et R. A. Eggleton, « The Natural Occurrence of Eta-Alumina (eta-Al2O3) in Bauxite », *Clays Clay Miner.*, vol. 44, janv. 1996.
[17] Y. Chen, J. Hyldtoft, C. J. . Jacobsen, et O. F. Nielsen, « NIR FT Raman spectroscopic studies of η-Al2O3 and Mo/η-Al2O3 catalysts », *Spectrochim. Acta. A. Mol. Biomol. Spectrosc.*, vol. 51, nº 12, p. 2161-2169, nov. 1995.
[18] R. W. G. Wyckoff, *Crystal structures*, Arizona. Wiley (Interscience)., vol. 1. Second edition. University of Arizona, Tucson, 1965.
[19] R. K. Hart, « The formation of films on aluminium immersed in water », *Trans Faraday Soc*, vol. 53, p. 1020-1025, 1956.
[20] M. Wintergerst, N. Dacheux, F. Datcharry, E. Herms, et B. Kapusta, « Corrosion of the AlFeNi alloy used for the fuel cladding in the Jules Horowitz research reactor », *J. Nucl. Mater.*, vol. 393, nº 3, p. 369-380, sept. 2009.

A POSSIBLE APPLICATION OF THE GRADED APPROACH TO GERMAN RESEARCH REACTORS

M. TRAPP
Reactor Safety Department, Plant Safety Division, Gesellschaft für Anlagen- und Reaktorsicherheit (GRS) gGmbH
Schwertnergasse 1, 50667 Cologne – Germany

K. NÜNIGHOFF
International Projects Department, International Management Division, Gesellschaft für Anlagen- und Reaktorsicherheit (GRS) gGmbH
Schwertnergasse 1, 50667 Cologne – Germany

ABSTRACT

In Germany, no dedicated regulatory framework for research reactors exists. Research reactors are regulated using the comprehensive regulatory framework for nuclear power plants by means of a so-called appropriate application i.e. applying a grading. In this paper, a systematic categorisation based on the three categories “utilisation of the research reactor”, “cooling of the fuel” and “confinement of radioactive material” of the German research reactors is proposed. Applying a “grading matrix” this procedure allows for a grading of the German Safety Requirements according to the risk potential of the research reactor under investigation.

1. Introduction

The IAEA Specific Safety Requirements SSR-3 “Safety of Research Reactors” [1] allows the use of the graded approach in application of the safety requirements for a research reactor commensurate with the potential hazard of the facility. As stated in Requirement 12, the application of the graded approach shall be based on safety analysis and regulatory requirements. The graded approach for research reactors is further detailed in the IAEA Specific Safety Guide SSG-22 “Use of a Graded Approach in the Application of the Safety Requirements for Research Reactors” [2]. This safety guide suggests in general that a qualitative categorisation should be performed on the basis of the radiological hazard potential (para. 2.6 in [2]) taking into account individual characteristics of the facility (para. 2.7 in [2]). How this categorisation and grading is implemented in practice in the national regulatory systems is left to the competent authorities.

The three examples given below show the wide range of different ways of application of the graded approach with respect to research reactors.

In the United States, the U.S. NRC used a grading for the assessment of the lessons learned from the Fukushima Dai-ichi to US research and test reactors. Here, only the thermal power served as a categorisation [3]. A threshold of 2 MW_{th} was defined in order to establish two categories. Also, for the licence renewal this threshold is used by the U.S. NRC. Here, facilities with a thermal power above or equal 2 MW_{th} undergo a full review according to NUREG-1537 [4]. Facilities with a smaller thermal power undergo a graded review which focuses on reactor, radiation protection, accident and technical specifications. The areas where this so-called “minimal regulation” is used are design criteria, fission product release, emergency planning, reactor siting and environmental requirements [5].

In Canada the regulatory document RD-367 [6] addresses the design of small reactor facilities (SMF). “A small reactor facility is defined as a reactor facility with a reactor with a power level of less than approximately 200 megawatts thermal (MW_{th}) that is used for research, isotope production, steam generation, electricity production or other applications.” [6] The document lists criteria which need to be considered when applying a grading according to SSG-22. In addition to the three fundamental safety functions “control of reactivity”, “removal of heat from the core” and “confinement of radioactive material”, the safety functions “control of operational discharges and hazardous substances”, “limitation of accidental releases” and “monitoring of safety critical parameters to guide operator actions” shall be respected.

In the Netherlands, Annex 6 of the Handreiking VOBK. (Handreiking voor een Veilig Ontwerp en het veilig Bedrijven van Kernreactoren) [7] describes the appropriate application of the safety requirements to research reactors. In this approach, a risk category and a cooling category are assigned to the research reactor. For the risk category which takes the radiological impact into account, the radiological consequences of a credible accident scenario which leads to the highest release of radioactivity shall be considered. The cooling category considers the necessary measures for residual heat removal. According to this categorisation, a grading of the regulatory requirements can be justified. A grading with respect to the safety function “control of reactivity” was not foreseen, because control of reactivity has to be ensured at any time.

The aim of the study presented here is to establish a structured method for the classification of German research reactors according to a graded approach. Therefore, the abstract concept of the graded approach is translated into a more technical classification scheme. This scheme is based on three categories: “utilisation of the research reactor”, “cooling of the fuel” and “confinement of radioactive materials”. The categorisation starts with the assignment to one of the classes in the category “utilization of the research reactor”. This procedure follows an approach proposed by the French TSO IRSN [8]. It serves as identification of additional aspects to be considered such as cold neutron sources or beam tubes in the case of neutron scattering facilities. In a next step, the fundamental safety functions “cooling of the fuel” and “confinement of radioactive material” are used for categorisation. The final result is a “grading matrix” which serves for the grading of the German regulations. Within this study a generic application of the graded approach on the German Safety Requirements for Nuclear Power Plants based on the derived “grading matrix” is studied in more detail. The subdivision of each category and the step by step classification of the German research reactors is given in detail in the following chapters.

2. Classification

2.1. Category “utilisation of the research reactor”

First the research reactor is classed according to its utilisation. In order to take into account the individual risk of a research reactor, three types of utilisation were identified (neutron source, zero power and teaching reactors and irradiation and test reactors) for German research reactors into which all reactors can be classed. This approach allows the identification of additional aspects to be considered such as cold neutron sources or beam tubes in the case of neutron scattering facilities or irradiation and test loops in case of an irradiation or test reactor. Tab. 1 shows the results for the German research reactors still in operation.

Cat.	Description
1	zero power reactors: SUR, AKR-2
2	irradiation and test reactors: FRMZ
3	neutron sources: FRM II, BER II

Tab. 1: Classification of the German research reactors according to its utilisation

2.2. Category “cooling of the fuel”

Second, the category for the cooling of the fuel is introduced by the need of active or passive cooling. For the category “cooling of the fuel” the need for an active cooling during operation and after shut-down was used to establish a categorisation.

Cat.	Description
1	No cooling needed after the shutdown of the reactor. Thermal radiation, air convection and thermal conductivity are sufficient to cool the fuel.
1a	Cat. 1 and passive cooling during operation
1b	Cat. 1 and active cooling during operation
2	Passive cooling needed after the shutdown of the reactor. This requires natural convection of water as the coolant.
2a	Cat. 2 and passive cooling during operation
2b	Cat. 2 and active cooling during operation
3	Active cooling needed after the shutdown of the reactor

Tab. 2: Classification according to the category “cooling of the fuel”

All zero power reactors are cooled by thermal radiation, air convection and thermal conductivity hence they are grouped into “cooling of the fuel” category 1. The FRMZ is cooled by natural convection during operation and belongs to “cooling of the fuel” category 2a. Both neutron sources BER II and FRM II have an active cooling after the reactor is shutdown and are in cooling of the fuel” category 3.

2.3. Category “confinement of radioactive material”

Finally, as a function of impact on the public and the environment the category “confinement of radioactive material” is established. For the third category “confinement of radioactive material” the approach developed in the IAEA Safety Report Series No. 53 “Derivation of the Source Term and Analysis of the Radiological Consequences of Research Reactor Accidents” [9] and intervention level for sheltering as recommended by the German Commission on Radiological Protection [10] are the basis for the categorisation according to the “confinement of radioactive material” criterion. The three defined subdivision can be found in Tab. 3.

Cat.	Description
1	Radiological consequences are restricted to supervised and controlled areas (i.e. the reactor building and guide halls) with an exceedance of limits for doses, contamination or incorporation defined for normal operation.
2	On-site consequences outside the reactor building. Exceedance of the effective dose limit of 1 mSv/year. No off-site measures necessary.
3	Off-site consequences. According to [10]: “10 mSv as the total of the effective dose due to external exposure within a period of 7 days and the committed effective dose from radionuclides inhaled during the same period.”

Tab. 3: Classification according to the category “confinement of radioactive material”

In a simplified approach following the IAEA Safety Report Series No. 53 [9] a realistic worst-case scenario with a complete release of the noble gases krypton and xenon with the strongest radiological impact is assumed. For caesium a release rate of 30 % was assumed.

The safety analysis reports of the SUR reactors did not contain information on the source term of the facilities. The SUR operate at a nominal power of 100 mW whereas the continuous power of the AKR-2 is 2 W. Therefore, the values of the SAR of the AKR-2 [11] were used as conservative estimate for the source term of the SUR. Comparing the exemption levels and the limits for high-activity radiation sources (HASS) according to German Ordinance on the Protection against Damage and Injuries Caused by Ionizing Radiation [12] with the source terms of the SUR/AKR-2 reactors it becomes clear that the reactors belonging to the zero power and teaching reactors should be assigned to the lowest subdivision of the “confinement of radioactive material” category.

For the FRMZ a study by the TÜV Rheinland [13] about the radiological consequences of an airplane crash with a fuel fire concluded that the maximal effective dose released during this event is 2.4 mSv in a distance of 200 m away from the reactor. Therefore, this research reactor is placed into the second subdivision of this category.

For both neutron sources BER II [14] and FRM II [15] the threshold for sheltering of 10 mSv in seven days is exceeded, hence both reactors belong to the highest subdivision in this category.

2.4. Resulting grading matrix

According to the classification developed in this chapter and the characteristics of each research reactor described, all German research reactors in operation (2019) were arranged in a “grading matrix” shown in Tab. 5.

	“Control of reactivity”	“Cooling of the fuel”	“Confinement of radioactive material”
SUR/AKR-2	1	1	1
FRMZ	2	2a	2
BER II	3	3	3
FRM II	3	3	3

Tab. 4: Categorisation of the German research reactors in operation

3. Application to the German Safety Requirements

In a next step, this classification was used to grade the requirement of the German Safety Requirements for Nuclear Power Plants [16]. Therefore, each requirement was checked against the three categories and given a rating. According to this rating the requirement can be (partly) graded as shown in the example for selected requirements in the category “cooling of the fuel” given below (Tab. 5).

Requirement	3.2 (1) The control of reactivity in the reactor core shall be ensured for all operational modes on levels of defence 1 to 4a as well as in the case of internal and external hazards and under very rare human induced external hazard.						
	Category “cooling of the fuel”						
	1	1a	1b	2	2a	2b	3
rating	Generally applicable						
Requirement	3.2 (5) The reactor shall have – at least one system for fast shutdown (reactor scram system) by means of control rod elements, and – at least one more shutdown system, being independent of and diverse from the reactor scram system, for reaching and long-term maintenance of subcriticality through injection of soluble neutron absorbers into the coolant. The control or limitation system for the reactor power may totally or in part be identical with the shutdown systems as far as the effectiveness of the shutdown systems is maintained to the required degree at any time.						
	Category “cooling of the fuel”						
	1	1a	1b	2	2a	2b	3
rating	The diverse shutdown system could be different to the injection of soluble neutron absorbers.						
Requirement	3.3 (1) Fuel cooling (heat removal from the reactor core) shall be ensured in all operational modes on levels of defence 1 to 4a as well as in the case of						

<table>
<tr><td></td><td colspan="7">internal and external hazards and under very rare human induced external hazards.
For this purpose, the heat produced in the fuel assembly shall be removed such that the safety-related acceptance targets and acceptance criteria for the fuel assemblies and the other safety-relevant equipment applicable on the respective levels of defence are met during their entire service life.</td></tr>
<tr><td rowspan="2"></td><td colspan="7">Category “cooling of the fuel”</td></tr>
<tr><td>1</td><td>1a</td><td>1b</td><td>2</td><td>2a</td><td>2b</td><td>3</td></tr>
<tr><td>rating</td><td colspan="3">Requirement can be waived</td><td colspan="4">Generally applicable</td></tr>
<tr><td>Requirement</td><td colspan="7">3.3 (2) Equipment shall be available by means of which during normal operation

a) the reactor can be started up and shut down reliably and according to the requirements, and

b) the residual heat can be removed reliably and according to the requirements also un-der consideration of all operational modes during refuelling and, if required, the simultaneous cooling of the spent fuel assemblies in the fuel pool as well as during maintenance measures.</td></tr>
<tr><td rowspan="2"></td><td colspan="7">Category “cooling of the fuel”</td></tr>
<tr><td>1</td><td>1a</td><td>1b</td><td>2</td><td>2a</td><td>2b</td><td>3</td></tr>
<tr><td>rating</td><td colspan="3">Requirement can be waived</td><td colspan="4">Generally applicable</td></tr>
<tr><td>Requirement</td><td colspan="7">3.3 (3) A reliable and redundant system for emergency cooling of the reactor core (emergency core cooling system) in case of a loss-of-coolant accidents shall be provided that ensures for the break sizes, break locations, operating states and accident-induced transients in the reactor coolant system to be considered that
a) the safety-related tasks are fulfilled also with respect to the requirements of Subsection 3.1 (7),
b) the respective applicable safety-related acceptance targets and acceptance criteria for the fuel assemblies, the core internals and for the containment are met.</td></tr>
<tr><td rowspan="2"></td><td colspan="7">Category “cooling of the fuel”</td></tr>
<tr><td>1</td><td>1a</td><td>1b</td><td>2</td><td>2a</td><td>2b</td><td>3</td></tr>
<tr><td>rating</td><td colspan="3">Requirement can be waived</td><td colspan="3">In case of loss of coolant, systems for refilling the reactor pool shall be provided.</td><td>Generally applicable</td></tr>
<tr><td>Requirement</td><td colspan="7">3.3 (4) A reliable and redundant system for reactor shutdown and residual heat removal in case of accidents without loss of coolant and after internal and external hazards shall be provided which ensures that the safety-related acceptance targets and acceptance criteria are met even following an interruption or disturbance of heat removal from the reactor to the main heat sink, also with respect to the requirements of Subsection 3.1 (7).</td></tr>
<tr><td rowspan="2"></td><td colspan="7">Category “cooling of the fuel”</td></tr>
<tr><td>1</td><td>1a</td><td>1b</td><td>2</td><td>2a</td><td>2b</td><td>3</td></tr>
<tr><td>rating</td><td colspan="3">The shutdown of the reactor should be ensured.
Requirement for the residual heat removal can be waived</td><td colspan="3">In case of loss of coolant, systems for refilling the reactor pool shall be provided.</td><td>Generally applicable</td></tr>
</table>

<table>
<tr><td>Requirement</td><td colspan="7">3.3 (5) Even in case of a loss of the primary heat sink as a result of loss of functions in the area of the circulating water intakes and returns, residual heat removal from the plant shall be ensured under all operating states by a diverse heat sink (possibly also by different heat sinks in combination). The equipment needed for this purpose shall satisfy at least the requirements for internal accident management measures; their effectiveness shall be demonstrated.
The availability of this diverse heat sink shall also be ensured in the event of external hazards.</td></tr>
<tr><td rowspan="2"></td><td colspan="7">Category “cooling of the fuel”</td></tr>
<tr><td>1</td><td>1a</td><td>1b</td><td>2</td><td>2a</td><td>2b</td><td>3</td></tr>
<tr><td>rating</td><td colspan="3">Requirement can be waived</td><td colspan="3">In case of loss of coolant, systems for refilling the reactor pool shall be provided.</td><td>Generally applicable</td></tr>
</table>

Tab. 5: Examples for the application of the classification scheme in order to apply a grading to the Safety Requirements.

The rating on the application of the requirement is split into three case: waiving of the requirement is marked in red in the table, suggested modifications of the requirement are marked in yellow and if the requirement is generally applicable, it is marked in green.

For example, three different ratings were obtained for the requirements 3.3 (3) to 3.3 (5) which reflects the core configurations of the different research reactors. The fuel of the SUR and AKR-2 reactors is cooled by air and a loss of coolant accident is therefore not a credible accident. Hence, the rating for categories 1, 1a and 1b is “requirement can be waived”. For category 2, natural convection of the water in the reactor pool is sufficient to remove the residual heat of the shutdown reactor. Therefore, care has to be taken that the core is always covered with water. For the highest category, the requirement is fully applicable.

Tab. 5 includes the proposal of waiving of requirements, especially for cooling categories 1, 1a and 1b, i.e. zero power reactors. This is in line with SSG-22 which allows explicitly a waiving of requirements (1.10) with reference to the then up-to date NS-R-4 [17]. In 2016, the NS-R-4 was superseded by the SSR-3 guide which now states in para. 6.18 that “the use of a graded approach in the application of the safety requirements shall not be considered as a means of waiving safety requirements…” [1]. Both guides, NS-R-4 and SSR-3, establish requirements specifically for research reactors. However, in Germany no dedicated regulatory framework for research reactors exists. Hence, a possible grading has to be performed on the requirements for power reactors. Especially with respect the zero power reactors where the thermal power is in the order of 1E+09 lower than for a nuclear power plant waiving of selected requirements may nevertheless be justified.

4. Conclusion

An extensive study of the international practice of the application of the graded approach to research reactors was performed and a proposal dedicated to the German research reactor landscape was developed. In this proposal, special emphasis was placed on the risk potential through the introduction of the categories “utilisation of the research reactor”, the different needs for the cooling of the fuel, ranging from air cooling in case of the SUR to an active cooling of the core after shutdown of the reactor are reflected in the “cooling of the fuel” category and the radiological impact on the public and the environment is accounted for in the category “confinement of radioactive material”.
The suggested classification scheme provides a structured and reproducible approach for a

classification of the German research reactors. This classification which can be visualised in a “grading matrix” allows possible grading of the German Safety Requirements for Nuclear Power Plants for the application of these requirements to research reactors as can be seen from the examples given.

Acknowlegement

The work presented in this article is supported by the Project 4717R01367 “Forschungsarbeiten zur Anwendung des kerntechnischen Regelwerks auf Forschungsreaktoren” funded by the German Ministry of Environment, Nature Conservation, and Nuclear Safety (BMU).

5. References

[1] International Atomic Energy Agency, Safety of Research Reactors, Specific Safety Requirements SSR-3, IAEA, Vienna (2016).

[2] International Atomic Energy Agency, IAEA Safety Standards, Use of a Graded Approach in the Application of the Safety Requirements for Research Reactors, Specific Safety Guide SSG-22, Vienna, IAEA (2012).

[3] Lynch, S., Adams, J., Adams, A.: Assessment of Lessons Learned from the Fukushima Dai-ichi Nuclear Accident to Research and Test Reactors in the United States, Proceedings of the 18th meeting of the International Group on Research Reactors, December 2017, Sydney, Australia.

[4] U.S.NRC, Guidelines for Preparing and Reviewing Applications for the Licensing of Non-Power Reactors (NUREG-1537), February 1996.

[5] The Application of Minimum Regulation to Research and Test Reactors at the U.S. Nuclear Regulatory Commission, annual meeting of the National Organization of Test, Research, and Training Reactors, September 21, 2017.

[6] Canadian Nuclear Safety Commission CNCS RD-367: Design of Small Reactor Facilities, June 2011.

[7] Dutch Safety Requirements for Nuclear Reactors: Fundamental Safety Requirements, ANVS, 8. October 2015.

[8] de Bellabre, C., et al.: Reassessment of research reactors - the approach implemented by IRSN based on the so-called "graded approach" and taking into account the first lessons learned from the Fukushima events. Proceedings des 14th IGORR 2012, Prague, Czech Republic.

[9] IAEA Safety Reports No. 53 “Derivation of the Source Term and Analysis of the Radiological Consequences of Research Reactor Accidents”.

[10] German Commission on Radiological Protection: Basic Radiological Principles for Decisions on Measures for the Protection of the Population against Incidents involving Releases of Radionuclides, February 2014.

[11] Sicherheitsbericht für den Ausbildungskernreaktor AKR-2 der TU Dresden, August 2002.

[12] Ordinance on the Protection against Damage and Injuries Caused by Ionizing Radiation (Radiation Protection Ordinance) of 20 July 2001, last Amendment of 26 July 2016.

[13] Stellungnahme zu den radiologischen Auswirkungen eines Flugzeugabsturzes auf den Forschungsreaktor TRIGA Mainz, TÜV Rheinland, November 2012.

[14] Sicherheitsgutachten für die Leistungserhöhung auf 10 MW des Forschungsreaktors BER II der Hahn-Meitner-Institut für Kernforschung Berlin GmbH, GRS-A-1080, April 1985.

[15] Gutachten über die Sicherheit des Forschungsreaktors München II (FRM-II), Standort Garching für das atomrechtliche Genehmigungsverfahren Gutachten zur Konzeption der Anlage (Konzeptgutachten), März 1996.

[16] Safety Requirements for Nuclear Power Plants, Federal Environment Ministry, March 2015.

[17] International Atomic Energy Agency, Safety of Research Reactors, IAEA Safety Standards Series No. NS-R-4, IAEA, Vienna (2005).

PRODUCTION OF ULTRACOLD NEUTRONS AT THE RESEARCH REACTOR TRIGA MAINZ

K. EBERHARDT, C. GEPPERT, C. GORGES, S. KARPUK,
J. RIEMER, D. RIES, K. ROSS
Institut für Kernchemie, Johannes Gutenberg-Universität Mainz
Fritz-Strassmann-Weg 2, 55128 Mainz – Germany

ABSTRACT

The TRIGA reactor at the Johannes Gutenberg-Universität Mainz is one of currently three German research reactors with a thermal power exceeding 50 kW. In steady-state mode the power level ranges from 100 mW_{th} up to 100 kW_{th}. Pulse-mode operation is also possible with a maximum peak power of 250 MW_{th}, a neutron flux of 10^{15} cm^{-2} per pulse and 30 ms pulse width. Two beam ports at the TRIGA Mainz are reserved for the production of ultra-cold neutrons (UCN) to determine fundamental neutron properties. Despite the low power, TRIGA Mainz is competitive for UCN production due to the possibility to pulse the reactor every five to ten minutes to produce a high density of UCN. With a super-thermal UCN source a density of 8.5 UCN cm^{-3} in a 32 liter storage volume has been achieved. Pulse mode is ideally suited for storage experiments, where the neutron storage trap has to be filled in similar cycles.

1. Introduction

Founded already in 1477 and named after the famous fifteenth-century printer who revolutionized printing with movable letters in Europe, the Johannes Gutenberg-Universität Mainz (JGU) is one of the largest universities in Germany. The university offers a wide research area, including the natural sciences, humanities, social studies, law, economics and medicine. The campus also hosts two Max-Planck-Institutes (MPI for Chemistry and MPI for Polymer Research), the electron accelerator facility MAMI and a research reactor type TRIGA Mark II [1]. On the 3rd of August 1965, the TRIGA Mainz became first critical with the insertion of the 57^{th} fuel element in the reactor core. Since this time the TRIGA Mainz has operated failure-free during about 200 days per year except a short break for a complete refurbishment of the cooling and purification circuits and the cooling tower in 1995. Since more than 50 years, the reactor is intensively used for basic research in nuclear chemistry and -physics, applied science as well as for educational purposes. The educational program is fully integrated into the curriculum of the faculties of Chemistry and Physics of JGU. TRIGA reactors are the most widely used research reactors in the world with steady state power levels ranging from 20 kW_{th} to 16 MW_{th} [1]. The research reactors of the TRIGA type [1,2] are light water cooled reactors using fuel-moderator elements composed of an alloy of uranium-zirconium-hydride (UZrH) with mostly below 20% enrichment in ^{235}U. TRIGA reactors offer inherent safety features due to the physical properties of the UZrH fuel-matrix [3-6], that gives the TRIGA core a large prompt negative temperature coefficient. Power rises initiated by the rapid insertion of even the total available excess reactivity, are automatically suppressed, and the reactor immediately returns to normal operating levels. Here, the so-called “warm neutron principle” [1,6] is used, where the moderation of neutrons is due to the hydrogen that is mixed with the fuel itself. Therefore, as the fuel temperature increases when a control rod (pulse rod) is suddenly removed, the hydrogen atoms inside the fuel rod gain more and more vibrational energy and consequently neutron moderation inside the fuel becomes less effective and the fission rate goes down. Due to the corresponding reactivity loss the reactor automatically reduces power within a few thousandths of a second, much faster than any engineered device can operate [3,7].

2 Reactor operation

The TRIGA Mainz is a swimming pool reactor with a graphite-reflected core placed inside an aluminum tank with a diameter of 2 m and a height of 6.25 m. The surrounding concrete biological shield and the de-mineralized water in the pool provide the required radiation shielding. The fuel-moderator elements are fixed in the core with a top and bottom grid plate containing 91 positions loaded with the fuel-moderator elements, control-rod guide tubes or irradiation channels and graphite dummy elements. Currently, the reactor core is equipped with 76 fuel elements, concentrically arranged by means of a lower and upper grid plate. For irradiations the TRIGA Mainz is equipped with a central experimental tube (central thimble), three pneumatic transfer systems (rabbit systems) and a rotary specimen rack with 40 positions which allows the irradiation of 80 samples at the same time [8]. In addition, the TRIGA Mainz includes four horizontal beam ports penetrating the concrete shielding and extending inside the pool towards the reflector. A graphite thermal column provides a source of well-thermalized neutrons suitable for physical research or biological/medical irradiations. Figure 1 shows a vertical cross section view of the TRIGA Mainz and a picture of the reactor core during operation at 100 kW power indicating the position of the core, the reflector and of various irradiation facilities together with the corresponding thermal neutron flux values (in [$cm^{-2}s^{-1}$]).

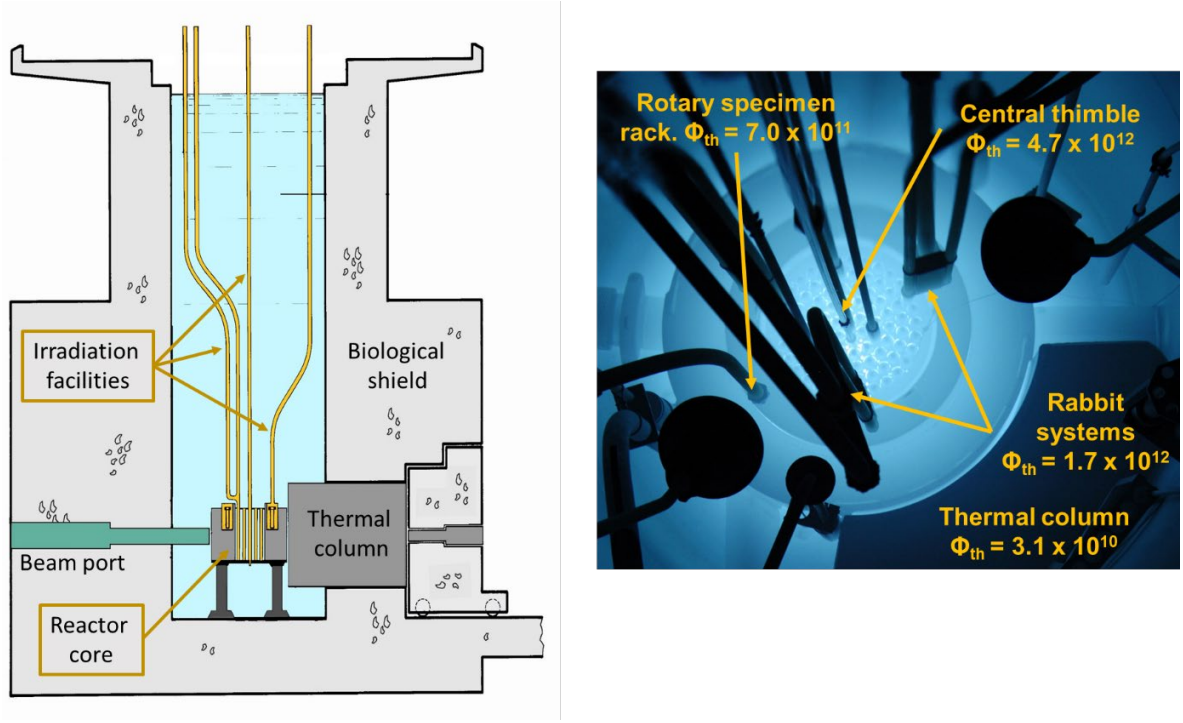

Figure 1: Vertical cross-section view of the TRIGA Mainz and picture of the reactor core during reactor operation at 100 kW power indicating the position of various irradiation facilities and corresponding thermal neutron flux values (given in [$cm^{-2}s^{-1}$]).

In steady state mode the reactor can be operated at power levels ranging from about 100 mW_{th} up to 100 kW_{th}, depending on the requirements of the different experiments. For pulse-mode operation the operation licence allows the insertion of an excess reactivity up to 2 Dollar[1], corresponding to a pulse peak power of 250 MW_{th} and a neutron flux of 10^{15} cm^{-2} per pulse, at a pulse width (FWHM) of about 30 ms [7]. For pulse mode operation, the reactor is

[1] *The term Dollar is used to denote the reactivity introduction that makes a reactor prompt critical. For the TRIGA Mainz 1 Dollar = 0.0073 [8].*

brought to criticality at a low steady state power, normally 50 W, and then a control rod is shot out of the reactor core with compressed air. Due to this sudden insertion of excess reactivity the power rises sharply with a reactor period of only a few milliseconds. With power, fuel temperature increases and in like manner neutron moderation by the UZrH-matrix becomes insufficient [1-6,7]. The pulses have a shape that can be approximated by a Gaussian function with a width at half maximum in the millisecond range. According to the operation license the maximum pulse frequency is 12 pulses per hour. So far, more than 25,500 pulses have been performed since 1965. There is no TRIGA reactor world-wide that performed more pulses. The average operation time of the TRIGA Mainz is about 200 days per year. In recent years, approx. 80% of the time is used for reactor operation at the nominal power of 100 kW_{th} and the rest for pulses, as well as for steady state operation with thermal powers ranging from 100 mW_{th} up to 100 kW_{th}. Under the typical operation conditions of the TRIGA Mainz, the burn-up is in the order of 4 g of U^{235} per year only. Thus, the TRIGA Mainz actually has a life-time core. However, a fresh fuel element is introduced about every four years in order to overcome the slow decrease of the reactivity over time.

3. Reactor utilization

Currently about 50 % of the available beam time is used for fundamental research, 25 % for applied science and 25 % for education and training, respectively. Applications include:

- TRIGA is part of the so-called Cluster of Excellence "Precision Physics, Fundamental Interactions and Structure of Matter“ (PRISMA$^+$) at the Johannes Gutenberg-University in Mainz. PRISMA$^+$ consists of leading research groups that work primarily in the areas of astro-particle, high-energy, and hadron physics, nuclear chemistry and precision physics with ultra-cold neutrons and ion traps. Beam ports C and D are reserved for the production of ultra-cold neutrons (UCN) to determine fundamental neutron properties with very high precision (see sections 4 and 5 of this contribution). Another high-precision experiment (TRIGA-TRAP) is installed at beam port B for the determination of ground-state properties of neutron-rich nuclei and actinide isotopes by means of Penning trap mass spectrometry [9-12]. TRIGA-TRAP is also part of PRISMA$^+$.

- Fast chemical separation procedures combining a gas-jet transport system installed in beam port A with either continuous or discontinuous chemical separation are being developed for the investigation of short-lived fission products and of the chemical properties of the heaviest elements [13-17].

- Neutron Activation Analysis (NAA) and isotope production for various applications in research and industry are also performed at the TRIGA Mainz [8,18-20]. For this, the rotary specimen rack, the central thimble and the rabbit systems are most often used.

- In a collaboration with the Goethe Universität in Frankfurt, Germany, neutron absorption cross sections for radioactive nuclides relevant for neutron capture processes in stars are measured. In recent experiments at the TRIGA Mainz neutron absorption experiments of the radioactive nuclei ^{60}Fe and ^{170}Tm have been performed [21,22]. During irradiation the reactor power was monitored every 10 s and showed only minor fluctuations in the order of about 0.5%.

- For education and training, various courses in nuclear and radiochemistry, reactor operation and -physics are held for scientists, advanced students, teachers, engineers and technicians.

Figure 2 shows a horizontal cross section view of the TRIGA Mainz indicating the position of the four beam ports and corresponding applications. Table 1 comprises the thermal and epithermal neutron flux for the different beam ports. At beam ports C and D sources for ultra-cold neutrons (UCN) are installed. Beam port B hosts the Penning-trap mass spectrometer facility TRIGA-TRAP.

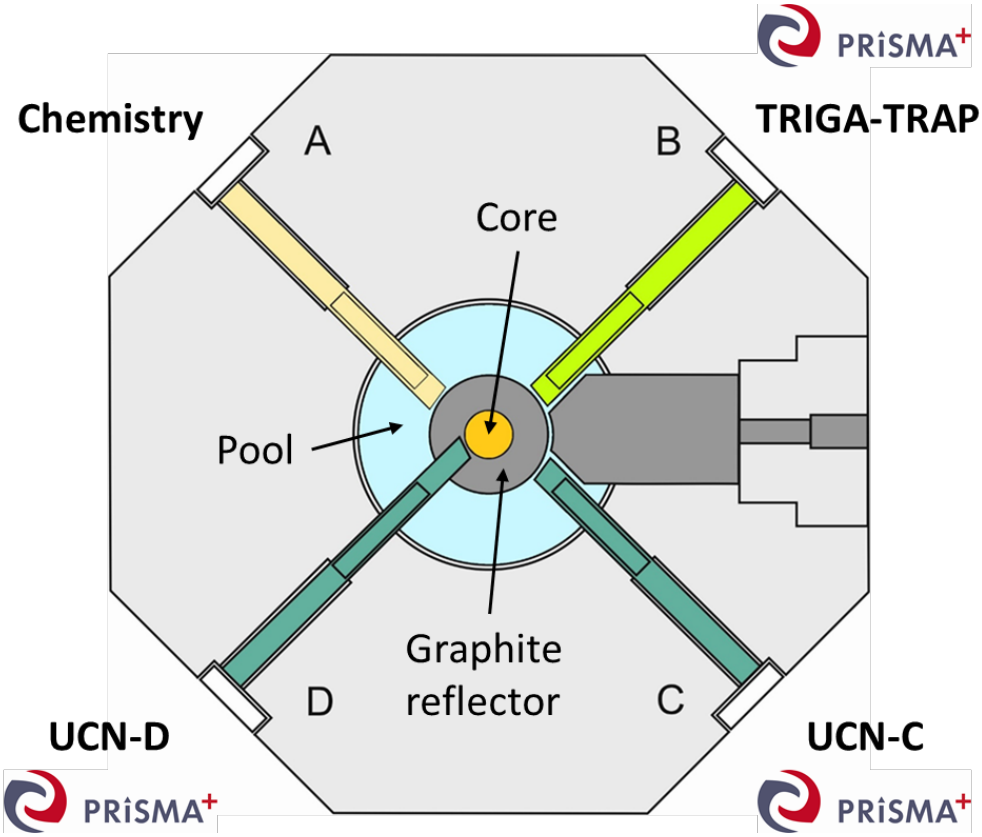

Figure 2: Horizontal cross-section view of the TRIGA Mainz showing the position of the four beam ports (A-D) and corresponding applications.

Beam port	Thermal flux[1)] [$cm^{-2}s^{-1}$]	Epithermal flux[2)] [$cm^{-2}s^{-1}$]
A	9.8×10^{10}	7.6×10^{8}
B	1.8×10^{11}	2.4×10^{9}
C	2.2×10^{11}	2.1×10^{9}
D	5.4×10^{11}	1.6×10^{10}

[1)] $E_n \leq 0.4$ eV [2)] $E_n \geq 0.4$ eV

Table 1: Thermal and epithermal neutron fluxes for the beam port positions at the TRIGA Mainz for a power of 100 kW_{th}

4. Production of ultracold neutrons (UCN)

In a beam of thermal neutrons with a kinetic energy of 0.025 eV neutrons travel with a velocity of more than 2,000 m/s. Even in cold neutron sources, e.g. in liquid H_2 or liquid D_2 at a temperature of 20-30 K, neutron velocity is still in the order of 400 m/s. Thus, in typical beam experiments observation times of only a few milliseconds are possible. In contrast, so-called ultracold neutrons with energies below 300 neV, corresponding to a velocity of only 7.6 m/s, are reflected by a number of materials at all incident angles and can be stored either in material bottles or confined by magnetic potential walls for times that approach the neutron´s ß-decay lifetime (880 s). Thus, highly precise and sensitive measurements of neutron properties are possible with UCN.

Sources for UCN are under construction at different research centers worldwide in order to tackle the existing count-rate limitations in these kinds of experiments. In close collaboration with the Institute of Physics of JGU and the Technical University of Munich (TUM) two sources for UCN have been developed and are operated at the TRIGA Mainz. Even a low-power reactor such as the TRIGA Mainz is strongly competitive for UCN production due to the possibility to pulse the reactor every twelve to fifteen minutes to produce a high density of UCN [23-26]. Pulse mode operation ideally meets the requirements of storage experiments, where the neutron storage trap has to be filled in similar cycles. With a so-called super-thermal UCN source installed at beam port D of the TRIGA Mainz [23,24] a density of 1.5 UCN per cm^3 for a storage time of 50 s was measured in a 32 liter storage volume [25] in 2015. A recent upgrade of the source resulted in a UCN density of 8.5 per cm^3 under identical experimental conditions [26]. Here, UCN are produced by the interaction of cold neutrons with a solid deuterium (sD_2) crystal kept at liquid helium temperature. In a first stage thermal neutrons as delivered from a reactor pulse are pre-moderated by means of 20 mol of solid hydrogen (sH_2) before they interact with the sD_2-crystal (8 mol). By inelastic scattering, the pre-moderated neutrons create phonon-excitations in the sD_2-matrix and thus loose further energy. UCN are then guided through the biological shield of the reactor and are fed into the specific experimental set-up placed in the reactor hall. Figure 3 shows a schematic drawing of the source, which is introduced for pulsed beam operation into beam port D (see also figure 5).

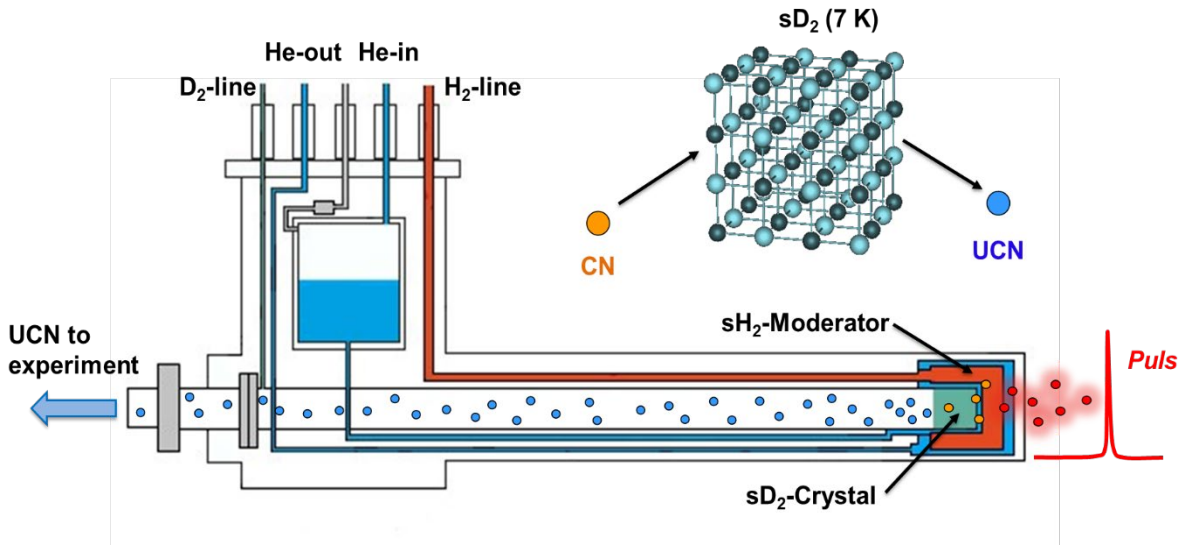

Figure 3: Schematic drawing (not to scale) of the super-thermal UCN source at the TRIGA Mainz. Thermal neutrons from a reactor pulse are pre-moderated with solid hydrogen (sH_2) and subsequently interact with a sD_2-crystal to become UCN with kinetic energies < 300 neV. The source has been developed in collaboration with the Institute of Physics at JGU.

Background interference during data taking is essentially zero for pulsed neutron beam operation since the reactor is off during the measurements between two subsequent neutron pulses. Low magnetic noise is another quality feature of this reactor. Current activities focus on the upgrade of the UCN-source to further increase the available UCN densities. Furthermore, at beam port C a similar UCN-source but without hydrogen pre-moderator is operational in 100 kW steady-state reactor mode. TRIGA Mainz and PRISMA$^+$ provide essential infrastructure to develop and sustain experiments at a facility well suited for UCN-storage experiments. A Helium-liquefier with a capacity of 14 L/h has been installed to supply the UCN sources. Figure 4 shows the available UCN-densities at the TRIGA Mainz, compared to other UCN-facilities at the reactor of the Institut Laue-Langevin (ILL) in Grenoble, France and at the spallation neutron source of the Paul-Scherrer-Institute (PSI) in Villigen, Switzerland. With the source operated at beam port C under steady-state reactor operation at 100 kW a rate of about 1000 UCN per second has been detected [27].

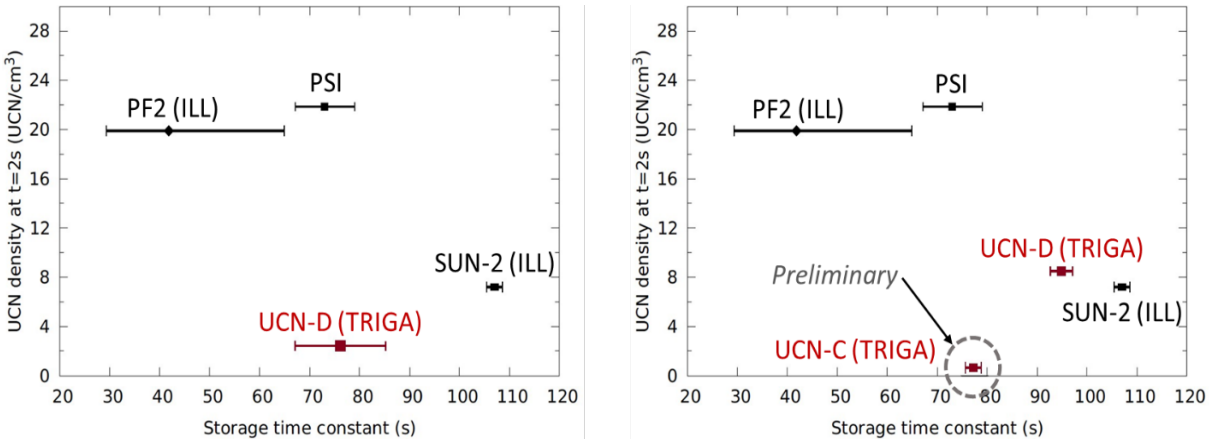

Figure 4: UCN-densities achieved at the TRIGA Mainz, compared to the UCN-facilities at the Institut Laue-Langevin (ILL) and at the Paul-Scherrer-Institute (PSI). The left graph shows the UCN density prior to the source upgrade (1.5 UCN cm^{-3}) [25], the right graph shows the current status for UCN-D (8.5 UCN cm^{-3}) [26] and UCN-C (about 1000 UCN s^{-1}). The data for UCN-C are still preliminary [27]

5. The τSPECT-experiment

One important experiment within PRISMA$^+$ at the TRIGA Mainz is the τSPECT experiment, which aims for the determination of the neutron lifetime, with high precision. The lifetime of the free neutron is of importance for precision tests of the standard model of particle physics. Besides this fundamental interest in the neutron lifetime, its re-determination is particularly relevant, since there are several precision measurements of neutron lifetime, which deviate from each other by far more than their uncertainties allow. Presently, the τSPECT experiment is being set-up in beam port area D of the TRIGA experimental hall, as shown in figure 5. τSPECT will measure the lifetime of the free neutron using the technique of neutron magnetic storage and in its final stage will be designed to detect both surviving neutrons and decay protons simultaneously. Thus, it will be possible to determine the neutron lifetime with improved control over systematic errors [28]. The current set-up is shown schematically in figure 6. UCN, as delivered from the pulsed source at beam port D, are guided into τSPECT where they are axially confined in the low field region of a superconducting magnet (see dashed red line in figure 6). Radial storage is performed with a Halbach-type octupole magnet placed inside the high-vacuum region of τSPECT in close proximity to the UCN-guide and a moveable neutron detector to measure the amount of neutrons in the storage trap. Every time after the neutrons have been counted, TRIGA performs the next pulse in order to fill τSPECT with “fresh”

neutrons. The integration and commissioning measurements for most components of τSPECT are currently under way. In a next step a measurement using full magnetic neutron storage will be performed. Then the systematic uncertainties will be investigated and optimized for a measurement of the neutron lifetime with a precision of 1 s (Phase 1). Subsequently, τSPECT will be optimized for a precision of 0.3 s (Phase 2).

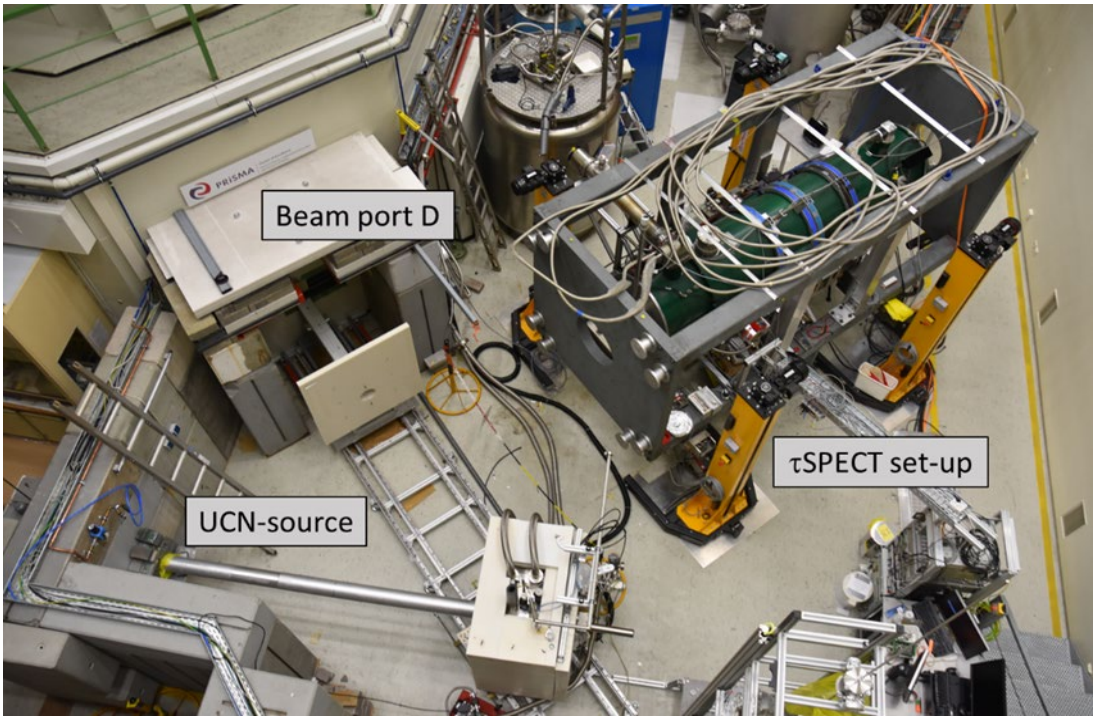

Figure 5: The τSPECT set-up at beam port D. In this picture, the UCN-source (on the bottom left) is not in use and thus extracted from the beam hole at port D. The τSPECT-facility (on the right) is mounted on four lifters (yellow pillars) in order to adjust its height to different arrangements of neutron guides that connect the UCN-source with τSPECT.

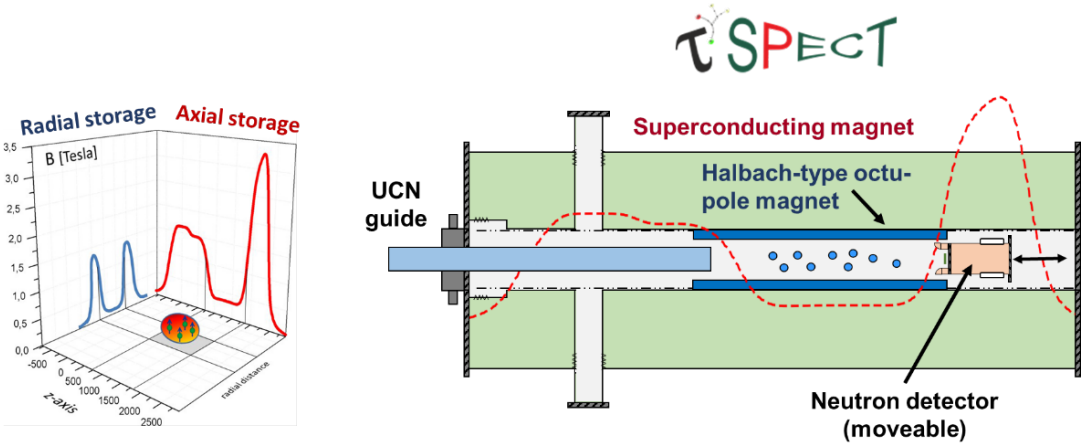

Figure 6: Schematic view of the τSPECT experiment [28]. UCN are guided into τSPECT and axially confined in the low field region of a superconducting magnet (dashed red line). For radial storage a Halbach-type octupole magnet is used. The amount of neutron in the storage trap is determined by means of a moveable neutron detector.

5. Conclusion and outlook

The research reactor TRIGA Mainz is intensively used for basic research, applied science and educational purposes. Furthermore, TRIGA is part of the so-called Cluster of Excellence "Precision Physics, Fundamental Interactions and Structure of Matter“ (PRISMA$^+$) at the Johannes Gutenberg-University in Mainz. PRISMA$^+$ consists of research groups that work primarily in the areas of astro-particle, high-energy, and hadron physics, nuclear chemistry and precision physics with ultra-cold neutrons and ion traps. Beam ports C and D of the TRIGA Mainz are reserved for the production of ultra-cold neutrons (UCN) to determine fundamental neutron properties with very high precision. For this, TRIGA Mainz and PRISMA$^+$ provide essential infrastructure to develop and sustain experiments at a facility well suited for UCN-storage experiments. Currently the τSPECT experiment dedicated to measure the lifetime of the free neutron is installed at beam port D.
Recently it was decided that the reactor will be operated at least until the year 2030. This decision was mainly made in connection with the research work performed and planned at the TRIGA Mainz and the training of students in the fields of nuclear chemistry, nuclear physics and radiation protection. Taking into account the past and future operation schedule and the typically low burn-up of TRIGA fuel elements, the reactor can be operated for more than the next decade with the fresh fuel elements on stock and without changing spent fuels.

6. References

[1] IAEA Technical Report Series No. 482, *History, Development and Future of TRIGA Research Reactors*, International Atomic Energy Agency, Vienna (2016)

[2] Koutz, S.L., Taylor, T., McReynolds, A.W., Dyson, F., Stone, R.S., Sleeper, H.B., Duffield, R.B.: *Design of a 10 kW Reactor for Isotope Production, Research and Training Purposes*. In: Proc. 2nd U.N. Intern. Conf. Peaceful Uses of Atomic Energy, 1017 (1958)

[3] Stone, R.S., Sleeper, H.P., Stahl, R.A., West, G.: *Transient Behaviour of TRIGA, a Zirconium-Hydride, Water - Moderated Reactor.* Nuclear Science and Engineering 6, 255 (1959)

[4] Merten, U., Dijkstra, L.J., Zimmermann, F.D., Hatcher, A.P., LaGrange, L.D.: *The Preparation and Properties of Zirconium-Uranium-Hydrogen Alloys*. In: Proc. 2nd U.N. Intern. Conf. Peaceful Uses of Atomic Energy, 789 (1958)

[5] McReynolds, A.W., Nelkin, M.S., Rosenbluth, M.N., Whittemore, W.L.: *Neutron Thermalization by Chemically-bound Hydrogen and Carbon*. In: Proc. 2nd U.N. Intern. Conf. Peaceful Uses of Atomic Energy, 1540 (1958)

[6] Dyson, F.: *The little red schoolhouse*. In: Disturbing the Universe, Basic Books, New York, (1979) pp. 94-103

[7] Menke, H., Trautmann, N., Krebs, W.J.: *Irradiations by means of Reactor Pulses*. Kerntechnik 17, 281 (1975)

[8] Eberhardt, K., Trautmann, N.: *Neutron Activation Analysis at the TRIGA Mark II research Reactor of the University of Mainz.* In: Utilization Realated Design Features of Research Reactors - A Compendium, International Atomic Energy Agency Technical Report Series No. 455, Vienna (2007)

[9] Ketelaer, J., Krämer, J., Beck, D., Blaum, K., Block, M., Eberhardt, K., Eitel, G., Ferrer, J., Geppert, C., George, S., Herfurth, F., Ketter, J., Nagy, Sz., Neidherr, D.,

Neugart, R., Nörtershäuser, W., Repp, J., Smorra, C., Trautmann, N., Weber, C.: *TRIGA-SPEC: A setup for mass spectrometry and laser spectroscopy at the research reactor TRIGA Mainz*. Nucl. Instr. Meth. A594, 162 (2008)

[10] Eibach, M., Beyer, T., Blaum, K., Block, M., Eberhardt, K., Herfurth, F., Geppert, C., Ketelaer, J., Ketter, J., Krämer, J., Krieger, A., Knuth, K., Nagy, Sz., Nörtershäuser, W., Smorra, C.: *Transport of fission products with a helium gas-jet at TRIGA-SPEC.* Nucl. Instrum. Methods A613, 226 (2010)

[11] Eibach, M., Beyer, T., Blaum, K., Block, M., Düllmann, Ch.E., Eberhardt, K., Grund, J., Nagy, Sz., Nitsche, H., Nörtershäuser, W., Renisch, D., Rykaczewski, K.P., Schneider, F., Smorra, C., Vieten, J., Wang, M., Wendt, K.: *Direct high-precision mass measurements on ^{241}Am, ^{243}Am, ^{244}Pu, and ^{249}Cf.* Phys. Rev. C 89, 064318 (2014)

[12] Grund, J., Düllmann, Ch.E., Eberhardt, K., Nagy, Sz., van der Laar, J., Renisch, D., Schneider, F.: *Implementation of an aerodynamic lens for TRIGA-SPEC.* Nucl. Instrum. Meth. Phys. Res. B 376 (2016)

[13] Altzitouglou, T., Rogowski, J., Skålberg, M., Alstad, J., Herrmann, G., Kaffrell, N., Skarnemark, G., Talbert, W., Trautmann, N.: *Fast Chemical Separation of Technetium from Fission Products and Decay Studies of ^{109}Tc and ^{110}Tc*. Radiochim. Acta 51, 145 (1990)

[14] Schoedder, S., Lhersonneau, G., Wöhr, A., Skarnemark, G., Alstad, J., Nähler, A., Eberhardt, K., Äystö, J., Trautmann, N., Kratz, K.-L.: *Level Lifetimes in Neutron Rich Ru Isotopes*. Z. Phys. A352, 237 (1995)

[15] Lhersonneau, G., Pfeiffer, B., Alstad, J., Dendooven, P., Eberhardt, K., Hankonen, S., Klöckl, I., Kratz, K.-L., Malmbeck, R., Omtvedt, J.P., Penttila, H., Schoedder, S., Skarnemark, G., Trautmann, N., Aystö, J.: *Spape Coexistence Near the Double-Midshell Nucleus ^{111}Rh*. Eur. Phys. J. A1 (1998) 285

[16] Alstad, J., Skarnemark, G., Haberberger, F., Herrmann, G., Nähler, A., Pense-Maskow, M., Trautmann, N.: *Development of New Centrifuges for Fast Solvent Extraction of Transactinide Elements*. J. Radioanal. Nucl. Chem. 189, 133 (1995)

[17] Even, J., Yakushev, A., Düllmann, C. E., Dvorak, J., Eichler, R., Gothe, O., Hartmann, W., Hild, D., Jäger, E., Khuyagbaatar, J., Kindler, B., Kratz, J.V., Krier, J., Lommel, B., Niewisch, L., Nitsche, H., Pysmenetska, I., Schädel, M., Schausten, B., Türler, A., Wiehl, N., Wittwer, D.: *In-situ formation, thermal decomposition, and adsorption studies of transition metal carbonyl complexes with short-lived radioisotopes.* Radiochim. Acta 102, 1093 (2014)

[18] Hampel J., Boldt, F.M., Gerstenberg, H., Hampel, G., Kratz, J.V., Reber, N., Wiehl, N.: *Fast determination of impurities in metallurgical grade silicon for photovoltaics by instrumental neutron activation analysis.* Appl. Rad. Isotopes 69, 1365 (2011)

[19] Conejos-Sanchez, I., Hampel, G., Zauner, S., Riederer, J.: *Reverse paintings on glass - A new approach for dating and localization.* Appl. Rad. Isotopes 67, 2113 (2009)

[20] Stieghorst, C., Hampel, G., Zauner, S., Plonka-Spehr, C.: *Archäometrie mittels instrumenteller Neutronenaktivierungsanalyse am Forschungsreaktor TRIGA Mainz.* METALLA, Sonderheft 5: Archäometrie und Denkmalpflege (2012)

[21] Heftrich, T., Bichler, M., Dressler, R., Eberhardt, K., Endres, A., Glorius, J., Göbel, K., Hampel, G., Heftrich, M., Käppeler, F., Lederer, C., Mikorski, M., Plag, R., Reifarth, R., Stieghorst, C., Schmidt, S., Schumann, D., Slavkovská, Z., Sonnabend, K., Wallner, A., Weigand, M., Wiehl, N., Zauner, S.: *Thermal neutron capture cross section of the radioactive isotope ^{60}Fe.* Phys. Rev. C92, 015806 (2015)

[22] Weigand, M., Heftrich, T., Düllmann, Ch.E., Eberhardt, K., Fiebiger, S., Glorius, J., Göbel, K., Haas, R., Langer, C., Lohse, S., Reifarth, R., Renisch, D., Wolf, C.: *66.7 keV γ-line intensity of ^{171}Tm determined via neutron activation.* Phys. Rev. C97, 035803 (2018)

[23] Frei, A., Sobolev, Yu., Altarev, I., Eberhardt, K., Gschrey, A., Gutsmiedl, E., Hackl, R., Hampel, G., Hartmann, F.J., Heil, W., Kratz, J.V., Lauer, TH., Lizon Aguilar, A., Mäller, A.R., Paul, S.,Pokotilovski, YU., Schmid, W., Tassini, L., Tortorella, D., Trautmann, N., Trinks, U., Wiehl, N.: *First production of ultracold neutrons with a solid deuterium source at the pulsed reactor TRIGA Mainz*. Eur. Phys. J. A 34, 119 (2007)

[24] Karch, J., Sobolev, Yu., Beck, M., Eberhardt, K., Hampel, G., Heil, W., Kieser, R., Reich, T., Trautmann, N., Ziegner, M.: *Performance of the solid deuterium ultra-cold neutron source at the pulsed reactor TRIGA Mainz*. Eur. Phys. J. A50, 78 (2014)

[25] Lauss, B., Bison, G., Daum, M., D. Ries, D., Schmidt-Wellenburg, P., Zsigmund, G., Brenner, T., Geltenbort, P., Jenke, T., Zimmer, O., Beck, M., Heil, W., Kahlenberg, J, Karch, J., Ross, K., Eberhardt, K., Geppert, C., Karpuk, S., Reich, T., Siemensen, C., Sobolev, Yu., Trautmann, N.: *Comparison of ultracold neutron sources for fundamental physics measurements.* Phys. Rev. C95, 045503 (2017)

[26] Kahlenberg, J., Ries, D., Ross, K.U, Siemensen, C., Beck, M., Geppert, C., Heil, W., Hild, N., Karch, J., Karpuk, S., Kories, F., Kretschmer, M., Lauss, B. Reich, T., Sobolev, Yu., Trautmann, N.: *Upgrade of the ultracold neutron source at the pulsed reactor TRIGA Mainz*. Eur. Phys. J. A53, 226 (2017)

[27] Ries, D.: Private communication

[28] Karch, J.: PhD-Thesis, Johannes Gutenberg-Universität Mainz (2017)

IS THERE A LIMIT FOR LEU MO PLATE IRRADIATION IN DOWNWARD FLOW?

A. S. DOVAL, F. SARDELLA
INVAP S.E. Comandante Luis Piedrabuena 4950, 8400 San Carlos de Bariloche, Río Negro, Argentina

I. GUIRADO
Instituto Balseiro, Universidad de Cuyo, Av. E. Bustillo km 9,500, R8402AGP, San Carlos de Bariloche, Rio Negro, Argentina

ABSTRACT

The last years the demand on medical radioisotope Mo99 was in constant increase together with the ageing of main "producer" research reactors of this radioisotope. From the production point of view, the more efficiently the Mo99 is obtained the better. For these reasons the focus is addressed in obtaining large amounts of Curies per plate which is strictly related with the power generated in the Mo plate, resulting in a maximum allowable heat flux. From the thermal-hydraulic point of view this requirement becomes a real challenge in the design of a Mo plate holder allowing the removal of large heat fluxes, mainly, for the case of coolant flowing downwards through the holder. This study presents an assessment on the effects on heat removal when enlarging the coolant gap between the Mo plates and to keep in mind that the pressure loss distribution in the rig has to be considered.

1. Introduction

The last years the demand on Mo99 as a medical radioisotope was in constant increase in parallel with the ageing of main "suppliers" research reactors of this radioisotope. As shown in Tab 1, most of the main suppliers are reaching the end of their lives in the coming decade which results in an increasing interest on the construction of new reactors as replacement. Such was the case of the Australian reactor (OPAL) and such is the case of the Dutch project reactor (PALLAS).

Reactor	Country	Power (MW)	Commissioning date	Expiration date	Global contribution %
BR-2	Belgium	100	1961	2026	20
HFR	Netherland	45	1961	2024	20
LVR-15	Czech Republic	10	1957	2028	10
Maria	Poland	30	1974	2030	10
NRU	Canada	135	1957	2018(*)	20
OPAL	Australia	20	2006	2055	10
Safari-1	South Africa	20	1965	2030	10

(*) already closed

Tab 1: Summary of main suppliers of Mo plates

It is clear that it is necessary to increase the Curies per plate in a more efficient way. This objective impacts directly on the power generated in the Mo plate, or better speaking, in the maximum heat flux that can be removed avoiding critical heat flux and fulfilling the design criteria adopted.

Regardless the fact of reaching a neutronic design to fulfil this production demand, there is a real challenge from the thermal-hydraulic point of view, regarding the cooling aspects of these plates.

The present analysis is focused on the thermal-hydraulic design of the Mo targets as the design of a reactor core providing the required neutron flux for irradiation does not seem to entail unsolved difficulties.

On dealing with the thermal-hydraulic assessment one of the first points to define is the direction of the coolant flow, upward or downward flow. In order to take a decision it is important to identify some of the "pros" and "cons" in each case. Tab 2 summarizes these differences.

	Flow direction	
	Upward	Downward
Pool access	Could be overcrowded	Clean access
Rig fixation	Special clamp to avoid withdrawal	Simple geometry
Loading/unloading	Reactor shutdown/sealed rig	During reactor operation
Coolant velocity	No restriction except vibration/erosion/critical velocity	Limited by available pressure drop
Heat flux	Not limited by coolant velocity	Limited by coolant velocity
Loss of Power Supply	No flow reversal	Flow reversal

Tab 2: "Pros" and "cons" regarding coolant flow direction

It is clear that it cannot be strongly concluded which flow direction is better. As the goal of the present study is to find out the limits in the heat flux, the assessment will be based on downward flow.

2. Analysis

It is well understood that the driver in the Mo production is the power that can be generated and it is related with the maximum heat flux that can be removed in the Mo targets and this last one with the coolant velocity and operation conditions.

The analysis consists in calculating the maximum coolant velocity between two plates to estimate the maximum heat flux that can be removed using a simple model and general assumptions for both coolant directions.

From the thermal-hydraulic point of view the larger the gap between the Mo plates the higher the coolant velocity that can be reached to fulfil the maximum available pressure drop.

3. Model and assumptions

The model adopted to calculate the coolant velocity is that of a coolant channel surrounded by two "generic" Mo plates, as shown in Fig 1.

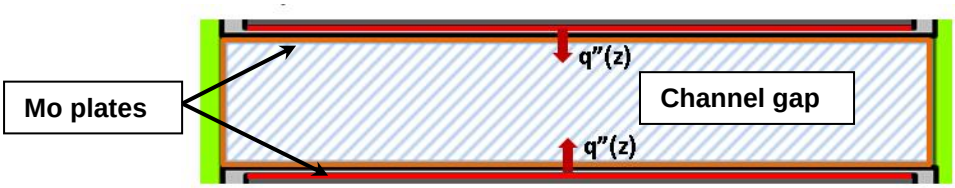

Fig 1: Calculation model

The analysis is performed for typical operational conditions considering that plates are placed in an irradiation position, in an open pool research reactor.

The first point is to calculate the maximum allowable coolant velocity, for a coolant flow moving downwards, as a function of the maximum "available" pressure drop in the plates ($\boldsymbol{DP_{plate}}$), for several channel gaps.

The channel gap was varied between 2 mm up to 10 mm, regardless any neutronic optimization. The minimum gap was adopted based on fuel assemblies gaps and the maximum value was defined arbitrarily.

Only the pressure loss due to friction over the walls of the Mo plates is considered. As the pressure drop depends on the inlet pressure to the channel, i.e., the height of the water column at the entrance of the channel, a maximum "available" DP_{plate} of 70 kPa is considered to avoid sub-atmospheric pressure at channel exit.
It is worth to notice that the plates are placed in a holder inside a rig, generating an additional pressure drop. To assess the impact on the coolant velocity and, consequently, on the heat flux due to the pressure losses in the rest of the rigs, besides of the Mo plates, a value of 35 kPa was considered, as well.

The figure of merit adopted for the assessment is the heat flux leading to Onset of Nucleate Boiling ($q"_{ONB}$).
The $q"_{ONB}$ was calculated with TERMIC code [1], an in-house developed code validated for rectangular channels [2], considering uncertainties.

Tab 3 presents a summary of this data.

Parameter	Description
Coolant	Light water
Flow direction	Downwards
Pressure drop in the plates	35 and 70 kPa
Mo plate dimensions for a generic plate	(36 x 130 x 2) mm^3
Channel gap	2 to 10 mm

Tab 3:Main data for the model and assumptions

4. Results

As previously described, the maximum velocity was calculated varying the channel gap between two Mo plates in order to estimate the maximum allowable heat flux that can be reached without exceeding ONB. This calculation was performed considering the two values adopted for the pressure drop, 35 kPa and 70 kPa. Fig 2 shows these results.

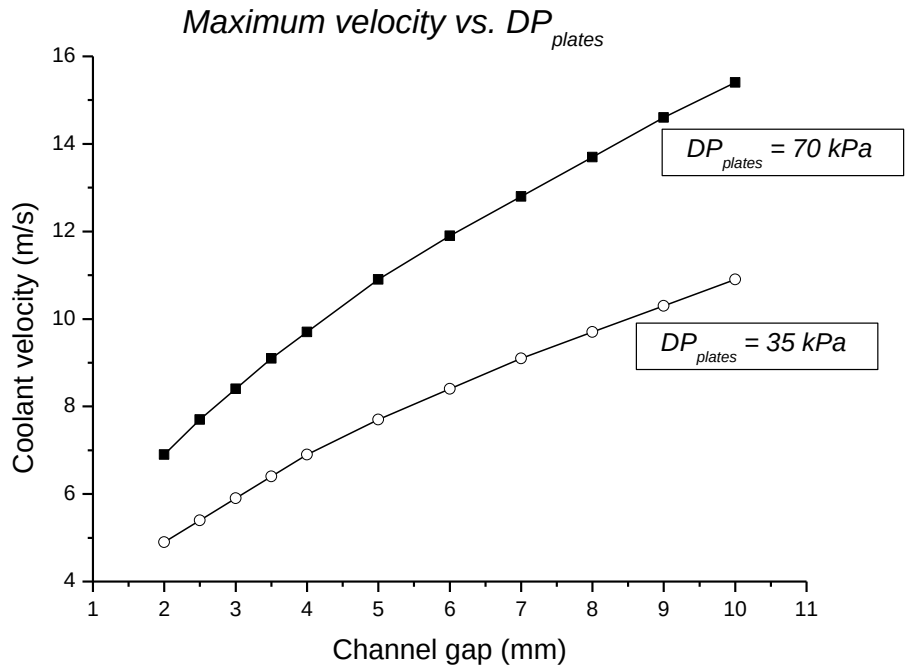

Fig 2: Maximum velocitiy vs. channel gap

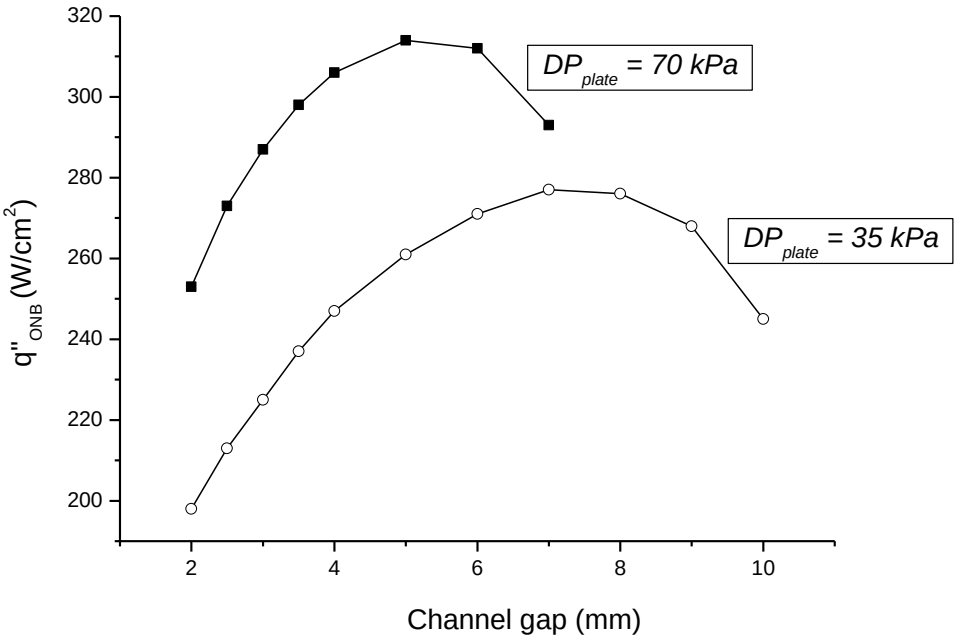

Fig 3: Maximum heat flux vs. channel gap

Fig 3 shows this behaviour for the $q"_{ONB}$, calculated for the two adopted values of DP_{plates}.

Although the calculated values give high velocities, always increasing (Fig 2), this behaviour is not the same when the heat flux is observed (Fig 3) and this is the consequence of the DP_{plate}.

The heat flux has a maximum depending on the available pressure drop as a consequence of the friction losses that grow up with coolant velocity in the channel. This value is between 7 and 8 mm, for a pressure drop of 35 kPa, and around 5 mm for a pressure drop of 70 kPa. Higher DP_{plates}, results in higher maximum heat flux. In other words, it means to design a rig optimizing the pressure drop distribution in the rest of components that are not the plates.
Needless to say that there are other constraints in the dimensions of these gaps, neutronic and mechanical, for example, regarding the available space for irradiation around the core.

Another interesting result is that, although the gaps are large (8 mm or more) and high velocities can be achieved, (for example 14 m/s), the pressure at the exit of the channel is so low, due to the pressure loss, that bubbles can appear due to cavitation or due to low saturation temperatures.

It is clear that the results presented in Fig 3 are intended to stress the idea that there is a limit on the heat flux that can be removed in Mo targets for a flow in downward direction.
For the sake of comparison, Fig 4 shows the $q"_{ONB}$ calculated for the same gaps and maximum coolant velocities, for downwards and upwards flow direction and for a DP_{plates} of 35 kPa.

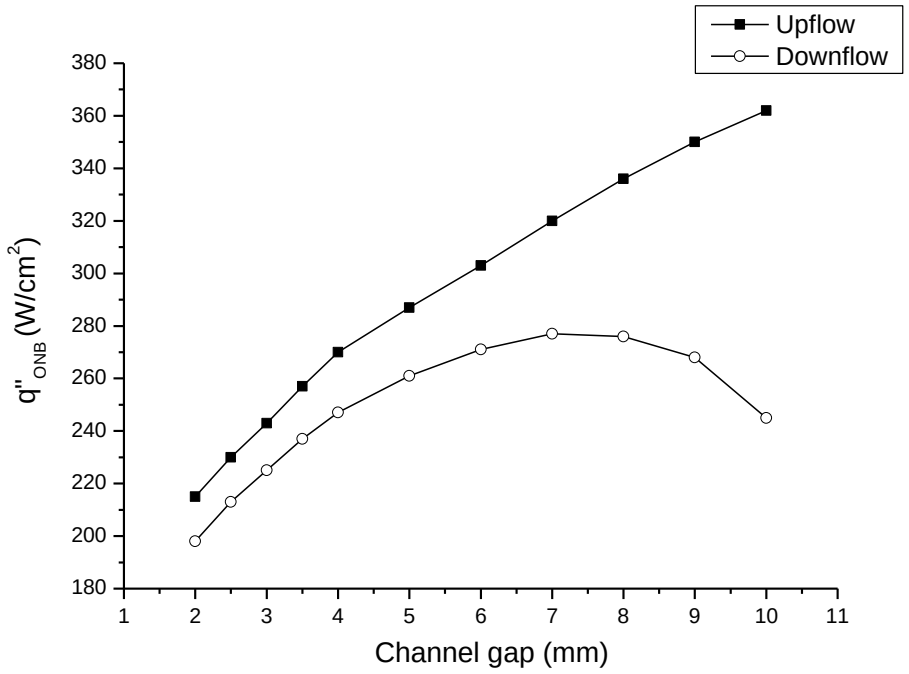

Fig 4: Maximum heat flux for upward and downward flow

5. Conclusions

There is a general consensus on the growing demand of Mo99 radioisotope production and, as a consequence of this, an increase in the power generated in the targets, leading to different designs and cooling configurations regarding the power removal of the plates.

Almost there is no doubt that there are no limits on the heat flux that can be achieved with the coolant flowing upwards but, the routine loading/unloading operations that could demand the shutdown of the reactor or a dedicated “sealed” cooling for each position resulting in an overcrowded pool appear as a disadvantage.

The present assessment is focused on the thermal-hydraulic aspects related to downward flow that, although it is not the ideal solution, developing a good design could allow large heat fluxes besides the advantages that downward flow presents.

Two aspects were considered in this analysis, the coolant gap between the plates and the pressure loss. The evaluation of these aspects leads to the following conclusions:

- Large gaps allow high coolant velocities and, as a consequence, high heat fluxes at the expense of large pressure losses.
- Optimization of the design of the rig is desirable to allow high pressure losses in the plates region
- Additional aspects, such as plate dimensions and available space for the rig, are important issues to define the maximum power achievable from the TH point of view

6. References

[1] 0275-DELC-SSITH-001, TERMIC – A program for the Thermal-hydraulic analysis of a MTR core in forced convection
[2] Validation and Verification of the MTR_PC thermo-hydraulic package, International Meeting on Reduced Enrichment for Research and Test Reactors, October 18 - 23, 1998, Sao Paulo, Brazil

Activation computation for MINERVE cleanup and dismantling

G. RITTER*
CEA, DEN, SPRC, F - 13108 St Paul-lez-Durance
** Tel: +33 (0) 442 254 180, Email: Guillaume.Ritter@CEA.Fr*

ABSTRACT

MINERVE was a French nuclear reactor mock up facility operated by the French Atomic Energy Commission, CEA.

It is now facing decommissioning and dismantling which requires an assessment of activation

Activation computations are based on a realistic model of the reactor including the main components of civil engineering.

The computations were performed with CEA code TRIPOLI4® for neutron transport and CEA DARWIN 2.3 reference evolution package for activation. Nuclear data came from EAF and JEFF3.1.1.

The neutron transport was made in two consecutive steps. First a criticality calculation to determine the leakage off the core and second a shielding calculation to propagate neutrons towards structural materials.

Eventually, the activation and decay process, computed with CEA DARWIN package, helped determine activities around the core.

The core power was limited to 100 W and the water layer between core and peripheral structural materials thick enough so that activities after 40 years of operations remain limited.

The goal of this study is to present the means to compute the specific neutron activation in the civil engineering.

1. Introduction

MINERVE was a nuclear reactor mock up facility, mostly dedicated to the experimental characterization of PWR's and BWR's [1]. It started operations in the sixties and is now ready for retirement.

The French Atomic Energy Commission, CEA, managed operations during the initial 50 years and is now facing decommissioning and dismantling. This new phase requires an assessment of activation, so that doses to personnel and activated inventories be evaluated and help make decisions in order to organize the project. For instance, some of the results may support decisions about keeping some parts of the facility or sending it to the waste disposal.

Activation computations are based on a realistic geometrical model of the reactor including reflectors and the main components of civil engineering.

The computations were performed with CEA Monte-Carlo TRIPOLI4® [2] for neutron transport and CEA DARWIN 2.3 [3] reference evolution package for activation.

The goal of this study is to present the means to compute neutron activation in the civil engineering of MINERVE. It has been used in the safety case for dismantling.

Dose rates are not evaluated here.

A synthesis of the study is given into the conclusion.

2. Reactor general description

MINERVE is located at the Cadarache Laboratory of CEA, in the south of France. It operated in the Experiments Section, Reactor Studies Department, Nuclear Energy Division of CEA, the French Atomic and Alternative Energies Commission.

The MINERVE facility [1] operated in the field of experimental Light Water Reactor (LWR) neutron physics. The maximum power was set to 100 W.

It first reached criticality in 1959 at Fontenay-Aux-Roses laboratory of CEA. Then it was moved to Cadarache, where a new campaign started in 1977.

It's a pool type reactor cooled by natural convection, as the core is located 3 m below the surface of water. The total water height in the pool is about 4.5 m. The core is made of an outer neutron feed zone with enriched uranium plates and an inner experimental area with various set ups. The feed zone itself is surrounded by a bit more than 100 graphite reflectors in aluminum casing, with various sizes.

On the axis of the central zone, a so-called ″oscillator″, carries several types of samples (inert materials, fissile compounds with a range of actinides or neutron poisons) in order to improve the validation of basic nuclear data (*e.g.* cross sections σ).

Eventually, it has also been used as a training tool for students and core control operators all across CEA.

3. Methods

A computation scheme consists in defining a sequence of operations with one or several computer codes in order to characterize targeted physics features of a type of system.
Here is a first attempt to assess activation in MINERVE. In the long term, a computer package dedicated to decommissioning and dismantling issues is to be developed and used for better predictions [4] [5].

This computer scheme includes the 3 following steps, with associated computer codes and specific data sets :

- Core characterization, including outgoing neutron source term : Monte Carlo Neutron Transport with TRIPOLI4 ®
- Source transport from core periphery to the outmost possibly activated regions of the facility : Monte Carlo Neutron Transport with TRIPOLI4 ®
- Materials activation with DARWIN-2.3

A further step should ultimately be included to the scheme with propagation of γ sources. This last step also uses TRIPOLI4, so that to evaluate dose rates in any point of the model, starting from γ spectra due to activation in each material. It will be useful to optimize operations scenarios when dismantling starts.

3.1 Assessment of core outgoing neutrons source term

The TRIPOLI4® data set operated with version 10 and corresponding to MINERVE reference core has been used to solve a criticality problem. This input deck was elaborated previously and dedicated to the validation of elementary nuclear data [1] and reactor Physics deterministic computation codes, like APOLLO2 [6].
The feed core is independent from the experimental area. So that, whatever the program inside, neutrons leaking the core will keep the same spectrum.

Transport computations have been achieved with the following resources : Dell Precision Tower 7810 with Linux 3.16.0-4-amd64 #1 SMP Debian 3.16.43-2 x86_64 GNU/Linux equipped with 8 processors type Intel(R) Xeon(R) CPU E5-2637 v3 @ 3.50GHz and 32 Gb RAM. The computation duration is 100 h for 10^8 histories.

This refined data set allows for a fine characterization of core physics. However, the associated model has outer boundaries at the location where core physics is no longer sensitive to further geometrical refinements.
It corresponds to the pool region, several 10cm outside the core and even beyond reflector (cf. Figure 1 below).

At this level, the computation scheme adds a fictitious frontier all around the core. This new volume bears a cylindrical shape (pink in Figure 1 below) and will later allow recording for all outbound leaking particles ($\rightarrow$) their distinctive features (Nature / Position / Direction / Energy / Statistical Weight). In TRIPOLI4 ®, this operation is called STORAGE and can be further used in a so-called ″surface restart″. Such features are the most representative of core physics as it comes from the most refined core model, the one dedicated to computer schemes validation and comparisons with experiments.

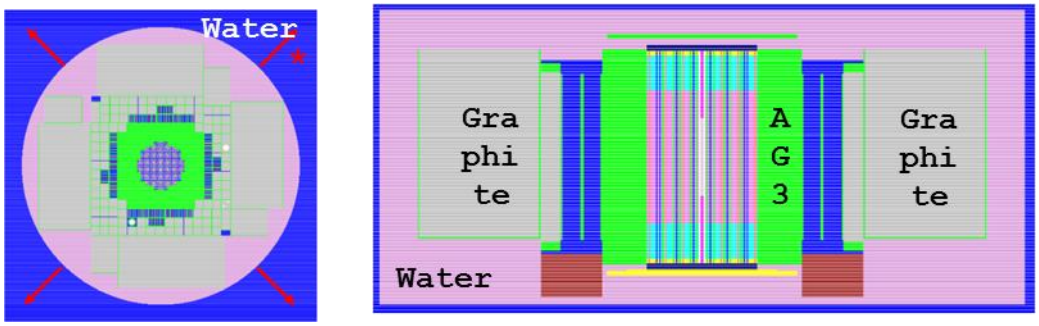

Figure 1 : MINERVE refined geometrical model

Figure 2 below shows a flux distribution in elevation and in a horizontal plane cut in the MINERVE fine core model.

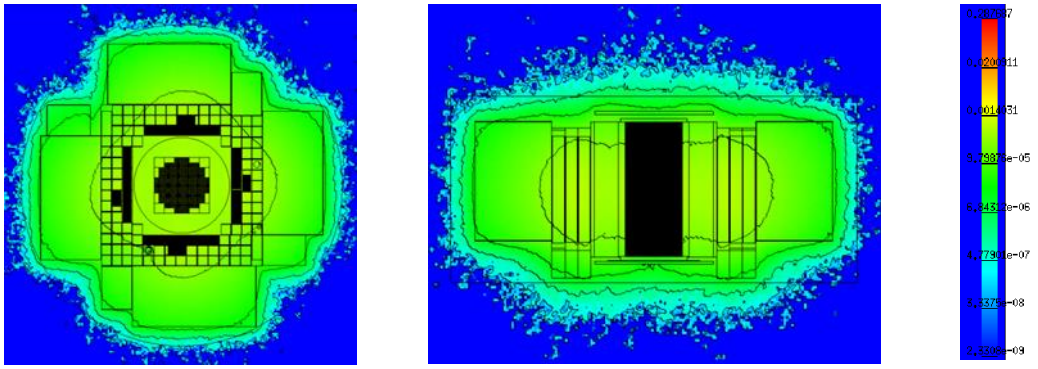

Figure 2 : Indicative flux distribution in the MINERVE fine core model (scale in n/cm².s)

Figure 2 shows neutron ″storage″ in the graphite reflector (large blocks outside the core) and how it is quick attenuated in the pool water around.

The energy deposited in the whole model is determined with a DEPOSITED_ENERGY response and the LOCAL_ENERGY_DEPOSITION score integrated over all volumes.
The computation yields 82.2 MeV/n, which is necessary to normalize the source intensity to the proper power.
This energy per neutron result will also be helpful to normalize the source intensity in the second phase ″surface restart″ computation.
It would not be realistic achieving the same level of refinement in the civil engineering over the whole facility as in the core first phase model, as it would take too much design effort. On top of that, the second phase source propagation transport would be much slower if the second model included every nuts and bolts, as in the core.
As a consequence, the idea is to stop computations at the boundary between a very accurate model of the core and a more global description of the rest of the facility. At this frontier point, all particles are frozen and stored, then, a new computation starts towards a more adapted geometrical model, while it is still representative of the building. This second phase is called a ″surface restart″, as frozen particles are generated and launched from the very surface where it was last frozen at the end of the first phase.
At the end of the first criticality computation phase, a Particles Storage File (PSF) has been generated and stored for each neutron coming across the limit.

In the case of this computation, the restart surface is made of a cylinder, all around the core. It has three faces : The upper and lower plates and the outer peripheral ferrule (cf. pink part of Figure 1).
On each face of the restart frontier, initial neutron characteristics are stored and can be used for the second phase computation.

3.2 Source restart and propagation in the building

A first neutron transport criticality computation in a most refined model was performed to characterize outgoing neutrons at its boundaries. The corresponding neutron distribution is now going to be used for their propagation with a so-called ″surface restart″ into a larger geometrical model that describes the facility.

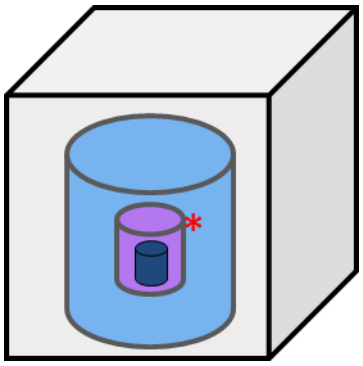

Figure 3 : First and second computation geometrical models

Figure 3 above shows the first geometrical model with its outer purple frontier* and the core, in dark blue. It also shows the second geometrical model with the same common inner frontier* in purple and the water around this boundary and eventually the concrete beyond.

At the frontier level, the restart intermediate neutron source has the location and energy distribution shown in Figure 4 below. This figure aims at giving a qualitative illustration of the source distribution in phase space and broadly shows a cylinder, which corresponds to the geometrical limits of the frontier.

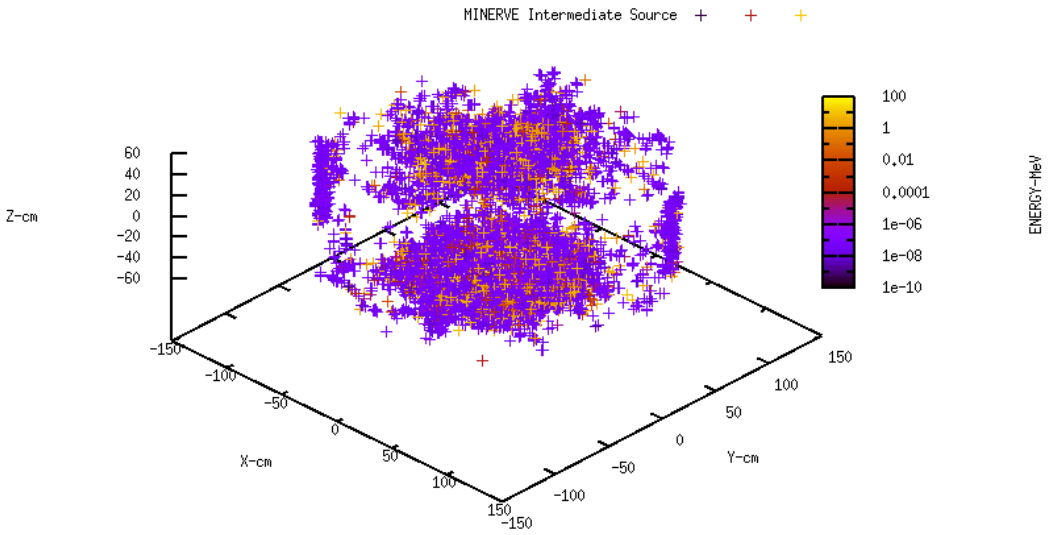

Figure 4 : Intermediate restart neutron source distribution (cm, MeV heat map)

This restart source, recorded at the boundaries of each geometrical model, corresponds to neutrons leaking outwards the core region.
Core physics analysis geometrical models are designed to characterize what happens inside the core and outgoing neutrons leakage is minimal.
For instance, among 2×10^{8} initial histories (~200 h cpu), only ~4.3×10^{6} neutrons (2.175%) remain at the boundary.

So that in order to have the same number of neutron histories coming to the edge of the second broad model, with civil engineering, and considering neutrons remain in the same compact cloud as in the core (which is optimistic, beyond more than 50 cm of water), about 1/0.01275≈80 more cpu power would be required.
The last hypothesis is not coherent as the computation goal during the second phase is no longer criticality but shielding transport, outside of a multiplication lattice, where neutrons will be dissipated in construction materials.
As a consequence, using directly the outgoing source, even with intermediate PSF files, could be misleading, either because the file would not contain as many neutrons as needed or because it would require more computation power, which is not compatible with the project needs, in terms of operational reactivity.
Then, rather than using a source with limited features, it was decided to extract its distribution in phase space. It meant separating direction, energy and location parameters at the boundary. It concerned a neutron population of ~4×10^6 neutrons, coming out of the upper or lower plate or from the peripheral side of the cylinder.

Effective number of neutrons across the restart surface for 2×10^8 initial histories	4,300,000
Share of neutrons leaking through the upper plate	33%
Share of neutrons leaking through the lower plate	51 %
Share of neutrons leaking through the ferrule	16 %

Table 1 : Restart source surface characteristics

A dedicated python2 script tool was developed in order to discretize each source neutron component in phase space (direction, energy and location). It was operated on each face (upper plate, lower plate and ferrule) of each MINERVE source. It was also used to check wether the second computation source parameters were in agreement with those extracted from the first computation, to prevent any syntax error when typing these parameters.

Figure 5 below shows a distribution of directions for upper and lower plate sources. This figure confirms that neutrons leaking through the upper plate are essentially oriented towards the top (0.<w<1.), while those leaking through the bottom plate are essentially oriented towards the ground (-1.<w<0.).

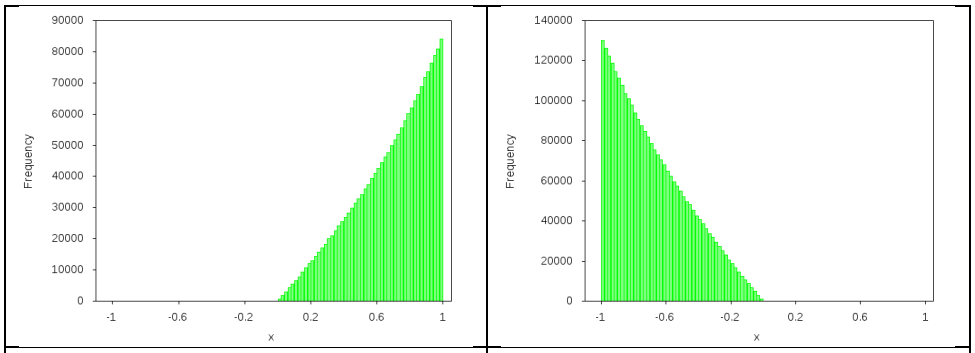

Figure 5 : Direction distributions according to Z for upper and lower faces of the frontier

The statistical weight for leakage neutrons *W* is also looked after, as Figure 6 below shows. Source processing shows 0,8 < *W* < 1,0, which is in agreement with expectations.

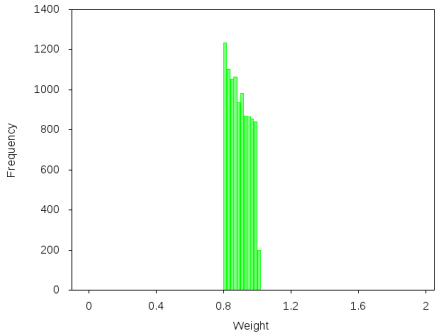

Figure 6 : Statistical weight for leakage neutrons (10^4 n sample)

The location distribution is determined beyond a given axial level (base or top of the cylinder) as a function of radius and, between both previous levels for a cylinder radius, as a function of the axial level and azimuth (cf. Figure 7 below).

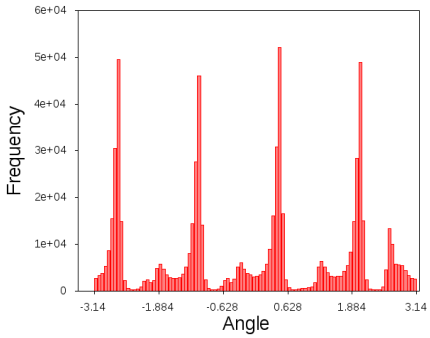

Figure 7 : Azimuthal location of sources around the cylinder

The azimuthal distribution around the cylinder (Figure 7 above) lets reflector blocks edges appear more clearly, as can also be seen on Figure 2.
Eventually in Figure 8 below, the energy distribution for each source component is determined in a 100 group constant lethargy increment binning. It basically corresponds to energy with a log scale.

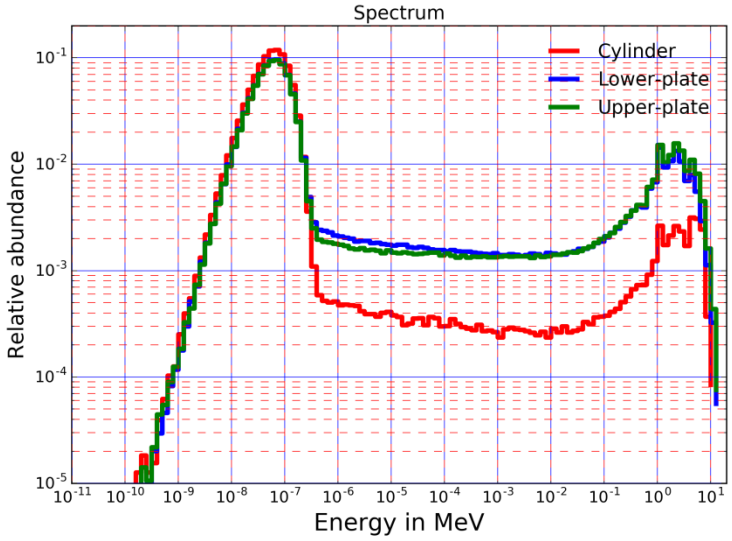

Figure 8 : Energy distribution for MINERVE sources

Figure 8 shows intermediate sources spectra. It corresponds to the energy distribution of neutrons leaking through the upper and lower plate, as well as across the cylinder.
It shows the maxwellian part of the spectrum is more important around the cylinder, from a qualitative standpoint, than above and below. It can be explained by a source frontier that is located in the pool, closer to the core above and below (in other words with less moderation) and closer to the graphite reflector (slightly more moderation) around the cylinder. Energy distributions above have each been averaged over one among three faces of each source frontier. In the second phase of the computation, it is then inserted as an independent source in the new global model.
And in this new model, each source keeps its original features (Location, Direction and Energy), as described previously. The source is discretized according to each dimension of phase space. In the end, 100 groups have been selected in each dimension (Location, Direction and Energy).
As a consequence, a direct sampling has been performed at the end of the first computation and then used in the second step for propagation of the restart surface source.
Restart sources sampled from PSF's generated by initial refined criticality computations are then propagated into a shielding type of computation in the building geometrical model. This model is no longer restricted to the technological description of the core but now includes structural pieces of the building like walls, slabs and the pool steel liner. The building geometrical model will be described further, but before, a precision is given below on the process of checking sources.

3.3 Checking sources

This part describes how the restart surface source is checked for each configuration. The goal of this process is to make sure the initial source sampling is correct and the parameters for the second phase computation are such that the restart source sticks to the PSF.

In other words, it means that sampling the restart source must give the same distribution as for the PSF.

As a consequence, the idea is to make sure the source generated in the second phase is basically a copy of that extracted in the first phase (PSF). It corresponds to the following two keywords in TRIPOLI4®, STORAGE and STORE_SOURCES_IN_FILE. It prevents mistakes occurring during sampling as well as when typing the second source.

This verification is successful as all distributions (Energy, Direction and Location) of both the initial sampling and the second source for all three surfaces (upper and lower plate as well as peripheral cylinder) stick one to the other.

It is also possible to take advantage of the restart surface location. This interface is located in open water, where neutron transport conditions are just identical. It then helps double checking the transport beyond that location as a PSF can be stored at the first interface and at another one further off the core. Sampling PSF's at both interfaces in the first and second restart computation also proves the method preserves neutron transport physics.

This operation was performed with fewer statistics at the second interface in the first computation, as for the same initial number of histories, even less neutrons can reach such remote frontiers. In the second computation, the source was closer, so that the statistics had to be better.
The results show that the source used in the global geometrical model (that including the building) is in agreement with the PSF extracted from the initial refined computation at the level of the restart surface.
Such results also validate the applied methodology as it proves, by similarity between distributions measured at the level of the second storage surface for first and second computations that neutron transport in between is identical.
As a consequence, the two step transport methodology, that helps saving a factor of several 100 in computation power is also validated from the Physics standpoint.

The following part extends the computation scheme description, providing details on the geometry where activation is determined.

3.4 Physics hypotheses

The volumes assembled in the geometrical model are a consistent reproduction of the actual civil engineering, and compositions for the corresponding materials are also described.

3.4.1 Geometrical model

This part gives a description of the geometrical model designed to determine the activation of civil engineering in the facility. It was built using the geometry surface syntax of TRIPOLI4® and depicted with its T4G module. This geometrical model is based on plans taken from the safety case.

Only four materials are used in this simpler model : The source core block, pool water, ordinary concrete and the pool steel liner.

The pool has a square, instead of a rectangular, cross section for simplification and conservatism.

The concrete comes in contact of the pool steel liner, just as if there was no intermediate layer.

The 4 scoring zones for the determination of spectra correspond to a 5 cm thick layer in concrete and to the whole thickness of the pool vessel. It is located in front of the source core region, with either the same hight or the same diameter.

The 5 cm thickness is determined by the following criteria : It is technologically representative, as it corresponds to the protection for structural steels (although steel is diluted into the whole volume of the numerical model), it is large enough to record enough events with best convergence criteria and it is not too thick, so that to avoid scraping one or several local peaking effects.

Dimensions are given on Figure 9 below.

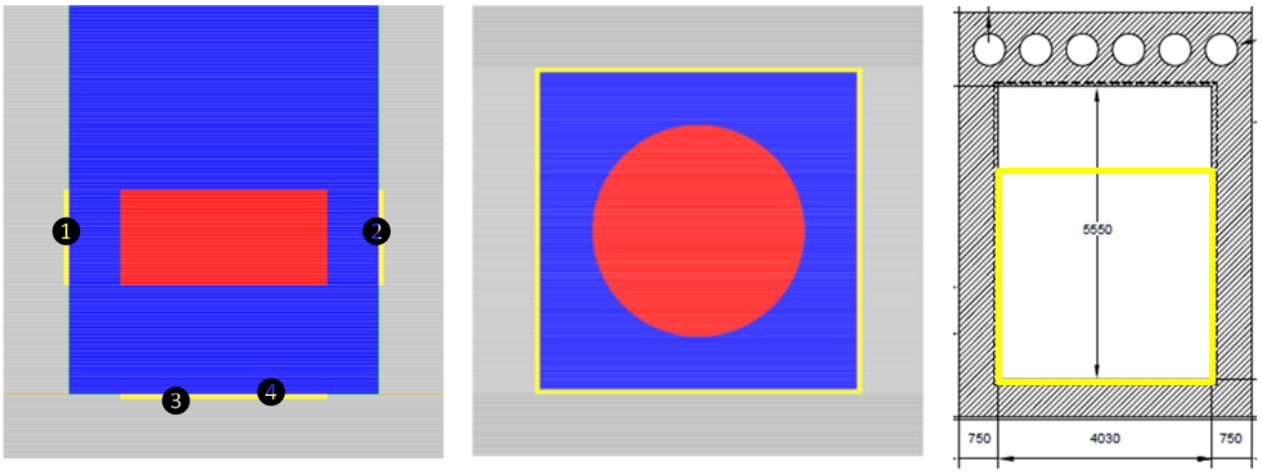

Elevation across core axis | Plane cut at core mid plane | Safety case plane cut

Figure 9 : Elevation and plane cut view

3.4.2 Materials compositions

This part presents hypotheses taken to enter materials compositions for all volumes of above geometrical models.

Concrete is the most abundant material in civil engineering. Several assumptions were made before selecting the figures that seem closest to the actual construction compositions.

For instance, it would have been too complicated and useless to enter an explicit description of structural steels in concrete. As a consequence, this composition was homogenized according to the specific steel volume fractions in the model.

In concrete, impurities often include some traces of heavy nuclides (~ 1ppm U and ~ 2 ppm Th) that have been removed from actual compositions as their natural decay adds a fictitious increment to activity while it is not caused by human activity (exposure to neutron flux).

Similarly the permanent natural activity, essentially due to initial ^{40}K and ^{87}Rb, mostly in concrete, is also removed as the computation only accounts for a balance between final and initial activity.

Those compositions combine two lists per material. The list of elements sufficient for neutron transport with TRIPOLI4® and the longer list of elements used for evolution computations with DARWIN 2.3.

The actual composition for concretes in civil engineering has not been recorded during construction. As a consequence, some assumptions were done. The reference concrete composition came from analytical chemistry measurements previously performed on the French RAPSODIE reactor dismantling experience as this fast breeder experimental reactor facility started decommissioning earlier in Cadarache as well.

This choice was determined by the observation that MINERVE and RAPSODIE concretes were produced locally, possibly with the same cement and aggregates from the same quarry, and at least during the same period of time (1960's).

The study considered the ordinary concrete sample of RAPSODIE corresponded to the mineral part of MINERVE concrete composition, and it was complemented with the adequate volume fraction of structural steel bars, so that the overall density is 2.42.

The pool steel liner was considered a stainless 304L type with a density of 7.96.

3.5 Source Propagation : flux distribution towards civil engineering

The TRIPOLI4® geometrical model includes all the facility, with outbound leakage boundary conditions. Instead, the source core region is considered a neutron black body (N(^{3}He)=10^{10} at/b.cm)), so that neutrons entering this region are lost, ″body and soul″, for the computation.

MINERVE SHIELDING computations with 50×10^9 histories last ~70 h wallclock. The convergence is poor as only very few particles reach scoring regions (60 cm off radially and 125 cm off axially).

These computations were performed with the following resources: 2 nodes type DELL Power Edge C6320 with 20 Intel Xeon E5-2660 v3 processors operating at 2,6Ghz with 128 Gb RAM and 4 nodes type Bull R424-E4 with 28 Intel Xeon E5-2680 v4 processors operating at 2.40GHz with 256 Gb RAM.

The sum of all source intensities is normalized to a total (fission and other nuclear reactions) power of 100 W and is worth 2.17% of 7.60×10^{12}n/s, as the energy deposited per history neutron in the refined core model is 81,37 MeV (2.17% is neutron leakage off the core).

In all integration zones, the scores are recorded with a TRIPOLI4® 315 groups energy binning, which is specific to activation computations.

3.6 Characterizing evolution

This part aims to show how the flux distribution evaluated in the past chapter will be used to assess the activation of specific materials in both facilities.
The evolution computation method will be described and the hypotheses on irradiation history will be presented.

3.6.1 General description of the evolution computation

315 group fluxes generated by TRIPOLI4® [2] are extracted for each scoring zone and inserted in DARWIN 2.3 [3], CEA reference package for isotopic evolution assessment.

Then it uses the INTERPEP and PEPIN2 modules of DARWIN 2.3 that generate 1 group reaction rates and solve the Bateman equation with a RK4 solver. In the end, it produces activities 3 years after shutdown, when clean up can begin.

Nuclear data (*M, E,* σ, λ, Y …) libraries are based on the JEFF3.1.1 evaluation [7] for transport and on EAF [8] for activation.

Materials' compositions include up to 60 elements in the evolution computation, whereas there are only 10 to 20 for TRIPOLI4® neutron transport. The reason is neutron transport is sensitive only to the major compounds, and except specific isotopes, like e.g. *B* or *Hf*, adding traces would only cost useless delays to this part of the computation. On the contrary, it is essential that evolution brings a comprehensive characterization of activation, meaning even the thinnest traces, that can add a significant contribution, must be included. For instance, it is the case of Co in steel or Cl in graphite.
On top of that, some materials, like concrete, may already contain naturally radioactive elements, like ^{40}K, ^{87}Rb, U or Th, from the beginning of construction. And such isotopes do not contribute to the artificially added activity. This study only accounts for activity increments caused by exposure to neutron flux.
The comparison of added activity for a U-Th composition when exposed to the operations history or not exposed to neutron flux ($\times 10^{-15}$) shows it is identical, meaning natural decay is the only cause for appearance of new radioactive isotopes, so that irradiation is not concerned.

3.6.2 Irradiation history

The irradiation history between the beginning on 09/1977 and the end in 12/2017 is a sequence of several active phases, with exposure to neutron flux, followed by decay periods.

A three years cooling phase is added at the end of operations, after reactor final shutdown on December 31st 2017. It leads to activities on January 1st, 2021. Three years is the minimum duration prior to start active dismantling.

Then, a first attempt to obtain more realistic results consisted in simulating a fictitious operations history, called a ″comb″, and corresponding to

- 30 minutes operations / day
- 20 days operations / month followed by 10 days ″cooling″
- 12 months / year
- 40 years of operation

The result is 9700 more refined steps.

Figure 10 below gives a schematic illustration of this "comb" approach :

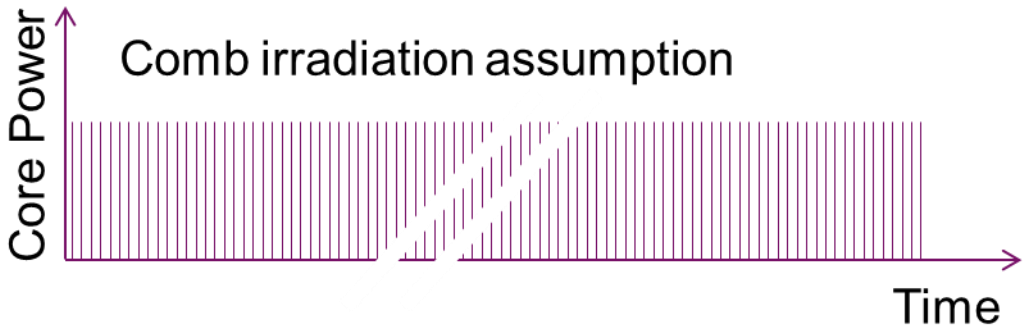

Figure 10 : Refined history (comb) assumption

This approach is certainly conservative as 100 W was the maximum power limit set by the safety case. It is probable that experiments were performed at a lower power.

Moreover, there have been maintenance and upgrade periods, when the reactor was not available for several months, so that the 12 months/year availability is envelope.

4. Results

This chapter gives a synthesis of activation results obtained on MINERVE. The first part is about flux distributions. The second one is about activities.

4.1 Flux distributions from TRIPOLI4®

The Monte-Carlo neutron transport computations were performed with TRIPOLI4® and based on JEFF3.1.1 nuclear data. It corresponds to the second phase with surface source restart. The results for the first phase are given in Figure 2. Spatial distributions are integrated over energy (1 bin) and energy spectra between 10^{-11} MeV and 20 MeV correspond to the 315 groups binning of TRIPOLI4® for activation.

The flux distribution in MINERVE is very much attenuated in water, so that pool liner and concrete activation is almost negligible.

4.1.1 Neutron energy spectra

Figure 11 below shows neutron spectra in the concrete wall around the pool and steel liner around the pool too. It shows the flux level for 100 W fission power in the core is extremely low. It is even lower at the bottom of the pool (steel liner and concrete base). This figure also shows the uncertainty is not negligible due to poor statistics in such remote scoring regions ($\sigma_{\text{vertical regions}}\approx4\%$ and $\sigma_{\text{horizontal regions}}\approx10\%$).

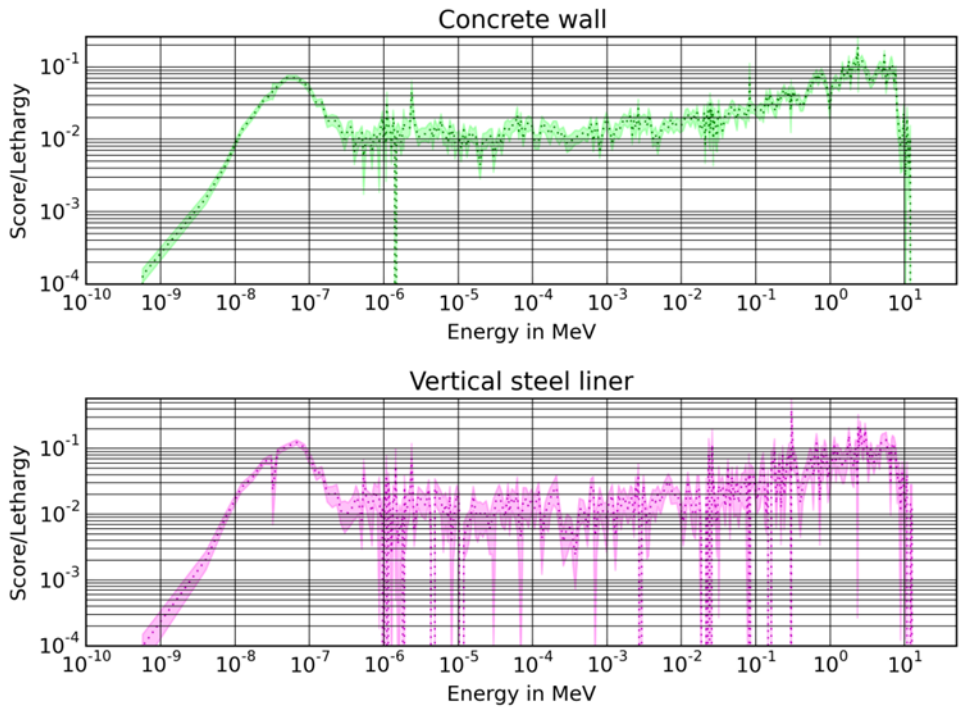

Figure 11 : Neutron spectra in the facility, beyond the core

The thermal maxwellian part of the spectrum is obviously the main component of both spectra It is similar in both materials.
At the pool bottom, the flux (and convergence) are lower (cf. Figure 13).

4.1.2 Flux spatial distribution

50×10^9 neutron histories were simulated and figures were generated with T4G, the graphics module of TRIPOLI4®.

The flux distribution was observed on the floor and on the vertical sides of the pool.

Figure 12 below shows the relative flux distribution on a log scale from TRIPOLI4® computation in plane cut (right) or in elevation (left) in the pool, steel liner and concrete.

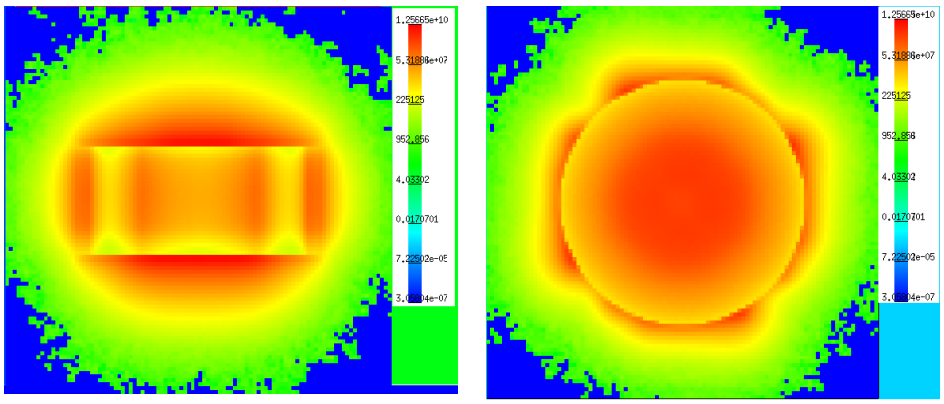

Figure 12 : Indicative flux distribution in the pool (Log scale)

Figure 12 above shows the very important flux attenuation in pool water (the heatmap is a log scale). It self explains why the activation in the steel liner and concrete is so low.

The log scale gives flux level values between 0 $n.cm^{-2}.s^{-1}$ (blue) and 1.2×10^{10} $n.cm^{-2}.s^{-1}$ (red).

This Figure 12 can also be compared with Figure 2 to understand how the flux propagates into the pool..

4.2 *Activity from DARWIN 2.3*

This part is relative to the assessment of activity from fluxes computed with TRIPOLI4® and the irradiation history described in § 0.

Figure 13 below shows the flux level at the location of main integration zones in MINERVE for a total power of 100 W.

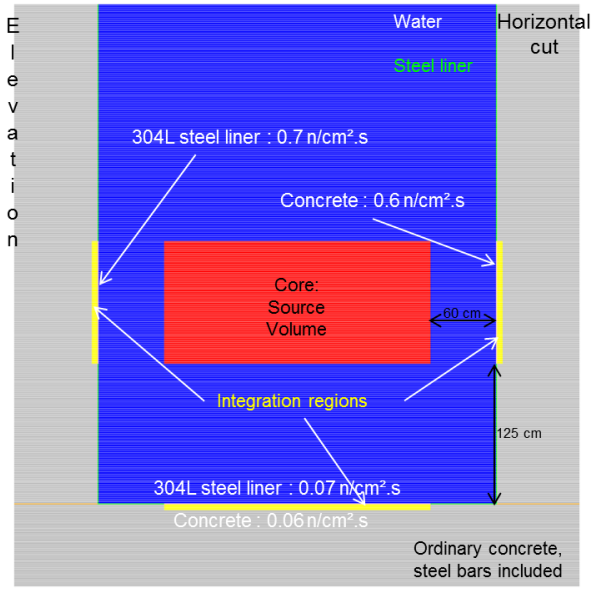

Figure 13 Flux levels (100 W)

Four integration zones can be seen on Figure 13 above. Two steel and two concrete, corresponding to the base and wall of the pool.

	Steel bottom			Concrete base			Vertical steel liner			Concrete wall	
^{55}Fe	7.5E-07	60%	^{3}H	1.5E-08	49%	^{55}Fe	9.4E-06	60%	^{3}H	1.4E-07	50%
^{60}Co	3.1E-07	25%	^{55}Fe	1.1E-08	36%	^{60}Co	4.0E-06	25%	^{55}Fe	1.0E-07	37%
^{63}Ni	1.7E-07	14%	^{39}Ar	2.5E-09	8%	^{63}Ni	2.3E-06	14%	^{39}Ar	2.1E-08	7%
^{54}Mn	6.1E-09	0%	^{152}Eu	6.3E-10	2%	^{54}Mn	1.2E-07	1%	^{152}Eu	6.5E-09	2%
^{59}Ni	1.6E-09	0%	^{54}Mn	4.0E-10	1%	^{59}Ni	2.1E-08	0%	^{54}Mn	3.4E-09	1%
^{14}C	3.6E-10	0%	^{45}Ca	2.1E-10	1%	^{14}C	4.6E-09	0%	^{45}Ca	2.0E-09	1%
^{93}Nb$_m$	6.0E-11	0%	^{60}Co	2.0E-10	1%	^{3}H	1.3E-09	0%	^{60}Co	1.7E-09	1%
Total	1.2 10^{-6}	1.6 10^{-7}	Total	3.1 10^{-8}	1.3 10^{-8}	Total	1.6 10^{-5}	2.0 10^{-6}	Total	2.8 10^{-7}	1.2 10^{-7}
	Bq/cc	Bq/g		Bq/cc	Bq/g		Bq/cc	Bq/g		Bq/cc	Bq/g

Such activities are very low and anyhow much lower than the natural activity due to ^{40}K (~0.3Bq/cc) or ^{87}Rb (0.04Bq/cc) in concrete. The bottom is about 10 times less active than vertical sides, which is coherent with the ratio on fluxes. And the activity in steel is about 50 times that in nearby concrete, which is coherent with the concentration in iron, as ^{55}Fe contribution to the activity also follows that ratio.

Such low activities are due to a low reactor power and a water layer thicker than at least 50 cm between core and steel liner.

5 Conclusion

This study presents the computation scheme developed in order to characterize the activation of MINERVE civil engineering.
It shows the hypotheses and protocol applied to TRIPOLI4® neutron transport and DARWIN2.3 evolution reference packages of CEA.
It justifies a necessary two step treatment for the neutron source.
It shows flux and activity results for both concrete and steel around the reactor pool. Fluxes and activities are very low.
Such results were used to characterize accidental release scenarios.
The maximum activity increment is lower than 2×10^{-6} Bq/g, which is less than 0,01% ^{40}K natural activity.

The study will now focus on activation of graphite reflector blocks in the core.

6 References

[1] A. Santamarina, P. Leconte, D. Bernard et G. Truchet, «Reactivity Worth Measurement of Major Fission Products in MINERVE LWR Lattice Experiment,» *NUCLEAR SCIENCE AND ENGINEERING,* vol. 178, n° %14, pp. 562 - 581, 2014.

[2] E. Brun, F. Damian, C. Diop, E. Dumonteil, F.-X. Hugot, C. Jouanne, Y. Lee, F. Malvagi, A. Mazzolo, O. Petit, J.-C. Trama, T. Visonneau et A. Zola, «TRIPOLI-4 CEA, EDF and AREVA reference Monte-Carlo code,» *Annals of Nuclear Energy,* vol. 82, pp. 151-160, 2015.

[3] L. San-Felice, R. Eschbach et P. Bourdot, «Experimental validation of the DARWIN2.3 package for fuel cycle applications,» chez *PHYSOR 2012*, Knoxville, Tennessee, USA, 2012, April 15-20.

[4] M. Soulard, G. Ritter, C. Le Loirec, R. Eschbach et O. Sérot, «Source Term Computation for reactor dismantling operations,» chez *DEM 2018*, Avignon (France), 2018.

[5] C. Le Loirec, M. Soulard, G. Ritter et Y. Peneliau, «Benchmark study of tripoli-4® for decommissioning purposes,» chez *DEM 2018*, Avignon, France, 2018.

[6] J. Vidal, P. Blaise et A. Calloo, «Qualification of APOLLO2.8-JEFF3.1.1. For the calculations of plutonium recycling PWRs using the EPICURE-UMZONE experiment,» chez *PHYSOR 2010, Int Conf on the Physics of Reactors*, Pittsburgh (USA), 2010.

[7] A. Santamarina, D. Bernard, P. Blaise, M. Coste, A. Courcelle, T. D. Huynh, C. Jouanne, P. Leconte, O. Litaize, S. Mengelle, G. Noguère, J.-M. Ruggiéri, O. Sérot, J. Tommasi, C. Vaglio et J.-F. Vidal, «The JEFF-3.1.1 Nuclear Data Library: Validation Results from JEF2-2 to JEFF-3.1.1,» *OECD Nuclear Energy Agency JEFF Report,* vol. 22, n° %16807, 2009.

[8] J.-C. Sublet, L. W. Packer, J. Kopecky, R. A. Forrest, A. J. Koning et D. A. Rochman, «The European Activation File: EAF-2010 neutron-induced cross section library,» CCFE, Abingdon, 2010.

BETA RADIONUCLIDE SOURCES FOR CANCER TREATMENT PRODUCED IN RESEARCH REACTOR

L. VIERERBL, J. ŠOLTÉS, M. KOLEŠKA, M. VINŠ, H. ASSMANN VRATISLAVSKÁ
Research Centre Řež, Ltd.,
Husinec-Řež 130, 25068, Czech Republic

P. POCHOP,
Motol University Hospital,
V Úvalu 84, Prague, 150 06, Czech Republic

ABSTRACT

Sealed beta radiation sources are often used in brachytherapy for eye cancer treatment. Mainly ^{106}Ru/^{106}Rh radionuclide sources are used for the eye applicator production due to its high beta radiation energy of 3545 keV. ^{42}K is suggested as an alternative radionuclide source for this purpose. Both sources have similar radiation characteristics. The main difference is their half-life parameter: 372 days for ^{106}Ru and 12.4 hours for ^{42}K. While ^{106}Ru/^{106}Rh production is based on a separation from a fission products mixture, ^{42}K can be produced by a simpler method of neutron activation of natural potassium. The possibility of ^{42}K production with treatment required parameters was theoretically and experimentally verified for the LVR-15 middle power research reactor. Another radionuclide with acceptable parameters for this application, especially for tumors with a lower depth treatment, is ^{76}As produced by thermal neutron activation from the ^{75}As(n,γ)^{76}As reaction. Advantages of this new method are discussed.

1. Introduction

Several types of ionizing radiation are used for cancer radiotherapy. Sealed beta radiation sources are often used in brachytherapy for the eye tumors treatment [1]. The ^{106}Ru radionuclide is usually used as a primary source of beta radiation in eye applicators [2]. The ^{106}Ru parent disintegrates with a half-life of 372 days to the ^{106}Rh radionuclide with a half-life of 30 s. The first decay is accompanied by beta radiation of a very low energy while in ^{106}Rh decay beta radiation with a maximum energy of 3545 keV is emitted. It is the highest value obtained from available radionuclides with longer half-life (or its parent half-life). The high energy is essential for tumor irradiation in a common eye tumor depth range. An alternative source with a lower beta radiation energy is the ^{90}Sr/^{90}Y radionuclide. The production of ^{106}Ru/^{106}Rh and ^{90}Sr/^{90}Y radionuclides is based on separation from fission products mixtures.

2. Methods and materials

This work describes a new idea based on a searching for a radionuclide with similar radiation parameters as ^{106}Ru/^{106}Rh, however, with a simpler production pattern using the neutron activation method. ^{42}K was found to be the most adequate radionuclide fulfilling this requirement and ^{76}As as the next prospective source.

Basic radiation parameters of the mentioned beta radiation sources taken from the ENDF/B-VII.1 nuclear data library [3] are listed in Table 1. The main differences between the old and new type of sources are their half-lives and the production way.

Production way	Fission products separation				Neutron activation			
Radionuclide	^{106}Ru+^{106}Rh		^{90}Sr+^{90}Y		^{42}K		^{76}As	
Half-life (days)	372		10500		0.52		1.08	
Radiation	**E_{max} (keV)**	**Intensity (%)**	**E_{max} (keV)**	**Intensity (%)**	**E_{max} (keV)**	**Intensity (%)**	**E_{max} (keV)**	**Intensity (%)**
β^-	3545	78.6	2280	100	3525	82.1	2962	51
	2411	10.0	546	100	2001	17.6	2403	35
	3033	8.1			1688	0.3	1746	7.5
	1983	1.8					1174	1.8
γ	512	20.4			1525	18.1	559.0	45.0
	622	9.9			313	0.3	657.0	6.0
	1050	1.6						

Table 1. Comparison of radiation parameters for radionuclides with high energy beta radiation.

3. Dose rate calculation

For a better comparison, calculations of dose rates in the eye with an applicator was made for the ^{42}K and ^{106}Rh radionuclides. A simplified model for this calculation is shown in Fig. 2. The model assumes an eye sphere diameter of 25 mm, a head sphere diameter of 180 mm, an applicator diameter of 14 mm, a radionuclide activity of 100 MBq and a soft tissue as a material. The influence of absorption in the front cover layer and self-absorption in the activated layer is taken to be equivalent to 0.5 mm layer of soft tissue.

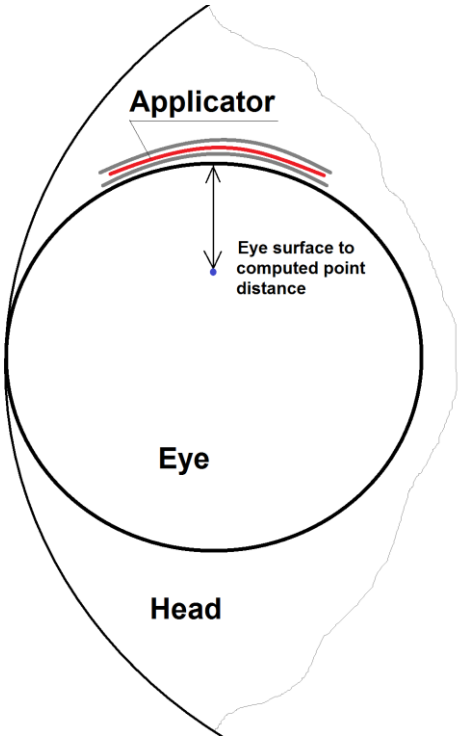

Fig. 1. Model for dose calculations in the eye with an applicator.

Radionuclide		^{42}K	^{106}Rh
Radiation	Distance (mm)	Dose rate (Gy/h)	
β^-	1	69.3	68.6
	3	35.9	35.1
	4	27.0	27.0
	6	16.4	17.7
	8	10.7	12.1
	10	8.1	8.6
	15	1.3	1.2
γ	10	0.027	0.023
	50	0.0011	0.0008

Table 2. Calculated dose rates in the eye with an applicator for radionuclide activity of 100 MBq.

4. ^{42}K production by neutron activation

Because the ^{42}K radionuclide looks to be a more promising source than ^{76}As for eye applicator preparation, in this and next chapter only ^{42}K is discussed. ^{42}K production is based on the irradiation of ^{41}K with thermal neutrons via the ^{41}K(n,γ)^{42}K nuclear reaction where the cross section for thermal neutrons is 1.3 b. According to the treatment requirements, activities of ^{42}K in the applicator should be in the range from 50 MBq to 500 MBq in the beginning of the application process. To verify if these activities can be reached using natural potassium irradiation in a middle-power research reactor, an estimation was made for five different vertical channels in the LVR-15 research reactor (Fig. 2) with a nominal thermal power of 9.5 MW [4]. The following values were used for the calculation: irradiation time - 6 hours, cooling time - 12 hours and the weight of natural potassium sample for activation - 50 mg. The calculated values of induced ^{42}K activities *A*, neutron fluence rates $\varphi_{thermal}$ (0 to 0.5 eV) and φ_{fast} (0.1 to 20 MeV) are shown in Table 3. The activities are roughly proportional to the thermal neutron fluence rates. Contributions to the activation of epithermal and fast neutrons are relatively small.

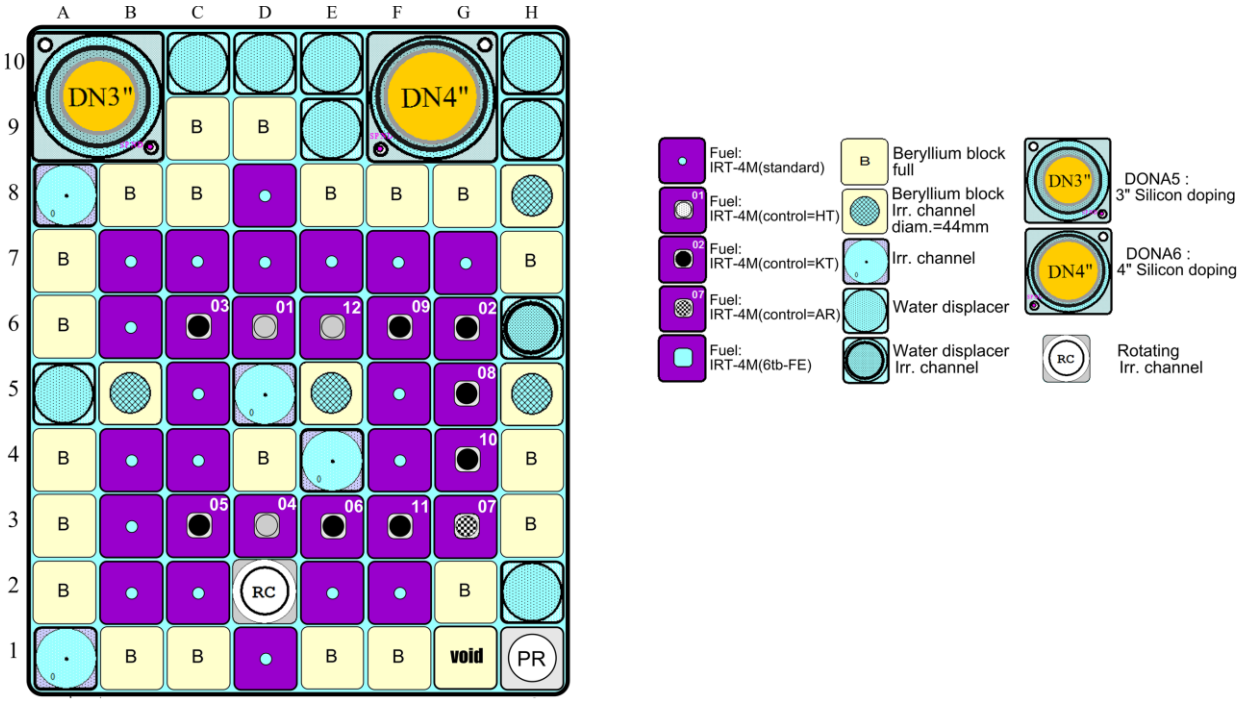

Fig. 2. Experimental core layout of LVR-15 in K163 reactor cycle.

Channel	A	$\varphi_{thermal}$	φ_{fast}
	(Bq)	(cm^{-2} s^{-1})	(cm^{-2} s^{-1})
H10	5.59E+07	6.00E+12	6.00E+11
H9	2.42E+08	2.60E+13	2.80E+12
H8	3.31E+08	3.55E+13	5.73E+12
H5	5.59E+08	6.00E+13	1.65E+13
D5	1.21E+09	1.30E+14	3.37E+13

Table 3. Fluence rates and ^{42}K activities in different vertical channels of LVR-15 research reactor. Induced activities were estimated for 50 mg of natural potassium, 6 h of irradiation time and 12 h of cooling time.

Experimental verification of activity estimation was made using a potassium iodide (KI) compound encapsulated in a polyethylene foil. The KI sample had a mass of 7.5 mg (i.e. 1.8 mg for natural potassium) and was irradiated for 2 hours in the H9 channel. After irradiation, the activity was measured by gamma spectrometry with a result of 6.51 MBq at the end of the irradiation process. The theoretical value calculated in the same way as it was described for values shown in Table 3 is 6.23 MBq, i.e. the difference between calculated and measured data is -4.3 %.

^{41}K enriched potassium can be used instead of the natural one. In this case, with 95 % enrichment and under the same conditions, the induced activities would be about 14 times higher compared to the values for the natural potassium.

5. Production and application examples

The whole treatment procedure includes the applicator preparation, neutron activation, cooling and treatment application. Relevant duration times are marked as t_{act}, t_{cool} and t_{appl}. Due to the ^{42}K half-life, these times should not much exceed 24 h. Five procedure examples are shown in Table 4. Neutron activation is calculated for vertical irradiation channels of the LVR-15 research reactor and similar values can be supposed for the other middle power research reactors. The cooling time serves for applicator activity measurement, transport and next applicator adjustment necessary for the treatment. t_{appl} is calculated to reach the required dose in specified depth of tumor in the eye. The depth of the tumor corresponds to „Eye surface to computed point distance" as is shown in Fig. 1. The required values for the treatment are listed in the first two columns of the table. The next parameters can be varied to gain suitable time of application in the last columns.

Depth of tumor (mm)	Required dose (Gy)	Potassium type	Potassium mass (mg)	Channel	$t_{irradiation}$ (h)	$t_{cooling}$ (h)	$t_{application}$ (h)
4	100	Natural	50	H9	1	12	10.6
6	100	Natural	20	H5	4	24	9.9
6	100	Natural	50	H5	2	24	6.9
10	100	Natural	20	D5	4	24	9.1
10	100	Enriched	10	D5	0.5	24	9.4

Table 4. Procedure examples of the ^{42}K radionuclide

The production of an applicator with pure metal potassium is possible however is rather complicated due to the high reactivity in air. In case a potassium compound is used, the self-absorption of beta radiation in the applicator slightly increases, however, it remains on an acceptable level. The most common compound used is potassium chloride (KCl). For example, 50 mg of K corresponds to 83 mg of KCl and for a 14 mm applicator diameter the area density is about 50 mg/cm^2 of KCl. This compound is also available with ^{41}K enriched potassium.

6. Discussion

The differences in half-lives and eye applicator production way result in advantages as well as disadvantages between the usage of ^{42}K and ^{106}Ru/^{106}Rh. A relatively low half-life of ^{42}K might be a disadvantage, however, the reduction of longer contamination and radioactive waste amount can be useful. The preparation of the applicator can be easily performed before the activation, e.g. from KCl and some plastic material. Thus, this can lead to larger variety of applicator dimensions and shapes or to tailor-made applicator for individual patients. The possibility to produce higher activities allows a decrease of the hospitalization time. The disadvantage of the ^{42}K method is the necessity of transport of the applicator from the reactor to the hospital.

Moreover**,** the use of enriched ^{41}K potassium can decrease self-absorption in the activated layer and/or the irradiation time in a reactor. However, the higher price of enriched potassium will probably prevail over this advantage in most of cases.

The other considered radionuclide with acceptable parameters for this application, especially for tumors with a lower depth treatment, is ^{76}As produced by thermal neutron activation based on the ^{75}As(n,γ)^{76}As reaction. It has a lower maximum beta energy (2962 keV) than ^{42}K. However, its other parameters are more preferable compared to ^{42}K. Namely, the cross section of ^{75}As for thermal neutrons is 3.8 b, the ^{75}As abundance in natural arsenic is 100 % and the ^{76}As half-life is 26.6 h.

7. Conclusion

This paper demonstrates the possibility of using the ^{42}K as an alternative radionuclide for eye applicators in terms of radiation parameters and production via neutron activation in research reactors. Its lower half-life and simpler production offer new opportunities compared to the currently used radionuclides. In case of routine usage of the method, a more precise procedure has to be developed for the applicator production including the selection of a material for support layers and preparation of thin potassium containing layers.

8. Acknowledgments

Presented results were obtained with the use of infrastructure Reactors LVR-15 and LR-0, which is financially supported by the Ministry of Education, Youth and Sports - project LM2015074.

9. References

[1] Nag S, Quivey JM, John D Earle JD, *et al*. The American Brachytherapy Society recommendations for brachytherapy of uveal melanomas. *Int. J. Radiation Oncology Biol. Phys.* 2003; 56; 2: 544–555.

[2] Šolc J. Monte Carlo calculation of dose to water of a 106Ru COB-type ophthalmic plaque. Journal of Physics: Conference Series 2008; 102; 012021: 1-6.

[3] Chadwick MB, Herman M, Obložinský P, et al.: ENDF/B-VII.1 Nuclear Data for Science and Technology. Nuclear Data Sheets 2011; 112; 12: 2887-2996.

[4] Koleška M, Lahodová Z, J. Šoltés J, et al. Capabilities of the LVR-15 research reactor for production of medical and industrial radioisotopes. J. Radioanal Nucl. Chem. 2015; 305: 51–59.

THE WORLD'S LARGEST PROFICIENCY TESTING EXERCISE FOR NEUTRON ACTIVATION ANALYSIS LABORATORIES BY INTERLABORATORY COMPARISON: FOCUS ON EUROPE

A. MIGLIORI, N. PESSOA BARRADAS, D. RIDIKAS, A. KATUKHOV
International Atomic Energy Agency, PO Box 100, A-1400 Vienna, Austria

P. BODE
NUQAM Consultancy, 3284LK-37 Zuid-Beijerland, The Netherlands

ABSTRACT

The IAEA facilitated in 2018, with the support of the IAEA Seibersdorf Analytical Laboratories, a new opportunity for proficiency testing by interlaboratory comparison based on a dedicated website, and the invitation for participation was extended to more NAA laboratories worldwide. Fifteen European laboratories operating activation analysis techniques registered for this proficiency test, making it the largest regional contribution within the gross total of 46 NAA laboratories from 32 Member States worldwide.

1. Introduction

Enhancement of low and medium power research reactor (RR) utilization is often pursued by increasing the neutron activation analysis (NAA) activities, being this analytical technique in principle available in more than half of the 226 operating RRs world-wide [1]. Whereas the markets for NAA laboratories may have been identified, penetrating these markets require demonstration of added value of NAA to existing 'on-site' analytical techniques. One advantageous characteristic of NAA is that matrix-matching reference materials for calibration are not needed. The degree of trueness of the measurement results is almost independent of the sample's composition, irrespective of its origin (geological, archaeological, environmental, biological or material science). Results from participating in interlaboratory comparison rounds is one of the approaches for objective and independent evidence of this proficiency.

The IAEA has regularly organized since 2010 interlaboratory comparison exercises for NAA laboratories to assess their proficiency in analysing material of various composition. The number of participating NAA laboratories increased from five, representing five Member States (2010), to 29 from 23 Member States in 2017. Recently held exercises in the period 2010-2017 have been complemented with feedback workshops for the participants to evaluate (potential) sources of error – both technical and managerial- and to discuss relevant methods for quality assurance and quality control. A significant improvement–in terms of analytical performance and reduced number of mistakes – could be concluded for most of the participating laboratories [2].

The IAEA facilitated in 2018, with the support of the IAEA Seibersdorf Analytical Laboratories, a new opportunity for proficiency testing by interlaboratory comparison based on a dedicated website, and the invitation for participation was extended to more NAA laboratories worldwide. Fifteen European laboratories operating activation analysis techniques registered for this proficiency test, making it the largest regional contribution within the gross total of 46 NAA laboratories from 32 Member States worldwide. It is probably the largest interlaboratory comparison amongst NAA laboratories ever held. Participants not only returned their measurement results but also answered an extensive questionnaire on their analytical practice and experimental condition.

The measurement results are evaluated against pre-defined criteria such as the acceptable number of results reported for which the bias is less than 20%, and the acceptable number of results for which the z-score is less than | 3|, similarly as in the exercises organized in the period 2010-2017.

We report on the results of the proficiency testing, with emphasis on the lessons learned, from which both good practices and follow-up correcting actions were derived.

2. Proficiency testing scheme

In previous NAA proficiency testing (PT) exercises facilitated by the IAEA, the samples have been provided by the Wageningen Evaluating Programmes for Analytical Laboratories (WEPAL) from The Netherlands, as part of their International Soil-analytical Exchange Programme (ISE) and International Plant-analytical Exchange Programme. The two matrices that have been selected as soil-type materials can be considered as a relatively simple material for neutron activation analysis laboratories, whereas plant material is more challenging as the often much lower element mass fractions, higher relative moisture content and more coarse particle size may introduce more analytical and practical difficulties.

The WEPAL programme does not define predefined target criteria as it aims at interlaboratory comparison rather than proficiency testing. Certified reference materials are not used, and the composition of the samples is not characterized a priori. The reports only provide indication of the deviation of the result from a given laboratory for a given element in a given sample, relative to the value of the robust mean result of all participants, taking into account the standard deviation of this mean value. This is made via calculated z-scores, defined as:

$$z = (\text{lab value} - \text{median value}) / (\text{standard deviation of all observations}) \quad (1)$$

In the 2018 exercise, a different approach was taken. Again sample types were selected that can be categorized as simpler and more challenging for NAA laboratories because of the differences in mass fraction levels. The following certified reference materials were used: IAEA-452 [3], which is animal tissue (scallop) – challenging material for NAA, with content certified for 9 elements, and IAEA-456 [4], which is Marine Sediment – simpler material for NAA, with content certified for 14 elements. However, participants were asked to report on all elements they wished, with advice given not to report elements for which results of replicates differed by more than 25% or counting statistics was above 20%. Moreover, in the 2018 PT round participants received only 1 gram of material whereas the amounts distributed in the WEPAL rounds was several tens of gram. The 1 gram of material is in principle sufficient for NAA, in which typically test portions of 200-300 mg are used, but limits the opportunity of analysing the samples in an uncommon multi-measurement procedure as was noticed in the past PT rounds. For the certified elements, the calculated z-scores were defined as:

$$z = (\text{lab value} - \text{median value}) / (\text{certified standard deviation}) \quad (2)$$

For the uncertified elements, z-scores were calculated from consensus values as defined by Eq. (1), using standard deviation by Horwitz function [5].

The laboratories that participated and reported results in the 2018 exercise are listed in Table 1. Five NAA laboratories in Europe participated for the first time (one in Czech Republic, in Poland, in Austria, and two in Germany). One laboratory (from Hungary) applied prompt gamma analysis which principle makes this technique almost equivalent to neutron activation analysis. A number of laboratories received samples but could not participate, for various reasons, including the reactor not being operational and difficulties with customs clearance. A few laboratories reported after the deadline and their results have not been taken in consideration in this report.

TABLE 1. NAA laboratories that participated and reported within deadline in the 2018 exercise

Laboratory	Member State
Neutron Activation Analysis Laboratory, Centre de Recherche Nucléaire de Draria	Algeria
Técnicas Analíticas Nucleares, Comisión Nacional de Energía Atómica	Argentina
NAA laboratory at RA6 reactor at Bariloche, Comisión Nacional de Energía Atómica	Argentina
Atominstitut, TU Wien	Austria
NAA Lab, Atomic Energy Research Establishment	Bangladesh
CDTN, CNEN	Brazil
Neutron Activation Analysis Laboratory, Nuclear and Energy Research Institute, IPEN-CNEN/SP	Brazil
Laboratório de Radioisótopos, Centro de Energia Nuclear na Agricultura, Universidade de São Paulo	Brazil
SLOWPOKE NAA Laboratory, Polytechnique Montreal	Canada
SLOWPOKE-2 Facility, Royal Military College of Canada	Canada
Neutron Activation Analysis, Chilean Nuclear Energy Commission	Chile
Neutron Activation Analysis Laboratory, China Institute of Atomic Energy	China
Neutron Activation Analysis Laboratory, Servicio Geológico Colombiano	Colombia
Nuclear Physics Institute, Czech Academy of Sciences	Czech Republic
Department of Nuclear Reactors, Czech Technical University in Prague	Czech Republic
NAA Lab - Egypt Second Research Reactor	Egypt
Radiochemie München, TU München	Germany
Institut für Kernchemie, Johannes Gutenberg-Universität Mainz	Germany
NAA laboratory,Nuclear Analysis and Radiography Department, Hungarian Academy of Sciences [1]	Hungary
Institute of Nuclear Techniques, Budapest University of Technology and Economics	Hungary
Center for Applied Nuclear Science and Technology, National Nuclear Energy Agency of Indonesia (BATAN)	Indonesia
Center for Science and Technology of Advanced Materials, National Nuclear Energy Agency of Indonesia (BATAN)	Indonesia
Center for Science and Accelerator Tecnology, National Nuclear Energy Agency of Indonesia (BATAN)	Indonesia
NAA group, MNSR Dep., Reactor School	Iran, Islamic Republic of
Neutron Physics lab, Nuclear Science and Technology Research Institute (NSTRI), Atomic Energy Organization of Iran (AEOI)	Iran, Islamic Republic of
INAA Lab, Radiation Applications Research School, Nuclear Science and Technology Research Institute	Iran, Islamic Republic of
Laboratorio per l'energia nucleare applicata - LENA, University of Pavia	Italy
Center of Complex Ecological Investigations, Institute of Nuclear Physics	Kazakhstan
Neutron Activation Analysis Lab, Malaysian Nuclear Agency	Malaysia
NAAL, Instituto Nacional de Investigaciones Nucleares	Mexico

Laboratory	Member State
Elemental and Radiometric Laboratories, CNESTEN	Morocco
Environmental Chemistry Group (ECG), Pakistan Institute of Nuclear Science and Technology (PINSTECH)	Pakistan
Laboratorio de Tecnicas Analiticas, Instituto Peruano de Energía Nuclear (IPEN)	Peru
Food and Environmental Laboratory, Institute of Nuclear Chemistry and Technology	Poland
Institute for Nuclear Research - Pitesti, Romanian Authority for Nuclear Activities (RAAN)	Romania
Frank Laboratory of Neutron Physics, IREN research facility, Joint Institute for Nuclear Research	Russian Federation
Department of Environmental Sciences, Jozef Stefan Institute	Slovenia
Neutron Activation Analysis, Atomic Energy Commission of Syria	Syrian Arab Republic
Department of Environmental, Earth & Atmospheric Sciences, University of Massachusetts Lowell	United States of America
Nuclear Engineering Teaching Lab, University of Texas at Austin	United States of America
Center for Analytical Techniques, Nuclear Research Institute (NRI)	Viet Nam

[1] Prompt gamma analysis

The performance of the laboratories in this IAEA facilitated project was evaluated on basis of the fraction of all data reported for which the absolute z-value, $|z| \leq 3$, similarly as in previous IAEA proficiency testing rounds for NAA laboratories in the years 2010, 2011, 2012, 2013, 2015 and 2017 [6-12].

Participants of the IAEA Training Workshop on Inter-Laboratory Comparison Feedback of NAA Proficiency Tests Performed in 2015 (Delft, The Netherlands, 31 August – 4 September 2015 [21]) decided to describe their performance by three categories, which will be used in this work:

1. Metrologically satisfactory performance, “excellent”, for those laboratories reporting more than 90 % of their data with $|z| \leq 3$;
2. Metrologically less satisfactory performance, “average”, for those laboratories reporting more than 70% and less than 90% of elements with $|z| \leq 3$. Minor to substantial improvements are needed to reach a higher level of performance;
3. Metrologically unsatisfactory performance, “poor”, for those laboratories reporting less than 70% of elements with $|z| \leq 3$. Major improvements are needed to reach an acceptable level of performance.

Previously, the IAEA implemented follow up feedback workshops for further discussion of the results and metrological feedback by IAEA experts on potential sources of analytical error. In these workshops, participants presented their activities, often with high level of detail that made it possible for the experts to direct on the most probably cause of the deficiencies.

However, it has been observed that similar sources of error are repeated by different laboratories over the years. In order to prevent this, in the 2018 exercise a summary of the most important lessons learned from previous IAEA facilitated interlaboratory comparison exercises was distributed to the participants prior to distribution of the samples. This included aspects on preparation and organisation, sample handling, calibration, internal quality control and reporting.

The IAEA distributed a questionnaire to all participants for providing information on the details of their sample preparation, irradiation and measurement procedures, and on the calibration methods used (such as relative method or k_0 method), software and data libraries used. These details might be useful for identifying correlations between experimental conditions and deficiencies in the submitted results.

3. Results and discussion

The results are shown in Figure 1 for Europe, and in Figure 2 in aggregate, for the "simpler" materials (soil, marine sediment) and "challenging" materials, plant and animal tissue, respectively. The evolution with time of number of laboratories in each of the performance categories (excellent-average-poor) agreed by the participants is shown. An initial marked increase in the aggregate performance was followed by some degree of stabilization, indicating consolidation of good performance by the majority of laboratories.

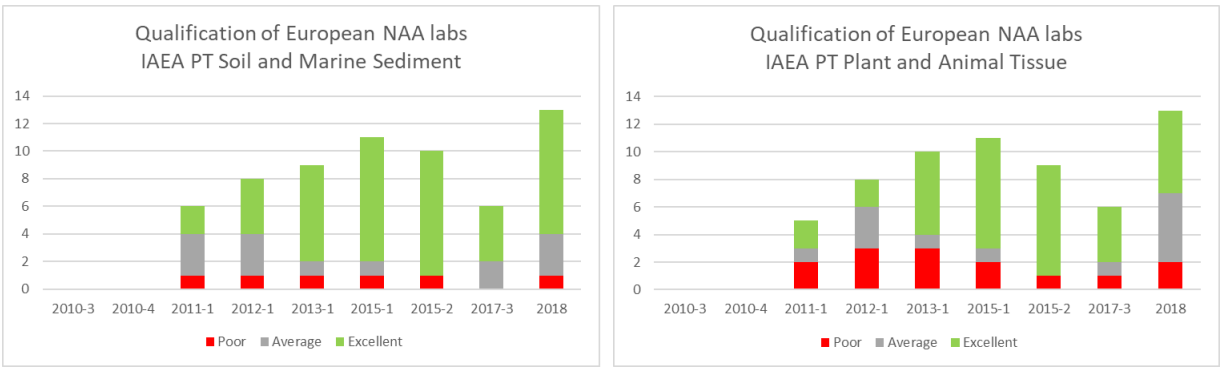

Figure 1. Number of European NAA laboratories in successive WEPAL rounds (2010-2017) and IAEA NAA PT round 2018, categorized by fraction of reported number of data with $z| \leq 3$.

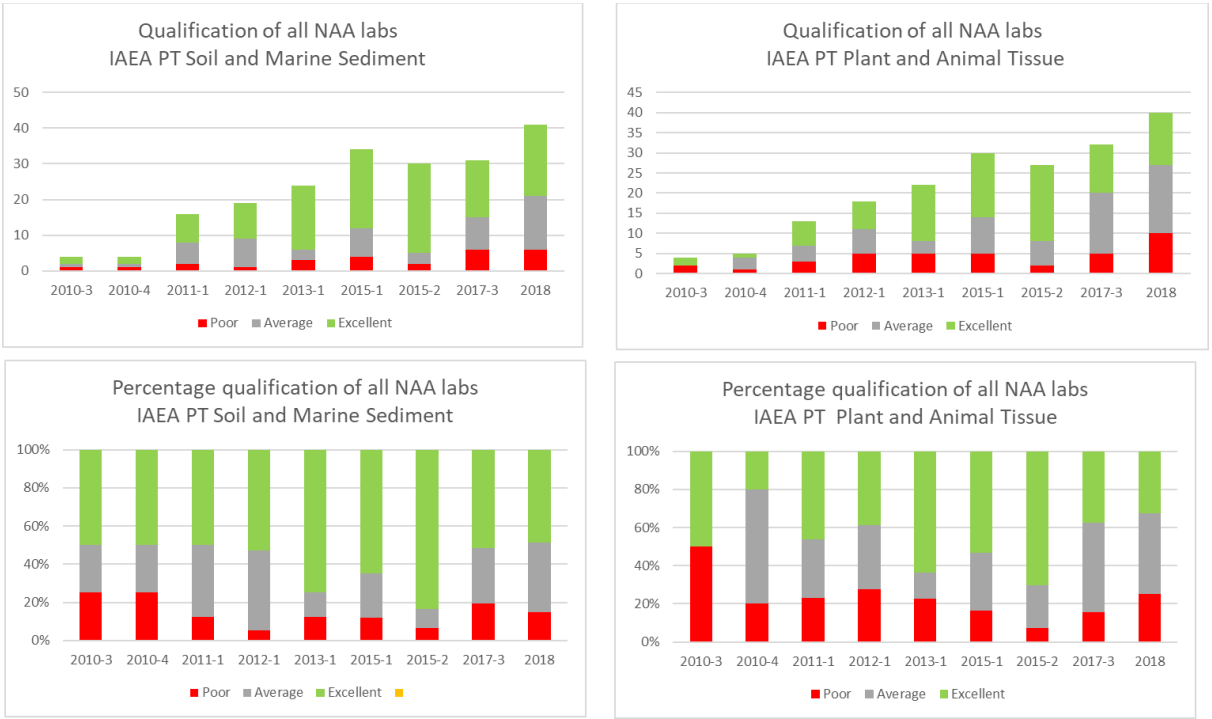

Figure 2. Total number of laboratories in the three performance categories for the "simpler" material: WEPAL Soil (2010-2017) and IAEA Marine Sediment samples (2018); and for the "challenging" material WEPAL Plant (2010-2017) and IAEA Animal Tissue (2018) samples, in successive years of IAEA facilitated proficiency testing exercise

The weak performance in 2018 by the Romanian laboratory, in comparison with their performances in previous years, can most likely be attributed to a systematic calculation error in the decay correction. The low score by the newcomer Czech laboratory (denoted as Cz-P) for the animal tissue resulted from reporting errors by a factor of 10-1000. If these mistakes had been observed and corrected before submitting the results, this laboratory would have had an ‘’Excellent”” score for this analysis.

The laboratory from Italy had a reporting error by a factor of 100 in one of their submitted results for the animal tissue analysis, which reduced their potential performance classification for “Excellent” to “Average”.

Almost all European laboratories have consistent excellent scores in these IAEA facilitated PTs, and it is promising to see that also ‘newcomer’ facilities share this category (Figure 3).

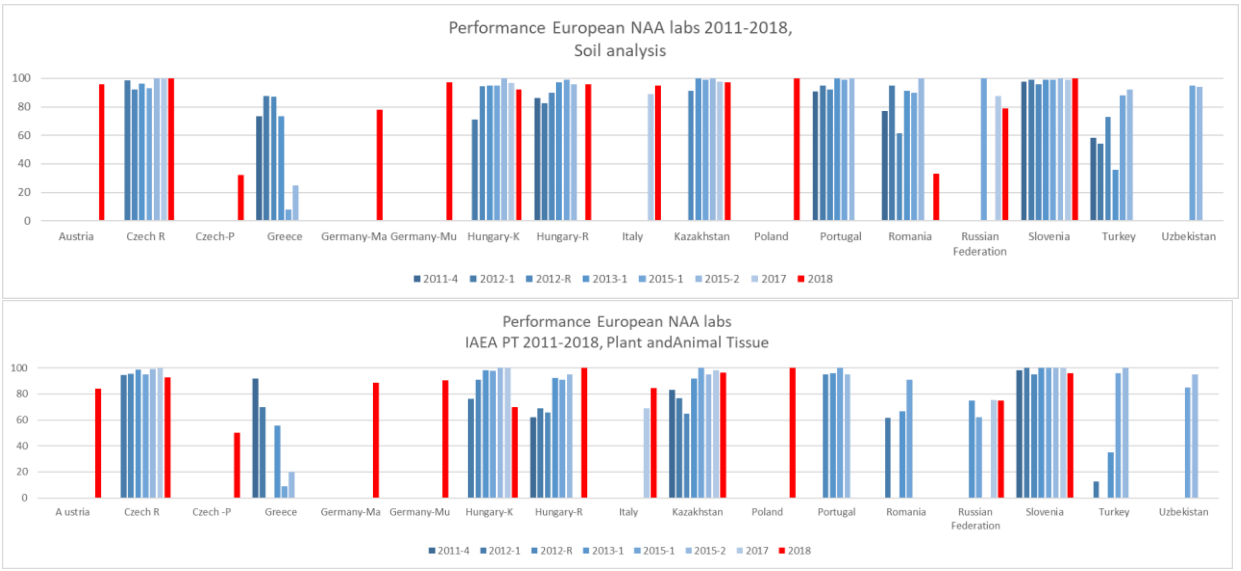

Figure 3 Performance of European NAA laboratories in the 2011-2018 IAEA facilitated PT rounds.

Considering the aggregate results for all participants, from the initial 2010-3 round to the 2018 round, the fraction of laboratories with excellent performance increased from 2010 to 2015 from 50% to 83% in the soil/sediment rounds but now decreased back to approximately 50%. A similar pattern is visible in the performance in the analysis of the more challenging materials, plant in the 2010-2017 rounds and animal tissue in 2018. Here again, the performance markedly increased from 2010 to 2015 but then steadily decreased to a value in 2018, even lower than in 2010. This can be partially attributed to the large increase in participants, with many newcomer labs, but also to inconsistent results in several labs, often due to turnover of experienced personnel.

Only 16 laboratories returned the questionnaire with information on their experimental conditions. Even so, the cause of several deficiencies remains difficult to resolve. There are, however, a few systematic cases.

Many participants reported approximately 15% higher Cr mass fractions in the marine sediment material than the assigned value for this element in this material (Figure 4). This could indicate that the assigned value has been based on the analysis results from techniques requiring sample digestion, such as ICP and AAS. It is well known that the chemical species containing Cr in sediments is extremely difficult to dissolve quantitatively, resulting in losses and too low estimates of the true value by the use of these techniques. NAA, on the other

hand, is not affecting by this problem, which explains the often higher NAA results. A similar, but less pronounced pattern is visible for the Co results.

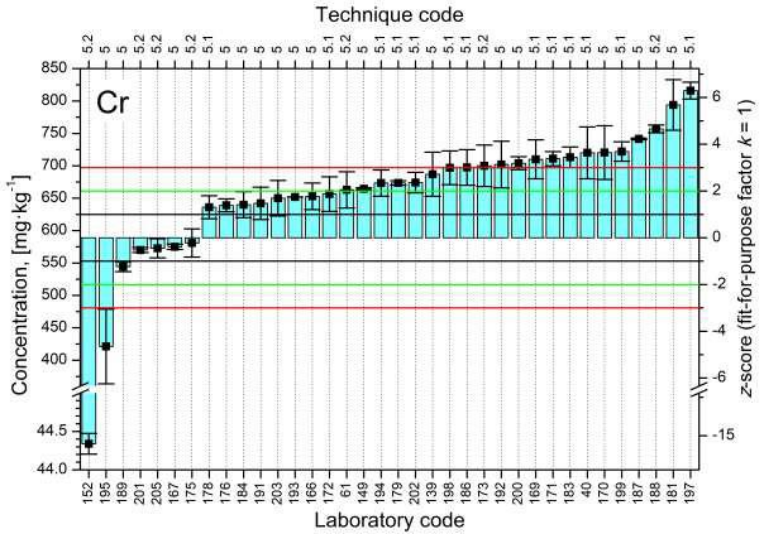

Figure 4. Distribution of Cr mass fractions in Marine sediment, indicating a systematic bias to the assigned value [13].

Other recurrent deficiencies were observed for the results of Al and Mg in the marine sediment. This could indicate to insufficient correction of the epithermal/fast neutron interfering reactions on the elements Si-Al-Mg.

This problem does usually not occur with biological materials, such as animal tissue (see Figure 5) but the high Cr results found by some of the participating NAA labs are most likely resulting from insufficient correction of the blank and/or by contamination.

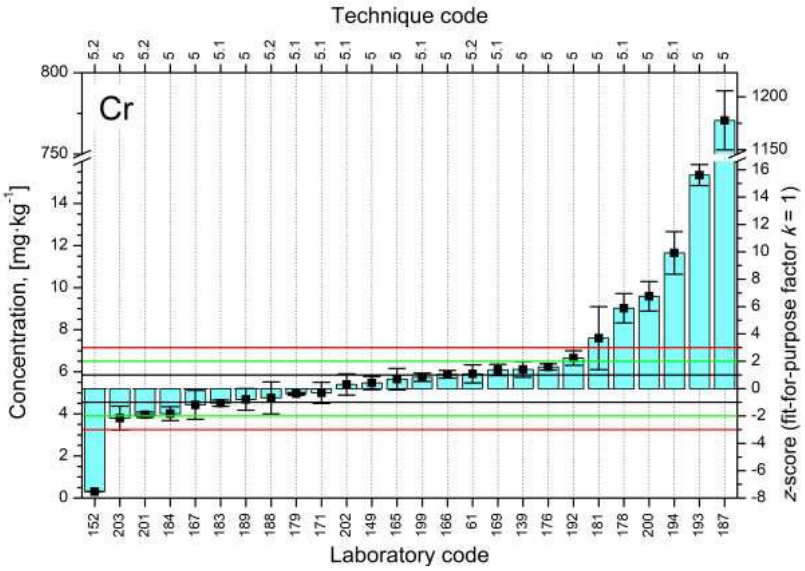

Figure 5. Distribution of Cr mass fractions in Animal Tissue, indicating a bias by contamination or by a contribution from the blank [13]

Contamination during sample preparation of the animal tissue may also be the reason that some laboratories reported too high mass fractions for elements like Na, K, Ca and Cl.

Several NAA laboratories also indicated which type of calibration method was used, i.e. the k_0 method (9 laboratories) or the relative method (7 laboratories). It is likely that the other laboratories also used the relative method, but this was not mentioned explicitly. The average number of elements for which mass fractions were reported for the sediment sample (22) is the same for this calibration technique. The laboratories using the k_0 technique reported, on the average, mass fractions for 19 elements, and those using the relative method, reported mass fractions for about 15 elements. This can be probably be explained by the fewer number of certified elements in biological reference materials, used as calibration standard in the relative method.

The laboratories using the k_0 technique had, overall, a better performance for both material types compared to the laboratories using other calibration methods, such as the relative method, although the number of laboratories with excellent performance was almost the same for the marine sediment.

4. Conclusions

It is encouraging to see that the NAA laboratories in Europe consolidated their performance and that newcomer European NAA laboratories performed equally well for at least the marine sediment. The animal tissue material was indeed more challenging as some of these newcomer laboratories may have noticed. In addition, the independent verification of calculations and data transfers is still not operational and/or effective in all laboratories. The latter deficiency is not only observed with the European NAA laboratories but also occurs in the NAA laboratories in the other regions.

Ever since the first IAEA PT rounds in 2010, the basic quality assurance and quality control concepts have been visited at each feedback workshop, and explicitly outlined in the related IAEA reports and publications, such as the IAEA TECDOC 1831 (February 2018) [14] in which the results, experiences and lessons learned from the 2010-2015 rounds have been compiled. The need for the processing of a quality control material (such as a portion of a certified reference material) simultaneously with the real samples as strongly been recommended as the analyses result thereof provides a first indication of potential systematic analysis of calculation errors. It can only be concluded that this is still either not common, or at least ineffective practice in many NAA laboratories in different regions. Also, as mentioned above, gross errors continued to occur, which, had they been eliminated, would have led to significantly better performance of some of the affected laboratories.

The increase in performance, or consolidation of excellent performance of several NAA laboratories, has been achieved by an increase in awareness of potential sources of error, technical and/or organizational, and related approaches of quality control and quality assurance that were implemented.

The foremost outcome of this IAEA project is that, since 2010, many of the participating laboratories have expanded their knowledge of the metrology of their techniques, and have implemented or improved quality control and quality assurance procedures, thus increasing their performance in obtaining valid results of known degree of trueness. However, in many countries in takes apparently substantial time and effort to reach a performance that is categorized as “excellent” reflecting the state of the practice of NAA.

The 2018 IAEA facilitated proficiency testing of neutron activation analysis laboratories has shown that there has not been a significant improvement in performance of laboratories that were categorized as less than ‘excellent’ in the 2017 PT testing. This indicates possibly insufficient follow-up to the lessons learned from the 2017 PT rounds, the related feedback workshop and from the consolidated IAEA TECDOC 1831 with recommendations for

improvement. One important factor for this is the retirement of turnover of experienced personnel, which leads to difficulties in maintaining or improving performance.

Quality assurance, quality control and methodologies for finding causes of analytical and technical errors are incorporated in great detail in the IAEA e-learning course on NAA [15]. It will contribute to the sustainability of NAA activities in research reactors, by providing an opportunity to maintain and further improve the quality of NAA analyses offered by the laboratories.

References

[1] INTERNATIONAL ATOMIC ENERGY AGENCY, IAEA Research Reactor Database, https://nucleus.iaea.org/RRDB/

[2] INTERNATIONAL ATOMIC ENERGY AGENCY, Proficiency Testing by Interlaboratory Comparison performed in 2010-2015 for Neutron Activation Analysis and other analytical techniques, IAEA TECDOC No. 1831, IAEA, Vienna (2017).

[3] Reference material IAEA-452, Biota, Scallop (Pecten maximus) (2012), <https://nucleus.iaea.org/rpst/referenceproducts/referencematerials/Trace_Elements_Methylmercury/IAEA-452/index.htm>.

[4] Reference material IAEA-456, Coastal Sediment (2017), <https://nucleus.iaea.org/rpst/referenceproducts/referencematerials/Trace_Elements_Methylmercury/IAEA-456/index.htm>.

[5] BODE, P., Basic evaluation of Interlaboratory Comparison results of participants in IAEA/AFRA project RAF 4/022, Report to IAEA C3-RAF4022-07-01 (2011).

[6] ORWITZ, W., KAMPS, L.R., BOYER, K.W., Quality assurance in the analysis of foods and trace constituents, J. Assoc. Off Anal. Chem. 63 (1980) 1344.

[7] BODE, P., Basic evaluation of Interlaboratory Comparison results of participants in IAEA/AFRA project RAF 4/022, Report to IAEA C3-RAF4022-07-02 (2012).

[8] BODE, P., Basic evaluation of Interlaboratory Comparison results of participants in IAEA project RER 4/032, Report IAEA C3-RER/1/007 01 01 (2012).

[9] BODE, P., Basic evaluation of Interlaboratory Comparison results of participants in IAEA project RLA 2/014 (2012).

[10] BODE, P., Evaluation of results of an Interlaboratory Comparison in 2013 by participants in IAEA/AFRA project RAF 4/022, IAEA ARCAL RLA 0037 and IAEA RER 4/032 - RER 1/007, Report IAEA CSA-RAF4022-29-01 (2013).

[11] BODE, P., Evaluation of results of proficiency testing by inter-laboratory comparison performed in 2015 for NAA under regional IAEA Technical Cooperation projects RAF1005, RAS 1019, RER 1007, and Regular Budget project 1.4.2.1 (2015).

[12] BODE, P., Report of the Training Workshop on Intercomparison Feedback of Neutron Activation Analysis Proficiency Tests Performed in 2017, under the IAEA projects NA-RB-1.4.2.1, TC-RAF1005 and TC-RER1016 (2017).

[13] INTERNATIONAL ATOMIC ENERGY AGENCY, Worldwide Open Proficiency Test for Neutron Activation Analysis Laboratories, PTNAAIAEA15, Determination of Major, Minor and Trace Elements in a Marine Sediment and in an Animal Tissue (2019).

[14] IAEA TECDOC 1831 Proficiency testing by Interlaboratory Comparison Performed in 2010-2015 for Neutron Activation Analysis and Other Analytical Techniques, IAEA, Vienna, 2018

[15] INTERNATIONAL ATOMIC ENERGY AGENCY, Neutron Activation Analysis e-learning course, <http://elearning.iaea.org/m2/course/index.php?categoryid=10>.

CALCULATION OF COMPLETE BURNUP HISTORY OF THE JSI TRIGA MARK II WITH SERPENT AND TRIGLAV

ANŽE PUNGERČIČ, DUŠAN ČALIČ, LUKA SNOJ
Reactor Physics Department, Jožef Stefan Institute
Jamova cesta 39, 1000 Ljubljana – Slovenia

ABSTRACT

Complete operational history of the TRIGA MARK II research reactor at the Jozef Stefan Institute was analysed in order to obtain the needed parameters for the detailed fuel burnup study in which two different neutron transport codes are used: Stochastic SERPENT and deterministic TRIGLAV. Results of complete burnup history simulation are presented with an emphasis on comparing the two codes with measurements of excess reactivity in order to validate our methodology and the code itself. The SERPENT results are in good agreement with the measured change of core reactivity. Furthermore a study done with SERPENT of the uncertainty propagation in initial fuel burnup throughout the operational history onto fresh fuel is presented. Effects of less than 6 % are observed. The presented results show great promise in adding the calculated fuel isotopic composition into existing JSI TRIGA benchmark models.

1. Introduction

The TRIGA Mark II research reactor at the Jozef Stefan Institute – JSI is an open pool type research reactor with a maximum steady-state power of 250 kW. It has been in operation since 1966, during which more than 300 fuel elements were used, arranged in 239 core configurations. Determining the final or the interim isotopic composition is challenging as we need to consider all the different types of fuel elements and their shuffling in the reactor core. Until recently all of the burnup calculations for the JSI TRIGA were performed using simplified operational history data together with deterministic codes, such as the in-house developed TRIGLAV code [1-4]. With such approach higher discrepancies were observed when comparing the criticality measurements and calculations with burned fuel in already validated MCNP geometrical models of the reactor [4]. Therefore we decided to analyse the complete operational history of the reactor in order to obtain more accurate data regarding released energy and fuel element movements, which were not taken into account prior of our work. Recently we also initiated activities to thoroughly extract the weekly performed measurements of excess reactivity for the purpose of validating the calculations and the methodology.

For the burnup calculations we wanted to replace the burnup calculations performed with deterministic TRIGLAV with stochastic SERPENT [5], due to its efficient and already built-in burnup routine. The TRIGLAV code package has a user friendly fuel shuffling interface, which made it easy for us to simulate the complete operation history, while for the SERPENT code a script was developed (called STRIGA) that creates a 3D Serpent 2 input of the TRIGA research reactor [6], based on a selected leading scheme, fuel element isotopic composition and burnup parameters. STRIGA thus enables automated Monte Carlo burnup calculations of the complete TRIGA operational history and also enables further axial, radial and angular division of individual fuel element. Such feature is especially important in TRIGA reactors, due to high heterogeneity of the reactor core. With the ability to simulate complete operational history we were able to perform multiple studies of the short-term and long-term fuel burnup effects [7].

In the first part of the paper the TRIGA MARK II research reactor and its operational history is presented, together with the used burnup calculation methodology. The second part focuses on the comparison of individual fuel element burnup calculated with both codes, where clear differences are observed, which are due to the fundamental differences between the two

codes. In order to explain the uncertainties in fuel burnup, a study of uncertainty propagation in initial burnup of already burned fuel el. throughout the TRIGA operational history and onto the burnup of the fresh fuel elements is presented. The last part focuses on the validation of our calculations, where calculated excess reactivity changes are compared to the measurements obtained from the operational history analysis.

2. Characteristics and operational history of the JSI TRIGA Mark II research reactor

The JSI TRIGA Mark II reactor is a pool type light water research reactor, with a maximum steady state power of 250 kW. The core is submerged into a 6.25 m high and 2 m wide aluminium pool filled with water and has an annular configuration. It consists of six concentric rings and total of 91 positions that can be either filled with fuel elements, irradiation channels, control rods or water (empty). A schematic view of the actual (13.2.2019) core configuration No. 240 is shown in Fig. 1. The core is surrounded by an annular graphite reflector which contains the rotary specimen rack. In total four different types of fuel elements, with characteristics given in Tab. 1, were used since the start of operation. Fuel elements are cylindrical rods with type 304 stainless steel (SS) or aluminium (Al) cladding. Fresh fuel is a homogeneous mixture of uranium (U) and zirconium hydride (ZrH), however in the HEU (high enriched uranium) fuel elements, which were in use in the past, burnable absorber erbium is present. The effect of burnable absorber is highly visible when comparing burnup of older and newer core configurations, presented in section 4.2. In the centre of the fuel rod is a region filled with zirconium rod with the exception of the aluminium fuel element.

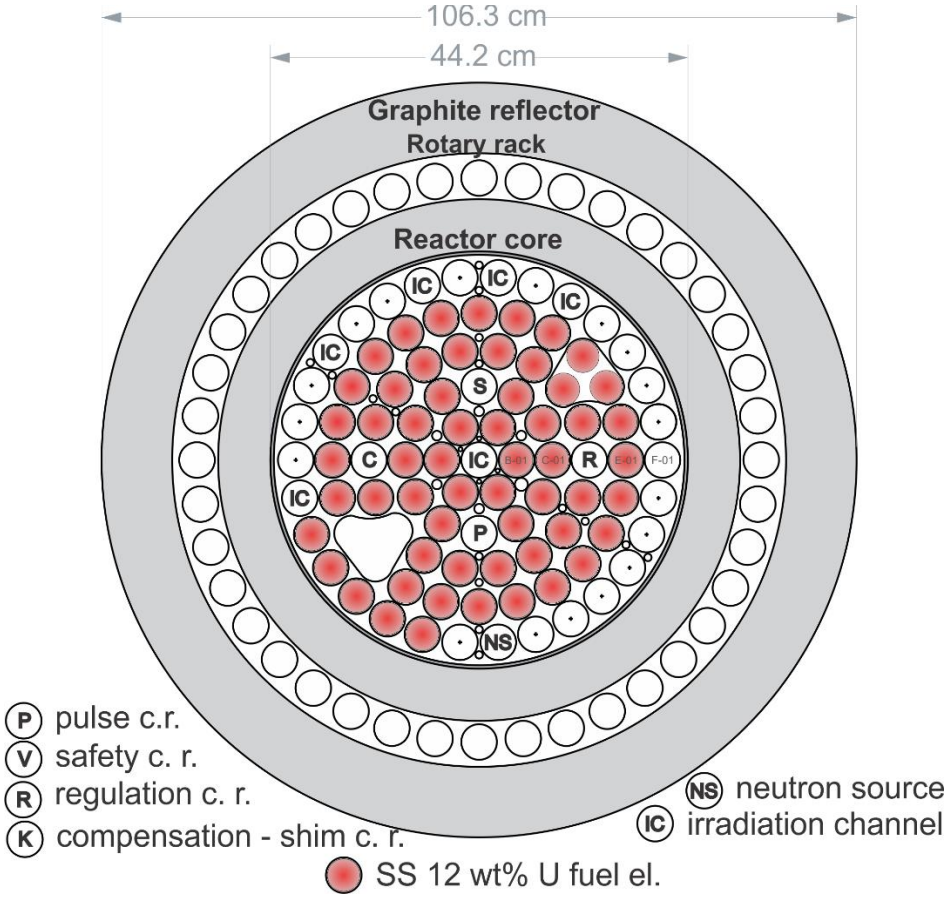

Fig 1. Schematic top view of the JSI TRIGA MARK II reactor core with denoted fuel elements, control rods (c.r.) and irradiation channels. The depicted core configuration was made operational on 13.2.2019 and it only consists of SS 12 wt% of U fuel elements.

Tab 1. Isotopic composition and properties of different types of fuel elements used in the JSI TRIGA MARK II reactor core [8].

	Aluminium 8.5 %	Standard 8.5 %	Standard 12 %	FLIP 8.5 %
Type → Composition*	LEU	LEU	LEU	HEU
Fuel	U-ZrH	U-ZrH	U-ZrH	U-ZrH-Er
Cladding	Al	SS 304	SS 304	SS 304
U content [wt%]	8.5	8.5	12	8.5
Mass(U) [g]	185	190	277	192
Enrichment [%]	20	20	20	70
Mass(^{235}U) [g]	37	38	55	134
Burnable poison	-	-	-	**Er (1.5 wt %)**
Years of usage	1966-1983	1970-1996	1991-	1973-1991

*Typical fuel element composition data. Individual fuel element compositions can slightly differ from the values depicted in this table.

Operational history analysis mainly focused on three burnup related parameters. First was the total energy released on each core configuration, which was calculated by taking into account each operation ever made with the reactor. The second was the determination of the positions of fuel elements in the reactor core over time. Fuel element movements were tracked throughout the complete history. In total 240 core configurations were analysed in order to collect the needed data for burnup calculations.
The third parameter analysed was the excess reactivity of the core. The measurements were performed weekly at the start of the week when the reactor was not poisoned with xenon. The measurements were used to validate the changes due to burnup and the changes due to fuel shuffling. The results are presented in section 4.2.

3. Description of burnup calculations

In the past criticality calculations were performed with MCNP [9] on TRIGA core benchmarks with burned fuel [4] [10], where the isotopic composition of burned fuel was calculated using the TRIGLAV code [1]. The differences in absolute k_{eff} have been observed and it is therefore essential to accurately describe the changes in fuel isotopic composition. Our goal is to use the detailed operational history data and in the future replace the use of deterministic TRIGLAV code and only use the stochastic Monte Carlo codes MCNP and Serpent for criticality and burnup calculations. For this purpose a script (STRIGA) for Serpent 2 neutron transport and burnup code was developed and used to calculate burnup of the TRIGA reactor.

3.1 Deterministic TRIGLAV code

Neutron transport and burnup deterministic code TRIGLAV was developed at the Jožef Stefan Institute at the Reactor Physics Department. Detailed description of the code can be found in [1], as only a brief description relevant for understanding burnup calculations and the presented results is described in this paper. The code was developed for TRIGA reactor geometry with annular fuel element rings. The calculations are performed in two-dimensional (r,ϕ) geometry. It is based on the four-group diffusion equation, where effective cross-sections together with isotopic composition are calculated in the unit-cell approximation using WIMSD-5B [11]. The geometry employed in the model encompasses the TRIGA cylindrical core in its entirety with a maximum of seven rings, subdivided into unit cells. Each fuel and non-fuel element position in the core is treated as a unit cell, which is represented with position coordinate and surrounded by water. Tracking position coordinates of inserted fuel elements enables us to simulate complete operational history with 240 core configurations with relative ease.

3.2 Stochastic Serpent code

Serpent 2 is a multi-purpose three-dimensional continuous-energy Monte Carlo particle transport code that is still under development at VTT Technical Research Centre of Finland [5]. The code has been publicly distributed by the OECD/NEA Data Bank and RSICC since 2009. Serpent burnup calculation capability was established early on, and is entirely based on built in calculation routines, without coupling to any external solvers. Irradiation history can be divided into multiple intervals with different normalizations, defined by power, power density, total flux, and fission or source rate. Depletion steps are given in units of burnup or time. With the increased multi-core CPU's capabilities, full 3-D burnup calculations of research reactors are possible in acceptable time.

A geometrically detailed 3-D Serpent TRIGA model was developed and criticality calculations were compared to MCNP model and validated on benchmark core configurations [6] [12-13]. The SERPENT calculated physical parameters are completely consistent with the MCNP ones and in very good agreement with the measurements, indicating that the TRIGA geometry and fresh fuel isotopic compositions employed in the model are well defined.

The most important aspect of the STRIGA tool is the fuel shuffling and storing the isotopic composition between different fuel cycles for each fuel element in so-called isotopic library. With such principle it makes the simulation of operational history or fuel management optimization user friendly. Stored isotopic composition enables us to perform criticality calculations for each selected core loading without additionally performing the burnup calculations. Flowchart of the STRIGA script is presented in Fig. 2. The STRIGA script was used to simulate the operational history and calculate the burnup of individual fuel elements at the JSI TRIGA Mark II research reactor.

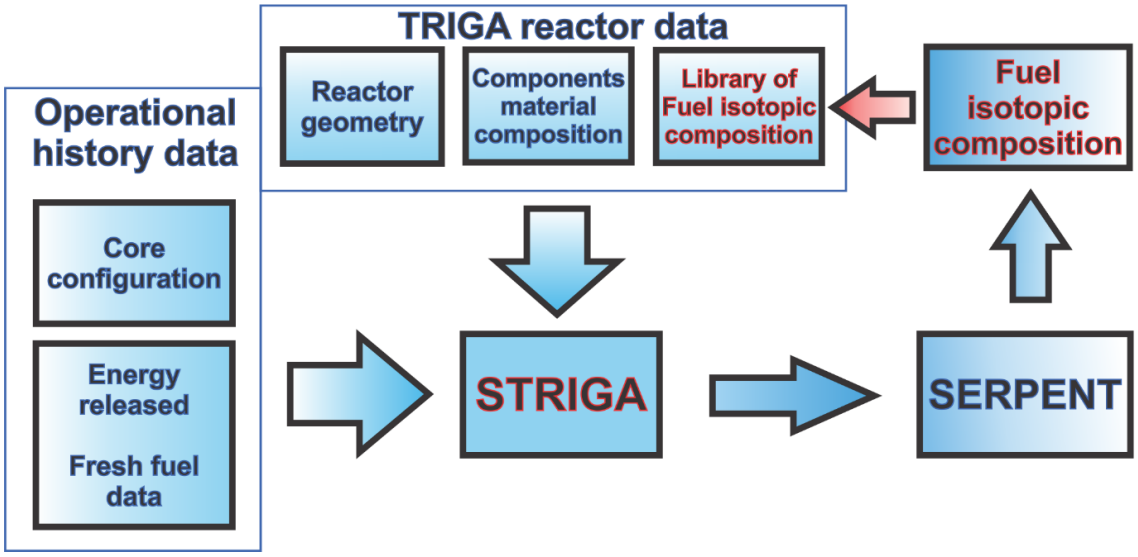

Fig 2. Schematic representation of the STRIGA methodology in which TRIGA reactor parameters are used to create Serpent 2 input for burnup calculations. The presented principle was used to simulate complete operational history of the JSI TRIGA MARK II reactor.

4 Results of complete burnup history calculations

The TRIGLAV and SERPENT codes, with the help of the STRIGA script, were used to simulate the operational history in which 239 core configurations were taken into account on which the actual diverse operation was simulated as one large on maximum power 250 kW with fuel cooldown at the end. Final individual fuel element burnup at the end of 2018, calculated with both codes, was compared, where higher discrepancy was observed for fuel elements with higher burnup. The results of 16 randomly chosen fuel el. are presented in Fig. 3.

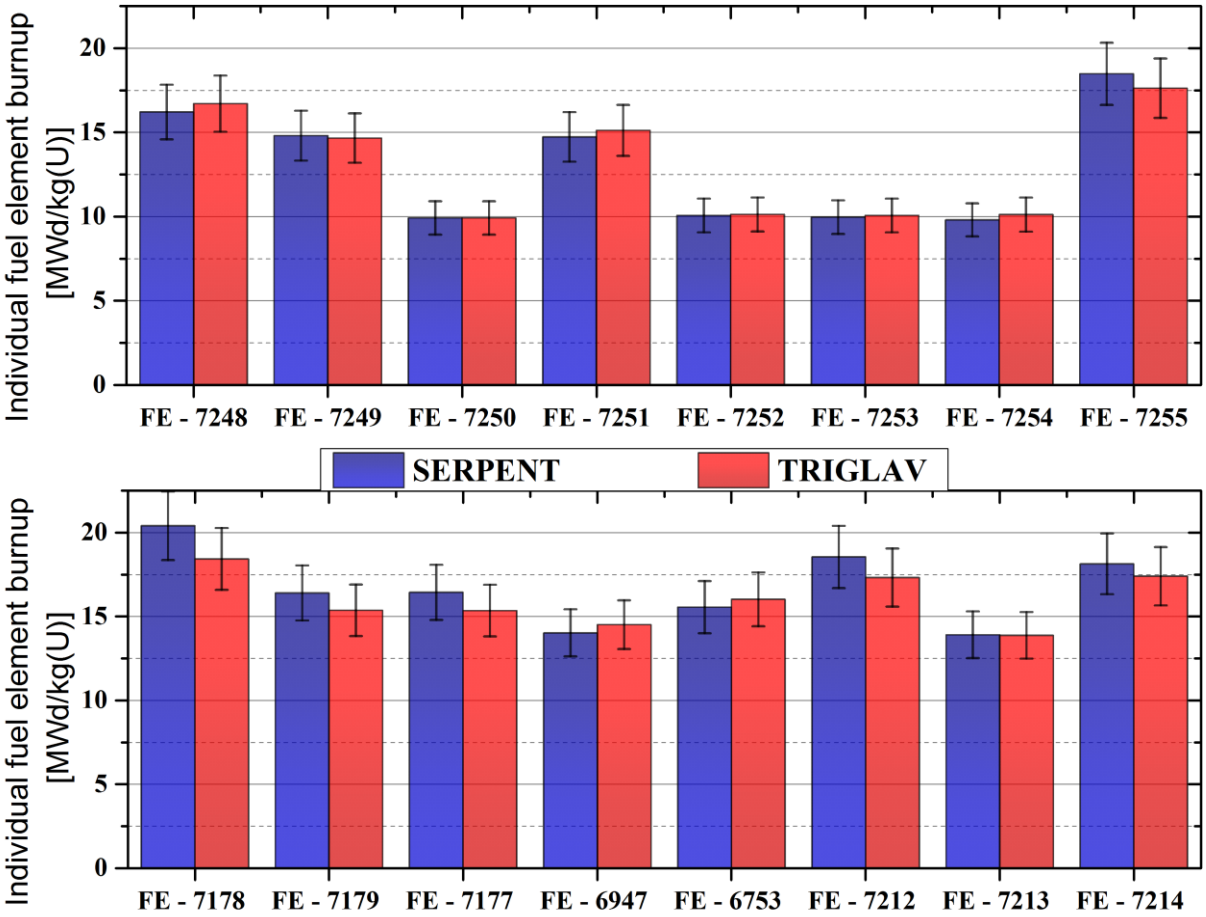

Fig 3. Burnup of individual fuel elements (FE), presented with 4 digit number, of the JSI TRIGA reactor at the end of 2018. Results were obtained with TRIGLAV and SERPENT code by simulating the complete operational history (1966-2018). The depicted 10 % uncertainty is due to uncertainty in reactor power [14] and uncertainty in initial burnup of some older fuel elements.

From the results of individual fuel element burnup we can observe the difference between different fuel elements, which was expected, due to their shuffling and position in the core. The second, more important observation, is the higher difference between both codes for fuel elements with higher burnup, which were inserted in the core at the beginning of 1991. The reason behind this is that in 1980s irradiated fuel elements were received from another TRIGA reactor and were later used in mixed core operation together with the mentioned fresh ones. The initial burnup of these older fuel elements is known with poor accuracy and therefore detailed study of the effect of not knowing the initial burnup was needed.

4.1 Propagation of uncertainty in initial fuel burnup

As mentioned, the initial burnup of some older fuel elements was uncertain. For this purpose the uncertainty propagation in initial burnup of the received fuel elements throughout the TRIGA operation history and onto the burnup of the newer ones was performed with the SERPENT code. The mixed core configurations were modelled using STRIGA. Ten different cases were studied, where the calculated burnup of the newer fuel el. was compared to the calculations at the reference value of 30 MWd/kgU, which served as a best estimate of the burnup of irradiated fuel elements. The initial burnup of the irradiated fuel elements was changed from -100 % (fresh) to + 30 % in comparison to the reference value. It was determined that the effect of not knowing the burnup of such fuel elements is less than 6 %. The statistical uncertainty propagation was under 0.5 %. The results are presented in Fig. 4.

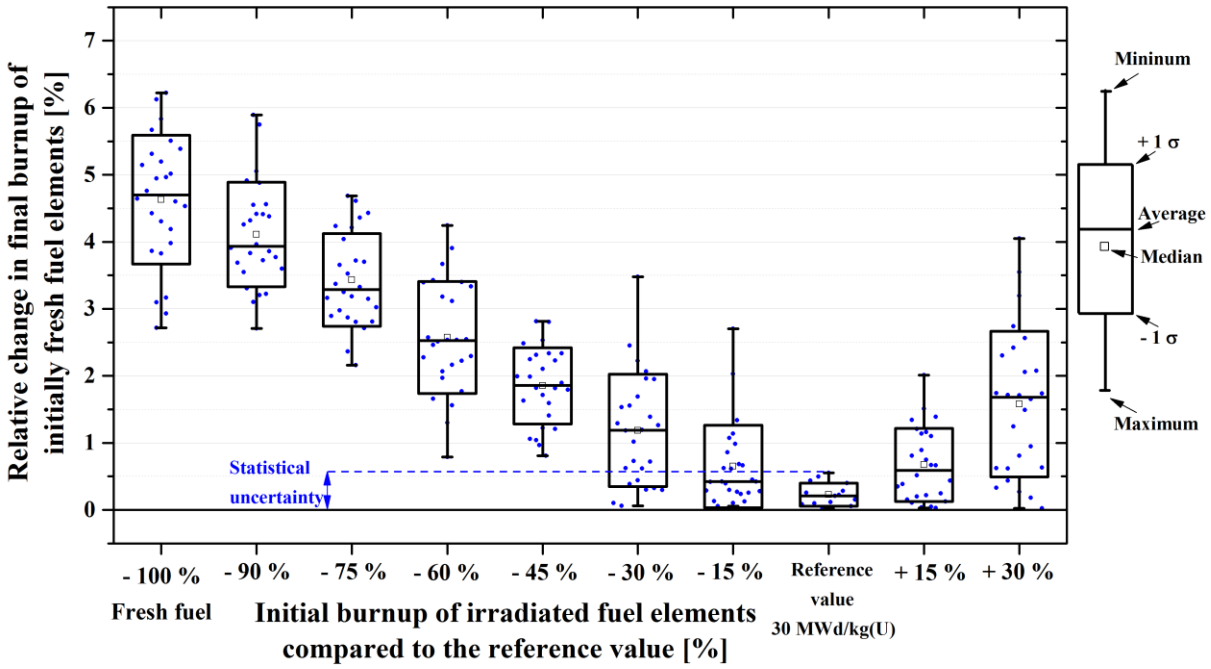

Fig 4. Relative change in final burnup (y-axis) of initially fresh fuel elements (blue dots) due to uncertainty in initial burnup of older already irradiated fuel elements, expressed as a relative change from reference value (x-axis).

4.2 Validation with excess reactivity measurements

Next step of our analysis was to validate the methodology and the results. Measurements of excess reactivity were compared to results obtained from simulating burnup history with both codes. As the comparison of absolute values of excess reactivity is difficult due to the fact that a single measurement has high uncertainty, we decided to study the smaller changes in excess reactivity of the core due to burnup. This was performed on four different core configurations, which were chosen based either on high burnup or high number of measurements. The comparison is presented on Fig. 5. For each core configuration linear change of reactivity due to burnup was assumed and the change expressed with the so-called burnup reactivity coefficient, which is defined as

$$Burnup\ reactivity\ coefficient = \frac{\Delta\rho_{Excess}\,[\mathrm{pcm}]}{\Delta\ Burnup\ \left[\frac{\mathrm{MWd}}{\mathrm{KgU}}\right]}.$$

The comparison between calculated and measured coefficients are presented in Tab. 2. The calculated values with SERPENT are within the 2σ uncertainty of the measurements, while the TRIGLAV calculations constantly slightly underestimate the measured coefficients, which is still satisfactory due to the simplicity of the code. We can conclude that the SERPENT code accurately describes the burnup changes in core reactivity on all core configurations.

The difference between older (69 and 130) and newer (189 and 218) cores in measured and calculated burnup reactivity coefficients was expected, because FLIP type fuel elements were used in the older core configurations. These elements contained burnable poison erbium, which introduces a positive reactivity change with burnup and in total decreases the change of reactivity per unit of burnup.

The analysis of small changes in reactivity and the comparison with the measurements also shows another advantage of the STRIGA tool. The initial fuel isotopic composition of a chosen fuel cycle was added from the library and the burnup step in SERPENT was further divided to study the small changes in reactivity. If the initial isotopic composition was not accurately described, the calculated relative changes would not be in such good agreement with the

measurements. This gives us motivation to compare the results from burnup calculations on other experiments and further validate our results.

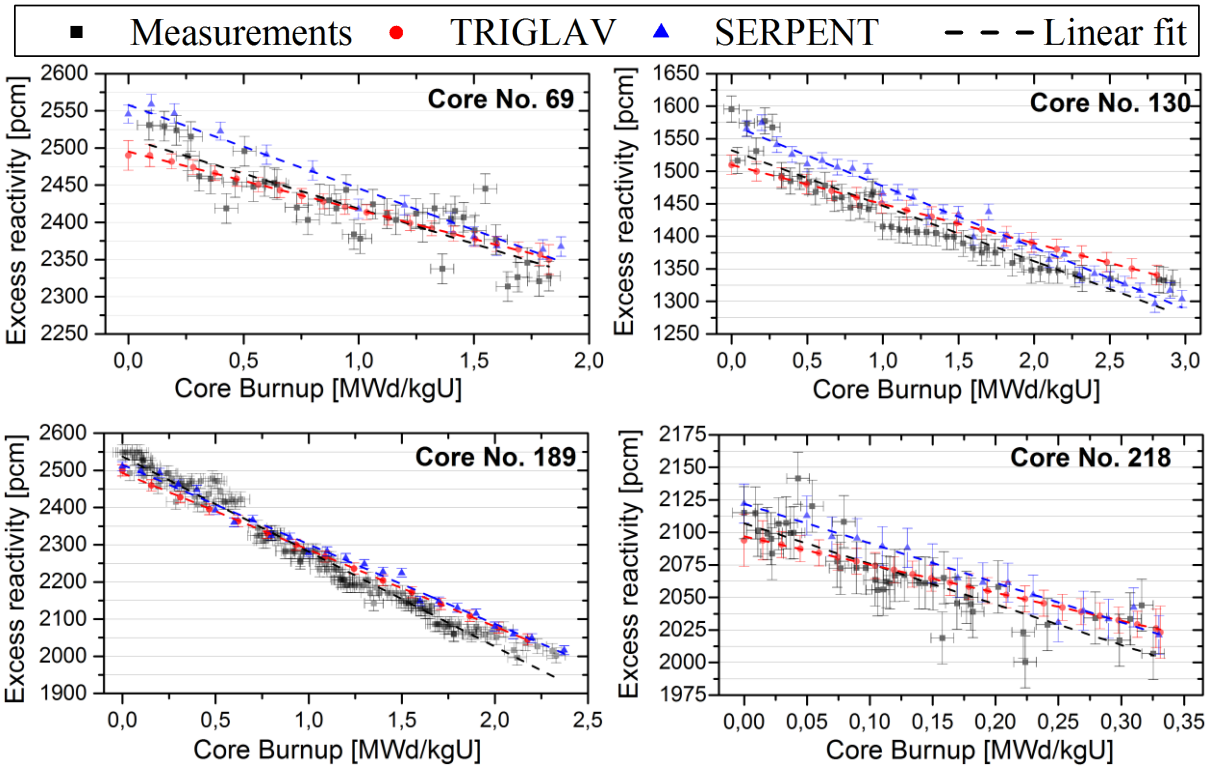

Fig 5. Excess reactivity as a function of reactor core burnup. Calculations with TRIGLAV and SERPENT are compared to weekly measurements for four different core configurations. Linear function is assumed for changes in excess reactivity due to burnup. It should be noted that core no. 69 and 130 contained HEU FLIP elements with burnable absorber erbium.

Tab 2. Measured and calculated linear coefficient of the reduction of excess reactivity due to burnup for four different core configurations, which were chosen for either higher burnup or higher number measurements. The quoted uncertainty is 1σ of the linear fit.

REACTOR CORE INFORMATION				REDUCTION OF EXCESS REACTIVITY $\left[\frac{pcm\ kgU}{MWd}\right]$		
Number	BURNUP [MWd/kgU]	Types of fuel elements	Number of measurements	Measured	TRIGLAV	SERPENT
69	1.826	FLIP*, Al 8.5%, SS 8.5%	40	**-94** ± 14	**-78.3** ± 0.5	**-112.1** ± 5.7
130	2.917	FLIP*, SS 8.5%	45	**-85** ± 12	**-60.26** ± 0.1	**-94.2** ± 2.5
189	2.330	SS 12 %	154	**-256** ±15	**-206.5** ± 0.8	**-213.9** ± 4.4
218	0.326	SS 12 %	42	**-312** ± 28	**-216.0** ± 1.0	**-303.6** ± 16.7

*FLIP fuel elements contained burnable absorber erbium

5 Conclusion

Complete operational history of the JSI TRIGA Mark II research reactor was analysed and the parameters needed for burnup calculations were collected. Calculations of complete burnup history were performed with the deterministic TRIGLAV and stochastic SERPENT. We compared the calculated final individual fuel el. burnup where higher discrepancies were observed on fuel el. that were used together with the already irradiated ones. Propagation study of the uncertainty in initial fuel burnup was performed with SERPENT, where it was

shown that the effect of the older fuel is less than 6 %. Consequently in the future only the history after 1991 could be taken into consideration, due to the low effect of the previous operations. The comparison of the SERPENT calculations with the weekly measurements of excess reactivity show good agreement within the 2σ of uncertainty. Higher discrepancies are observed for TRIGLAV calculations, however in our opinion still satisfactory due to the simplicity of the code. With this we can conclude that the methodology for TRIGA burnup calculations with SERPENT is acceptable and will be further validated in the future and used for improving the already validated Monte Carlo geometrical models of the reactor [15-17].

6 References

[1] A. Peršič, T. Žagar, et al., "TRIGLAV: A program package for TRIGA reactor calculations", IJS-DP-7862, Nuclear Engineering and Design, Volume 318, July 2017, Pages 24-34.

[2] M. Ravnik, T. Žagar, A. Peršič, "Fuel element burnup determination in mixed TRIGA core using reactor calculations", Nucl. Technol., 128, 1999, pp. 35-45.

[3] A. Peršič, M. Ravnik, T. Žagar, "TRIGA Mark II criticality benchmark experiment with burned fuel", Nucl. Technol., 132, 2000, pp. 325-338.

[4] R. Jeraj, T. Žagar, M. Ravnik, "Monte Carlo Simulation of the TRIGA Mark II Benchmark Experiment with Burned Fuel", Nucl. Technol., 137, 2002, pp. 169-180.

[5] J. Leppänen, et all, "The Serpent Monte Carlo code: Status, development and applications in 2013." Ann. Nucl. Energy, 82 (2015) 142-150.

[6] D. Ćalić, G. Žerovnik, A. Trkov, L. Snoj "Validation of the Serpent 2 code on TRIGA Mark II benchmark experiments" Applied Radiation and Isotopes, 107 (2016) 165-170.

[7] A. Pungerčič, D. Ćalić, L. Snoj, "Burnup calculations of the TRIGA research reactor using deterministic and stochastic codes", Proceedings of the RRFM 2018, European Nuclear Society, Münich, Germany, 2018.

[8] T. Žagar, M. Ravnik, "Fuel Element Burnup Determination in HUE - LEU Mixed TRIGA Research Reactor Core", 2000 International Meeting on Reduced Enrichment for Research and Test Reactors, Las Vegas, Nevada, October 1-6, 2000.

[9] T. Goorley, et al., "Initial MCNP6 Release Overview", Nuclear Technology, **180**, pp 298-315 (Dec 2012).

[10] I. Mele, M. Ravnik, A. Trkov, "TRIGA Mark II Benchmark Experiment, Part I: Steady- State Operation", Nucl. Technol., 105, 1994, pp. 37-51.

[11] Askew, J.R., Fayers, F.J., Kemshell, P.B., 1966. A general description of the code WIMS. J. Br. Nucl. Energy Soc. 5, 564.

[12] R. Jeraj, M. Ravnik, "TRIGA Mark II Reactor: U(20)-Zirconium Hydride Fuel Rods in Water with Graphite Reactor, IEU-COMP-THERM-003", International Handbook of Evaluated Criticality Safety Benchmark Experiments. NEA/NSC/DOC(95)03, OECD NEA, Paris, France, 2010.

[13] Ž. Štancar, L. Snoj, L. Barbot, "Reaction Rate Distribution Experiments at the Slovenian JSI TRIGA Mark II Research Reactor, TRIGA-FUND-RESR-002", International Handbook of Evaluated Reactor Physics Benchmark Experiments. NEA/NSC/DOC(2006)1, OECD NEA, Paris, France, 2016.

[14] Ž. Štancar, L. Snoj, L. Barbot, “Evaluation Of The Effect Of Burn-Up On Neutron Flux And Reaction Rate Distributions In The Triga Mark II Reactor”, Proceedings of the PHYSOR 2016 – Unifying Theory and Experiments in the 21st Century, American Nuclear Socitey, Sun Valley, Idaho, USA, May 1-5, 2016.

[15] T. Kaiba, G. Žerovnik, A. Jazbec, Ž. Štancar, L. Barbot, D. Fourmentel, L. Snoj, “Validation of neutron flux redistribution factors in JSI TRIGA reactor due to control rod movements”, Applied Radiation and Isotopes, 104, 2015, pp. 34-42.

[16] L. Snoj, G. Žerovnik, A. Trkov, “Computational analysis of irradiation facilities at the JSI TRIGA reactor”, Applied Radiation and Isotopes, 70, 2012, pp. 483-488,

[17] V. Radulović, Ž. Štancar, L. Snoj, A. Trkov. “Validation of absolute axial neutron flux distribution calculations with MCNP with $^{197}Au(n,\gamma)^{198}Au$ reaction rate distribution measurements at the JSI TRIGA Mark II reactor”, Applied Radiation and Isotopes, 107, 2016, pp. 165-170.

Utilization of BAEC TRIGA Research Reactor in the field of Nuclear programs and Human resource development in Bangladesh

HASAN, MD. Rakibul[1]; UDDIN, Mohammad Mezbah[1]; HAQUE, Ashraful[1]; SONER, MD. Abdul Malek[1]; SHOHAG, MD. Bodhroddoza[1]; SALAM, MD. Abdus[2].

[1]Center for Research Reactor (CRR), Atomic Energy Research Establishment (AERE) Ganakbari, Savar, Dhaka, Bangladesh

[2] Bangladesh Atomic Energy Commission, E-12/A, Agargaon, Dhaka.

E-mail of main author: rakibmist@gmail.com

Abstract. Bangladesh Atomic Energy Commission (BAEC) has been operating the BAEC TRIGA research reactor (BTRR) since September 1986. This is a unique facility in Bangladesh and the reactor has been used for manpower training, education and various R&D activities. Center for Research Reactor (CRR) of BAEC is responsible for operation and maintenance of the reactor as well as human resources development in the area of nuclear science and power program. A strategic plan has been developed for BAEC TRIGA Research Reactor (BTRR) with a view to enhancement of utilization of the reactor. The plan has identified facility's strengths, achievements, weaknesses, opportunities and threats, strategic issues and prepares a time bound action plan for achieving the goals. BAEC with its limited resources is always trying hard to strengthen the safeguards and physical protection programs around its research reactor and associated facilities. The BAEC plays a leading role in the planning, implementation, and evaluation of the nuclear safeguards and security activities in different nuclear and radio-logical facilities. Bangladesh government has strong commitment to implement nuclear power programs (NPP) in the country. The knowledge and experience gain from operating the research reactor, directly or indirectly can support the development and implementation of nuclear power programs. In addition with that, nuclear reactor technology related training and education program has been extended to provide necessary supports to the students undertaking nuclear engineering courses in various public universities of the country. The reactor facility has been used for training and retraining programs of the reactor operating personnel. The facility also arranges several practical experiments on nuclear safety parameters measurements for the participants of different training courses. Research, education and human resource development programs enhance significantly with a view to implement the NPP. BTRR is playing an important role for human resources and infrastructure development for nuclear science and nuclear power programs in the country. The experience from managing nuclear material at research reactors promotes a better understanding of the infrastructure and issues that need to be addressed in the field of nuclear power programs.

Key Words: TRIGA Research Reactor, Utilization of the reactor, Manpower training, Nuclear power program.

1. Introduction

The BAEC TRIGA Research Reactor (BTRR) has been in operation for almost 33 years (first critical in 1986). This is the only research reactor operated in Bangladesh under BAEC. BTRR is a light water cooled, graphite reflected reactor, designed for maximum steady state power level 3 MW (thermal) and for pulsing operation with maximum pulse power of 852 MW. The reactor uses Erbium-Uranium-Zirconium Hydride material as fuel elements. The uranium enrichment of the BTRR fuel is 19.7% [1], [2]. The BTRR was operated by analogue console system from its commissioning of Sept 1986 to July 2011. The analogue based control console system has been replaced by digital control console on June, 2012. Besides this, two neutron beam port facility has been modernized by the addition of a digital neutron radiography set-up at the tangential beam port and installation of a high performance neutron powder diffractometer at the radial beam port-2 of the reactor. After modernization of reactor control console systems and neutron beam port facilities, reactor based research has increased significantly [1]. The government considers this reactor facility to be one of the most valuable

installations of the country. The government funds the facility as and when needed for safe, efficient and reliable operation, maintenance and utilization of the research reactor. Recently an annual development project has been taken by the government for the balancing modernization and renovation of BTRR to increase operational life time as well as safety of the reactor. This is a prime facility in the field or nuclear research and training in Bangladesh.

FIG.1. Shield structure of the BTRR

Fig 1 shows the shield structure of BTRR. The reactor has so far been used in various fields of research and utilization such as, Neutron Activation Analysis (NAA), Neutron Radiography (NR), Neutron Scattering (NS), experimental reactor safety research, academic research, training of manpower (local and foreign) etc. It will play a major role for construction and operation of future NPP of Bangladesh as the basic issues consider in infrastructure building for NPP's are common with research reactor. Primary responsibility for the safety of nuclear facilities rests with the operating organization that mean BAEC. CRR is performing a very important role in this field. CRR routinely carries out certain activities which are considered as part of the international obligations that fall on Bangladesh as a signatory of different treaties, agreements and protocols signed between Bangladesh and the International Atomic Energy Agency (IAEA) under the International Nuclear Non-proliferation regime.

2. Research Activities

Research and Development (R&D) works on reactor physics and reactor engineering are oriented around the TRIGA MARK-II research reactor which constitutes a complex, multidisciplinary task involving basic nuclear safety research, studies on control and operational parameters applications of reactor neutrons to useful analytical and testing procedures. The activities in these areas are: (i) Development of computational facilities for nuclear engineering and nuclear data processing (ii) Neutronics, burn-up and in-core fuel management study of nuclear reactor (iii) Development of shielding materials and related technology (iv) Heat transfer and thermal hydraulics studies of nuclear reactor (v) Control and

monitoring studies of nuclear devices (vi) Development of digital reactivity meter for TRIGA reactor.

Beside those different groups of the Institute of Nuclear Science and Technology (INST) used the neutron beam of the reactor for carrying out various R&D activities. The reactor user groups have research collaboration with national and international research institute and universities [3].

2.1. Neutron Activation Analysis

The neutron activation analysis (NAA) Group is one of the vital users of the BTRR. NAA group is engaged in the determination of major, minor and trace elements in geological, biological, industrial, nutritional and health-related environmental samples. At present arsenic toxicity in groundwater is a serious problem for the nation. The NAA laboratory has therefore given special emphasis on the determination of arsenic toxicity in water, soil, foodstuff and biometrics of arsenic-affected patients. For the analysis of the sample mostly the pneumatic system is used. Fig 2 shows the pneumatic system controller and sample loader/unloaded.

FIG.2. Pneumatic transfer system: (a) Sample load/unload unit, (b) controller

2.2.Neutron Radiography

Another vigorous user group of BTRR is Neutron Radiography (NR) group. The Neutron Radiography (NR) group used the NR technique to detect voids, cracks, internal continuity in materials and determine water absorption behaviour of jute plastic composites and various types of building materials e.g. bricks, tiles, etc. In addition with that, they are also engaged with determination of irradiation time of Electronic spare parts to determine internal defects and determination of exposure time growth in plant, determination of double layer collagen bandage (sheet) blood serum absorption. Fig 3 shows the schematic diagram of the neutron radiography and neutron radiography experimental set-up.

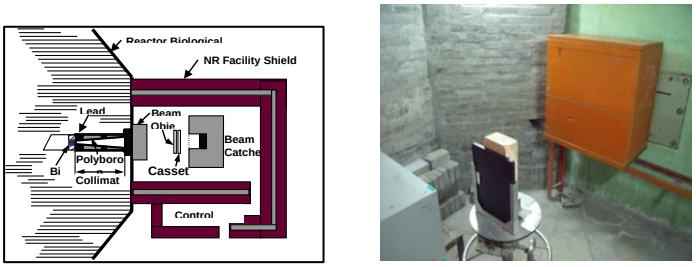

FIG.3. NR facility: (a) Schematic Diagram of the NR, (b) experimental set-up

2.3.Neutron Scattering

Neutron Scattering (NS) group performed Neutron Powder Diffraction studies as well as Small Angel Neutron Scattering and Texture studies. The High Performance Powder Diffractometer (HPPD) has been set up at the reactor to enhance the R&D facilities in neutron scattering technique. Structural studies of materials are being done by this technique to characterize materials crystallographic and magnetically. The micro-structural information is obtainable by neuron scattering method which is very essential for determining its technological applications. This technique is unique for understanding the magnetic behaviour in magnetic materials. Ceramic, steel, electronic and electric industries can be benefited from this facility for improving their products and fabrication process. Fig 4 shows the experimental setup for Neutron diffraction.

FIG.4. Experimental setup for Neutron diffraction.

3. Utilization of BTRR:

During the year 2017, the reactor was operated at power levels of 50 W to 2400 kW for reactor physics experiments conducted by CRR personnel and to provide neutron beam for various reactor users. During this period, the total operating hour was about 253 and total burn-up of the reactor fuel was about 441 MWh. Monthly fuel burn-up is graphically represented in Figure 5 and monthly operation data of the reactor during the reporting period are shown in Table 1.

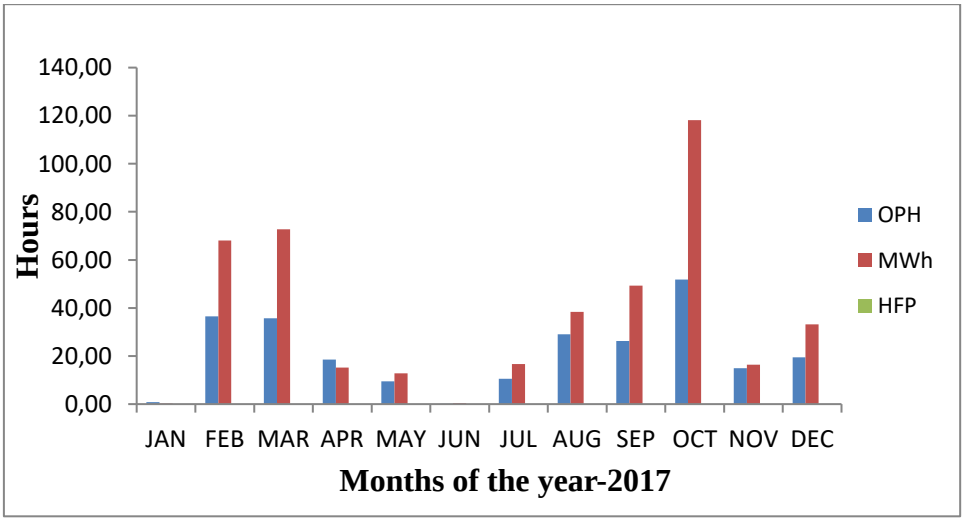

FIG 5: Monthly Operational Data for 2017

Table 1: Monthly Operational Data for 2017

MONTH	OPH	MWh	CuOPH	CuMWh	DOP	CuDOP
JAN	0.88	0.25	0.88	0.25	3	3
FEB	36.45	68.11	37.33	68.36	9	12
MAR	35.75	72.74	73.08	141.10	9	21
APR	18.50	15.23	91.58	156.33	10	31
MAY	9.50	12.83	101.08	169.16	7	38
JUN	0.20	0.48	101.28	169.64	1	39
JUL	10.53	16.61	111.81	186.25	3	42
AUG	29.07	38.39	140.88	224.64	12	54
SEP	26.27	49.32	167.15	273.96	7	61
OCT	51.78	118.08	218.93	392.04	11	72
NOV	14.93	16.37	233.86	408.41	7	79
DEC	19.433	33.1703	253.29	441.58	8	87

In the last 5 years, a total of 1820 samples were irradiated through the 574-irradiation request using neutron beam of the reactor for carrying out various research and development activities.

4. Experimental Research on Nuclear Safety

Study on reactor physics safety parameters of the nuclear reactor is the most important for reactor safety and efficient operation. Some important reactor safety parameters were measured such as control rod worth, core excess reactivity, shutdown margin, loss of reactivity with power increases, power defect, fission product poisoning, fuel temperature reactivity coefficient, coolant temperature reactivity coefficient, void coefficients and thermal power calibration of the reactor. Most of the measured safety parameters were found within the safety limit as mentioned in the Safety Analysis Report (SAR) of the BAEC research reactor.

5. Human Recourse Development

CRR arranged routinely different types of training program for professionals from different govt. and non govt. organizations and students from different universities**.** BTRR is playing an important role for human resources development for nuclear power. Scientists, engineers are being trained up at various levels of reactor engineering, operation, control and maintenance. Students from Universities do R&D works for their thesis and carry out industrial training. In addition with that a number of foreign and Bangladeshi officials have pay a visit to the reactor facilities.

Fig.5. Practical works going on for engineering students at BTRR

5.1.1. Senior Reactor Operator (SRO) and Reactor Operator (RO) Training Program

The facility has been used to train up reactor personnel up to the level of Senior Reactor Operator (SRO) and Reactor Operator (RO). However, at present three licensed SROs and Five ROs are working at the facility. The facility routinely arranged SRO & RO training and retraining programs for Scientists/Engineers/Officers at the reactor facility.

5.1.2. In-house Training Program

The facility routinely arranged in-house training programs for Scientist/Engineers and technical staffs on radiation protection and different systems & equipment of the reactor. The BTRR is also used for demonstration on reactor operation for BAEC scientists who are participating in different training programs such as BNOC, reactor engineering course, FTC course etc.

In-house training programs for technical supporting personnel on the following fields:
(i) Radiation protection; (ii) Reactor I&C system; (iii) Reactor auxiliary systems;
(iv) Improvement of safety culture; (v) Emergency preparedness, etc.

5.1.3. Industrial Attachment Training program for Engineering Students

Theoretical and experimental demonstration has given to the students on nuclear engineering. One hundred and ten students from different engineering universities are also complete their industrial attachment program from CRR.

5.2 Education Programs

University students took essential help from the reactor and its associated laboratories for Master, M. Phil and Ph.D. programs. For the last 5 years, 34 students have completed their Master/M.Phil. /PhD level thesis using reactor facility. 37 (Thirty Seven) students from Nuclear Engineering department of Dhaka University have completed their practical works as a part of their master's course in this year. Almost sixty technical/scientific papers have been published for last 5 years in various national and international journals, using reactor facility.

6. Nuclear power programs

The Government is determined to implement the nuclear power plant named RNPP for meeting the long-term electricity demand of the country. An agreement was signed on 2 November 2011 between the Government of the Russian Federation and the Government of the People's Republic of Bangladesh for the construction of a NPP (2400 MW) on the territory of Bangladesh. A programme has been undertaken by the BAEC to perform the following activities: (i) to evaluate sustainable energy strategies for addressing climate change issues employing analytical tools of IAEA such as MESSAGE, ENPEP, WASP, Air Pacts etc. (ii) to perform the feasibility of a nuclear power plant in the power system expansion planning for the long term power generation (iii) to assess energy indicators to identify the barriers of under-development of the power sector and to recommend future strategies to resolve those issues (iv) to compare the cost effectiveness of the nuclear power plant with different alternatives and calculate the loan repayment at different rates. These programs are solely dependent on BTRR and its associated professionals. In addition with that there are 19 issues consider in infrastructure building for NPP and among those issues a lot of similarity has been presents for NPP and research reactor [4-5]. With a vast operating experience of operating a research reactor for about 3 decades, BAEC is playing the key impending areas of research reactor contribution to the building for NPP are: Nuclear safety, regulatory activities, safeguards, radiation protection, human resource development environmental protection, emergency planning, security and physical protection, nuclear fuel handling and storage, radioactive waste, etc. These issues are handling by customarily by the BAEC and regulatory personnel successfully. The supporting infrastructures, experience and expertise by the existing research reactor would be helpful for taking knowledgeable decision regarding NPP. Currently the RNPP is in the second phase of construction and a company has already formed to take over that. Pre-construction surveys and construction of supporting facilities are now on-going on the project site.

The radiation protection program at the reactor facility showed that the reactor could be operated safely and maintained the international goal of keeping personnel doses and release of radio nuclides As Low as Reasonably Achievable (ALARA). Different presentations on this topic were delivered by CRR engineers/scientists at different seminars/workshops to share the knowledge among the engineers/scientists working on RNPP project. It is to be mentioned that BTRR is an important facility for providing training to the manpower that would be needed for nuclear power program of the country.

7. Conclusions

The reactor has been operated safely for various peaceful applications of nuclear technology. Different user group performed various experiments, which plays an important role in perspective of nuclear science and technology in Bangladesh.The reactor facility is used for training and educational and research purpose. Bangladesh government has a strong commitment to implement nuclear power plant (NPP) in the country. BTRR is playing an important role for human resources development for new research reactor as well as nuclear power program in the country. Knowledge and experience gather from operation and maintenance of BTRR over the last three decades in different fields like regulatory supervision, safeguards, radiation protection, licensing, nuclear fuel management etc. will be very helpful for the successful implementation of country's first nuclear power plant.

8. References

[1] HASAN, M. R., et al., Annual Report of Center for Research Reactor, BAEC, Savar, Dhaka (2017).

[2] GENERAL ATOMICS (GA), Safety Analysis Report of BAEC 3MW TRIGA Mark-II Research Reactor, Savar, Dhaka (1986).

[3] REACTOR AND NUCLEAR PHYSICS DIVISION, Report of reactor utilization group, BAEC, Dhaka (2013).

[4] INTERNATIONAL ATOMIC ENERGY AGENCY, nuclear energy series NP-T-5.1.

[5] SALAM M. A.; HASAN, M. R.; et al, Role of BAEC TRIGA Research Reactor in the Development of Nuclear Science and Power Programs in Bangladesh, IAEA CN-231 (2016).

Orano Decommissioning and Waste Management services for Research Reactors.

When approaching the research reactor's end of life, operators are facing multiple new challenges as they have to prepare the reactor for future works, establish the most adapted decommissioning programme and resource management strategy, while managing major issues related to budget, finance and relations with regulatory authorities.

This paper aims to provide research reactors' operators with an overview of the areas of support Orano can offer, with a strong focus on the optimization of the decommissioning plan and the transition period, in which risks for the future of the programme can be limited, and opportunities created.

As an owner-operator and service provider, Orano has accumulated extensive experience in D&D of nuclear facilities over the last decades. Orano is indeed in charge of the decommissioning of its own facilities and is involved in several major international decommissioning programmes in France, in the UK, in Japan and in the United States with the North Star alliance. It has also delivered several research reactors decommissioning projects such as SVAFO in Sweden, Phebus in Cadarache, Phenix in Marcoule, Ulysse in Saclay, as well as other French research reactors TRITON, EL3, PEGASE, MELUSINE, SCARABE.

In addition, with more than 10,000m3 of waste conditioned each year, coupled with continuous D&D efforts, Orano has built a comprehensive range of waste management solutions for transport, characterization, treatment and conditioning.

These experiences provided Orano with strong expertise in defining the optimal strategy for various types of projects in a given legal and political environment, and capacities in project cost control and optimization. As for waste management, Orano's approach aims to minimize the costs, the volume and toxicity of the final waste as well as the incremental investments, while achieving environmental, safety, political and legal requirements.

Orano is ready to set up sustainable partnerships with research reactors operators and support them with robust and optimized solutions.

NEUTRON ACTIVATION MEASUREMENTS AND CALCULATIONS IN SUPPORT OF DETECTOR TESTING EXPERIMENTS AT THE JSI TRIGA REACTOR

V. RADULOVIĆ, K. AMBROŽIČ, T. GORIČANEC, B. KOS, S. RUPNIK, A. JAZBEC, L. SNOJ

Reactor Physics Division, Jožef Stefan Institute

Jamova 39, 1000 Ljubljana - Slovenia

ABSTRACT

Recently, the utilization of the Jožef Stefan Institute (JSI) TRIGA reactor in Ljubljana, Slovenia, for dedicated experimental testing campaigns of neutron detectors has steadily been increasing. In 2018, three dedicated experimental testing campaigns were performed, aimed at the validation of the response of self-powered neutron detector (SPND) assemblies, thermocouples and fission chambers in representative reactor conditions. This paper presents neutron activation measurements and calculations, performed at the JSI TRIGA reactor as required support for the experimental testing campaigns. The measurements represent an independent experimental means of verification and adjustment of the calculated neutron flux levels and spectra, obtained through Monte Carlo particle transport calculations with the MCNP6 code. These calculated results serve as input data for subsequent computational determination of the detector responses and comparison to the experimental values obtained in the experiments.

1. Introduction

In the last few years, the utilization of the Jožef Stefan Institute (JSI) TRIGA reactor in Ljubljana, Slovenia, for dedicated experimental testing campaigns of neutron detectors has steadily been increasing. In 2018, three dedicated experimental campaigns were performed, aimed at demonstrating and validating the functioning of self-powered neutron detector (SPND) assemblies, thermocouples and fission chambers in representative reactor conditions. Additionally, the experimental results served as validation of dedicated computational schemes for the calculation of SPND signals. The tested SPNDs were of different material compositions and geometry; the experimental tests were performed in different locations in the core of the JSI TRIGA reactor. The entry data required in the computational schemes used to calculate the detector response signals are neutron and gamma flux levels and energy spectra in close vicinity of the tested detector assemblies. The entry data was calculated by the Reactor Physics Division of the JSI through the use of the MCNP6 code [1] in conjunction with the ENDF/B-VII.1 nuclear data library [2]. The calculations were performed by explicitly modelling the tested detector assemblies and including them in a detailed, verified and validated computational model of the JSI TRIGA reactor, which has been in use at the JSI for over a decade and which is being constantly improved

and refined. The computational model has been validated for calculations of the effective multiplication factor [3], kinetic parameters [4], neutron flux distributions [5-6], and can offer the possibility of in-depth computational support to experimental campaigns [7-8]. Recently a new benchmark on the comparison of measurements with CEA-developed miniature fission chambers and Monte Carlo calculations, performed in collaboration with the CEA has been published in the International Handbook of Evaluated Reactor Physics Benchmark Experiments (IRPhE) [9].

Neutron activation measurements were performed as an independent experimental means of verification of the neutron flux calculations. Measurement of the ^{197}Au(n,γ) and ^{27}Al(n,α) reaction rates were performed using samples of Al-0.1%Au certified reference material obtained from the Institute of Reference Materials and Measurement – IRMM, Belgium (now JRC). The performed neutron activation irradiations were reproduced in the JSI TRIGA reactor model and reaction rates in the locations of the irradiated samples were calculated for comparison. This paper gives a general overview of the performed detector testing experiments and presents the comparison between calculated and experimentally determined ^{197}Au(n,γ) and ^{27}Al(n,α) reaction rates in support of detector testing experiments at the JSI TRIGA reactor.

2. Performed experimental campaigns

The first experimental campaign was performed in the framework of the DISCOMS (DIstributed Sensing for COrium Monitoring and Safety) project, part of the French National Research Agency program on nuclear safety and radiation protection [10-11]. The project aims at the development of new under-vessel instrumentation based on both distributed Optical Fiber Sensors and Self-Powered Neutron Detectors (SPNDs). Two CEA laboratories (the Instrumentation Sensors and Dosimetry Lab - LDCI and the Sensors and Electronic Architecture Lab - LCAE) and the Thermocoax SAS company co-developed a sensing instrumentation device including SPNDs and thermocouples as well as a standalone low current acquisition system. The experimental campaign was performed in January 2018. One sensor was irradiated in three irradiation locations in the JSI TRIGA reactor.

The second experimental campaign consisted in irradiations of SPND detector assemblies and fission chambers in the framework of a project on development of new instrumentation for in-core neutron flux monitoring in a nuclear reactor. The campaign was performed in October 2018. SPND detector assemblies were irradiated inside Measurement Positions (MPs), i.e. positions located between the fuel elements in which it is possible to irradiate objects with a maximum diameter of 10 mm.

The third experimental campaign was performed for the Thermocoax SAS company, which develops, manufactures and commercializes neutron detectors, including SPNDs. Several SPND detector assemblies were irradiated in one MP in the reactor core. The requirements for the performance of the testing campaign were stringent, and included highly accurate positioning of the SPND detector assemblies in the reactor core in the axial (vertical) direction as well as the angle of rotation about the vertical axis. Assembly positioning to the required tolerances was achieved through a

dedicated positioning system, designed in collaboration with Thermocoax and manufactured at the JSI. The campaign, which was performed in a two week period [12], involved irradiations of four detector assemblies and numerous changes in the assembly position in the reactor core and reactor start-up – shutdown sequences.

Figure 1 displays the JSI TRIGA reactor core configuration and a photograph of the reactor core at full power. Figure 2 displays a schematic 3D-view of 6 JSI TRIGA fuel elements located by the top and bottom reactor grid plates and the Measurement Positions in which detector assemblies can be inserted for testing.

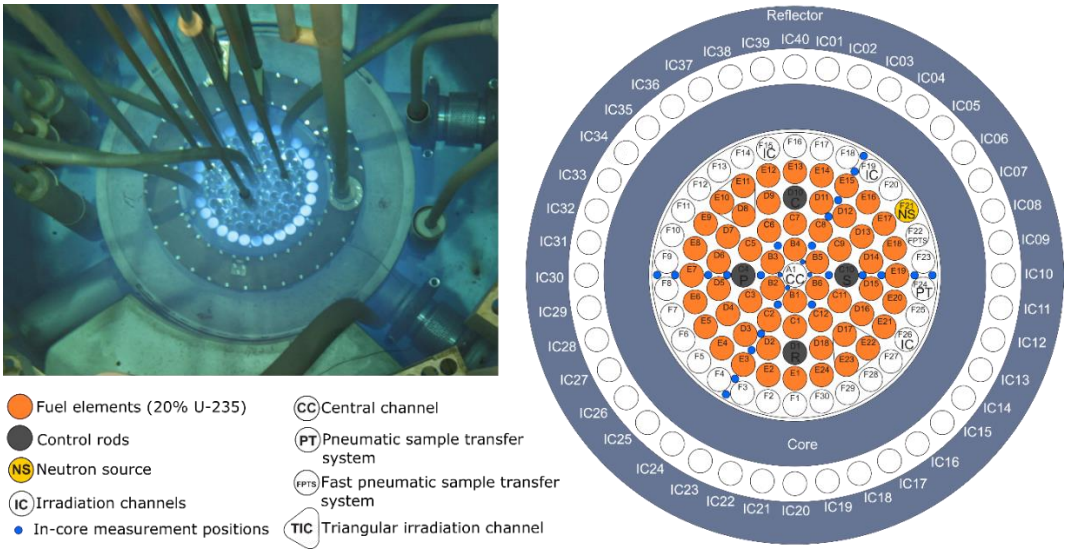

Figure 1. Left: JSI TRIGA reactor core at full reactor power (250 kW). Right: reactor core configuration.

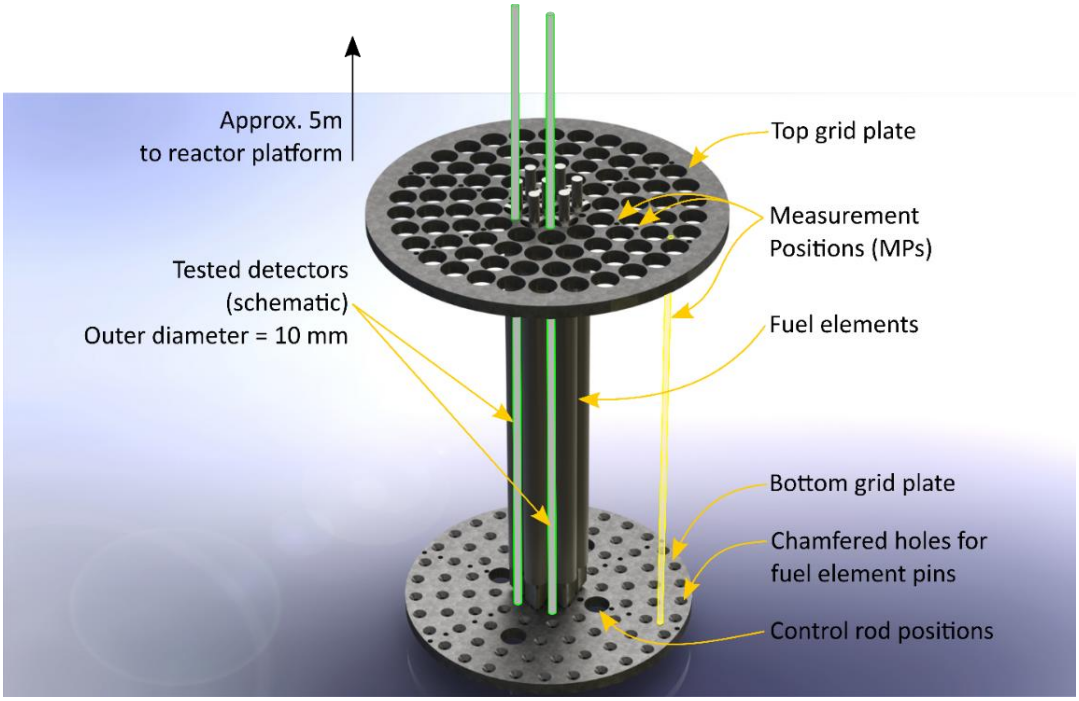

Figure 2: Schematic 3D view of 6 fuel elements located by the top and bottom reactor grid plates, the Measurement Positions in which detector assemblies can be inserted for testing.

3. Neutron activation measurements

Neutron activation measurements were performed in the framework of the three experimental campaigns, to experimentally determine reaction rates for the ^{197}Au(n,γ) and ^{27}Al(n,α) reactions. Both reactions are dosimetry reactions with well-known reaction cross sections and are included in the International Reactor Dosimetry and Fusion File (IRDFF) [13]. The ^{197}Au(n,γ) reaction is sensitive to thermal and resonance energy neutrons, the ^{27}Al(n,α) reaction is a threshold reaction (the threshold energy being approximately 3.25 MeV) therefore it is sensitive to the fast neutron energy range. Figure 3 displays plots of the groupwise ^{197}Au(n,γ) and ^{27}Al(n,α) reaction cross sections (data taken from the IRDFF-v1-05 nuclear data library).

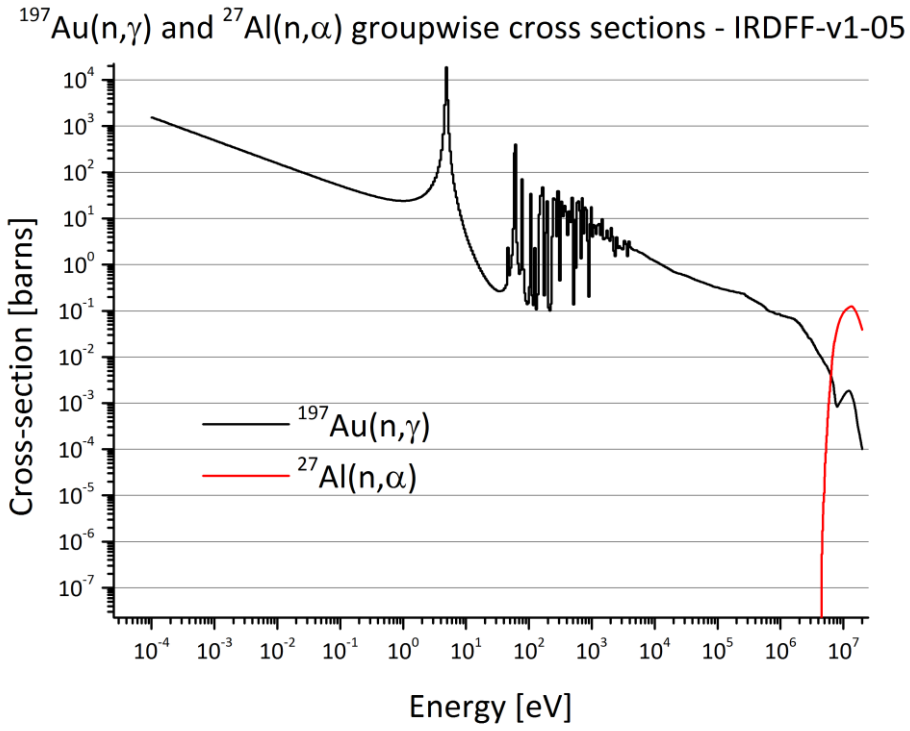

Figure 3: Groupwise cross-sections for the ^{197}Au(n,γ) and ^{27}Al(n,α) reaction cross sections vs. incident neutron energy. Data taken from the IRDFF-v1-05 nuclear data library.

The same reference material was used for the measurement of both reactions, i.e. Al-0.1%Au alloy, obtained from the Institute of Reference Materials and Measurements (IRMM), now Joint Research Centre (JRC) in Geel, Belgium. Samples in both wire and foil form were employed. The foils had a diameter of approximately 5 mm and a thickness of 0.1 mm, the wires had a diameter of 1 mm and were approximately 5 mm in length.

Depending on the experimental testing requirements, samples were irradiated in close proximity of the tested detector assemblies in the reactor core or in dedicated sample holders, without the tested detectors present. In the first and third testing campaign, samples in foil form were used. They were sealed in polyethylene film in order to avoid contamination; the sealed samples were attached to aluminium centering components, in turn attached to the detector assemblies. The centering components bearing the

samples were designed to enable detachment from the detector assemblies underwater, inside the JSI TRIGA reactor pool, in order for this operation not to cause significant radiation exposure to personnel. The centering components were extracted from the reactor pool after a suitable cooling time and the samples were extracted. In the second campaign, samples in wire form were irradiated inside aluminium probes, consisting of inner aluminium rods, 5 mm in diameter with 69 1.5 mm diameter holes, perpendicular to their axis, at 1 cm increments, into which samples can be inserted. The inner rods fit inside aluminium sleeves. The top section of the rod treads onto the top section of the sleeve. The top section of the sleeve also has several steps, which rest on the top surface of the top reactor grid plate and determines the vertical position of the probe in the reactor core during irradiation. Figure 4 displays a technical drawing and a photograph of the probes.

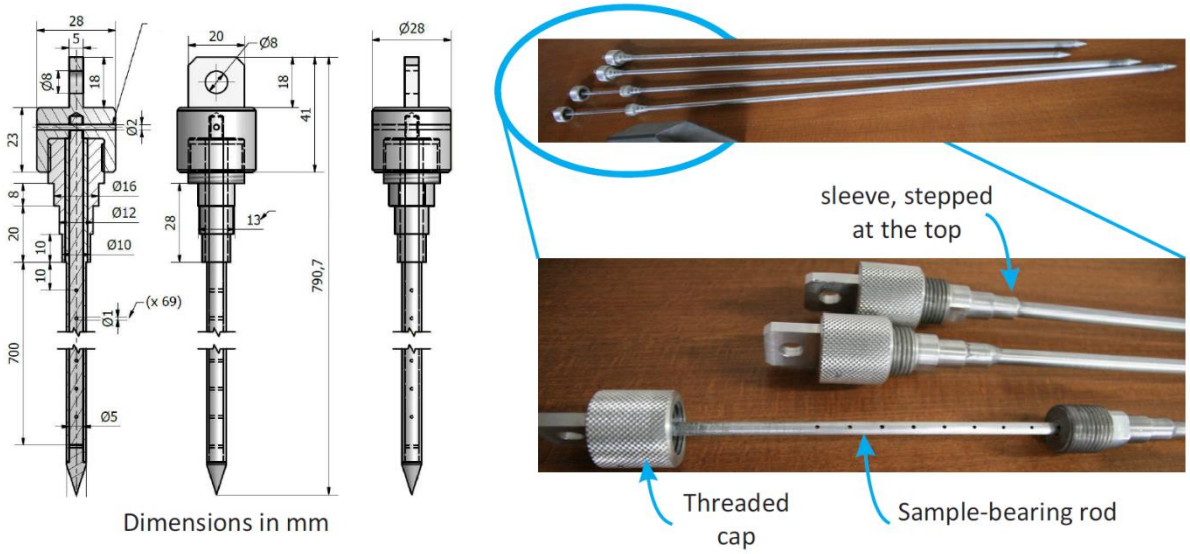

Figure 4. Aluminium probes used for the neutron dosimetry measurements. Left: technical drawing, right: photograph of 4 probes.

After extraction, the samples were measured using an absolutely calibrated High Purity Germanium (HPGe) detector. The gamma rays of interest in the measurements were at energies 411.8 keV (^{198}Au) and 1368.6 keV (^{24}Na), resulting from the ^{197}Au(n,γ) and ^{27}Al(n,α) reactions, respectively. From the recorded peak areas in the gamma spectra and the sample and timing data, the specific saturation activities per target atom (in Bq / target atom) were computed using the JSI-developed code SPCACT, which computes the saturated activities (reaction rates) per target atom and the associated uncertainties. At infinite dilution (i.e. if self-shielding effects are negligible, as in the present case) the specific saturation activities correspond to the reaction rates and can be directly compared to the values obtained by Monte Carlo calculations. The experimental uncertainties were calculated from the individual contributions due to the uncertainties in the sample mass, irradiation, measurement and cooling times, the recorded peak areas and the detection efficiencies. The 1-σ experimental uncertainties for the ^{197}Au(n,γ) and the ^{27}Al(n,α) reaction rates ranged from around 2% to 3% and from around 3% to 4%, respectively.

4. Reaction rate calculations

Monte Carlo calculations of the ^{197}Au(n,γ) and ^{27}Al(n,α) reaction rates were performed with the MCNP6 code in conjunction with the ENDF/B-VII.1 nuclear data library, for direct comparison with the experimental values. Tallies were defined in 1-cm sections of the aluminium centering elements or aluminium probes, centered on the sample locations. This approach was favoured over explicitly modelling the samples, which would require significantly longer calculation runs to achieve satisfactorily low statistical calculation uncertainties. The experimental configurations during the sample irradiations were reproduced in the computational model (presence or not of detector assemblies, centering components, sample-bearing probes, control rod positions). The raw calculation results were normalized with respect to the reactor power, according to Equation (1)

$$R_{abs} = R_{calc} \frac{P\nu}{w\, k_{eff}}, \quad (1)$$

where R_{abs} is the absolute reaction rate value, R_{calc} is the raw calculated result, P is the reactor power level during the irradiation, ν is the average number of neutrons emitted per fission, w is the recoverable energy per fission and k_{eff} is the calculated effective multiplication factor [14]. The uncertainties in the calculated values are quadratically combined from the statistical uncertainties and an additional estimated 5% contribution due to the uncertainty in the reactor power normalization factor [6]. The resulting 1-σ uncertainties in the calculated values were between 5% and 6% for the ^{197}Au(n,γ) reaction and between 5% and 8% for the ^{27}Al(n,α) reaction.

5. Comparison of experimental and calculated results

Figures 5-8 display the calculated and experimental ^{197}Au(n,γ) and ^{27}Al(n,α) reaction rates and 1-σ uncertainties in MP17, MP20, MP25 and MP26, respectively, as a function of the depth from the top surface of the top reactor grid plate.

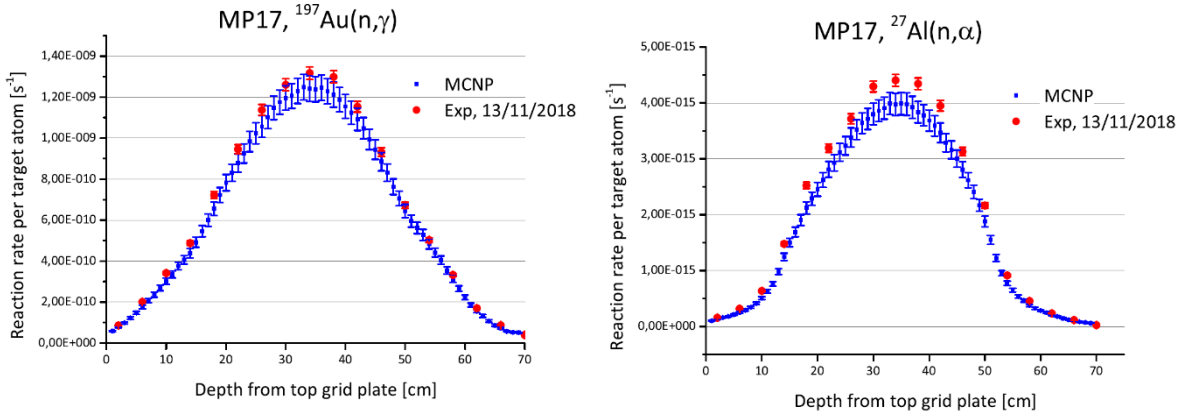

Figure 5: Comparison of experimental and calculated ^{197}Au(n,γ) and ^{27}Al(n,α) reaction rates in MP17.

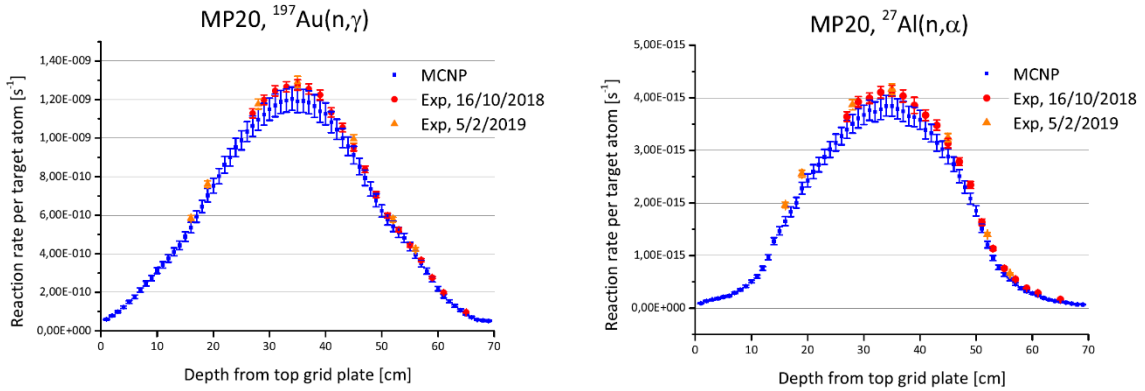

Figure 6: Comparison of experimental and calculated ^{197}Au(n,γ) and ^{27}Al(n,α) reaction rates in MP20.

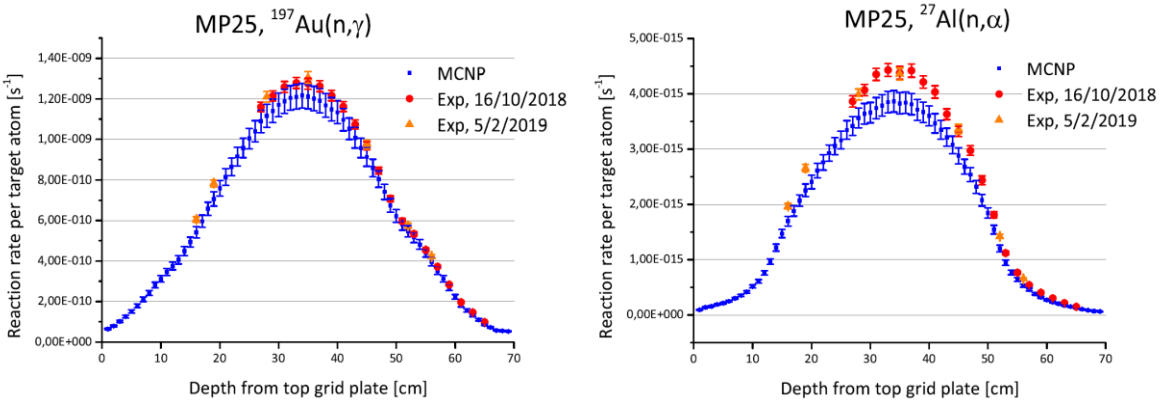

Figure 7: Comparison of experimental and calculated ^{197}Au(n,γ) and ^{27}Al(n,α) reaction rates in MP25.

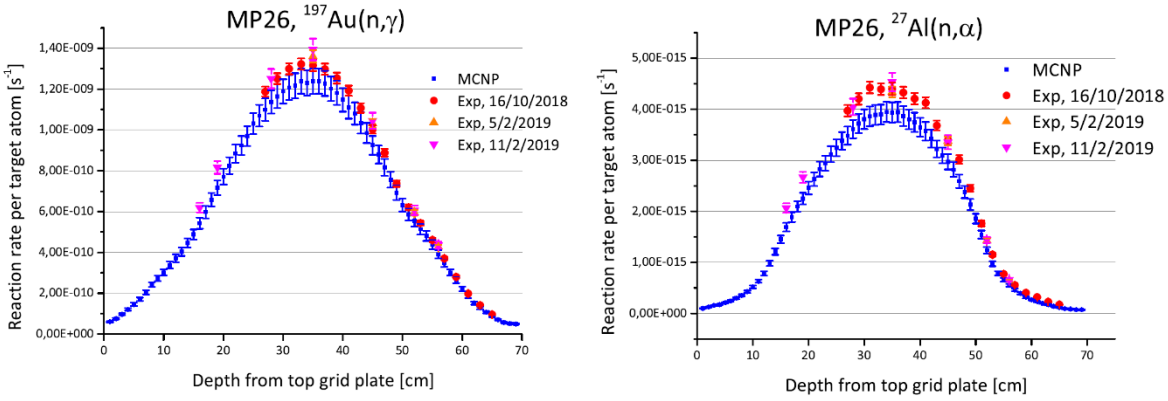

Figure 8: Comparison of experimental and calculated ^{197}Au(n,γ) and ^{27}Al(n,α) reaction rates in MP26.

Overall, the experimental and calculated reaction rate profiles for all the MPs have a consistent shape, indicating that the calculations reproduce very well the relative neutron flux distribution within the reactor core. The experimental results from independent irradiations and measurements were seen to agree consistently within the

experimental uncertainties, indicating a good repeatability of the experimental conditions in the reactor.

The comparison of absolute reaction rate values showed that for both reactions, the experimental values are consistently higher than the calculated values. For the ^{197}Au(n,γ) reaction, the experimental and calculated values are in agreement within their respective 1-σ uncertainties; the observed relative differences are consistently around 6%. For the ^{27}Al(n,α) reaction, the relative differences between the experimental and calculated values are higher, i.e. around 10 % - 15 %. A possible cause for the observed discrepancies are fuel burnup effects, the fuel burnup not being treated explicitly in the calculations. On the basis of the comparison between the experimental and calculated reaction rates, adjustment were made in the calculated neutron flux levels, to be used for computational determination of the detector responses.

6. Conclusions

This gives presents an overview of dedicated neutron detector testing experiments performed at the JSI TRIGA reactor. In the framework of the experimental campaigns, neutron activation measurements for the ^{197}Au(n,γ) and ^{27}Al(n,α) reactions were carried out through irradiations of Al-0.1%Au material. Dedicated Monte Carlo particle transport calculations of the ^{197}Au(n,γ) and ^{27}Al(n,α) were carried out for comparison with the experimental values. Overall, for the ^{197}Au(n,γ) reaction, agreement between the experimental and calculated values was observed, within their respective 1-σ uncertainties, the relative differences being around 6 %. For the ^{27}Al(n,α) reaction, the agreement was less good, the relative differences being around 10 % - 15 %. The discrepancies can be attributed to fuel burnup effects, not treated in the calculations. Work is currently in progress at the JSI, aimed firstly at collecting and consolidating the TRIGA reactor operational history, and secondly, to obtain realistic fuel element isotopic composition data through the use of computational methods, in order to improve the performance of the computational model. On the basis of the comparison, adjustments to the neutron flux levels, used for subsequent computational determination of the detector responses were made. The successful outcome of the recent testing activities further confirms the status of the JSI TRIGA reactor as a reference facility, able to host dedicated nuclear instrumentation detector testing experiments.

7. References

[1] Goorley, J. T., James, M. R., Booth, T. E., Brown, F. B., Bull, J. S., Cox, L. J., Durkee, J. W. J., Elson, J. S., Fensin, M. L., Forster, R. A. I., et al., Jun 2013. Initial MCNP6 Release Overview - MCNP6 version 1.0. Los Alamos National Laboratory (LANL), Report number: LANL Report LA-UR-13-22934.

[2] Chadwick, M.B. et al., ENDF/B-VII.1 Nuclear Data for Science and Technology: Cross Sections, Covariances, Fission Product Yields and Decay Data. Nuclear Data Sheets, 112 (12), 2887-2996, 2011.

[3] Jeraj, R., Ravnik, M., 2010. TRIGA Mark II Reactor: U(20)-Zirconium Hydride Fuel Rods in Water with Graphite Reflector, IEU-COMP-THERM-003. International Handbook of Evaluated Criticality Safety Benchmark Experiments, NEA/NSC/DOC(95)03, OECD-NEA, Paris, France.

[4] Snoj, L. et al., Calculation of kinetic parameters for mixed TRIGA cores with Monte Carlo. Ann. Nucl. Energy, 37, 2, 223-229, 2010.

[5] Snoj, L., et al., Analysis of neutron flux distribution for the validation of computational methods for the optimization of research reactor utilization, Appl. Radiat. Isot., 69, 1, 136-141, 2011.

[6] Radulović, V. et al., Validation of absolute axial neutron flux distribution calculations with MCNP with $^{197}Au(n,\gamma)^{198}Au$ reaction rate distribution measurements at the JSI TRIGA Mark II reactor, Appl. Rad. Isot., 84, 57-65, 2014.

[7] Snoj, L., Žerovnik, G., Trkov, A., Computational analysis of irradiation facilities at the JSI TRIGA reactor, Appl. Rad. Isot., 70 (3), 483-488, 2012.

[8] Ambrožič, K., Žerovnik, G., Snoj, L., Computational analysis of the dose rates at JSI TRIGA reactor irradiation facilities, Appl. Rad. Isot., 130, 140-152, 2017.

[9] Štancar, Ž., et al. Reaction Rate Distribution Experiments at the Slovenian JSI TRIGA Mark II Research Reactor, TRIGA-FUND-RESR-002. In: International Handbook of Evaluated Reactor Physics Benchmark Experiments [DVD]/Nuclear Energy Agency. - Paris OECD Nuclear Energy Agency, 2017. - 251 pp. (NEA;7329).

[10] Barbot, L., Villard, J-F., Fourrez, S., Pichon, L., Makil, H., The Self-Powered Detector Simulation 'MATiSSe' Toolbox applied to SPNDs for severe accident monitoring in PWRs, EPJ Web Conf. 170 08001 (2018).

[11] Brovchenko, M., Duhamel, I., Dechenaux, B., Neutron-gamma flux and dose calculations for feasibility study of DISCOMS instrumentation in case of severe accident in a GEN 3 reactor, EPJ Web Conf. 153 07030 (2017).

[12] https://www.thermocoax.com/successful-test-campaign-on-neutron-sensors/ (9.3.2019)

[13] Capote, R., Zolotarev, K. I., Pronyaev, V. G., and Trkov, A., "Updating and Extending the IRDF-2002 Dosimetry Library," Journal of ASTM International, Vol. 9, No. 4, 2012, pp. 1-9.

[14] Žerovnik, G. et al., On normalization of fluxes and reaction rates in MCNP criticality calculations, Ann. Nucl. Energy, 63, 126-128, 2014.

NETWORKING MULTINATIONAL FUEL AND MATERIALS TESTING CAPACITIES FOR SCIENCE, SAFETY AND INDUSTRY:

THE P2M JOINT PROJECT PROPOSAL IN THE FRAME OF THE OECD/NEA

D. P. PARRAT, M.C. ANSELMET
CEA, DEN, DEC
Commissariat à l'Energie Atomique et aux Energies Alternatives, Nuclear Energy Division
Building 151, CEA Cadarache, 13108 Saint Paul lez Durance (FR)

M. MIKLOS
Centrum vyzkumu Rez s.r.o., CVR
Husinec-Rez 130, 250 68 Husinec-Rez (CZ)

B. BOER, M. VERWERFT, S. VAN DEN BERGHE
Studiecentrum voor Kernenergie, SCK•CEN
Boeretang 200, 2400 Mol (BE)

A. AMBARD
Electricité de France, Research and Development, Department MMC
Avenue des Renardières, 77250 Écuelles (FR)

M. TON THAT, N. WAECKEL
Electricité de France, Direction Technique
19 Rue Pierre Bourdeix, 69007 Lyon (FR)

G. BIGNAN
CEA, DEN, DER
Commissariat à l'Energie Atomique et aux Energies Alternatives, Nuclear Energy Division
Building 151, CEA Cadarache, 13108 Saint Paul lez Durance (FR)

ABSTRACT

Recent changes in the European irradiation infrastructure landscape opened a period with reduced experimental capability for addressing the needs in the field of nuclear fuel and materials development and qualification, waiting for new irradiation facilities such as the Jules Horowitz MTR. To overcome these uncertainties, and to preserve skilled staff and knowledge, an efficient way is to establish and maintain collaborations through international joint research projects with the use of multiple infrastructures (MTRs and hot cell laboratories) in parallel.

This way has been recognized as essential by the JHR Consortium, and a first experimental program was proposed to the OECD/NEA by a "core group" gathering SCK•CEN, CEA and EDF. Main objective is to discriminate, rank and quantify mechanisms that appear in a LWR fuel rod during any type of power transients, with a focus on those provoking a moderate to high load on the clad. This focus includes power levels initiating a central melting of the fissile material.

This paper describes the context of this proposal, the scientific objectives in relation with stakes for power reactors operation, details on experiment implementation and measurements done on-line or through PIEs. A specific OECD/NEA/NSC workshop will be held beginning of March 2019, for discussing this proposal. The main outcomes will be presented at this Conference.

1. Introduction

The landscape of the irradiation infrastructures worldwide changed dramatically in recent years: large MTRs such as the Halden Boiling Water Reactor (HBWR, NO), Japan Material Test Reactor (JMTR, JA) and OSIRIS at CEA (FR) experienced a definite shutdown respectively in June 2018, mid-2017 and end of 2015. These events opened a period with reduced experimental capability for addressing the needs in the field of nuclear fuel and materials development and qualification. Major MTRs (water cooled high power research reactor for fuels and materials testing) still in operation today are ATR (USA), MIR and SM3 (Russia), BR2 (Belgium), HFR (Netherlands), LVR-15 (Czech Republic) and there is up-to-now one new irradiation facility under construction; the Jules Horowitz MTR [1], [2]. To overcome these uncertainties, and to preserve skilled staff and knowledge, an efficient way is to establish and maintain international collaborations through international joint research projects. One example among others is the case of the Halden Reactor Project (HRP), managed under the umbrella of the OECD/NEA (Nuclear Energy Agency), which demonstrated the value of such a synergy for decades. However, the closure of the HBWR led HRP members to consider other joint projects in order to maintain this fruitful international cooperation: the goal is to use several alternate facilities in parallel (i.e. MTRs and hot cell laboratories for post-irradiation examinations) to reduce the impact of a possible defaulting facility on the experimental programs.
In coherence with this view, the Jules Horowitz Reactor (JHR) Project has set up an International Consortium, for close partnership between the funding organizations. This Consortium has organized in 2013 three Working Groups, namely Fuel, Materials and Technology. They gather scientific representatives and experts from industry (utilities and fuel suppliers), research and international organizations. As a key output of these working groups, it has been decided that “pre-JHR” irradiation programs of common interest should be defined, addressing generic scientific issues of interest for the whole MTR community.
These programs are proposed in the coming years in existing MTRs and/or hot cell laboratories, according to their possibilities, before potentially continuing them in JHR [3], [4].

The first in pile experimental program, which has been recommended by the Fuel WG experts (formerly called “SLOWTRANS” and now called “P2M”), aims at determining and quantifying of the main physical phenomena activated during any type of power transients, including potential incipient fuel melting at fuel pellet center. Such transients may generate moderate to high straining of the fuel cladding. This program covers transverse R&D topics exploring Light Water Reactor (LWR) fuel rod behavior in operating conditions (incidental and accidental) rarely covered before and for which a lack of data is obvious. Moreover, this program catches the interest of various potential partners: R&D organizations, fuel vendors, plant operators and Safety Bodies.

2. Presentation of the new multinational program to the OECD/NEA

The Nuclear Science Committee (NSC) of the NEA organized in January 2018 a workshop titled “Enhancing Experimental Support for Deployment of New Fuels and Materials”. This workshop gathered industry (utilities, fuel makers), regulatory bodies, technical support organizations, research organizations and experimentalists in order to reach a mutual understanding of the requirements of the validation/qualification process for innovative fuel and to enhance the effectiveness of experimental programs. Discussions during the workshop helped to identify multiple directions for international collaboration where the NEA can play an important role as integrator and central coordinator in several potential tasks. However, due to the HBWR situation, a proposal was made to urgently form a joint experimental project to test selected Accident Tolerant Fuels (ATF) concepts, for LWRs with the aim to perform them in the Halden reactor and other research reactors, including those represented at the workshop.
At this workshop, a CEA presentation entitled “Some pending issues in nuclear fuel and in-core materials development for LWRs: experimental support for modeling and simulation”, detailed three R&D experimental program proposals in the nuclear fuel domain, gathering irradiation in MTRs

and/or examinations and separate effect tests in hot cells. The first one dealt with fuel behavior under slow power transients that addressed fuel safety and flexibility under plant operation. This proposal was the primary structure of the current P2M program.

A second NEA workshop held in October 2018, gathering NSC and CSNI members, was the first one held after the HBWR closure, and provided the basics of a new vision for building multilateral programs [5]. In particular, involvement of stakeholders to oversee the transition from the Halden Reactor Project to a new Framework was underlined. It has been confirmed, that International Joint Projects are the best way to ensure a continuity of coordination and cooperation in the use of experimental facilities to meet the needs of the community. Within the due respect of budgetary capacities, it is relevant to involve multiple test facilities that offer mutual benefit and advance the international vision for an integrated fuel and materials research.
A "Core Group" gathering three partners, SCK•CEN, CEA and EDF, presented the P2M proposal at this workshop. The aim is to launch a new ambitious NEA joint project based on a few advanced in-pile experiments.
The first task of this program is to implement an irradiation program in the BR2 MTR (SCK•CEN, BE). This choice is driven by the following benefits:

- The anticipated irradiation device is available on-the-shelf and fully operational,
- BR2 exhibits a high neutron flux (for achieving a high terminal linear power on a high burn-up experimental rod),
- SCK•CEN experienced staff has already implemented similar tests.

The proposed irradiations will be supported by pre-test and post-test simulation, and completed by non-destructive and destructive PIEs in hot cell Laboratories (see more details in § 6.2).
The second Task aims at testing modern and innovative fuel and cladding materials (such as Accident Tolerant Fuel or Advanced Technology Fuel concepts). It will include the use of advanced irradiation devices and innovative on-line instrumentation.

3. Objectives and interest of the P2M proposal

3.1 Scientific and R&D objectives

The in-pile experiment will focus on quantification of:

- Fuel thermal expansion, due to the global temperature increase during the power transient,
- Fuel gaseous swelling, due to increased diffusion of fission products and to the formation of gas bubbles, within the fuel grains and at the grain boundaries (see figure 1 below),
- Fission gas release (FGR), due to temperature elevation and temperature gradient between the pellet center and the periphery,
- Supplementary fission gas release as a consequence of the phase change when fuel material starts to melt,
- Fuel volume change and its impact on the cladding in case the central part of the fuel pellet melts. That will imply very high linear heat generation rate (LHGR) levels.

This program will combine several scientific objectives (with a view to enhance fuel behavior knowledge during power transients) in one experiment such as:

- Quantifying the FGR for high LHGR values and for fuels with high burn-up levels,
- Monitoring the clad deformation as a function of the loadings resulting from the physical mechanisms above mentioned,
- Defining local irradiation conditions susceptible to generate a given quantity of melted fuel,
- Studying impact of a partial melted volume on the overall fuel rod behavior and properties.

To achieve this, a specific in-pile irradiation test has to be defined to enable power transient test conditions significantly different from those of standard "power ramp" ones and covering, on a conservative approach, all the hypothetical situations. In particular, objective is (i) to reach, on a mastered way, the incipient fuel melting limit in the central part of the hottest fuel pellet(s) (i.e. at the maximum rod temperature plane), whatever the burn-up of the tested rod, and (ii) to avoid the fuel rod failure, either during the power transient phase or at the occurrence of incipient melting.

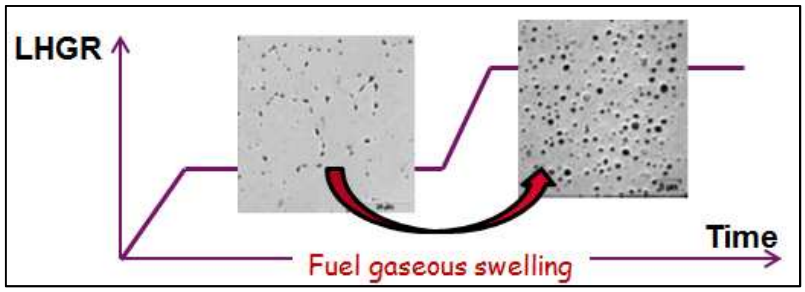

Fig. 1: Schematic of fuel gaseous swelling during a power increase

3.2 Improvement of modeling and codes on fuel rod behavior

The current databases need to be updated to account for the advanced irradiation conditions targeted by P2M. Such conditions include high burn-up fuels, high LHGR levels, new fuels and modern cladding materials, including Accident Tolerant Fuel (ATF) products, properties change at the melting, etc… The experimental results will be made available to all the participants and will be used to update the fuel performance codes models thanks to benchmarks.

Modeling will be used to design the experiment itself to make it as relevant as possible. To define the test conditions and to specify the instrumentation performances (range, sensitivity...), pre-calculation of the fuel rod behavior will be carried out to assess the evolution of the parameters of interest (centerline fuel temperature, anticipated incipient melting temperature, fission gas distribution, fission gas release, cladding strains, etc..) and to detect potential thresholds.

These calculations will help building the safety case of the experiment itself (this will be a specific task using validated models). They will also streamline the post-test comparisons between prediction and experimental results.

3.3 Industrial motivations

Integral tests on nuclear fuel have always been precious to support a safety demonstration because they enable actual phenomena observation within a fuel rod during a transient. Hence, from a nuclear industry point of view, it is crucial to maintain the ability to carry out such transients in MTR at a reasonable cost.

Because of the strong coupling between the various physical phenomena taking place within the fuel, separate effect experiments are insufficient to provide directly the requested safety margins. Integral or semi-integral tests are thus necessary. Various integral tests have been carried out in the recent years such as in-pile LOCA tests in Halden (Halden Reactor Project) or in-pile RIA transients in CABRI (Cabri International Program CIP). Numerous power ramps have also been performed to determine the PCI-SCC failure thresholds in test reactors such as R2 (Studsvik), OSIRIS (CEA) and HBWR (Halden), all of them being now shutdown. Regarding slow transients, the current fuel integrity demonstration relies on data derived from old tests, performed on obsolete fuel designs with limited (and not always reliable) instrumentation. As a result, it is worth updating the database using modern fuel designs (fuel and cladding alloys) and comprehensive online measurements.

3.4 P2M as a program gathering crosscutting interests

The targeted scientific information gained from P2M will help addressing safety and reliability issues related to NPP flexible operation, fuel manufacturing and procurement processes:

- For R&D organizations: the Project will enhance the overall knowledge on fuel and cladding behaviors, provide reliable data to validate fuel performance codes models and extend international databases with updated experimental data in temperature/power domains where very few data exist, especially on modern fuel products.
- For utilities: the Project will provide the maximal allowable cladding strain at high linear heat rate, the margin to incipient fuel melting and, more globally, will improve the quantification of the available margins in the current fuel management schemes (the potential benefit being eventually a relaxation of the current limitations on in-reactor power change rates),

- For fuel vendors: the Project will provide licensing data usable for new fuel products and for new fuel licensing methodologies and for safety enhancement (e.g. for ATF products),
- For Technical Support Organizations (TSOs) and safety organizations: the Project will help harmonizing the safety approach methodologies.

4. Implementation of the P2M program

The proposed project is divided into two tasks:
➔ **The first Task** should be started as soon as possible using the devices already available within the Core Group (see § 2). In practice, the choice made is to implement an irradiation program in the BR2 MTR (SCK•CEN, BE) driven by the following benefits:

- The anticipated irradiation device is available on-the-shelf and fully operational,
- BR2 exhibits a high neutron flux, for achieving a high terminal linear power on a high burn-up (BU) experimental rod,
- SCK•CEN experienced staff has already implemented similar tests.

The proposed irradiations will be supported by pre-test and post-test simulation, and completed by non-destructive and destructive post-irradiation examinations (PIEs) in hot cell Laboratories (see more details in § 6.2).
➔ **The second Task** will provide complementary scientific information by investigating the fuel rod cladding deformation during the transient caused by the fission gas and the solid and gaseous swelling of the fuel stack. Such a goal requires to adapt or to develop a specific device welcoming devoted sensors capable to measure on line the fuel rod diameter changes.
Combining the results of Task 1 and Task 2 will result in an extended database on transients to help establishing the safety cases.

5. Proposed project plan and test matrix

To implement the program in a timely manner, the first experiment will be a “scoping test” on standard fuel products (fuel and clad) to commission the test device, to master the experimental protocol and to confirm that the results fit with models predictions. To maximize the parameters values accessible during the test (internal pressure, clad deformation...), the test rods should be preferably selected in the high burnup range (to enhance fission gas effects), e.g. in the range 40-65 GWd.t_U^{-1}. However, the BU value is open and will be adapted depending on available candidates and participant’s proposals. The proposed two first tests for the Task 1 are:

Task	P2M Test #	Type of fuel	Type of cladding	Targeted volume fraction of melted fuel at maximum T plane	Comments
Task 1	1	Standard UO_2 BU # 50 GWd/t_u	M5 / Zirlo	5%	Calibration of the experimental protocol
	2	Standard UO_2 BU # 50 GWd/t_u	M5 / Zirlo	15%	Same fuel as #1 (from an adjacent stack) Go / No Go for Task 2

In order to monitor on-line the kinetics of the evolution of the parameters of interest during the test, the refabricated rod (refabrication process is detailed in [6]) will be equipped with sensors enabling on-line evolutions of i) the rod internal gas pressure (RIP) and/or the gas composition [7] and ii) the fuel centerline temperature. Other qualified sensors might be implemented if available. In particular, on-line clad outer diameter measurement is of prime interest and shall be implemented as early as possible in the test device, so in the test matrix.

6. Experimental irradiation device and experimental protocol

6.1 Overview of the project

The overall transient that the project wants to explore is schematized on figure 2 below. It also indicates the main physical phenomena affecting the fuel or the fuel-clad gap and impacting potentially the clad deformation.

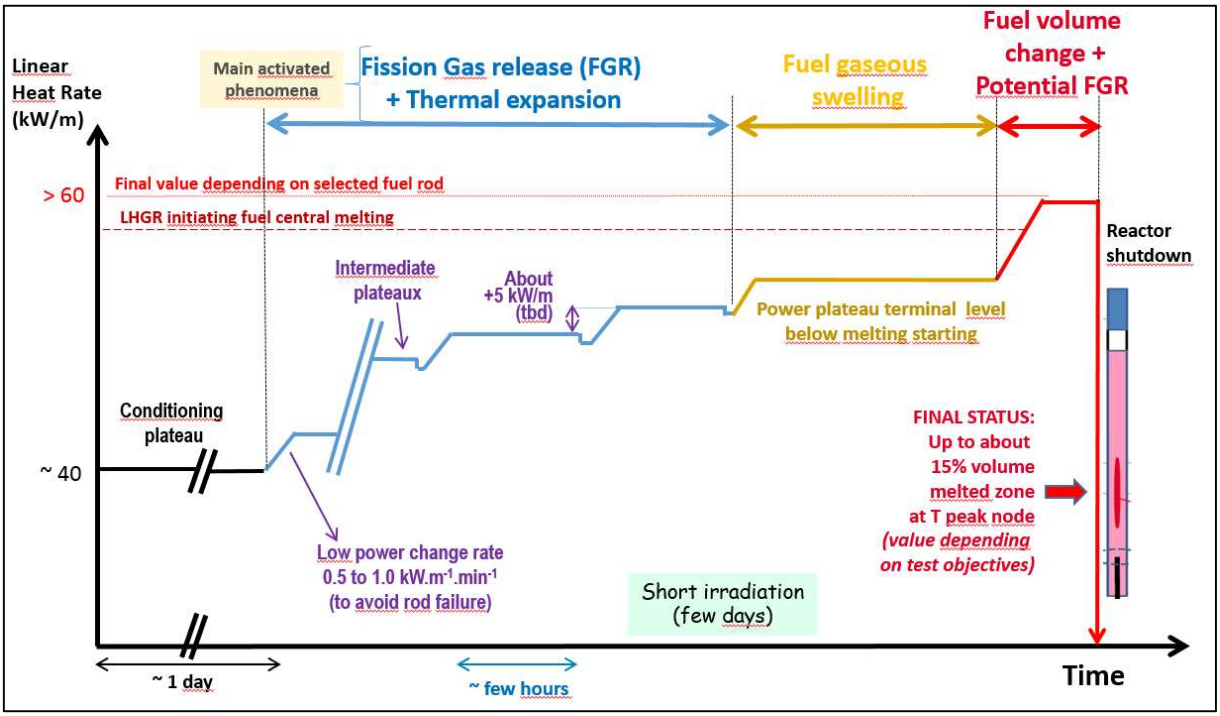

Fig. 2: Schematic of the envelope configuration of the transient that the project wants to investigate

To implement an in-pile test in a timely manner, a 2 phases approach has been proposed and detailed in § 4. The first one, corresponding to Task 1, will address the "fuel melting issues" and the second one (Task 2) mainly the "fuel swelling issues" (the "fuel melting issues" will be also considered). "Melting" is first investigated because devices are operational whereas the in-situ cladding deformation measurement required for the "fuel swelling phase" is still under development or integration work (see [8] for the status of melting from the design point of view and the reference herein).

6.2 Task 1 implementation

The main objective is to reach high LHGR values (beyond 60 $kW.m^{-1}$) on high burn-up fuels, such requesting high neutron flux environment. The proven Pressurized Water Capsule (PWC) in BR2 reactor (SCK•CEN, Mol, Belgium) is well suited for power to melt transients (see figure 3). The LHGR of a high burnup test rod will be increased stepwise until the incipient fuel melting threshold is reached, and then the targeted melted volume fraction (see figure 2 and [9]).
The test device allows internal pressure measurements (or rod axial extension measurements, alternatively). Temperature in the center of the bottom of the fuel stack is also measured.

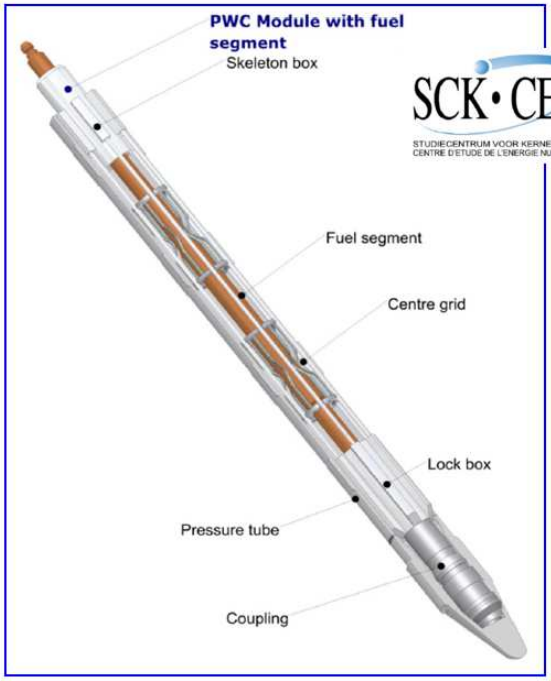

Fig. 3: Schematic of the PWC capsule to be used in BR2

Compare to the envelope configuration represented on figure 2, the experimental protocol will focus on last power plateaus. The test itself is anticipated to last 2 days, but the process in BR2 will last about one week, including test preparation and post-test handling. It is possible to run a direct power-to-melt ramp test, which would be shorter (a few minutes, see [10]), but it would not fit with the overall objective of the project which is to investigate the behavior of fuel rods during a **slow** transient. Therefore it was chosen to reproduce a whole slow transient terminated with a power-to-melt transient.
The terminal plateau at very high power level should initiate a “lens” of molten fuel at the peak power node. More precisely, the target is to obtain a melted zone representing a volume fraction ranging from 5 to 15% in the 2 first tests at the hottest elevation of the tested rod. The reactor power will then be shutdown in such a way that final status of the rod is preserved and rod failure during the power decrease is precluded. Destructive PIEs will be performed and should exhibit similar feature as those shown on figure 4 below. It represents a crosscut of an experimental rod, which have experienced a power-to-melt test in another program.

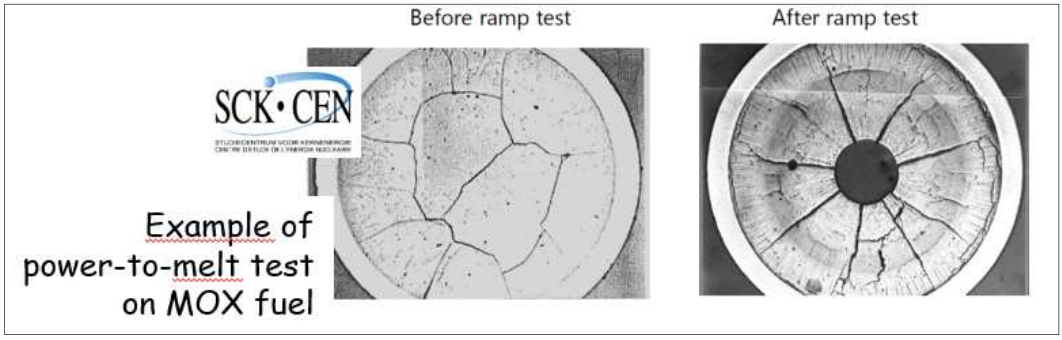

Fig. 4: Crosscut of an experimental rod after a test reaching the central melting

The axial extension of the melted zone will be mastered using the measured in-reactor axial neutron flux profile (figure 5 represents an example of BR2 power axial profile) and the calculated “power to melt” based on models validated on former experiments. It is a challenging issue, but feasible thanks to the previous experience feedback (see for example the program in ref. [11]).

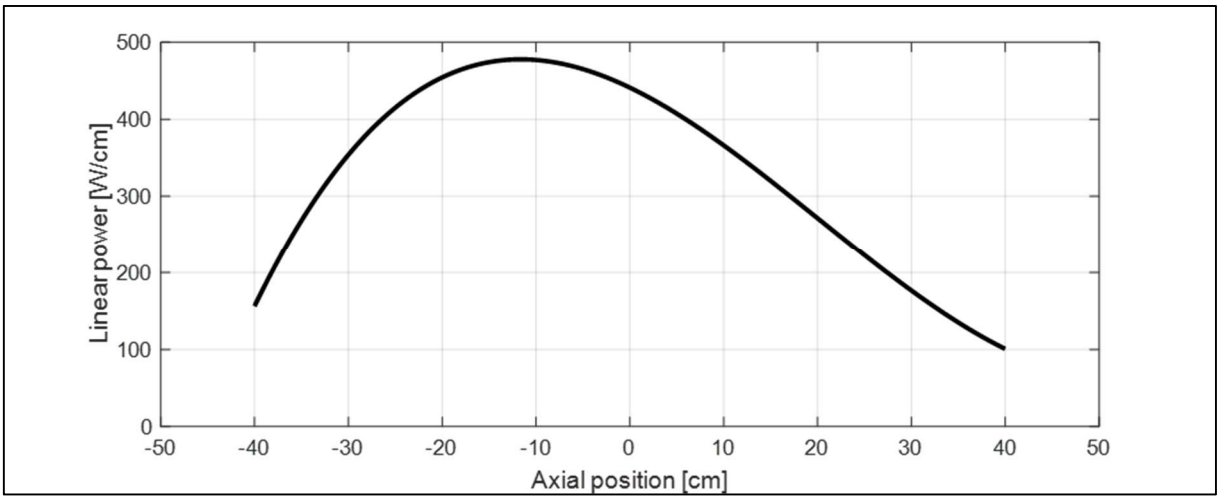

Fig. 5: Example of axial power profile in the BR2 reactor

Regarding post-irradiation examinations, the hot cell laboratories used for tests #1 and #2 (Task1) will be the LHMA at SCK•CEN at Mol and the LECA-STAR at CEA Cadarache, for non-destructive examinations and destructive examinations respectively:

➔ **Non-destructive post-irradiation examinations (NDEs)** for both tests will implement proven techniques. Before the test the reference status of the rod will be based on visual inspection, axial profilometry and gamma scanning. After the test, visual inspection, axial profilometry, gamma scanning and clad structure (by Eddy Current) will be the main examinations.

➔ **Destructive post-irradiation examinations (DEs)** will be performed after rod puncturing (measurements of the released gases and of the internal free volume). Proposed program consists of making three metallographic cuts (radial and/or axial) on interest zones determined by NDEs. On each cut, metallographies will be implemented before and after chemical etching (measurement of the spectrum of fuel grain sizes versus the pellet radius, study of the pellet-cladding interface…).
Then microanalyses with Electron Probe Micro-Analysis (EPMA) and Secondary Ion Mass Spectrometry (SIMS) will be performed on a coupled way (quantitative balance for the xenon distribution, to be compared to building codes, distribution and chemical forms of some fission products of interest, by co-localization…). Two other microanalysis techniques will be also proposed: micro-beam X-Ray Diffraction at various radius values and Electron Back-Scattered Diffraction (EBSD) to know the microstructure and the orientations at the fuel grain level.

6.3 Task 2 implementation

Task 2 of the Project aims at studying the cladding deformation induced by fuel solid and gaseous swelling during a slow transient. To achieve this goal specific development or adaptation of the test device are requested, favoring the use of a rig with multiple on-line instrumentation. In particular a reliable and accurate **on-line clad outer diameter sensor allowing axial scans,** has to be implemented.
It is recommended to benefit from IFE (Institute For Energy, Halden, NO) experience feedback in this matter. Options including a PWR loop or capsule in a MTR at RIAR, ROSATOM, or a dedicated loop or capsule in ATR at INL, DOE, USA, or a new capsule in BR2 should be investigated.
It must be understood that Task 2 is less well-defined than Task 1 as it requires further developments. So the proposed test matrix is preliminary. It includes Cr-doped UO_2 and Gd – doped UO_2 fuels (standard or large grains) with M5 or Zirlo cladding, and also E110 or equivalent cladding. ATF products will be also discussed (U_3Si_2, fuel with high thermal conductivity, SiC cladding...). Moreover, final test conditions will be defined by participants.

7. Conclusion

The recent Halden BWR definite shutdown opened a period with reduced experimental capability for addressing the needs in the field of nuclear fuel and materials development and qualification. In 2018, the OECD/NEA held several workshops or technical meetings, gathering NSC and CSNI members, for providing the basics of a new vision for building international joint research projects, as they are considered as an efficient way for improving the R&D knowledge and maintaining skilled teams. For that aim, an implementation, networking several infrastructures (MTRs and hot cell laboratories for post-irradiation examinations) on a same program, is clearly a relevant approach.

Within this objective, the P2M R&D program, proposed to the OECD/NEA by a “core group” gathering SCK•CEN, CEA and EDF, is currently the first and the most developed proposal. It aims at discriminating, ranking and quantifying mechanisms that appear in a LWR fuel rod during any type of power transients, with a focus on those provoking a moderate to high load on the clad. This focus includes power levels initiating a central melting of the fissile material. A first step (called “Task 1”) contents two tests and will be implemented in the BR2 MTR thanks to the PWC-CD boiling capsule. It aims at obtaining a predetermined melted volume fraction at the hottest part of the experimental rod. Then this final status will be analyzed by non-destructive and destructive examinations at the LHMA (SCK•CEN) and LECA-STAR (CEA Cadarache) respectively. The both tests are planned fall 2020 and fall 2021 respectively, and end of Task 1 is expected at mid-2023.

Detailed content of the Task 1 will be discussed during an OECD/NEA/NSC workshop beginning of March 2019. The main outcomes will be presented at this Conference.

REFERENCES

[1] BIGNAN G., “The Jules Horowitz Reactor: A new high performance European MTR with modern experimental capacities – Toward an international user Facility”, 16th IGORR Conf., 17-21 November 2014, Bariloche (AR).

[2] MARCILLE O., et al., “Jules Horowitz Reactor Project: Preparation of the commissioning phase and normal operation”, RRFM-IGORR 2019 Conf., 24-28 March 2019, Dead Sea resort (JO)

[3] GONNIER C., et al., “Preparing JHR international Community through the developments of the first experimental capacity”, 17th IGORR – RRFM 2016 Conf., 13-17 March 2016, Berlin (D)

[4] GONNIER C., et al., “Update of the JHR experimental facility and first orientations for the experimental programs”, RRFM-IGORR 2019 Conf., 24-28 March 2019, Dead Sea resort (JO)

[5] IRACANE D., “Multinational NEA Joint Project on nuclear fuel and material qualification testing”, RRFM-IGORR 2019 Conf., 24-28 March 2019, Dead Sea resort (JO)

[6] BERDOULA F., et al., “Fuel rod instrumentation techniques implemented in LECA facility – Development of advanced instrumentation techniques”, IGORR 2009 Conf., 27-30 October 2009, Beijing (CN)

[7] ROSENKRANTZ E., et al., “An Innovative Acoustic Sensor for In-Pile Fission Gas Composition Measurements”, IEEE Transactions on Nuclear Science, 2013

[8] NEA/WGFS “Nuclear Fuel Safety Criteria Technical Review”, 2012, second edition available at www.oecd-nea.org/nsd/reports/2012/nea7072-fuel-safety-criteria.pdf

[9] VAN DYCK S., et al., “Experimental irradiations of materials and fuels in the BR2 reactor”, IAEA Tech. Meeting on commercial products and services of research reactors, 28 June – 2 July 2010, Vienna (AT)

[10] SANNEN L., BODART S., GYS A., VAN DER MEER K., VERWERFT M., “Nuclear fuel rod qualification by ramp testing and pre- and post-irradiation examination”, Research Facilities for the Future of Nuclear Energy – Proceedings of an ENS Class 1 Topical Meeting, 1996, Edited by Hamid Aït Abderrahim, World Scientific, Page 187

[11] MACDONALD P. E. et al., Response of unirradiated and irradiated PWR fuel rods tested under power-cooling mismatch conditions, Nuclear Safety, Vol. 19, N°4, July-August 1978, p. 440

RRFM EUROPEAN RESEARCH REACTOR CONFERENCE 2019

IGORR

Theoretical and experimental reactor physic on the BME Training Reactor (TR) during the periodic safety review

András Horváth

Budapest University of Technology and Economics (BME), Institute of Nuclear Techniques

e-mail: horvath.andras@reak.bme.hu

Introduction:

The purpose of the work was the assistance for the last periodic safety review of the BME Training Reactor (TR).
The work has 2 parts, one of is the theoretical reactor physic calculations using the code MCNP6. Every relevant reactor physics parameter was calculated, for example: safety and control rod integral and differential worth's, isothermal reactivity coefficient, neutron flux in relevant core positions, etc. The experimental part of this periodic safety review was performed in an extended measuring project. Every reactor physics parameter was been measured in minimum 2 different methods. According to the simulation results in comparison with the measurements yields, the codes perform within an acceptable margin of error resulting almost identical data.

The BME Training Reactor

- **Location:** Campus of the BME
- **Type:** pool-type reactor (Hungarian design)
- **First criticality:** 1971
- **Nominal power:** 100 kW
- **Fuel:** EK-10 (soviet design), 24 assemblies
- **Moderator and coolant:** light water
- **Control:** 2 safety rod, 2 control rod,
  5 nuclear measurement channel
- 5 horizontal and 18 vertical irradiation channels (IC)
- 2 pneumatic rabbit system
- Thermal coloumn

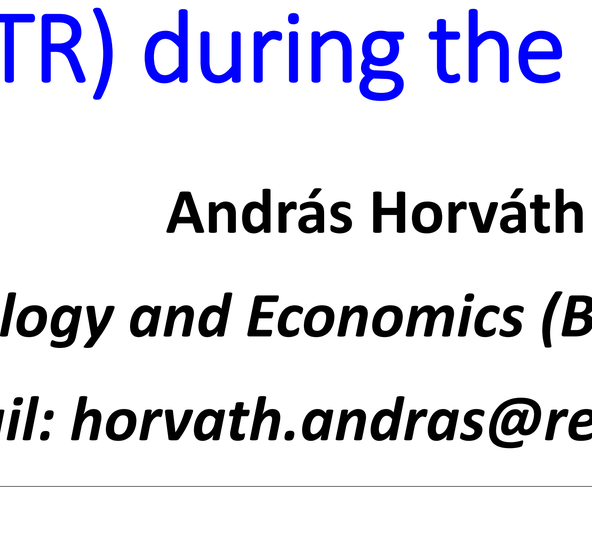

(*a* – automatic CR; b_i – safety rods; *c,d* – penumatic rabbit system; *e* – vertical IC; *f* – fuel elements; *g* – graphite reflector elements; *h* – IC in graphite; *i* –IC in fuel assemblies; j – start-up neutron source)

Total Reactivity worth of the safety and control rods

- Measuring method: rod drop and inverse kinetics
- Calculation method: MCNP 6.1 (using KCODE)

Rod type	Material	Reactivity worth [$]		Difference [%]
		Measured	Calculated	(calc./meas.)
SR-1	B_4C	2,25 ± 0,01	2,15 ± 0,005	-4,4
SR-2		3,41 ± 0,02	3,64 ± 0,005	6,7
Manual (K)		1,88 ± 0,01	1,92 ± 0,005	2,1
Automatic (A)	Cd on steel rod	0,86 ± 0,01	0,89 ± 0,005	3,95

Differential reactivity worth of the control rods

- Measuring method: inverse kinetics, 1/N method
- Count rates measurement: boron lined, Ar-filled proportional counter
- Calculation method: MCNP 6.1
- Fitted curve: *z* – actual position, H – length of the rod (H = 600 mm), C – parameter

$$\rho(z) = C \cdot \left[\frac{H - z}{2} + \frac{H}{4\pi} \sin\left(\frac{2\pi \cdot z}{H} \right) \right] \qquad \left. \frac{\partial \rho(z)}{\partial z} \right|_{z=\frac{H}{2}} = -C$$

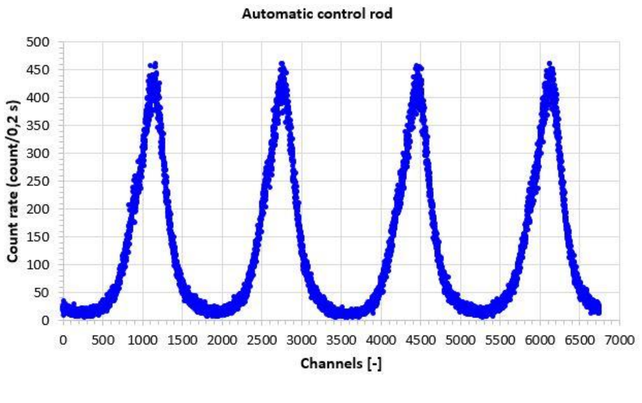

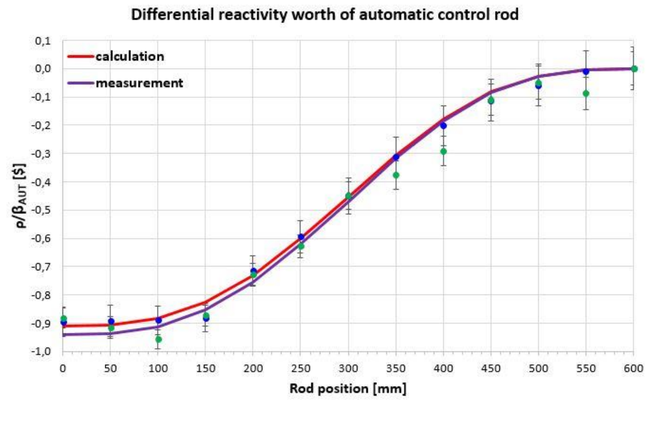

Periodic Safety Review (PSR)

- **Number of PSR done so far:** 1996, 2006, **2016**
- IAEA / HAEA guidlines was used
- **PSR team:** 8 – 10 persons
- **Quality Assurance:** review in pairs, director review
- **PSR report length:** 400 pages (6–100 / Safety Factors)
- **Reactor physics:** specific feature in TR

Isotermic reactivity coefficient measurement (δρ/δT)

- Measuring method: P = 1 W, automatic mode, heating the primary water
- Data collection: every half hour (T_{in}, T_{out}, h_{MAN} = 400 mm)
- Reactivity calculation: from the automatic rod curve

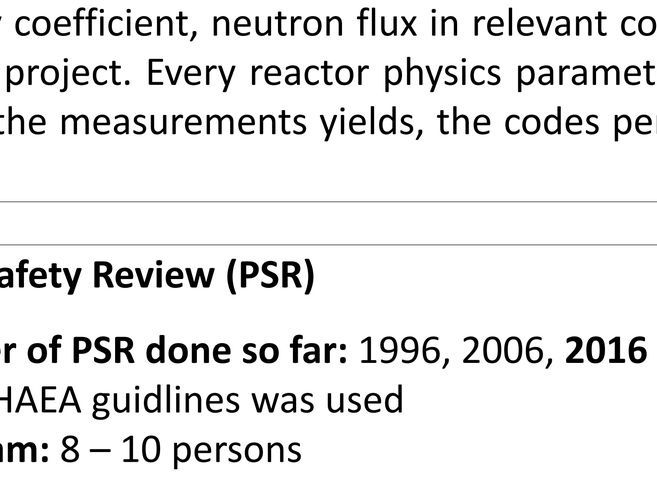

$$\rho(T) = a \cdot T^2 + b \cdot T + c \qquad \frac{\partial \rho(T)}{\partial T} = -2 \cdot a \cdot T - b = -0{,}02406 \cdot T + 0{,}170$$

Thermal neutron flux measurements

- Measuring method: distribution: Dy-Al wire in the core
  absolute: Gold foil activation
- Calculation method: MCNP 6.1

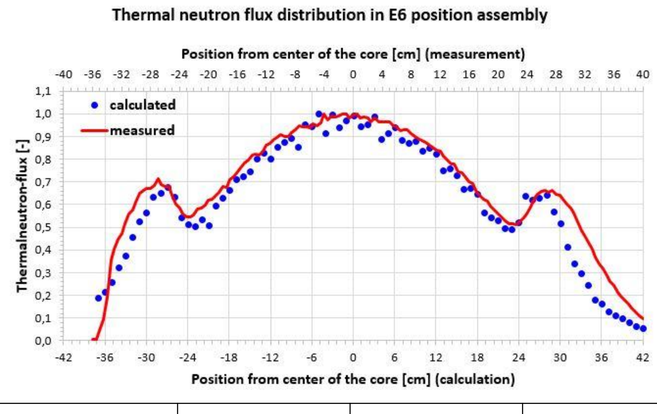

Position	G5	D5	E8
F4 tally ($\times 10^{-4}$)	4,115	8,874	3,12
k_{eff}	1,01177		
$\Phi_{calc.}$ [$cm^{-2}s^{-1}$]	$3{,}05\times10^{11}$	$6{,}58\times10^{11}$	$2{,}31\times10^{10}$
$\Phi_{meas.}$ [$cm^{-2}s^{-1}$]	$2{,}52\times10^{11}$	$3{,}38\times10^{11}$	$2{,}26\times10^{10}$

ON HOW A BEST ESTIMATE PLUS UNCERTAINTY ANALYSIS CAN IMPROVE THE DESIGN OF A RESEARCH REACTOR

J.LUPIANO CONTRERAS, A.S. DOVAL, P.A. ALBERTO
Nuclear Engineering Division, INVAP S.E.
Av. Cmte. Luis Piedrabuena 4950, R8403CPV San Carlos de Bariloche – Argentina

ABSTRACT

Thermal-hydraulic system codes have been used to evaluate the behaviour of research reactors in the steady state and during transients. The existence of uncertainties has forced the analyst to use a conservative approach to absorb deviations and guarantee that design criteria are satisfied. The best estimate method (BEPU) is an alternative providing a more realistic simulation of the case being studied. The best estimate calculation is complemented by an uncertainty analysis to obtain upper and lower bounds for relevant figures of merit.
RELAP5 is used to model the behaviour of OPAL research reactor. Both, the conservative and BEPU approaches are considered.
The study is divided into sections, including: a validation of the model, the determination of set point values for reactor trips and the evaluation of an initiating event considered for reactor design.
The BEPU methodology results in a more efficient reactor design with improvements in its operation.

Acknowledgment*: the authors very much appreciate the valuable commissioning data provided by ANSTO*

1. Introduction

Thermal-hydraulic system codes have been specifically developed to evaluate transients in Nuclear Power Plants (NPP) and they have been successfully used in the design of Nuclear Research Reactors (RR). Most best-estimate thermal-hydraulic system codes, such as RELAP5 solve the mass, energy and momentum equations for the liquid and the vapour phases and they make use of validated empirical correlations to close de problem. Sources of uncertainties, including geometrical deviations, the lack of knowledge in the physical phenomena involved, the existence of undefined or uncertain boundary conditions, the deviations in the empirical correlations and the extensive use of approximate mathematical methods, have forced the designer to use conservative values, boundary conditions and hypotheses to absorb all deviations and guarantee that all design criteria are satisfied.
The best estimate modelling is an alternative approach providing a more realistic simulation of the case being studied, with a precision commensurate with the current knowledge of the phenomena involved. The best estimate calculation is complemented by an uncertainty analysis to obtain upper and lower bounds for the relevant figures of merit.
The Best Estimate Plus Uncertainty (BEPU) methodology has been implemented to assess transients in NPP but its application has not been extended to the analysis of RR yet. In the design of NPP, the BEPU approach has proved useful as it has resulted in more economic designs and improved reactor performance.
The present study uses the thermal-hydraulic system code RELAP5 to model the behaviour of OPAL reactor in the steady state and during transients. Both, the conservative and the BEPU approaches are considered, thus resulting in two alternative ways to assess reactor behaviour. For the BEPU calculation approach, the “input error propagation” technique has been adopted. Uncertainties in operating parameters have been settled based on engineering judgment, measurements and experience.
The study is divided into different sections, including a) a validation of both calculation approaches by comparing calculated values of figures of merit, such as coolant flows with experimental values, b) a comparison between the set point values of parameters used for reactor trips as calculated by the two methodologies and, c) the evaluation of a loss of flow

accident (LOFA) to determine the size of the inertia flywheel of the primary cooling system pumps.
The analysis performed shows that the BEPU calculation approach may result in a more efficient reactor design with improvements in its operation. In particular, set points can be defined in such a way that the spurious triggering of a safety system due to a noisy signal is reduced. It also allows an optimization of the moment of inertia of the cooling pumps. Finally, the importance of validating the BEPU calculation approach also becomes relevant as it has been used for safety analysis and in the licensing of NPP and it could be extended to RR.

1. Description of the cooling circuit

The reactor considered for the analysis is the 20 MW OPAL reactor. During normal operation, the heat generated in the core is removed by demineralized light water flowing in an upward direction in a forced circulation cooling regime. The coolant is provided by a set of pumps which are part of the Primary Cooling System (PCS). Heat exchangers remove the heat to the Secondary Cooling System (SCS) and a decay tank has been added to allow activated nitrogen to decay.
During normal operation at low powers (≈ 400 kW) or following a pump stop, the power in the core is removed in the natural circulation cooling regime. Two set of flap valves have been placed in each inlet pipe for such purpose. The flap valves open when the pressure difference between the inlet pipes and the reactor pool is reduced, allowing the water in the pool to flow upwards through the core. The pumps in the PCS contain an inertia flywheel which provides the flow required to guarantee a smooth transition from the forced to the natural circulation cooling regime.

2. Reactor design based on thermal-hydraulic design criteria

The reactor design must guarantee that the fundamental safety function of heat removal is satisfied, so to preserve the integrity of the fuel. Thermal-hydraulic design criteria based on limiting physical phenomena have been established. These design criteria are considered for the reactor design and also to establish some of the set points values leading to the triggering of trips resulting in reactor shutdown.
The limiting phenomena considered in reactor design are Departure From Nucleate Boiling (DNB) and Flow Redistribution (RD). While different in nature, both of them result in vapour blanketing and a degradation of heat transfer which may lead to fuel damage. At low flows, these phenomena are known as Burn-Out (BO) and Boiling Power (BP) respectively.
Thermal-hydraulic design criteria have been established considering a margin to these limiting physical phenomena. These margins are summarized in Tab 1 and they are conservatively evaluated in a “hot channel”. The hot channel is the hottest channel in the core and it acts as an envelope to all the cooling channels. A peaking factor (PF) accounting for the non-homogeneous power distribution among the reactor core is considered to calculate the power in this hot channel.

Parameter	**Design criteria**		
	Normal Operation		**Postulated single failure initiating events**
	Forced circulation	**Natural circulation**	
$DNBR=q''_{DNB}/q''_{max}$	≥ 2.0	N/A	≥ 1.5
$RDR=P_{RD}/P_{max}$	≥ 2.0	N/A	≥ 1.5
$BOR=q''_{BO}/q''_{max}$	N/A	2.0	≥ 1.5
$BPR=BP/P_{max}$	N/A	2.0	≥ 1.5

Tab 1: Thermal-hydraulic design criteria

In Tab 1:
q''_{DNB}: Heat flux leading to DNB

P_{RD}: Power leading to RD
$q"_{BO}$: Heat flux leading to BO
BP: Boiling Power
$q"_{max}$: Maximum heat flux, calculated as PF*$q"_{ave}$, being $q"_{ave}$ the average heat flux which is the ratio between the thermal power in the core and the total heat transfer area

The $q"_{DNB}$ is calculated by the Mirshak correlation (1). The P_{RD} is calculated by the Whittle and Forgan correlation with the French formulation recommended by Fabrega (2). For low flows (coolant velocities < 1.3 m/s) the $q"_{BO}$ is calculated by using the Fabrega correlation (3) while the BP is calculated as the power required to achieve the saturation temperature.

3. Thermal-hydraulic design

The thermal-hydraulic design of a nuclear reactor relies on calculation codes. These codes make use of empirical correlations which introduce uncertainties to the calculations. Deviations from nominal operating parameters and fabrication tolerances are also a source of uncertainty. Therefore, both, the selection of an adequate calculation code and the treatment of uncertainties in the thermal-hydraulic analysis are two factors to be considered.
A calculation code which results adequate to perform a thermal-hydraulic calculation is that which can efficiently predict the behaviour of the reactor. A validation procedure is usually required and it implies a comparison between the measured and calculated value of a thermal-hydraulic relevant figure of merit.
In reference to the uncertainty treatment, two different approaches have been used: the conservative and the best estimate approach.
In the **conservative approach**, uncertainty factors, boundary conditions and modelling hypotheses are chosen in such a way that a pessimistic model of the reactor behaviour is obtained. The values to be chosen in the conservative approach depend on the operating condition of the reactor or the transient under analysis and also on the figure of merit chosen to evaluate the reactor behaviour. For the thermal-hydraulic design, these figures of merit are the design criteria in Tab 1. The conservative approach aims at absorbing all the deviations and uncertainties to guarantee that the design criteria are satisfied.
The **best estimate approach** considers boundary conditions, parameters and hypotheses leading to a realistic prediction of the reactor behaviour. This approach requires an uncertainty analysis to obtain upper and lower bounds for the thermal-hydraulic figure of merit under evaluation, so to account for the uncertainties in the model. This calculation methodology is known as Best Estimate Plus Uncertainty (BEPU) and the results are given in terms of probabilities and confidence levels.
The thermal-hydraulic analysis can be used in reactor design for different purposes. The present study is divided into three parts:

- A validation of the calculation tool and methodology
- A study of the reactor behaviour in the steady state to determine the set point values of the parameters used to trigger the actuation of the First Shutdown System (FSS)
- The determination of the moment of inertia of the pumps in the PCS based on the reactor behaviour to a Loss of Flow Accident (LOFA)

All the items mentioned above are analysed considering both, the conservative and the BEPU methodologies and results are compared.

4. Description of the study

The present section describes the calculation tool, the model and the methodologies used to perform the study.

1.1 Calculation tool

The calculation tool used is the thermal-hydraulic system code RELAP5 v. 3.4, with uncertainty package. RELAP5 solves the mass, energy and momentum equations for the

liquid and the vapour phases and it makes use of empirical correlations to solve the problem. The cooling system is modelled by a series of volumes and junctions connecting them. The heat transfer to and from the cooling fluid is modelled by components known as heat structures. Specific components usually found in plants, such as pumps, are also included. The mass and energy equations are solved in the centre of the volumes while the momentum equation is solved in the junctions.
The uncertainty package is an additional module which has been added to perform uncertainty analysis based on a “base case” (best estimate) in which no uncertainties are considered. This additional module allows the user to specify the uncertainty distribution for a specific parameter, including both, input parameters and parameters calculated by the source code such as heat transfer coefficients or water properties. Details of the methodology used to perform the uncertainty analysis are given in this section.

1.2 Calculation model

The nodalization used to model the reactor and the PCS is schematically illustrated in Fig 1. It includes the components inside the reactor pool: core, chimney and inlet pipes and the main components of the cooling circuit such as pumps, decay tank and heat exchangers. The reactor core is modelled by two pipes which represent the hot (HFA) and an average (AFA) channel. Heat structures have been attached to these two pipes to model the heat transfer from the fuel to coolant. Flap valves have also been included on the inlet pipes, so to model the natural circulation cooling regime. The SCS is considered as a boundary condition.

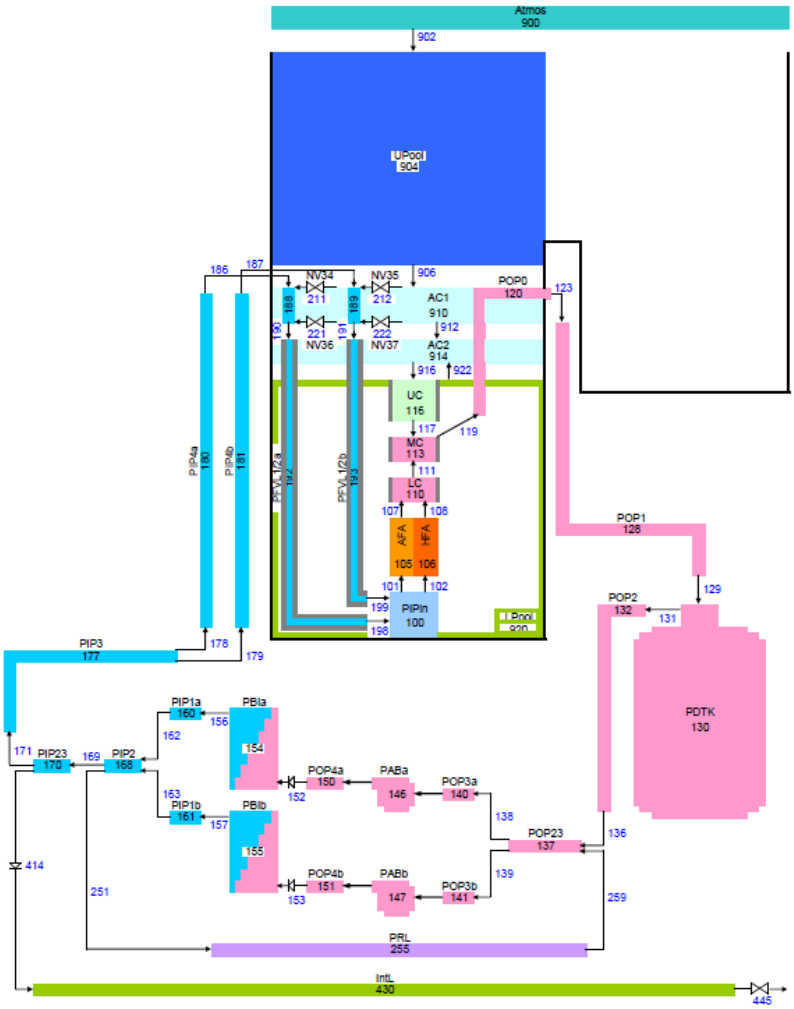

Fig 1. Nodalization of PCS

1.3 Calculation methodologies

The conservative and the BEPU calculation approaches are used to perform the study and the conclusions will be based on the comparison of the results obtained by both methodologies.

1.1. Conservative calculation approach

A single calculation run is performed and the input parameters, boundary conditions and hypotheses are chosen in such a way that the reactor behaviour, as calculated by the model, is a pessimistic one in terms of a pre-established thermal-hydraulic figure of merit

1.2. BEPU calculation approach

An uncertainty distribution and the parameters describing such distribution are defined for a group of "relevant" parameters. The calculation consists of:

- A "best estimate" or a "base case" calculation in which uncertainties are not considered in the modelling of the reactor
- An uncertainty analysis based on the input error propagation technique. In this case, weighting factors are randomly generated for each parameter, considering the uncertainty distribution defined by the user. These weighting factors are applied to the nominal value of the variable, thus modifying the input value. The new values are randomly combined generating a number of inputs or cases to be run.

The result of the BEPU approach is a "best estimate" prediction for a thermal hydraulic relevant figure of merit, with the upper and lower bounds achieved for such figure of merit. Results are given in terms of probabilities and confidence levels, which are a function of the number of calculations performed and which can be estimated by using Wilk's formula (4, 5). The uncertainty module included in version 3.4 of RELAP 5 makes use of such formula to generate the number of cases to be run according to the desired probability and confidence level specified by the user. It also allows the user to specify the number of runs to be performed regardless of Wilk's formula.

1.4 Analysis

As mentioned before, the study is divided into different parts. Each of them is described in the present section:

1.4.1 Validation of the model and calculation methodologies

Measurements for a Loss of Normal Power Supply (LNPS) Test at 20 MW were performed during the commissioning of OPAL reactor. The experimental values of core flow are used to validate the calculation tool, model and methodologies. This is done by comparing the measured values with the values of core flow as calculated by RELAP5 during the steady state normal operation and during the LNPS event for the conservative and the BEPU calculation approaches.

The event under analysis consists of a pump stop, actuation of the FSS and interruption of the SCS at t=0, when the loss of power takes place. Flap valves open when the pressure difference between the inlet pipes and the reactor pool falls below a given value, thus changing from the forced to the natural circulation cooling regime. The FSS is modelled by means of a table describing the negative reactivity inserted as a function of time.

1.4.2 Determination of set points

The values of set points for some of the parameters triggering the FSS are determined by modelling the steady state with the conservative and the BEPU approach. The set point values for reactor power, core flow and inlet temperature are evaluated in this study, as the FSS can be triggered either by high reactor power, by low core flow or by high inlet temperature.

For the conservative evaluation, the steady state of the reactor is modelled considering conservative values of input parameters and boundary conditions. A series of calculations are performed varying the value of the set point parameter accordingly (i.e., increasing reactor power, decreasing coolant flow, increasing inlet temperature) until the thermal-hydraulic design criteria fails to be accomplished.
The procedure is similar for the BEPU evaluation. The steady state value of the set point parameter in the best estimate case is varied until the upper or lower bound of the uncertainty analysis fails to comply with the design criteria.

1.4.3 Determination of the moment of inertia of the pumps

A LOFA is the event studied to determine the moment of inertia of the pumps in the PCS. The pumps are stopped at t=0, together with the pumps in the SCS. The coolant in the PCS falls according to the coast-down curve of the pump, which depends of its moment of inertia. The FSS is triggered either by a low flow or by a high inlet temperature trip. The forced circulation cooling regime is therefore maintained until the flap valves open, when the pressure difference between the inlet pipe and the reactor pool falls below a given value. The moment of inertia of the pumps is specified in such a way that, at the time at which the flap valves open and the natural circulation cooling regime establishes, the decay power is low enough so as to satisfy the thermal-hydraulic design limits.
The LOFA is modelled by using both, the conservative and the BEPU approaches.

1.4.4 Input data

The calculation model at the best estimate steady state is adjusted to a thermal power of 18.8 MW, a core flow of 1900 m^3/h, and an inlet temperature of 37 °C. Tab 3 summarizes the input parameters on which an uncertainty distribution has been considered, the type of distribution and the parameters characterizing it.

Parameter	Uncertainty distribution	Characterization of distribution
Heat transfer coefficient for modes 2 and 3 (*)	Uniform	Min / max value: 0.8 / 1.2
Reactor power	Normal	Mean: 1; Deviation: 0.025
Reactivity insertion	Normal	Mean: 1; Deviation: 0.010
Rated flow of pumps	Normal	Mean: 1; Deviation: 0.025
Friction coefficients (**)	Uniform	Min / max value: 0.3 / 1.7
Pump torque and coefficients	Normal	Mean: 1; Deviation: 0.05
Moment of inertia of pumps	Normal	Mean: 1; Deviation: 0.1
Inlet temperature to the SCS	Uniform	Min / max value: 0.9968 / 1.003 (***)

(*) According to RELAP5 heat transfer map
(**) Loss coefficients on the junctions in the core
(***) Resulting in a +/- 1°C deviation

Tab 3: Parameters with uncertainty distribution and its characterization

For most of the cases, the uncertainty distribution has been determined and characterized based on engineering judgement and experience. For the case of reactivity insertion, the errors committed in neutronic calculations are considered. The uncertainty distribution for the heat transfer coefficient is based on the comparison between published experimental values with the values as calculated by the correlations used in RELAP5.
For the steady state, a total number of 59 runs are performed in the uncertainty analysis. This means that, for a particular thermal-hydraulic figure of merit, there is a 95% probability that its value falls within the calculated upper and lower bounds, and this is guaranteed with a 95% confidence level, according to Wilk's. For the transients, i.e., the LNPS and the LOFA the number of runs performed is increased to 90, thus increasing the confidence level to

99%. For the conservative evaluation, the maximum and minimum values corresponding to each parameter are combined to obtain the most pessimistic behaviour of the reactor in terms of a particular thermal-hydraulic figure of merit obtained as calculation output.

1.4.5 Evaluation of results

For the validation process, the thermal-hydraulic figure of merit considered is the core flow. For the conservative approach, the input parameters are combined in such a way that the core flow falls below the experimental values, resulting in a reduction of the time taken for the flap valves to open. For the BEPU approach, it is expected that the experimental values fall within the upper and lower bounds. The margins to the limiting thermal-hydraulic design criterion, RDR for the steady-state normal operation and BPR for the transient, are also evaluated for completeness. .

For the analysis of set points in the steady-state, the thermal-hydraulic figure of merit considered is the RDR, being RD the limiting phenomenon. In case of the LOFA, the thermal-hydraulic figure of merit considered is the BPR, being the BP the physical phenomenon conditioning the result.

5. Results

1.5 Validation of the model and calculation methodologies

Fig 2 shows the calculated and measured values of the core flow at steady-state normal operation and during the LNPS.

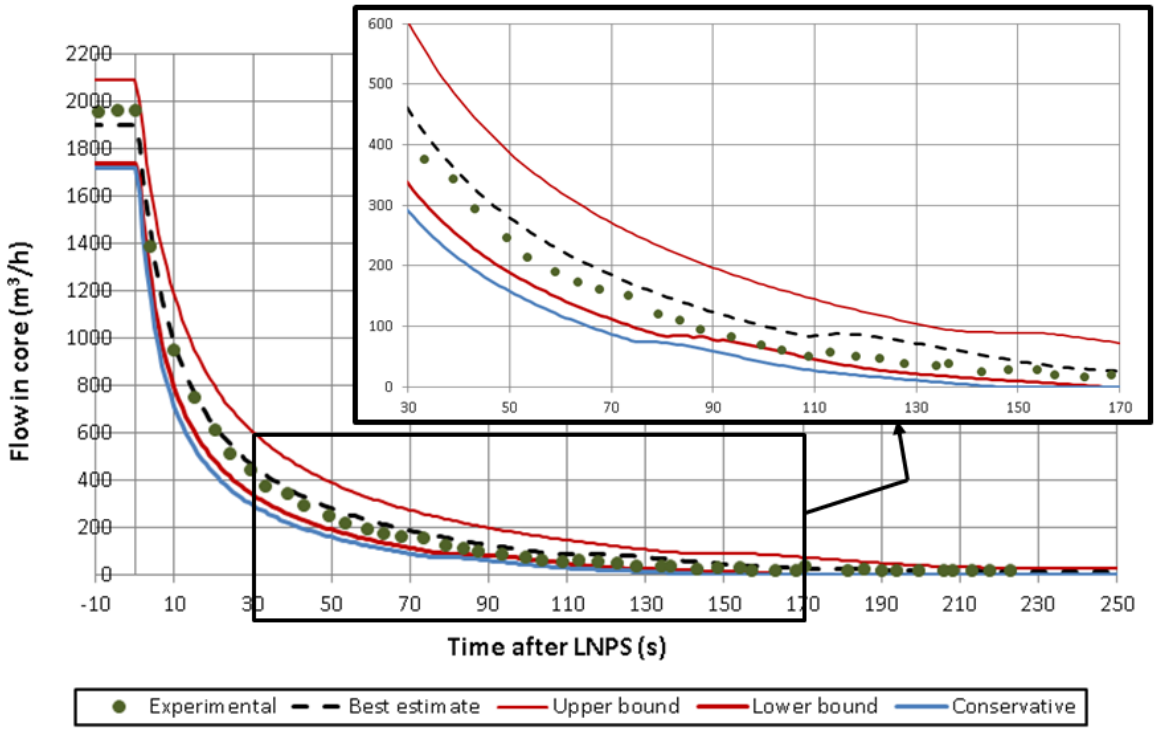

Fig 2. Calculated and measured core flow during a LNPS

For the steady-state normal operation, the experimental values of core flow falls within the upper and lower bound of the BEPU analysis. For the conservative case, the calculated core flow falls below the experimental value. In reference to the RDR, the minimum value of the lower band in the BEPU analysis is equal to 2.8. This value falls to 2.5 for the conservative case. Consequently, all thermal-hydraulic design criteria are satisfied at steady-state normal operation, regardless the calculation approach.

In reference to the LNPS, flap valves open at 114 seconds according to measurements. For the best estimate prediction, this value is equal to 110 seconds and the measured values of

core flow fall within the uncertainty band, thus validating the calculation model and methodology. In reference to the BPR, the minimum value of the lower bound exceeds the design limit (1.53).
The time taken for the flap valves to open according to the conservative prediction is equal to 74 seconds. The core flow as calculated by this approach falls below the experimental values. In reference to the minimum BPR, this is equal to 1.35, meaning that the thermal-hydraulic design limit is not accomplished.

1.6 Determination of set points at steady state

Tab 4 summarizes the results obtained for the set point values as determined by both, the conservative and the BEPU prediction. The design values, which have been established with a different methodology and calculation tool, have been included for completeness.

Parameter	Set point value		
	Design value	**Conservative**	**BEPU**
Thermal power	115% of nominal value	120% of nominal value	130% of nominal value
Core flow	90% of nominal value	80% of nominal value	75% of nominal value
Inlet temperature (°C)	Nominal value + 9	Nominal value + 16	Nominal value + 18

Tab 4: Set point values as calculated by the different methodologies

1.7 Determination of the moment of inertia of the pumps

Fig 3, Fig 4 and Fig 5 show the evolution in the BPR throughout the transient under analysis for a moment of inertia of pumps equal to 70 kg.m^2, 60 kg.m^2 and 50 kg.m^2 respectively.

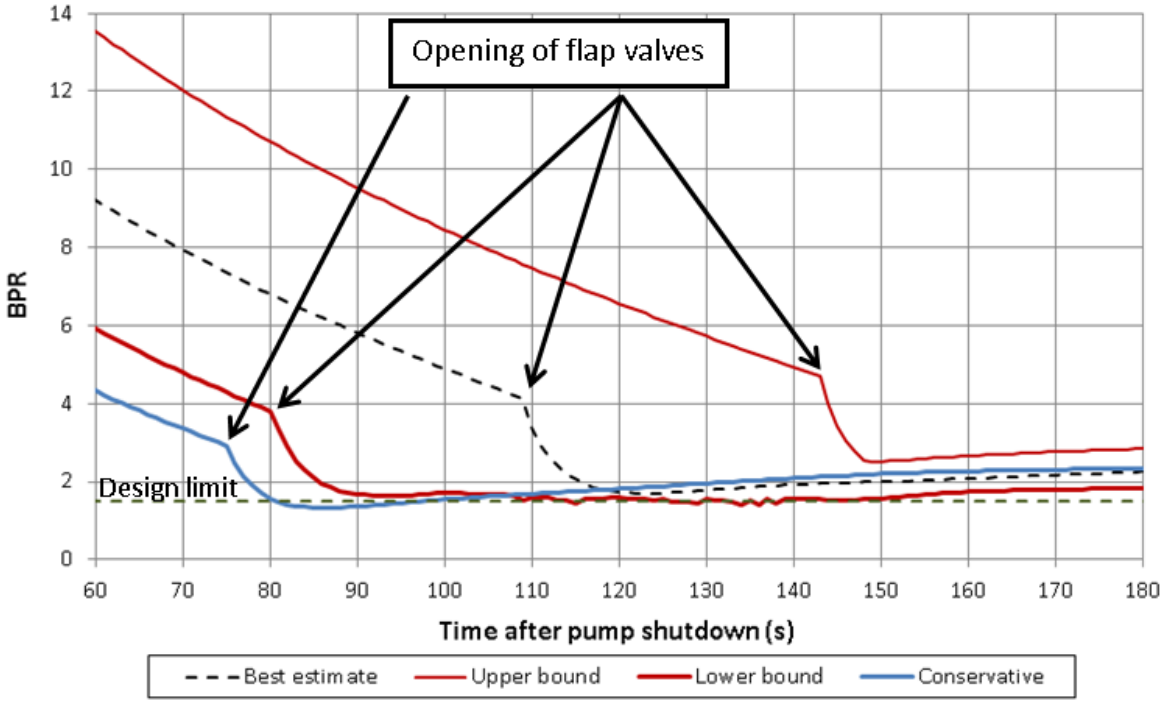

Fig 3: Evolution for the BPR during a LOFA for a moment of inertia of pumps of 70 kg.m^2

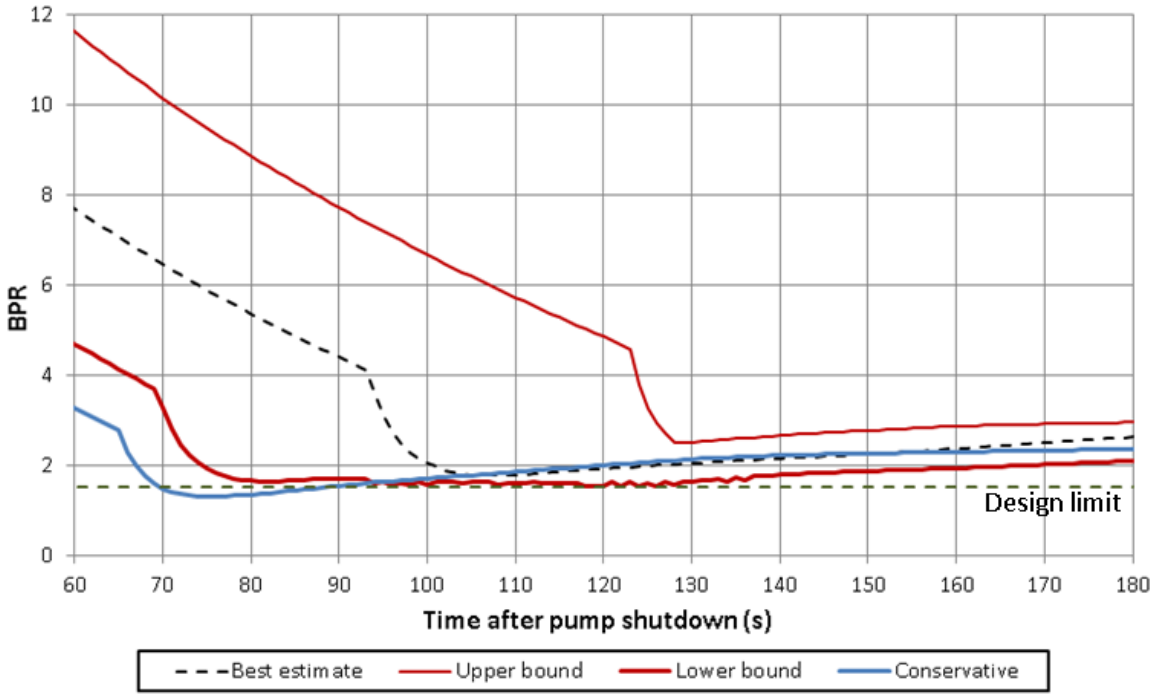

Fig 4: Evolution for the BPR during a LOFA for a moment of inertia of pumps of 60 kg.m^2

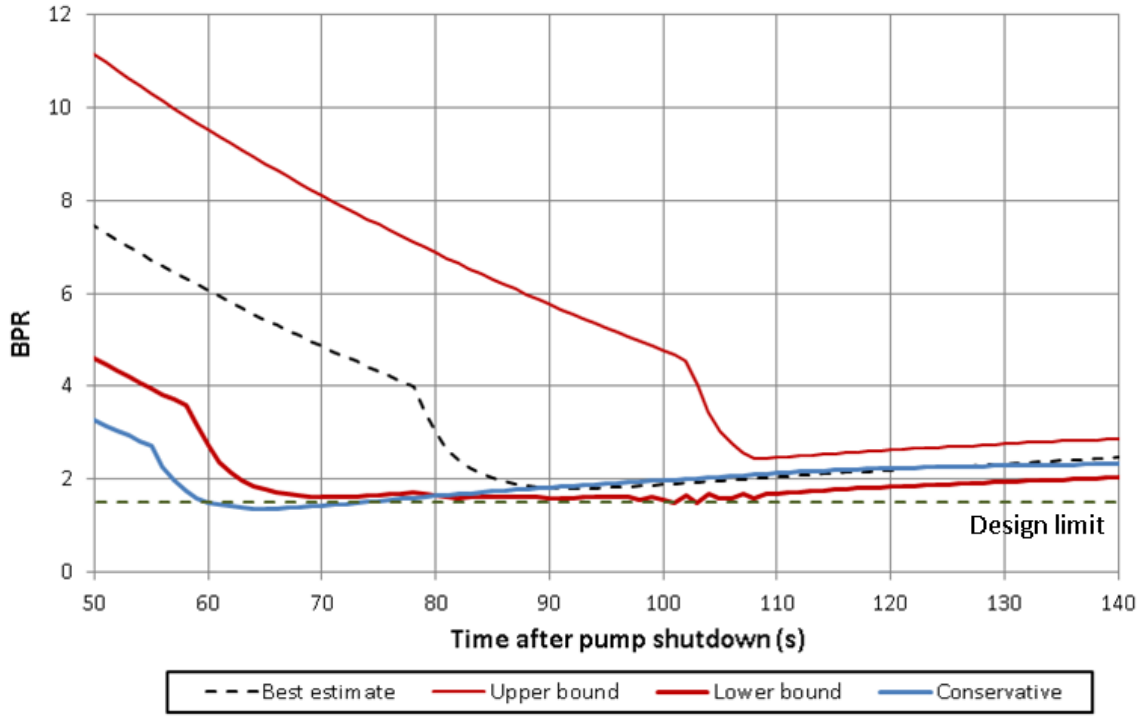

Fig 5: Evolution for the BPR during a LOFA for a moment of inertia of pumps of 50 kg.m^2

As observed in results, a single minimum value for the BPR is obtained for the conservative and for the best estimate cases. Based on this observation, an increase in the moment of inertia of pumps results in an increase in the BPR. However, this conclusion changes when the minimum value of the lower bound is considered. As observed, there is a period of time in which the minimum value of BPR remains almost constant and an increase in the moment of inertia of pumps does not necessarily result in an increase in the minimum value of the BPR. Results are summarized in Tab 5.

Moment of inertia of pumps ($kg.m^2$)	Minimum BPR		
	Conservative	BEPU	
		Lower bound	Best estimate
50	1.3	1.5	1.8
60	1.31	1.52	1.82
70	1.34	1.41	1.85

Tab 5: Minimum BPR for different moments of inertia of pumps

6. Conclusion

The conservative and BEPU calculation approaches have been used to evaluate the design of OPAL reactor. The evaluation is made in terms of the most limiting thermal-hydraulic design criterion. The model and calculation methodologies were validated by comparing calculated with experimental values. While the BEPU methodology efficiently predicts the behaviour of the reactor at steady state and during the LNPS, the conservative estimation is too pessimistic for the evaluation of the transient. Both methodologies were used to determine the set point values of parameters triggering the FSS. The BEPU approach results in less conservative values, thus reducing the possibility of spurious actuation of the FSS. In reference to the analysis of a LOFA used to determine the moment of inertia of the pumps in the PCS, the conservative calculation approach would result in designs far exceeding the 70 $kg.m^2$, making it not viable. The results obtained from the BEPU calculation approach shows that the moment of inertia perhaps could be reduced from 70 $kg.m^2$ to 60 $kg.m^2$, although more calculations are required. It can also be seen that such moment of inertia may improve reactor performance, as the lower bound in this case exceeds the design limit while the lower bound for the moment of inertia of 70 $kg.m^2$ falls below such value, this behaviour could be, probably, the result of uncertainties combination.

7. References

1. IAEA-TECDOC-233 Research Reactor Core Conversion from the use of Highly Enriched Uranium to the use of Low Enriched Uranium. ANL, USA, 1980.
2. R. H. Whittle and R. Forgan, 1967, “A Correlation for the Minima in the Pressure Drop vs. Flow-Rate Curves for Subcooled Water Flowing in Narrow Heated Channels,” Nucl. Eng. Design **6**, pp. 89–99.
3. S. Fabrega, “Le calcul thermique des Reacteurs de Recherche refroidis par Eau”, Commissariat a l’energie atomique, CEA-R-4114
4. S. S.Wilks, 1941, “Determination of sample sizes for setting tolerance limits,” Annals of Mathematical Statistics, 12 (1), pp. 91-96.
5. S. S. Wilks, 1942, “Statistical prediction with special reference to the problem of tolerance limits,” Annals of Mathematical Statistics, 13 (4), pp. 400–409.

DESIGN OF NEUTRON FLUX FLATTENERS FOR NTD FACILITIES

I. FERRARI(*), D. HERGENREDER(+), P. CAMUSSO(+)
Nuclear Engineering Department, INVAP SE
(*)Esmeralda 356, C1035ABH, CABA – Argentina
(+)Cmte Luis Piedrabuena 4950, R8403CPV, S.C.de Bariloche – Argentina

ABSTRACT

INVAP has designed and built NTD facilities and flux flattener devices for several reactors such as ETRR-2 and OPAL. The present document will describe the design process carried out for the Brazilian Multipurpose Reactor (RMB).
The RMB is a 30 MW multi-purpose open-pool research reactor designed by INVAP S.E. (Argentina) for CNEN (Brazil). The reactor is a versatile facility which will be used for several applications such as the irradiation of materials, neutron activation analysis, radioisotope production for medical and industrial applications and the doping of silicon ingots for the semiconductor industry, among others.
Silicon ingots of different sizes can be irradiated at different flux levels in the five Neutron Transmutation Doping (NTD) facilities located inside the Reflector Vessel of the reactor.
The NTD facilities are surrounded by the heavy water reflector ensuring the high thermal-to-fast flux ratio required to produce high quality semiconductors.
Applications for which this technique is used demand a high level of uniformity in the dopant spatial distribution, therefore, a high level of uniformity in the irradiation conditions of the ingot during the NTD process is required.
The neutron flux perturbations induced by the five neutron beams located in the vicinity of the NTD facilities increase the axial asymmetry of the neutron flux profile in the ingots. The design of a customized “neutron flux flattener” for each irradiation position, used to achieve the required irradiation conditions, represents a challenging task, since the flux uniformity must be obtained for a very large irradiation volume (60 cm of active length for both, 6 inches and 8 inches silicon ingots facilities).
The present work describes the main aspects and current state of the design of the NTD facilities and the neutron flux flatteners, including the characterization of the irradiation conditions achieved in the silicon ingots.

1. Introduction

The Neutron Transmutation Doping (NTD) technique is based on the uniform generation of a controlled amount of impurities on an intrinsic or extrinsic semiconductor by means of a nuclear reaction. This technique is widely used to produce Phosphorus-doped Silicon for the manufacturing of high quality semiconductors. The reaction is induced by thermal neutrons on Silicon atoms:

$$^{30}Si + n \rightarrow {}^{31}Si \rightarrow (\beta^{-})^{31}P.$$

Nuclear reactors provide an appropriate option for generating the neutron field which is required to induce such reaction, however, this neutron field is not uniform and, considering that the volume of Silicon targets is rather large, irradiation conditions can vary significantly across the different sections of the irradiation target.

The neutronic design of NTD facilities for Phosphorus-doped Silicon production consists in adapting the irradiations conditions in the reactor in order to obtain highly uniform dopant

spatial distributions. INVAP has designed and built NTD facilities for several reactors such as ETTR-2 and OPAL, and is currently developing the design for the Multipurpose Brazilian Reactor (RMB).

RMB is a 30 MW multi-purpose open-pool reactor designed for CNEN (Brazil). The core is composed of twenty-three fuel assemblies using low enriched Uranium arranged in parallel-plate geometry. The core is confined in a chimney and cooled by light water. Inside the core are two irradiation facilities for fast neutron flux irradiation and material testing experiments. The core chimney is surrounded by heavy water which is contained in the Reflector Vessel, providing appropriate irradiation conditions for multiple applications. The facilities located in the Reflector Vessel include nineteen irradiation positions for radioisotope production such as ^{99}Mo, ^{192}Ir and ^{131}I, fourteen pneumatic devices with multiple irradiation positions for neutron activation analysis, two thermal neutron beams, a cold neutron source with two cold neutron beams, a neutrography beam, a testing loop for Power Plants fuel assemblies testing and five NTD facilities.

The present work describes the main aspects and current state of the design of the NTD facilities and the neutron flux flatteners, including the characterization of the irradiation conditions achieved in the Silicon ingots.

2. NTD facilities and design objectives

RMB reactor has three NTD facilities for the irradiation of 6''-ingots and two NTD facilities for the irradiation of 8''-ingots, consisting of vertical irradiation positions located in the Reflector Vessel. The Silicon ingot is encapsulated inside an Aluminium can and is axially reflected by a lower Silicon/graphite plug and upper Silicon plug which increase the neutron thermal flux in the ends of the ingot and avoids abrupt changes in the axial flux profile. The complete ensemble is contained in a rotation tube.

The quality of a semi-conductor is measured, mainly, by the uniformity of its resistivity. The most important advantages of the NTD technique is that it can produce an extremely uniform dopant distribution, provided that an equally uniform Silicon activation rate (or equivalently, thermal neutron fluence) is achieved in the irradiation target. Uniformity is normally represented by its radial and axial components, and complementary strategies are used in order to adjust each of them.

Radial uniformity is controlled by rotating the Silicon ingot during the irradiation, and thus, compensating the effects of the thermal flux gradient and other radial effects induced by nearby components such as the neutron beams and other irradiation facilities, however, the self-attenuation effect produced by the Silicon ingot cannot be eliminated.

Axial uniformity is controlled by surrounding the irradiation device with a neutron filtering screen called “neutron flux flattener”. The neutron flux flattener consists of a cylindrical shell of 0.9 mm of width. The adjustment of the axial shape of the thermal neutron flux is produced by combining different Aluminium and Stainless Steel layers in order to control the absorption rate produced in each axial region of the neutron flux flattener. Each of the five NTD positions require a custom-made flux flattener since the axial neutron flux profile varies significantly across the different positions in the Reflector Vessel.

In addition to the uniformity, there are other parameters associated to the irradiation target that should be analysed in order to assess the performance of the NTD facilities, namely, the thermal neutron level flux, the fast neutron flux level and the gamma-ray flux level.

Thermal neutron flux level is directly related to the irradiation time required to reach the required resistivity in the target, since the resistivity of the semi-conductor is inversely proportional to the thermal neutron fluence. Although a higher neutron thermal flux level

reduces irradiation time, if the irradiation time is too short, the irradiation accuracy may be affected.

Fast neutrons and gamma rays produce undesirable effects in the Silicon target, mainly due to the production of lattice defects in the ingot and to the heating produced by nuclear reactions, which can lead to highly demanding cooling conditions.

Considering that radial uniformity is adjusted by the rotation of the Silicon target during irradiation, the characterization of the irradiation conditions for NTD production is then summarized through four parameters: the axial thermal neutron flux uniformity, the thermal neutron flux level, the thermal-to-fast flux ratio and the heat deposition. In order to assess the quality of the irradiation conditions, a set of design objectives for each of these parameters is established, based in common requirements of the industry:

- Axial thermal flux uniformity lower than 8%
- Thermal neutron flux between 1.7 x 10^{12} n cm^{-2} s^{-1} and 1.7 x 10^{13} n cm^{-2} s^{-1}
- Thermal-to-fast flux ratio greater than 200
- Heat deposition as low as possible

With the exception of thermal neutron flux uniformity, all design objectives can be adjusted by a proper selection of the distance that separates the core from the NTD facility. The heavy water reflector located in the Reflector Vessel of RMB reactor ensures a higher thermal-to-fast flux ratio and lower gamma deposition far away from the core, at the expense of a lower level of thermal neutron flux. Additional restrictions can be imposed by the layout of the facilities since NTD facilities occupy a significant volume of the Reflector Vessel.

The design of the neutron flux flatteners is a challenging task because the thermal neutron flux uniformity must be achieved in a large volume of the reactor. In the following section, the neutronic model for the evaluation of design objectives and the methodology used to design of the neutron flux flatteners is described.

3. Neutron flux flatteners design

INVAP calculation line [1] is composed of a set of in-house developed computational codes, utilities and third-party codes, together with nuclear data libraries and calculation procedures which encompasses the different aspects of the design of the reactor (Figure 1).

The deterministic line (namely, CONDOR-CITVAP [2-3]) provides a fast methodology for the design of the main features core, together with the definition of the operation cycle. CONDOR-CITVAP is integrated with general multipurpose 3D Monte-Carlo transport codes, which allow the design of ex-core irradiation facilities such as the NTD irradiation positions. Additional computational codes are frequently used for specific calculations, including dynamic coupling, inventory and activation calculations or independent core-level verifications.

The design of the NTD flux flatteners is developed through a series of transport calculations performed with MCNP6 [4] with ENDF/B-VII.0 nuclear data [5]. The thermal axial neutron profile adjustment is performed by using two different models. The “full” model (Figure 2) includes the core and the chimney, the Reflector Vessel, the ex-core irradiation positions, neutron beams, cold neutron source, pneumatic devices, etc. The “reduced” model includes the NTD facilities only, together with a surface source at the boundary of each facility.

The operation cycle of RMB reactor consists in three sub-cycles with a duration of 33 days. The analysis of the design objectives for NTD facilities is performed for each Beginning of Cycle (BOC) and End of Cycle (EOC) of the equilibrium core. In order to represent the burnup of the fuel, the active length of the core is divided in twenty axial segments and each

segment has a specific material composition taken from the deterministic calculations of the equilibrium core (performed with CONDOR-CITVAP) trough NDDUMP [1] code.

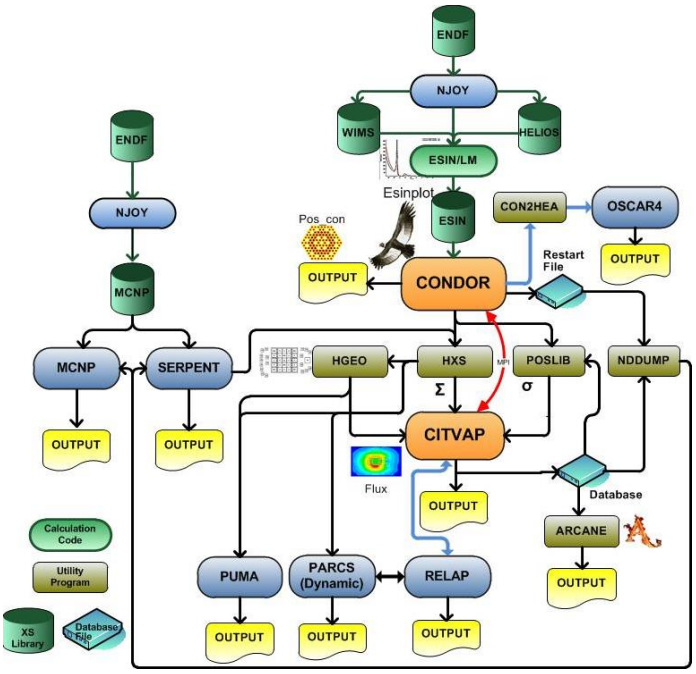

Figure 1: INVAP calculation line

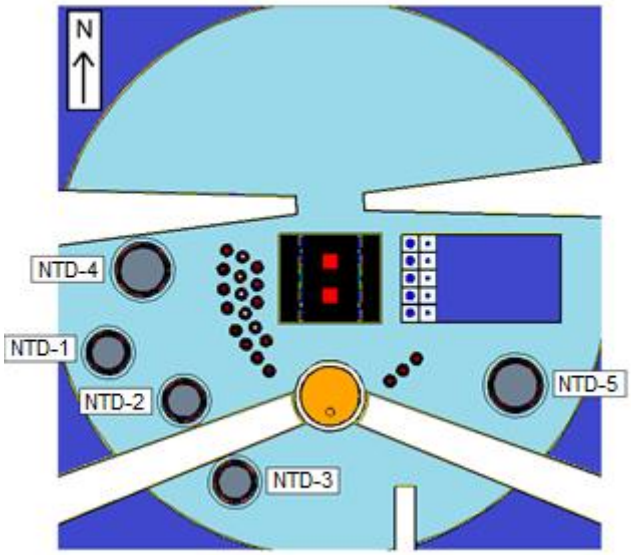

Figure 2: MCNP "full" model

Figure 3 shows an axial cut of the NTD facility model and a detail of the different layers of the flux flattener (Aluminium in red and Stainless Steel in orange). The Silicon ingot is centred 5 cm below the active length of the core and is divided in 60 axial segments.

The flux flattener is divided in 15 axial segments of 4 cm of height allowing to locally modify the axial neutron flux profile with the required precision. Each axial segment composed of an inner Aluminium layer and, if required, an external Stainless Steel layer which increase thermal neutron absorption in that particular region.

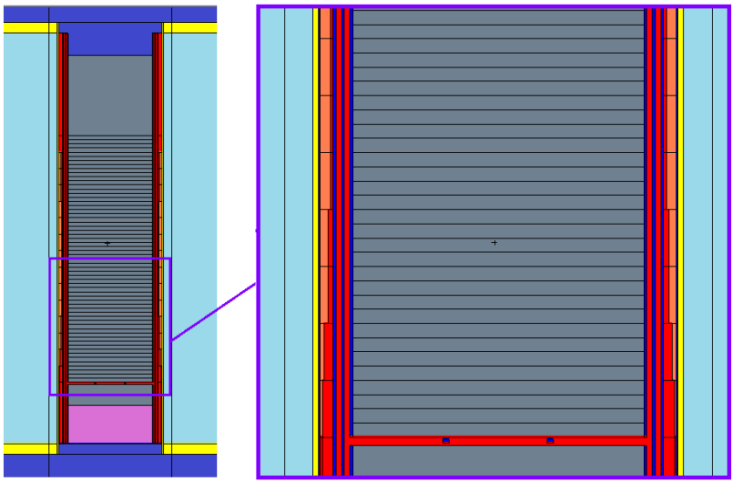

Figure 3: Axial cut of the NTD facility model with a detail showing the layers of the flux flattener

In order to quantify the neutron flux axial uniformity (FAU) for a given NTD position, the Silicon ingot is divided in 60 axial segments of 1 cm of height, and the thermal neutron flux is computed for each segment. The FAU is then obtained through the expression:

$$\mathrm{FAU} = \max_i \frac{|\phi_i - \overline{\phi}|}{\overline{\phi}} \mathrm{x}\, 100\%$$

where ϕ_i is the thermal neutron flux in layer i and $\overline{\phi}$ is the average thermal neutron flux in the Si ingot. For the initial condition, where the neutron flux flatteners are purely made of Aluminium, the FAU for the NTD facilities is approximately 20%.

The design of the neutron flux flatteners is performed iteratively: first, a surface source file surrounding each of the NTD facilities is written using the “full” model. Then, using the “reduced” model the Stainless Steel width of each of the 15 axial segments of the neutron flux flattener is adjusted, seeking to minimize the FAU. The use of the reduced model significantly reduces the computational cost of each run. Finally, a new surface source file is written using the “full” model with the updated flux flattener design in order to include the perturbations effects in the boundary source induced by the Stainless Steel layers. The process is repeated until the convergence between the results of the two models and the required thermal neutron uniformity level is reached.

Perturbations over the reactor configuration used to design the neutron flux flattener can affect the shape of the axial neutron profile (e.g., the unloading of Molybdenum irradiation devices located in the vicinity of some of the NTD facilities). For this reason, a conservative limit of 3% is considered in the design stage in order to cover the effect of these perturbations, along with other calculation uncertainty due to the computational codes, nuclear data, etc.

4. Results

Table 1 shows the FAU obtained for the five NTD facilities in the different states of the reactor. As it can be noticed from the results, the flux flattener is effective to improve the uniformity; in all cases a FAU lower than 3% was achieved. The width of the Stainless Steel layer as a function of the axial position and the neutron flux obtained for the final design of the neutron flux flatteners is exemplified in Figure 4, corresponding to the case of NTD-1 at BOC-1. The 3%- limit for the FAU is shown in red dashed lines.

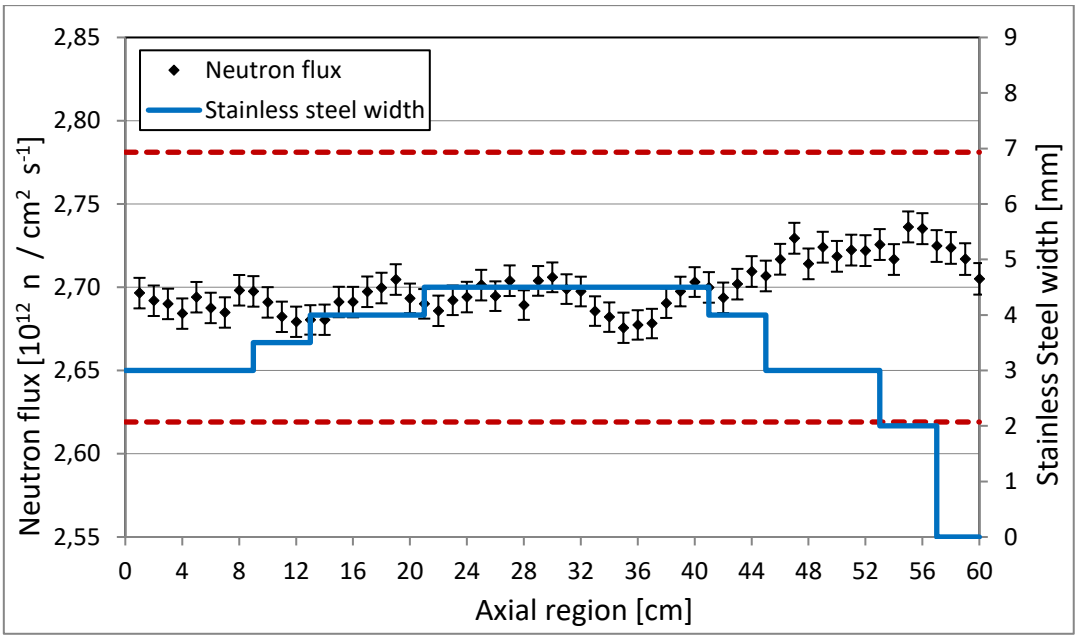

Figure 4: Axial thermal neutron profile and Stainless Steel width for NTD-1

Core state	Device				
	NTD-1	NTD-2	NTD-3	NTD-4	NTD-5
BOC-1	1.3%	1.0%	1.5%	1.0%	1.3%
EOC-1	1.1%	1.5%	1.8%	1.8%	2.0%
BOC-2	1.4%	1.3%	1.3%	1.2%	1.3%
EOC-2	1.3%	1.3%	1.7%	1.7%	1.7%
BOC-3	1.5%	1.1%	1.6%	0.8%	1.2%
EOC-3	1.2%	1.7%	2.2%	1.7%	2.0%

Table 1: FAU for the different sub-cycles

Core state	Device				
	NTD-1	NTD-2	NTD-3	NTD-4	NTD-5
BOC-1	2.70	10.0	7.21	9.69	4.95
EOC-1	2.69	9.96	7.05	9.66	4.78
BOC-2	2.70	10.0	7.23	9.70	5.01
EOC-2	2.70	9.98	7.08	9.70	4.83
BOC-3	2.70	10.0	7.26	9.67	5.06
EOC-3	2.69	9.97	7.10	9.67	4.87

Table 2: Average thermal neutron flux [10^{12} n cm^{-2} s^{-1}]

Core state	Device				
	NTD-1	NTD-2	NTD-3	NTD-4	NTD-5
BOC-1	1750	420	540	310	1090
EOC-1	1960	400	520	310	1050
BOC-2	1890	420	550	320	1020
EOC-2	1910	410	540	310	1100
BOC-3	1780	410	540	310	1150
EOC-3	2070	420	530	310	1100

Table 3: Thermal-to-fast flux ratio

Table 2 and Table 3 show the thermal flux level and the thermal-to-fast flux ratio at the BOC and EOC states equilibrium core. The average thermal flux levels in the Silicon ingots is found in the range of 2.7 x 10^{12} n cm^{-2} s^{-1} and 1.0 x 10^{13} n cm^{-2} s^{-1}, in accordance with the design objective.

The thermal-to-fast flux is greater than 200 in all cases indicating low damage irradiation effects in the target. Additionally, gamma-ray heating on the irradiation targets was computed, obtaining values between 0.1-0.2 W/cm^3, which are acceptable in terms of cooling conditions.

5. Conclusions

The design of NTD facilities for the doping of Silicon is a complex task that requires achieving a high uniformity of the thermal neutron flux in a significantly large volume of the reactor. In the present work, the design of the NTD facilities and the neutron flux flatterers for RMB reactor is presented, describing the associated design objectives and design process.

The reactor has five NTD facilities, three for production of 6''-diameter Phosphorus-doped Silicon ingots and two for production of 8''-diameter Phosphorus-doped Silicon ingots, which allow the irradiation of targets for thermal neutron flux levels between 2.7 x 10^{12} n cm^{-2} s^{-1} and 1.0 x 10^{13} n cm^{-2} s^{-1} with a thermal-to-fast flux ratio greater than 300, and therefore providing reasonable irradiations times without compromising the irradiation accuracy, while reducing irradiation damage effects. The gamma-ray heating takes values between 0.1-0.2 W/cm^3.

The design and placement of neutron filtering screens or “neutron flux flatteners”, which are custom-made for each NTD facility, ensure the axial uniformity of the neutron flux through the operation cycle of the reactor. The uniformity obtained in the five NTD facilities is lower than 3%.

6. References

[1] E. Villarino, I Mochi and P. Sartorio. “INVAP neutronic calculation line”. XXI Congreso sobre Métodos Numéricos y sus Aplicaciones 23-26 September 2014, Bariloche, Rio Negro, Argentina.

[2] E. Villarino, “Condor Calculation Package,” Proceedings of the PHYSOR 2002, Seoul, South Korea, October 2002

[3] E. Villarino and C. Lecot, “Neutronic calculation code CITVAP 3.1,” in IX Encontro Nacional de Fisica de Reatores e Termo-Hidrualica, Caxambu, Brazil, October 1993

[4] T. Goorley, et al., "Initial MCNP6 Release Overview", Nuclear Technology, 180, pp 298-315 (Dec 2012).

[5] ENDF/B-VII.0: Next Generation Evaluated Nuclear Data Library for Nuclear Science and Technology

METHODOLOGY FOR THE DESIGN OF THE PRIMARY COOLANT CIRCUIT SHIELDING FOR AN OPEN POOL RESEARCH REACTOR

A. MAITRE, R. REY, F. ALBORNOZ
Nuclear Engineering Department – Radiation Transport Group, INVAP S.E.
Avenida Comandante Luis Piedrabuena, R8403CPV Bariloche – Argentina

ABSTRACT

This work presents INVAP's methodology for the design of the primary coolant circuit shielding of a 30 MW open pool reactor.
The light water that circulates through the core and the irradiation facilities is activated by the high thermal and fast neutron flux present in the core and its neighbourhood, producing mainly ^{16}N, ^{19}O, ^{41}Ar and ^{24}Na. In addition, the fuel and the ^{99}Mo production targets have aluminium cladding which is also activated producing mainly ^{28}Al, ^{27}Mg and ^{24}Na.
The production of the mentioned radionuclides is calculated for the given design of the reactor. Then, a mathematical model of the main cooling circuits is solved in order to obtain the activity of mentioned radionuclides at points of interest.
Finally, gamma radiation transport models are developed with the MCNP code in order to calculate the dose rate in the rooms of the reactor and to design the shields that the main cooling circuits need.

1. Introduction

1.1 Company

INVAP is an Argentinean company whose main nuclear activities are the design, construction and commissioning of nuclear facilities such as Research Reactors, Radioisotope Production Plants, Fuel Manufacturing Plants, Waste Management Plants, Small Modular Reactors and Nuclear Medical Centre Facilities.

The latest research reactor projects in which INVAP is involved are 30 MW open pool reactors inspired by the design of the reactor OPAL.

This work presents INVAP's methodology for the design of the primary coolant circuit shielding.

1.2 Objectives

The latest research reactor projects in which INVAP is involved are 30 MW open pool type MTR reactors that include a light water cooling circuit for the refrigeration of the core and of the irradiation facilities and a heavy water cooling circuit for the refrigeration of the heavy water reflector.

The light water (containing dissolved air and traces of impurities) that circulates through the core and the irradiation facilities is activated by the high thermal and fast neutron flux present in the core and its neighbourhood, producing mainly ^{16}N, ^{19}O, ^{41}Ar and ^{24}Na. In addition, the fuel and the radioisotope production targets have aluminium cladding which is also activated producing mainly ^{28}Al, ^{27}Mg and ^{24}Na. These radioisotopes are dispersed into the cooling

circuits by diverse physical processes such as corrosion or recoil products of specific nuclear reactions.

^{16}N and ^{24}Na are high energy gamma emitters (main gamma lines in the range from 1 MeV to 7 MeV). As a consequence the rooms of the reactor where the light water cooling circuit equipment is located, are susceptible to present high enough dose rates that may prohibit access to these rooms.

Moreover, as the mentioned reactors are open-pool type, the upper part of the reactor pool is an interface through which a fraction of the radioisotopes produced is transferred to the reactor containment. These radionuclides are contributors to the dose received by the reactor workers due to both internal and external exposure. Their concentrations have also to be considered in order to estimate how much of them is not retained by the filtering components before they are released through the ventilation stack. This is part of the estimation of the dose to the public needed to verify compliance with applicable regulations.

Finally, the radioactive isotopes (except noble gases) accumulate inside the resins of the Reactor Water Purification System. Long term accumulation causes a potentially high dose rate inside the resins bunker and adjacent rooms.

As a consequence, when designing an open pool reactor, the activities of mentioned radionuclides in the Core Cooling System and in the In Confinement Pool Cooling System and resulting dose rates have to be calculated. Adequate shields and filters are added after such an analysis when required.

This work focuses only in the details of the calculation of the radionuclide activities and dose rate related to the Core Cooling System inside the reactor containment, close to the coolant pipes. It does not address the release of airborne nuclides into the containment nor the accumulation of activity in the resins of the coolant purification system.

2. Radionuclide activity calculation method

2.1 Reactor main cooling circuits overview

The core of the reactor studied in this work is cooled by a light water circuit called Core Cooling System. The core is surrounded by a heavy water reflector tank cooled by the Heavy Water Cooling and Purification System. The ensemble core and reflector tank is submerged in an open pool which has a height of light water of more than 10 m. This pool is cooled by the In Confinement Pools Cooling System. The reactor has Radioisotope Production Facilities and a Fuel Irradiation Facility in the reflector tank. These facilities are also cooled by the In Confinement Pools Cooling System.

The Core Cooling System and the In Confinement Pools Cooling System are inter-connected, for that reason there is a constant mix of part of the water in both cooling systems.

Fig 1 is an overview of the main pipes of the Core Cooling System (in red) and the In Confinement Pool Cooling System (in blue).

Letters a to z represent points of interest where specific activities of the radionuclides are calculated. The Q_i are the coolant flow in the pipes.

Abbreviations used in Fig 1: CCS (Core Cooling System), HL-RP (Hot water Layer-Reactor Pool), HL-SP (Hot water Layer-Service Pool), HWL-PC (Hot Water Layer-Purification Circuit), Mo (Molybdenum production facility), LOOP (Fuel Irradiation Facility), Ir (Iridium production facility), ICPCS (In Confinement Pool Cooling System), RWPS (Reactor Water Purification System).

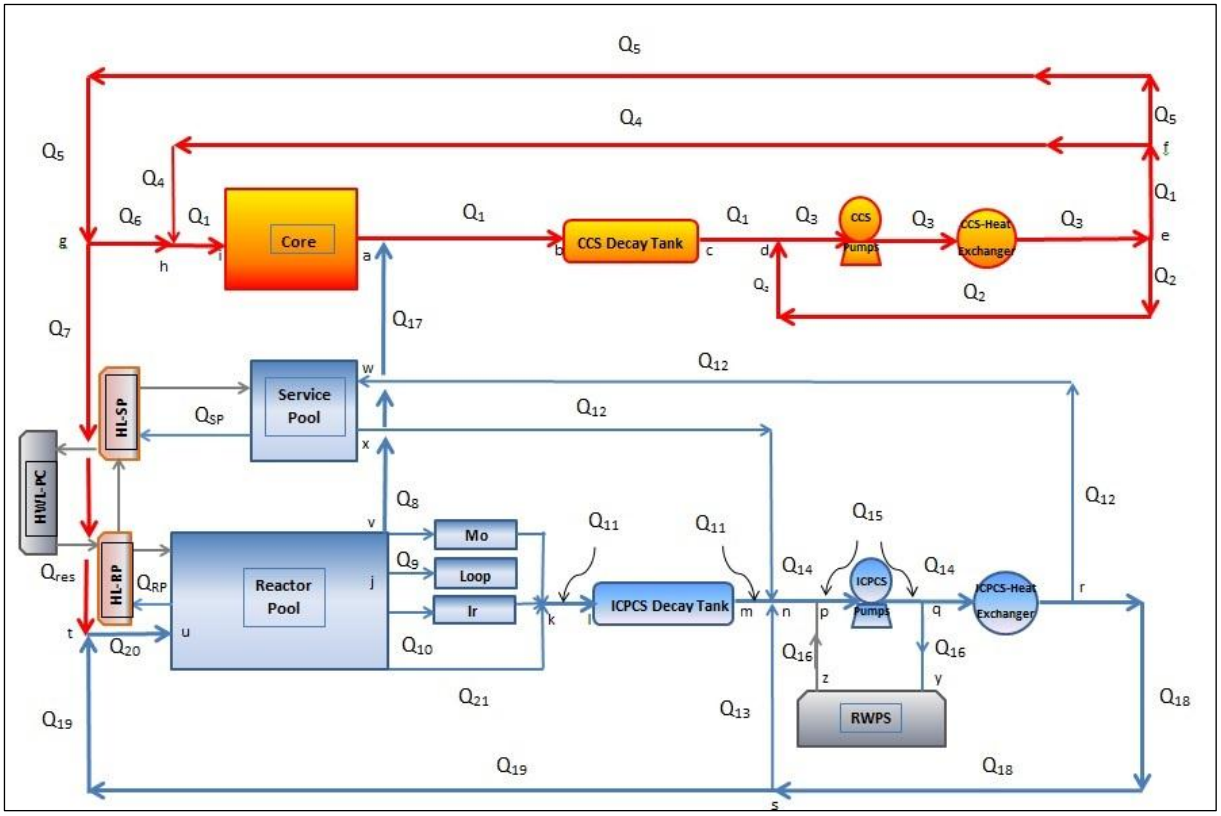

Fig 1: Diagram of the Core Cooling System and the In Confinement Pool Cooling System

2.2 Flux calculation

The production of the radionuclides occurs in the water volumes of the Core Cooling System and the In Confinement Pools Cooling System exposed to neutron flux.

Tab 1 shows the main nuclear reactions studied with their energy threshold and one-group weighted cross-sections.

For capture cross-sections, the cross-section value indicated corresponds to the thermal cross-section, weighted with the neutron flux below 0.625 eV, as considered in this work.

Nuclear reaction	Energy threshold	Cross-section
$^{16}O(n, p)^{16}N$	10.2 MeV	25.5 mb
$^{18}O(n, \gamma)^{19}O$	-	0.14 mb
$^{23}Na(n, \gamma)^{24}Na$	-	0.45 b
$^{27}Al(n, \alpha)^{24}Na$	3.2 MeV	3.9 mb
$^{27}Al(n, p)^{27}Mg$	1.9 MeV	9.1 mb
$^{27}Al(n, \gamma)^{28}Al$	-	0.20 b
$^{40}Ar(n, \gamma)^{41}Ar$	-	0.56 b

Tab 1: Nuclear reactions considered

Fig 2 shows an example of MCNP [1] model used to calculate the neutron fluxes in the core, the Fuel Irradiation Facility and the Radioisotope Production Facilities.

The calculated neutron fluxes enable to estimate the reaction rates of the reactions mentioned in Tab 1.

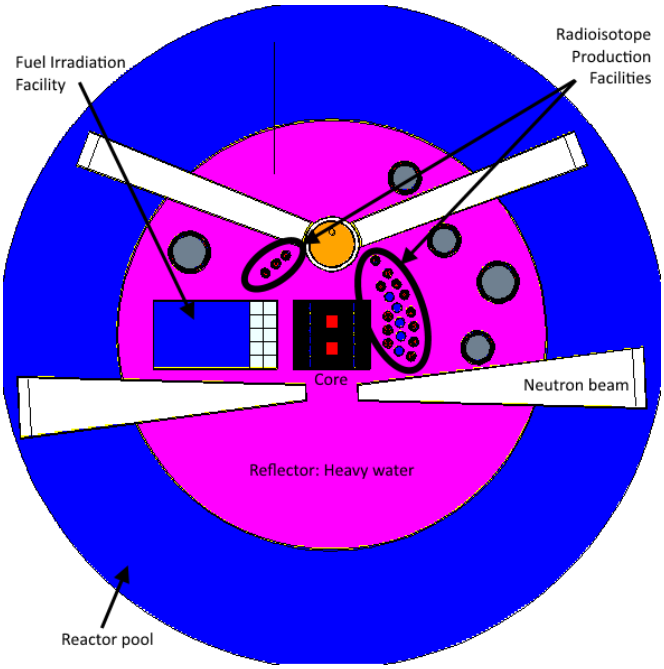

Fig 2: MCNP model – horizontal slice at the center of the Core

2.3 Radionuclide production

The production of ^{16}N, ^{17}N, ^{19}O and ^{41}Ar results from the nuclear reaction due to neutron bombardment of the parent nuclides ^{16}O, ^{17}O, ^{18}O and ^{40}Ar, respectively. These parent nuclides are either present in the water molecules or dissolved in the water.

The production of ^{24}Na results from 3 phenomena:

- Neutron activation of ^{23}Na impurities present in the water,
- Reaction $^{27}Al(n,\alpha)^{24}Na$ from the ^{27}Al present in the water due to corrosion of the aluminium of structural elements of the core (for instance the cladding of the fuel),
- Reaction $^{27}Al(n,\alpha)^{24}Na$ from the ^{27}Al present in the aluminium structural elements of the core and then released into the water by recoil.

For the corrosion process, the transfer rate W_k (expressed in at/cm^3/s) of ^{27}Al from a component k (Core, Irradiation facility…) to water can be calculated with equation 1:

$$W_k = 10^{-5} \cdot \frac{mdd_k}{24 \times 3600} \cdot \frac{N_A}{27} \cdot \frac{A_k}{Q_k t_k} \quad (1)$$

Where mdd_k is the aluminium mass transferred per surface unit and per time unit and is 1 mg/(dm^2·day) [2] [3], N_A is the Avogadro number, A_k is the surface of component k exposed to water (in cm^2), Q_k is the water flow in the component k and t_k is the residence time of the water in component k.

For the recoil process, the effective length of recoil is supposed to be l_{rec} =1.37 µm and only 25% of the ^{24}Na produced in the aluminium is transferred to water [4] [5]. Then, the transfer of specific activity R_k (in Bq/cm^3/s) of ^{24}Na from component k to water is calculated with equation 2:

$$R_k = \frac{\lambda \sigma N \phi_k V_{Al,k}^{\text{eff}}}{4V_k} \quad (2)$$

Where $V_{Al,k}^{eff} = l_{rec} \, . \, A_k$ is the effective volume from which recoil nuclides are transferred to water (A_k is the surface of component k exposed to water), $V_k = Q_k . t_k$ is the volume of component k, N is the number density of ^{27}Al in the component k, λ is the decay constant of ^{24}Na, σ is the microscopic cross section of the reaction $^{27}Al(n,\alpha)^{24}Na$ and ϕ_k is the neutron flux above 3.2 MeV in component k.

The production mechanisms of ^{27}Mg are similar to those for ^{24}Na, but changing the value of the parameters involved. The equations remain the same.

The production of ^{28}Al comes from the reaction $^{27}Al(n,\gamma)^{28}Al$ in the aluminium of structural elements. The transfer of ^{28}Al to water is calculated through an equivalent aluminium [6] thickness where its production is equal to its release into the water. This thickness is l_{eff}=0.42 µm.

2.4 Radionuclide distribution in the water circuits

Once the production terms for each isotope are calculated in every element of the water circuit, a set of equations is established with the residence time of water in each element of the circuit and in each pipe section in order to determine the specific activity of each isotope at every point of the circuit in stationary condition.

In this step, the data used are the water flow rate and the size of the pipes, the residence time of water in pumps and heat exchangers (can be calculated with flow rate and volume), the decay constant of the specific isotope and the production terms of the isotope (from section 2.3).

The Core Cooling System and the In Confinement Pool Cooling System have a decay tank whose goal is to reduce the activity of ^{16}N in the pipes to negligible levels, as compared to the activity of other radioisotopes present in the coolant. The calculation of the residence time of the coolant in these tanks is a crucial point for shielding design because it has a huge impact on the amount of high energy gammas to be shielded. As a consequence, a CFD (Computational Fluid Dynamics) calculation of the effective residence time of the isotope in the decay tanks in stationary condition is carried out with the methodology explained in [7].

Complete development is not needed to understand the methodology so what follows is the beginning of the development of the equation set for production and distribution of ^{16}N.
Let us begin with the equation 3 which shows the specific activity of ^{16}N at Primary Decay Tank inlet a_b (point b in Fig 1) in function of the specific activity of ^{16}N at core outlet a_C^o (point a in Fig 1). This section of the circuit is a pipe so there is only a decay term:

$$a_b = a_C^o * e^{-\lambda t_1} \tag{3}$$

Where λ is the decay constant of ^{16}N and t_1 is the residence time of water in the corresponding pipe.

Let us express the specific activity of ^{16}N at core outlet a_C^o in function of the specific activity of ^{16}N at core inlet a_C^i (point i in Fig 1) [8] [9]. Beside the decay term, this section of the circuit also includes a production term which depends on the results of sections 2.2 and 2.3.

$$a_C^o = a_C^i * e^{-\lambda t_c} + n\sigma\varphi_c(1 - e^{-\lambda t_c}) \tag{4}$$

Where t_c is the residence time of water in the core, n is the number density of ^{16}O (parent) in the water, σ is the microscopic cross section of the reaction $^{16}O(n,p)^{16}N$ of Tab 1 and φ_c is the neutron flux at corresponding energy.

The same reasoning is used to create a coherent set of linear equations for the unknown specific activities of each radionuclide at every point of the circuit. The number of equations is equal to the number of unknown (typically a system of coupled linear equations).

This set of equations is represented in a matrix form and then is solved by hand calculation or with any mathematics program in order to obtain the vector solution of the matrix system. The results of the resolution of the matrix of every radionuclide are the specific activities of every radionuclide at every point of the water cooling circuits.

3. Results

3.1 General use

The specific activities calculated with the methodology of section 2 are used into 3 different ways:

- Shielding calculations in the rooms of the reactor where the pipes with water containing radionuclides pass.
- Estimation of radionuclide accumulation in the resins of the Reactor Water Purification System in order to estimate the shield required by the reactor resins. It is also used to estimate the inventory of the resins when removed from the reactor for its processing as radioactive waste. It enables to estimate the dose rate in contact with the transport containers and the impact of their eventual leak.
- Calculation of the release of airborne radionuclide into the containment by natural evaporation at the surface of the open pool. This is the source term for dose calculation to operators by external exposure and inhalation of airborne radionuclides and for dose calculation to critical group for public dose assessment.

For the 2 last points the external contamination of the fuel elements of the core must be taken into account too. Since external contamination of the fuel elements is out of the scope of this work, the accumulation of radionuclides in resins and the calculation of the release of airborne radionuclide into the containment are not treated here.

Nevertheless, sections 3.2 and 3.3 show example of shielding calculations carried out that use the specific activities calculated with the method presented in section 2.

3.2 Dose rates in the Decay Tanks Bunker and adjacent rooms

3.2.1 Dose rate criteria

As an example let us use the Argentinean regulation to explain the radiological criteria used for such a reactor.

The regulatory criterion for workers is an annual effective dose limit of 20 mSv [10]. The limit for ALARA demonstration is an annual dose of 5 mSv. This limit for ALARA demonstration is normally used by INVAP as it is a very demanding criterion for shielding design.

Besides this, an occupancy factor (between 0 for no occupancy and 1 for full time occupancy) is established for every room of the reactor. Assuming 2000 working hours per year, the ALARA criterion is derived to a dose rate limit per room which depends on the occupancy factor of the room. Tab 2 shows the dose rate limit depending on the occupancy factor, resulting from the application of these design criteria.

Occupancy Factor	Dose rate limit for ALARA (µSv/h)
1	2.5
0.5	5

0.1	25
0.01	250

Tab 2: Dose rate limit to comply with ALARA criterion (example)

The limits presented in Tab 2 are normally tailored to be consistent with the regulations applicable of the country where the reactor is built, considering also particular requirements from INVAP's client, if needed.

The Decay Tanks Bunker is classified as a forbidden area and its occupancy factor is 0. In adjacent rooms, the occupancy factor depends on the use of the room which can differ from one reactor to another.

3.2.2 Dose rate calculation

With the specific activities calculated with the methodology presented in section 2, a 3D calculation model is built with the code MCNP [1].

In this shielding calculation, the main radionuclide is ^{16}N since it has the highest concentration at the Core Cooling System Decay Tank inlet and also is the isotope of highest energy gammas.

To make the best estimation of the dose rate inside the Decay Tanks Bunker and adjacent rooms, a particular attention must be given to the concentration of ^{16}N in the different segments of the Decay Tanks in order to avoid sub estimation or over estimation of the source and of the dose rates.

Fig 3 shows a view of the decay tanks INVAP uses along with its MCNP model. It can be seen the division into 4 segments in order to take into account the decay of ^{16}N while water goes further inside the tank.

This shielding calculation is normally carried out by applying conservative assumptions: the density of the shield material is reduced to account for engineering margins; the material of the pipes (in general, stainless steel) is ignored in the modelling; the volume of the radiation source contained in the pipes is slightly increased (by incorporating the piping thickness into the source volume, while maintaining the specific activity of the radionuclides involved). All of these conservative assumptions contribute to obtain a robust design of the shields involved in the analysis, which is an important design goal during the basic design stage. Thus, small changes or re-evaluations of input data that normally occur during more advanced design stages can be absorbed into the design, without compromising to achieve the design criteria adopted and then time consuming or potentially expensive and non-planned re-works are avoided.

Fig 4 shows a typical dose rate map inside a Decay Tanks bunker with reactor at full power. The entrance labyrinth of the bunker can be seen. Inside the bunker the dose rate reaches values superior to 100 mSv/h. Cylinders representative of operators are placed along the bunker walls and at the beginning of the labyrinth in order to check compliance with the dose rate criteria in adjacent rooms.

In the particular case of this calculation, the highest dose rate calculated in adjacent rooms is inferior to 2.5 µSv/h. As a consequence, the design criteria are fulfilled.

The 2 main results of such a calculation are:

- Establishing the adequate thickness of the bunker walls in order to fulfil the design criteria in the adjacent rooms,

- Designing an entrance labyrinth for the Decay Tanks Bunker able to reduce the dose rate to values lower than the design criteria.

In both cases, the dose rate is reduced by about 5 orders of magnitude.

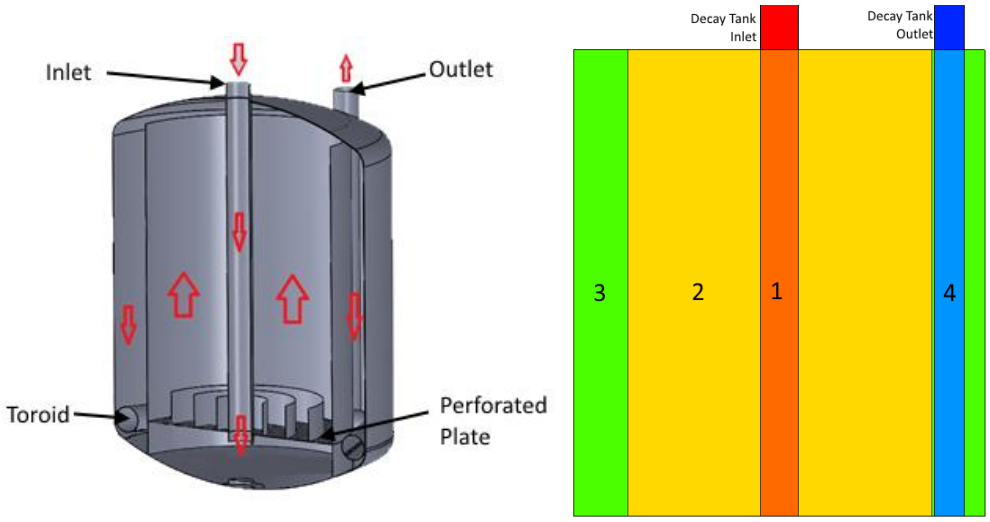

Fig 3: Design and MCNP model of the Decay Tanks

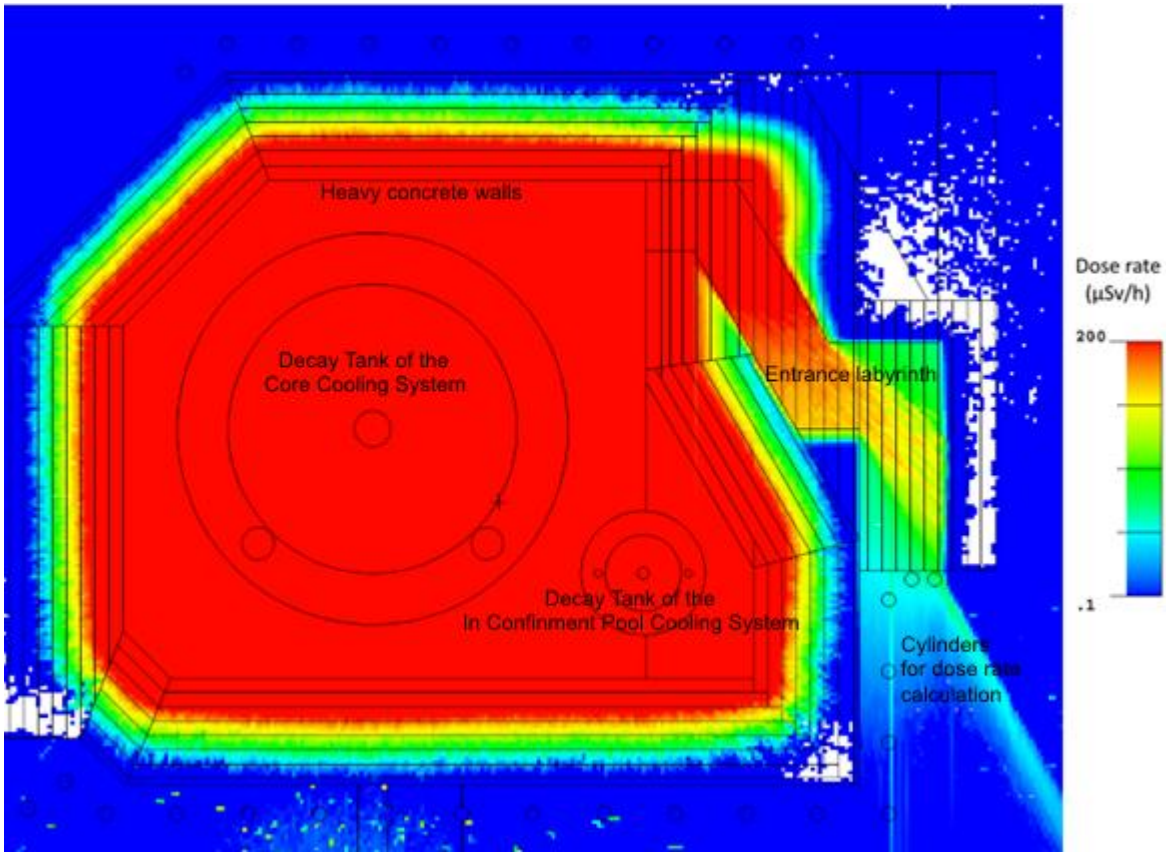

Fig 4: Dose rate map inside the Decay Tanks Bunker and adjacent rooms

3.3 Dose rate in the Core Cooling Pump Room

3.3.1 Dose rate criteria

The studied reactor has 3 Core pooling pumps, each one in a different Core Cooling Pump Room. Two out of the three pumps are working at the same time. Access is not required in

any of the pump rooms during operation, except for very short periods of time as part of the routine inspection by reactor staff. However, the dose rate inside the room with the pump not working should allow maintenance tasks which means, in the Argentinean regulation, a dose rate inferior to 200 µSv/h [11].

For the adjacent rooms, the same criteria as for the Decay Tanks Bunker apply.

3.3.2 Dose rate calculation

With the specific activities calculated with the methodology presented in section 2, a 3D calculation model is built with the code MCNP [1].

In this shielding calculation, the main radionuclide is no longer ^{16}N because it has almost fully decayed during its journey inside the Core Cooling System Decay Tank. Here, all the radionuclides in Tab 1 participate significantly to the calculated dose rates.

To obtain a reliable estimation of the dose rate inside the pump rooms and adjacent rooms, a particular attention must be paid to the concentration of all remaining radionuclides in the heat exchangers (components with the highest volume), in the different pipes and in the pumps themselves.

This shielding calculation is carried out with similar conservative hypothesis, as described in section 3.2.2.

Fig 5 shows a typical dose rate map inside the Core Cooling Pump Rooms with reactor at full power. Here, it is assumed that the not-working pump is the one in the central room. Cylinders representative of operators are placed along the rooms' walls and at relevant positions in order to check compliance with the dose rate criteria in the not-working pump room and adjacent rooms.

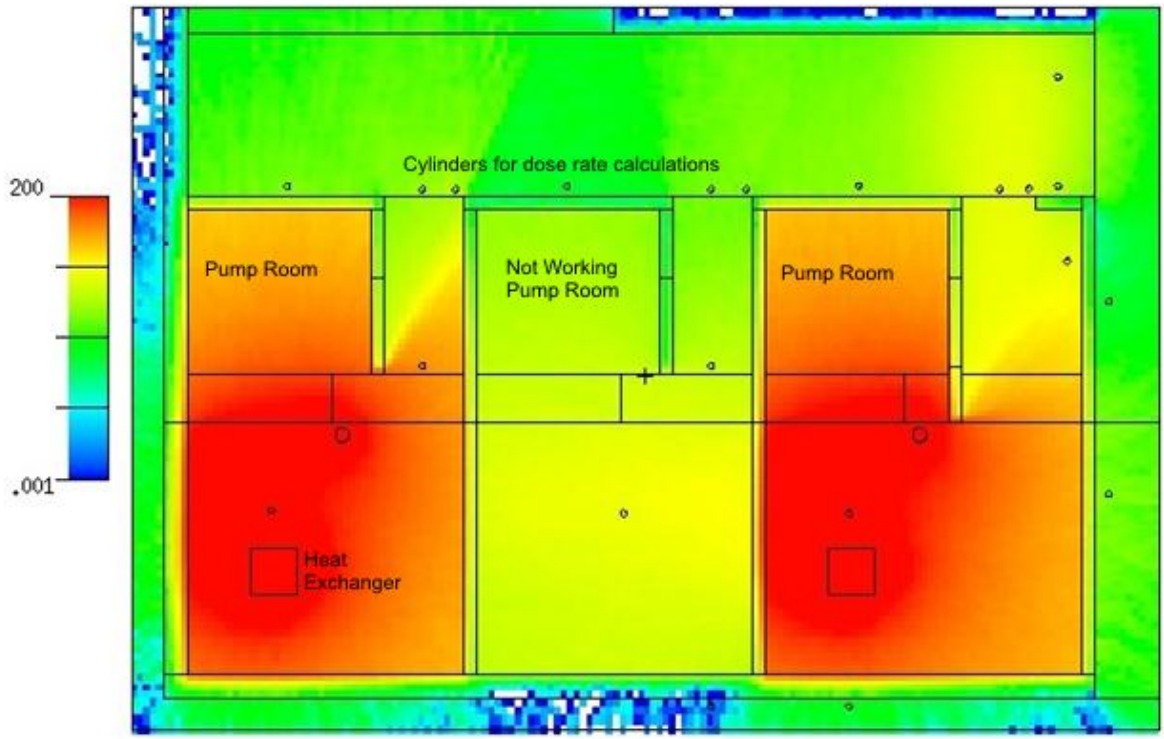

Fig 8: Dose rate map inside the Pump Rooms and adjacent rooms [µSv/h]

In the particular case of this calculation:

- Inside the working pumps rooms the dose rate reaches values up to 200 µSv/h.
- The highest dose rate calculated in the not-working pump room is inferior to 5 µSv/h.
- The highest dose rate calculated in adjacent rooms is inferior to 2.5 µSv/h.

As a consequence, the design criteria are fulfilled.

The main results of such a calculation are:

- Establishing that the not-working pump room is accessible for maintenance tasks during operation,
- Establishing the adequate thickness of the rooms' walls in order to fulfil the design criteria in the adjacent rooms,
- Determining the appropriate location within the rooms with operating pumps to place any instrument or component that should be protected from radiation.

4. Conclusions

The methodology proposed in this work for calculation of the concentration of the main radionuclides (the ones important for shielding analysis) enables to make a conservative dose rate calculation in the main cooling circuits' rooms of a research reactor and to design the radiological shields they need.

5. References

[1] T. Goorley, et al., "Initial MCNP6 Release Overview", Nuclear Technology, 180, pp 298-315 (Dec 2012).

[2] Water Corrosion of Aluminum Alloy Claddings, Argonne National Laboratory. Publicado en IAEA-TECDOC-643 Research reactor core conversion guidebook, Volume 4, Appendix I-3.1. International Atomic Energy Agency, Austria, April 1992.

[3] H. Piper, Water and Corrosion Technology of Light Water Research Reactors. Publicado en IAEA-TECDOC-643 Research reactor core conversion guidebook, Volume 4, Appendix I-3.6. International Atomic Energy Agency, Austria, April 1992.

[4] H. Mitsui, Measurement and Calculation of Recoil Ranges of 27Mg and 24Na in the Reactions 27Al(n,p)27Mg and 27Al(n,α)24Na, Journal of Nuclear Science and Technology, Vol. 1, No. 6, p. 203-209 (1963).

[5] J. C. Ward, Radioactivity of Nuclear Reactor Cooling Fluids, ORNL-3152, Oak Ridge National Laboratory, October 1961.

[6] Byung Jin Jun et al., Estimation of Aluminum and Argon Activation Source in the HANARO Coolant, *Nuclear Engineering and Technology*, Vol. 42 No. 4, Aug. 2010.

[7] Mataloni, Laura et al. "CFD Analysis of Residence Time Distribution in a Decay Tank and Comparison with Experimental Measurements". IYNCWiN2018, Bariloche, Argentina, 2018, Track 4 Thermal hydraulics.

[8] Engineering Compendium on Radiation Shielding, Vol. III : Shield Design and Engineering, R. G. Jaeger, Ed. Springer-Verlag, Berlin-Heidelberg-New York 1970.

[9] Reactor Shielding Design Manual, T. Rockwell III, Ed., United States Atomic Energy Commission, 1stedition, 1956.

[10] Autoridad Regulatoria Nuclear. AR 10.1.1. Norma básica de seguridad radiológica. REVISIÓN 3. Aprobada por Resolución del Directorio de la Autoridad Regulatoria Nuclear Nº 22/01 (Boletín Oficial 20/11/01). Modificada por Resolución del Directorio de la Autoridad Regulatoria Nuclear N°230/16 (Boletín Oficial 29/04/16).

[11] Autoridad Regulatoria Nuclear. AR 6.1.1. Exposición ocupacional de instalaciones radiactivas Clase I. REVISIÓN 1. Aprobada por Resolución del Directorio de la Autoridad Regulatoria Nuclear Nº 36/01 (Boletín Oficial 15/1/02).

METHODOLOGY FOR THE DESIGN OF THE HEAVY WATER COOLING AND PURIFICATION SYSTEM SHIELDING IN HIGH PERFORMANCE MULTIPURPOSE RESEARCH REACTORS

H.G. MEIER, M. BRIZUELA, A. MAÎTRE
INVAP S.E. Av. Comandante Luis Piedrabuena 4950, 8400 San Carlos de Bariloche, Río Negro, Argentina, hgmeier@invap.com.ar, http://www.invap.com.ar

ABSTRACT

Some high performance multipurpose research reactor designs include a heavy water reflector tank that amplifies the available space with appropriate high neutron flux to accommodate more irradiation facilities. Neutron flux irradiation of the heavy water in the reflector tank generates activated heavy water that circulates through the heavy water cooling and purification system. The room that accommodates the heavy water cooling and purification system has to be appropriately shielded against decay gamma and also against neutrons produced by these same high energy decay gammas via photo-neutron reactions in the circulating heavy water contained in pipelines, pumps and heat exchangers.
The aim of this work is to present INVAP´s methodology for the design of the biological shields of the heavy water cooling and purification system rooms. INVAP´s methodology includes: a neutron flux irradiation calculation of heavy water in order to obtain the circulating heavy water activity in full power normal operation, then 3D detailed geometry modelling of the heavy water cooling and purification system room with the heavy water pipelines, pumps and heat exchangers as gamma and photo-neutron radiation sources and finally the MCNP coupled neutron-gamma transport calculation using a weight windows mesh prepared with ADVANTG as a variance reduction in order to calculate the expected dose rates on operators, verifying the designed biological shields.

1 Introduction

This paper presents INVAP S.E. methodology for designing and verifying the biological shields in high performance multipurpose research reactors of the heavy water cooling and purification system rooms in order to achieve As Low As Reasonably Achievable (ALARA) operators dose rates.

1.1 Problem Description

Heavy water reflector tanks are included in some high performance multipurpose research reactor designs with the aim of amplifying the available space with appropriate high neutron flux to accommodate more irradiation facilities.
The heavy water circulating through the reflector tank vessel is irradiated by neutron flux from the core; the neutron flux irradiation produces activated heavy water that is the radiation source that has to be appropriately shielded.
The radiation source came from decay gamma and neutrons from in reflector vessel activated isotopes and via photo-neutron reactions in the circulating heavy water contained in pipelines, pumps and heat exchangers.
Activated heavy water circulates through the heavy water cooling and purification system produces dose rate at the room that accommodates this system and has to be appropriately shielded against radiation.

2 Methodology

INVAP´s calculation methodology diagram is shown in Fig 1.

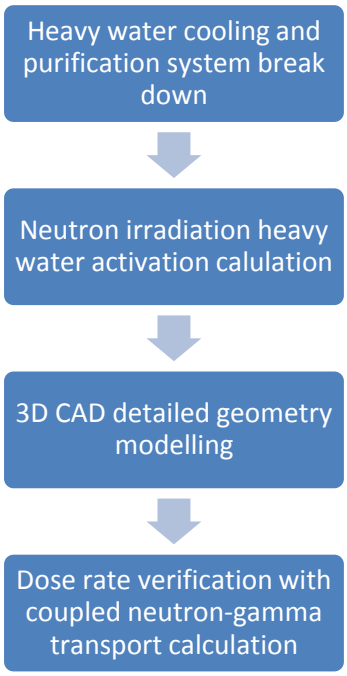

Fig 1. INVAP´s calculation methodology diagram

2.1 System Break Down

A typical heavy water cooling and purification system flow diagram is depicted as the one presented in Fig2. Generally, a heavy water cooling and purification system comprises the following subsystems:

i. Heavy water cooling circuit: a heavy water circulating circuit with pumps and heat exchangers in order to transfer heat from the reflector vessel heavy water to the intermediate circuit.
ii. Heavy water purification circuit: a heavy water circulating circuit with filters and ion-exchanger resins in order to maintain heavy water chemistry within the specified values for safe reactor operation.
iii. Heavy water intermediate circuit: a light water circulating circuit with pumps and heat exchangers in order to transfer heat from the heavy water cooling circuit to the final cooling source and serves the purpose of creating an additional barrier to avoid any possible tritium migration into the environment.
iv. Heavy water recombination circuit: a heavy water circulating circuit with pumps and recombination units in order to recombine deuterium with oxygen to avoid the accumulation of explosive gases.

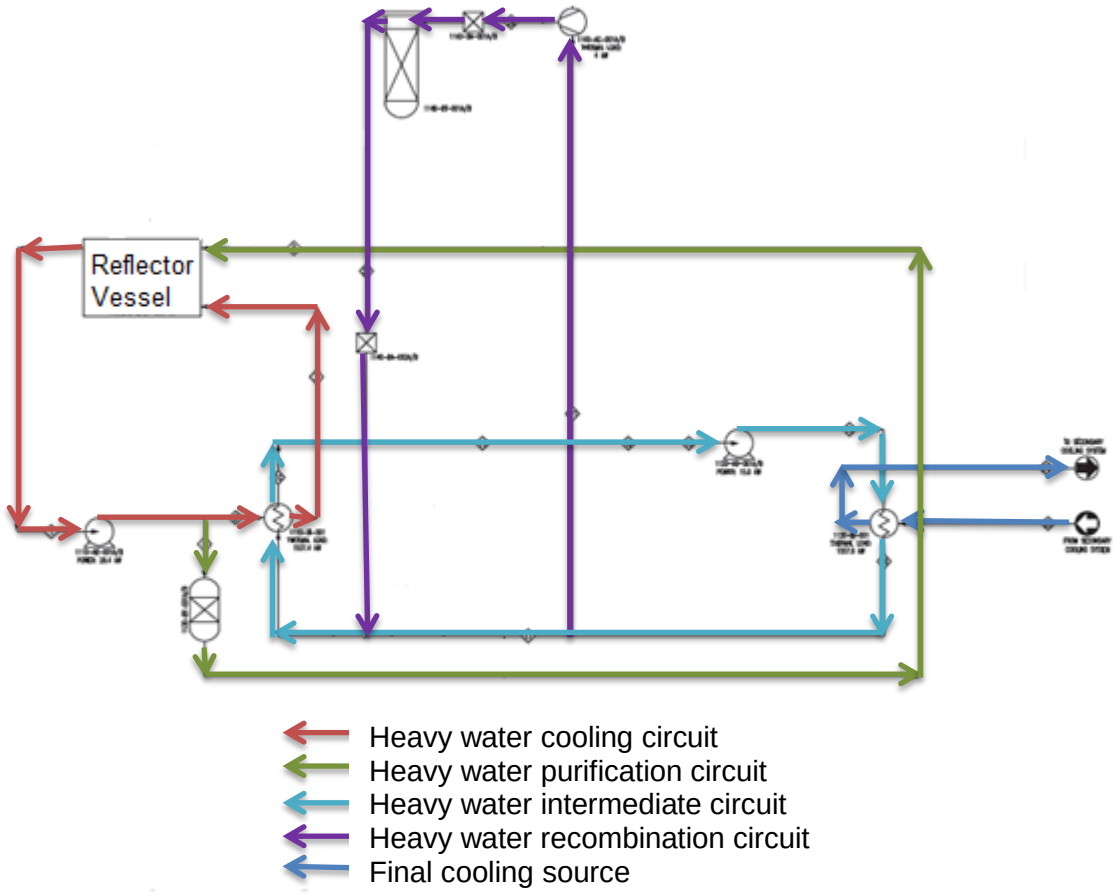

Fig 2. Typical heavy water cooling and purification system process flow diagram.

From the description above the following assumptions can be considered:

i. Heavy water cooling circuit: To be conservative the heavy water activity at the circuit is calculated at the exit of the reflector vessel.
ii. Heavy water purification circuit: The heavy water activity is assumed to be equal to the heavy water activity of the Heavy water Cooling Circuit
iii. Heavy water intermediate circuit: This circuit is a light water closed loop that does not contain heavy water activity.
iv. Heavy water recombination circuit: Due to the low flow rate, this circuit is not studied.

2.2 Activation Calculation

2.2.1 Main radioisotopes

Due to the heavy water high purity and the corrosion resistance of the materials in contact with the heavy water (typically Zircaloy-4 and stainless steel), heavy water activation comes mainly from the activation of deuterium and oxygen isotopes. Therefore, the most relevant activation products and their main specifications are presented in Tab1.

Parent nuclide	Isotopic abundance	Atomic density (at/bcm)	Reaction	Activation product	Half life
^{16}O	99.757%	3.31E-02	$^{16}O(n,p)^{16}N$	^{16}N	7.13 s
^{17}O	0.038%	1.26E-05	$^{17}O(n,p)^{17}N$	^{17}N	4.173 s
^{18}O	0.205%	6.79E-05	$^{18}O(n,g)^{19}O$	^{19}O	26.88 s
^{2}H	100.000%	6.63E-02	$^{2}H(n,g)^{3}H$	^{3}H	12.32 y

Tab 1: Heavy water neutron activation products and their main specifications [1].

2.2.2 Physics model

The concentration of any radioisotope (N) is obtained via a balance of radioisotope production via neutron flux irradiation and the losses via radioactive decay.
The system can be modelled as the simple coolant circuit of Fig 3 [2].

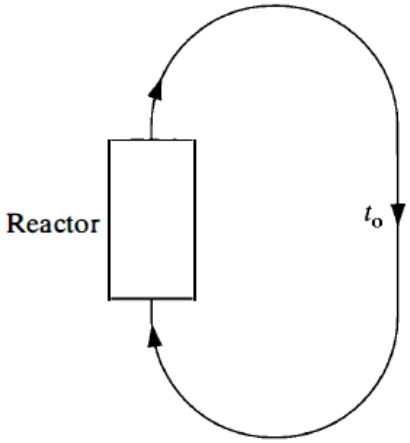

Fig 3. A simple coolant circuit [2].

The specific activity (A) of a radioisotope at the exit of the irradiation region for a recirculation circuit exposed to a neutron flux during time Ti and a total circuit time Tc is:

$$A(t)=\Sigma\cdot\Phi\cdot\frac{\left(1-e^{-\lambda\cdot Ti}\right)}{\left(1-e^{-\lambda\cdot Tc}\right)} \quad (1)$$

Finally, the activity in the heavy water cooling circuit is calculated from Eq. 1.

2.2.3 Residence time estimation

The residence time outside the reflector vessel is obtained dividing the total volume of circulating heavy water by the heavy water cooling circuit flow rate. In this study it will be assumed that the resulting circulation time outside the reflector vessel is of 30 seconds.
The heavy water residence time inside the reflector vessel is more difficult to be precisely calculated, if the heavy water does not completely mix inside the reflector vessel an effective irradiated reflector vessel volume is generated that could have less volume than the real reflector vessel volume. The size of the effective irradiated reflector vessel volume may affect the heavy water activity in two opposite ways:

i. A reduced effective irradiated reflector vessel volume can produce that circulating heavy water passes through an average higher neutron flux increasing the final heavy water activity.
ii. A reduced effective irradiated reflector vessel volume also reduces the irradiation time reducing the final heavy water activity.
iii. At further distances from the core the fast neutron flux decreases faster than thermal neutron flux, thus a larger effective irradiated reflector vessel volume has an average neutron flux more thermalized than a smaller one. This neutron flux thermalization in larger effective irradiated reflector vessel volume reduces the reaction rate for $^{16}O(n.p)^{16}N$ and $^{17}O(n.p)^{17}N$ reactions that have threshold energy.

To precisely calculate all effects complex coupled thermohydraulics-neutronic calculations are needed. However, conservative results can be obtained using only neutronic calculations to calculate a maximum heavy water activity.
INVAPS´s methodology calculates the ^{16}N, ^{17}N. ^{19}O and ^{3}H activity in function of the effective irradiated reflector vessel volume. With this approach the real effective irradiated reflector vessel volume does not matter because the heavy water activity is going to be inferior or

equal to the maximum heavy water activity calculated for the most conservative effective irradiated reflector vessel volume. Then the maximum heavy water cooling circuit activity is assumed to be the maximum calculated activity of each radioisotope.

2.2.4 Neutron flux calculation

In a fission reactor the neutron flux comes from the reactor core and it is transported to the heavy water reflector vessel, for this study it is assumed a Material Testing Reactor (MTR) type of 30 MW_{th} power with U_2Si_3 fuels and light water as moderator/refrigerator.
A detailed 238 group neutron flux (ϕg) is calculated using the reactor model of Fig4 with MCNP6 [3] and the group reaction cross sections (Σg) are obtained from SCALE6.1 JEFF238g library [4]. The total neutron flux (ϕ) is obtained using Eq. 2 and the condensated monoergetic reaction cross section (Σ) is obtained using Eq. 3.

$$\Phi = \sum_{n}^{238} \Phi_g \quad [2]$$

$$\Sigma = \sum_{n}^{238} \frac{\Sigma_g \Phi_g}{\Phi} \quad [3]$$

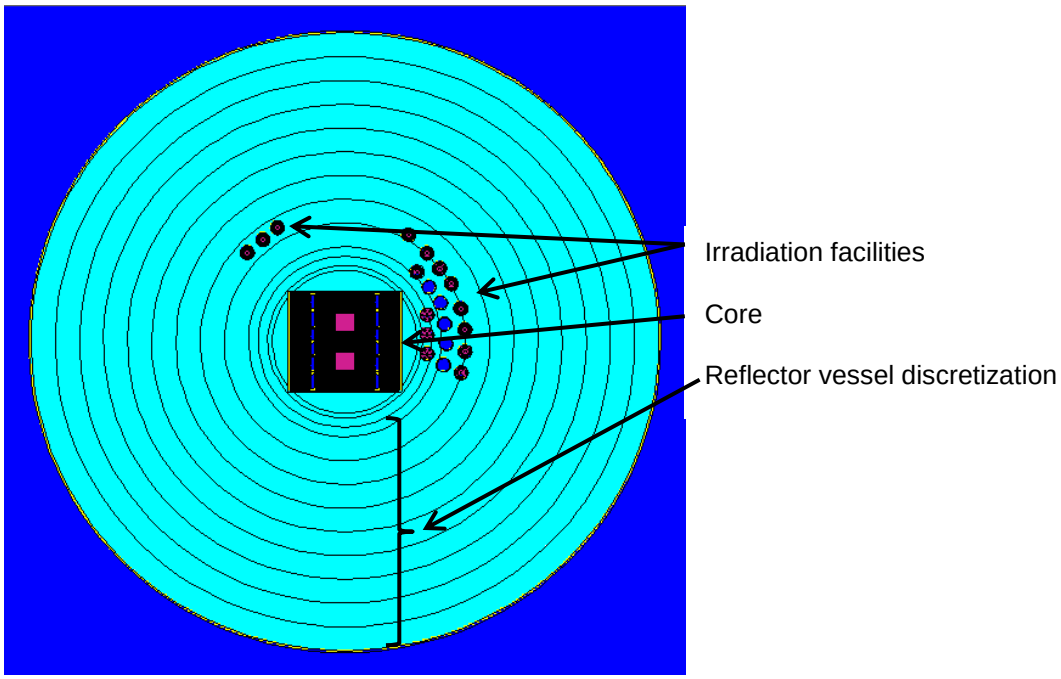

Fig 4. Heavy water reflector vessel discretization model.

2.3 Geometry modeling

3D drawings coming from civil and mechanical engineering groups are used as model input.
An example of 3D drawing is shown in Fig5, it feeds the geometry conversion software for conversion of CAD models into the Monte Carlo (MC) geometries. This software generates a 3D detailed geometry model of the heavy water cooling and purification system room with the heavy water pipelines, pumps and heat exchangers as gamma and photo-neutron radiation sources and the biological shields.
Adopted shielding materials are heavy concrete and standard concrete with conservative densities of 3.2 g/cm^3 and 2.1 g/cm^3.

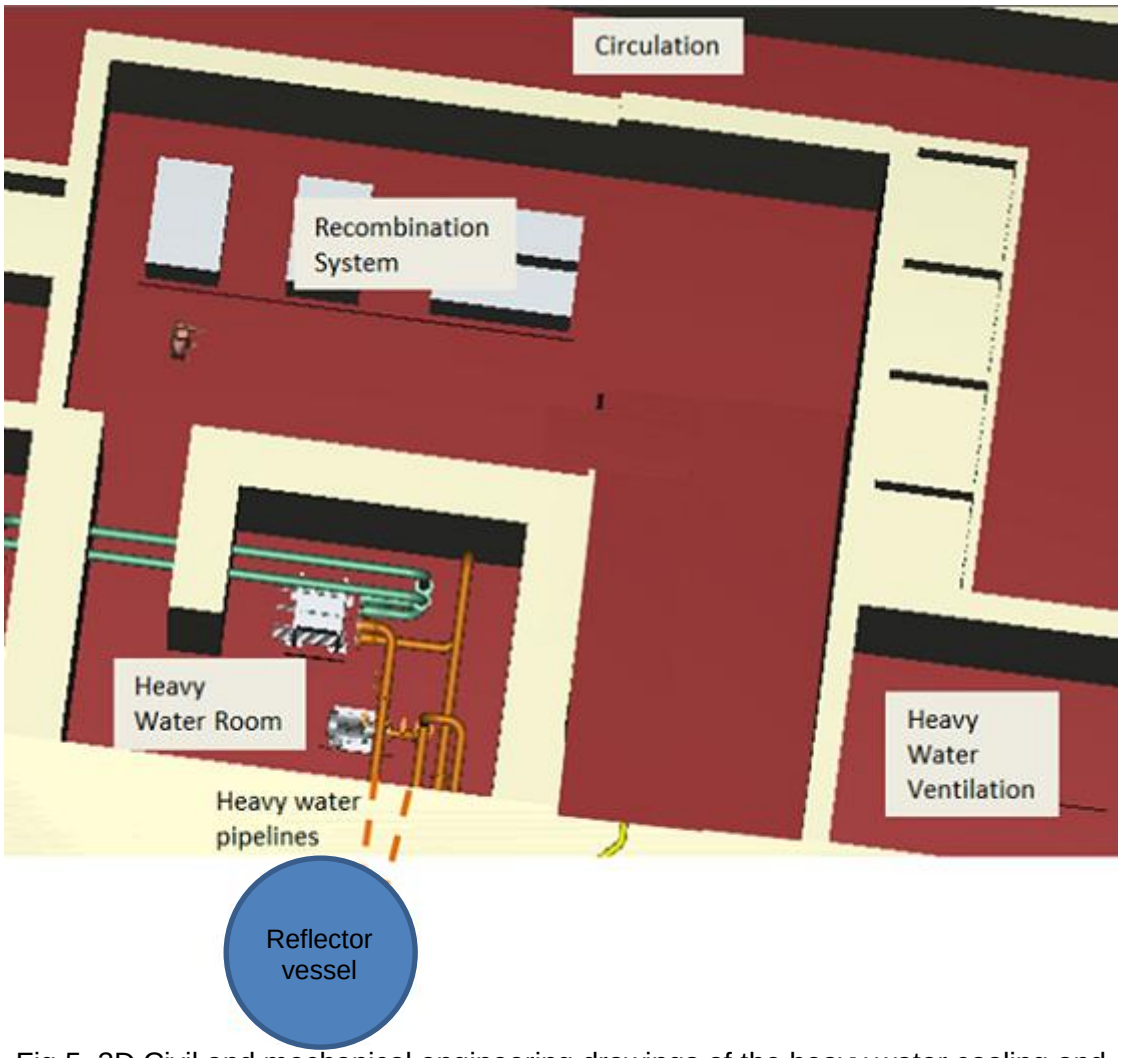

Fig 5. 3D Civil and mechanical engineering drawings of the heavy water cooling and purification system rooms.

2.3.1 Source modeling

The radioactive specific activities (Bq/cm^3) calculated in Section 2.2. have to be included in the calculation model.
Sources are modelled in MCNP6 [3] as simple geometry cells (spheres, cylinders, cubes, etc.) Source photons are homogenous and isotropically generated in the whole source cell volume.
Tab2 shows the calculated total source activity, considering respective cell volume and decay time considered in the source cells.
ORIGEN-S code from the SCALE 6.1 software package [4] is used to obtain the photon emission spectra of the respective source activity.
Additionally, neutrons produced via ^{2}H (γ, n) ^{1}H photoneutron reaction in heavy water it is considered via MCNP6 [3] option.

Source	**Geometry**	**Decay time (s)**	**Activity (Bq)**		
			^{16}N	**^{17}N**	**^{19}O**
Inlet piping in block	Cylinder (r=10 cm)	2	2E+11	2E+07	2E+10
Exit piping in block	Cylinder (r=5 cm)	15	3E+10	1E+06	8E+09
Income piping in air	Cylinder (r=10 cm)	3	2E+11	2E+07	2E+10

Source	Geometry	Decay time (s)	Activity (Bq)		
			^{16}N	^{17}N	^{19}O
Exit piping in air	Cylinder (r=5 cm)	13	3E+10	1E+06	8E+09
Pump	Sphere (r=5 cm)	5	1E+12	5E+07	1E+11
Heat exchanger simplified model	Cylinder (r=30 cm)	10	1E+12	5E+07	1E+11

Tab 2: Radioactive sources activities.

2.3.2 Variance reduction

Deep penetration neutron and gamma shielding transportation is difficult to calculate without appropriately reduction variance technics.
One available reduction variance technic is the superposition of a weight window mesh. To create the appropriate weight window mesh the code used is ADVANTG[5], it is an automated tool for generating variance reduction parameters for fixed-source continuous-energy Monte Carlo simulations based on approximate 3-D multigroup discrete ordinates adjoint transport solutions.
The variance reduction parameters generated by ADVANTG[5] consist of space and energy-dependent weight-window bounds and biased source distributions, which are output in formats that can be directly used.
ADVANTG[5] has been applied to neutron, photon, and coupled neutron-photon simulations of radiation detection and shielding scenarios.

2.4 Dose Rate Verification Calculation

2.4.1 Calculation Criteria

INVAP's methodology performs the dose rate calculations with the following criteria:

i. The used dose rate is the equivalent ambient dose rate from calculated with the flux-to-dose conversion factors to translate photon flux into dose rate from ICRP-116 [6].
ii. The operator dose rate is calculated in a representative position of an operator in cylinders of 180 cm of height and 20 cm of diameter 30 cm away from the external surface of a shield. Fig. 6 shows the cylinders that represent the operator position.

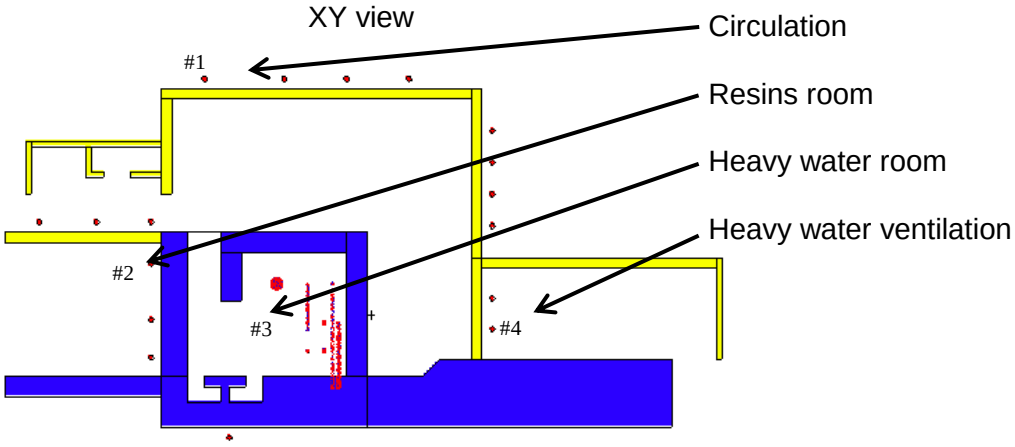

Fig. 6 XY view calculation model showing operator position control volumes identified with # symbol (yellow=standard concrete and blue=heavy concrete)

2.4.2 Acceptance Criteria

The dose rate acceptable in relevant rooms of this study comes from the applicable regulatory body, but generally acceptance criteria depend on the Occupancy Factor as follow:

i. Optimization is not required when, under normal operation conditions, the average effective dose does not exceed 1 mSv per annum.
ii. Dose rate acceptable in Controlled area depends on the Occupancy factor of each room considering 2000 working hours per year.

In Tab 3 it is shown an example of Occupancy factor for the studied rooms.

ROOM		Occupancy factor	Optimized dose rate (μSv/h)
#1	Circulation	0.10	5.0
#2	Resins room	0.01	50
#3	Heavy Water Room	0.00	No limit
#4	Heavy Water Ventilation	0.01	50

Tab 3: Occupancy factors for the studied rooms.

Dose rate mesh maps are usually also calculated in order to easily see the convergence and the absence of unexpected dose rate field behaviour.

3 Results

3.1 Specific activity results

Fig. 7 shows the curves of Heavy water Cooling Circuit radioisotope activity for ^{16}N. ^{17}N. ^{19}O and ^{3}H versus the effective irradiated reflector vessel volumes. In all this curves it is observed that the activity reaches a global maximum.
The different behaviour of ^{16}N and ^{17}N curves than ^{19}O and ^{3}H curves in Fig 7 shows the influence of the neutron flux thermalization at larger effective irradiated reflector vessel volumes. This thermalization decreases the number of ^{16}O(n.p)^{16}N and ^{17}O(n.p)^{17}N reactions because of their threshold energy.

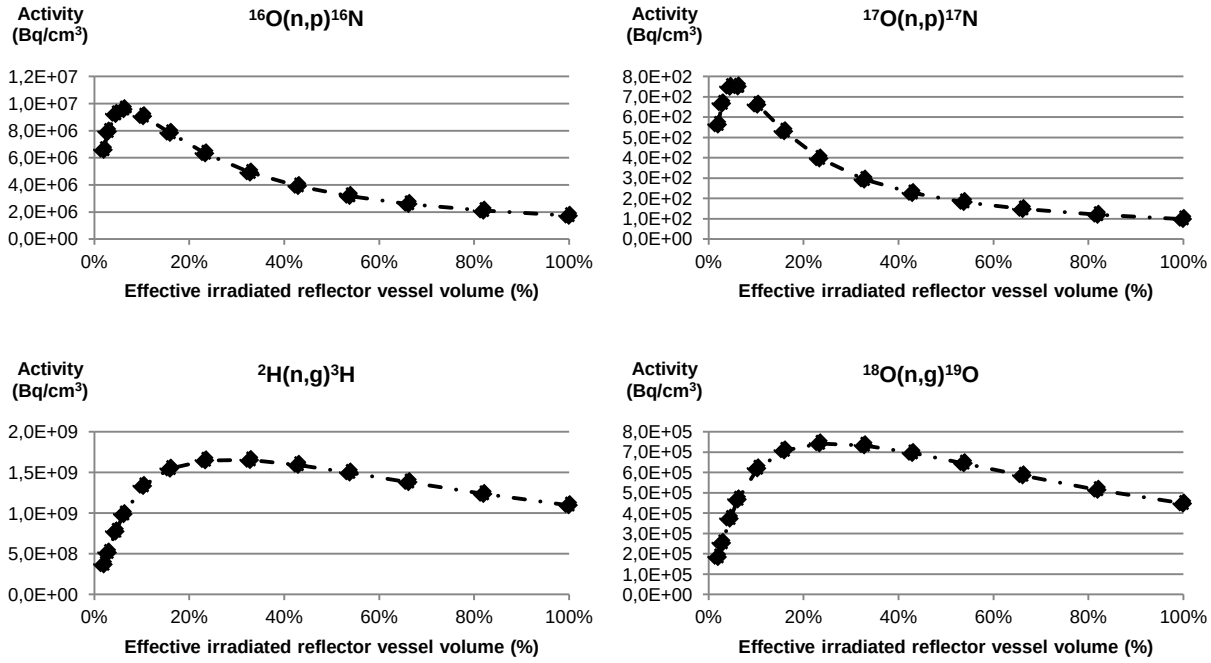

Fig. 7: Heavy water cooling circuit activity versus effective irradiated reflector vessel volume.

3.2 Weight window results

In Fig. 8 it is shown the neutron weight window mesh generated with ADVANTG[5] for the heavy water cooling and purification system rooms transport model.

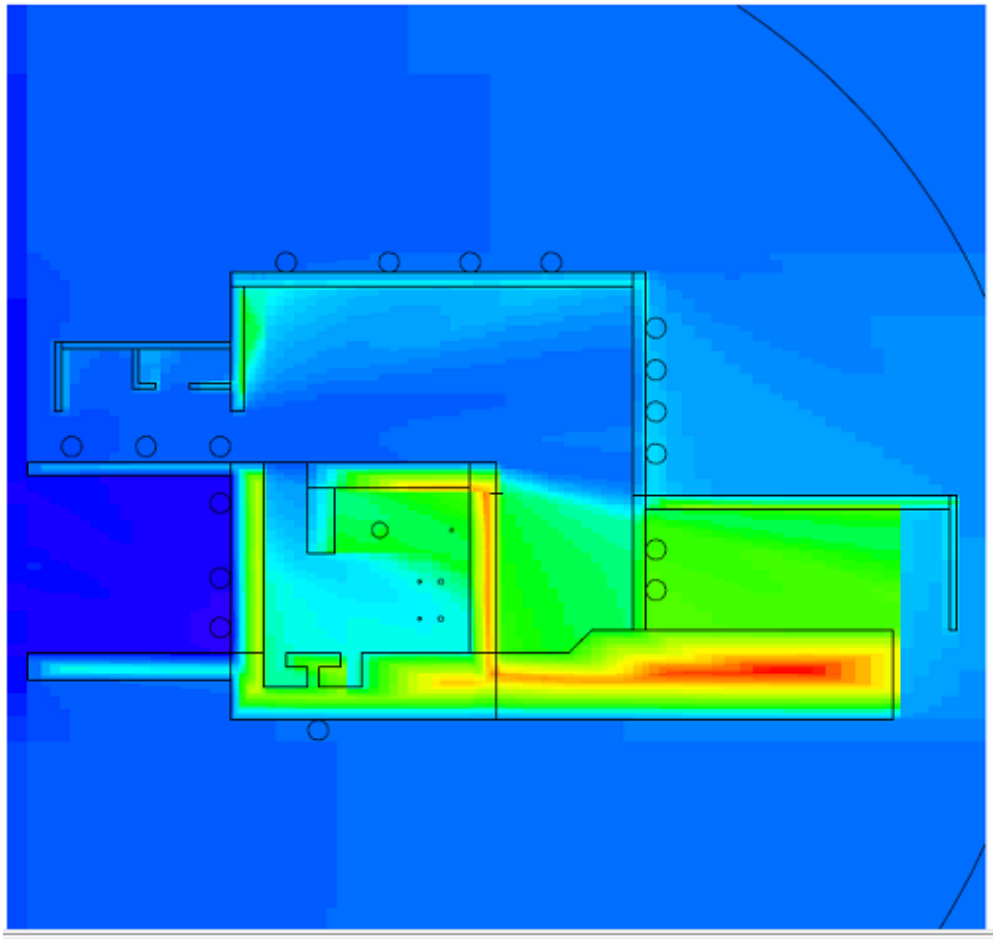

Fig. 8 ADVANTG[5] generated neutron weight window mesh for the transport model.

3.3 Dose rate results

Tab 4 shows the dose rate calculation results for the studied rooms at the operator position as described in Section 2.4.2.

ROOM		Occupation factor	Optimized dose rate (μSv/h)	Dose Rate (μSv/h)			
				Neutron	RE (%)	Photon	RE (%)
#1	Circulation	0.10	5.0	0.1	1.0	0.8	5.5
#2	Resins room	0.01	50	2.4	8.8	30	4.5
#3	Heavy Water Room	0.00	No limit	1E4	0.2	1E5	0.5
#4	Heavy Water Ventilation	0.01	50	0.2	0.6	2.3	5.7

Tab 4: Dose rates results for operator position for the studied rooms.

Fig. 9 and Fig. 10 present photon and neutron dose rate mesh maps respectively.
The neutron and photon dose rate field show the convergence achieved (more convergence for neutron transportation than from gamma transportation) and the absence of strange dose rate field behaviour.

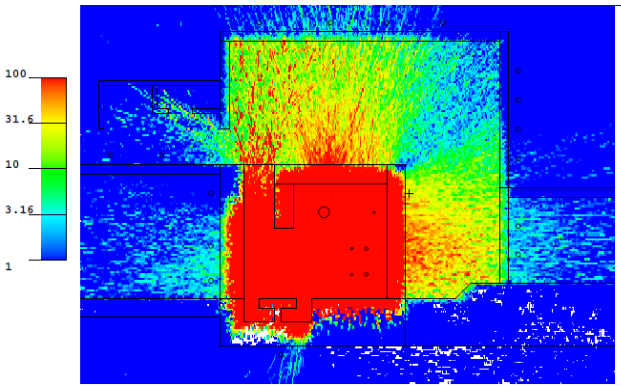

Fig 9. XY view of photon dose rate (µSv/h)

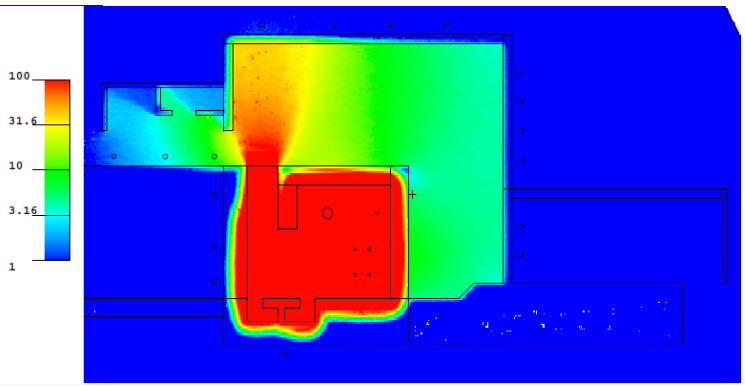

Fig 10. XY view of neutron dose rate (µSv/h)

4 Conclusion

This document shows INVAP´s methodology for designing the biological shields and verification of the operator dose rates at the heavy water cooling and purification system rooms of a representative multipurpose research reactor.
The result shows that the obtained operator dose rates are lower than the required for optimization. Therefore, the design fulfils the applicable regulatory body requirements.
All the analysis and the calculations were carried on assuming a conservative approach.

5 References

[1] Live Chart of Nuclides. Nuclear Structure and Decay Data. Nuclear Data Center. IAEA.

[2] Lamarsh, J.R. Introduction to Nuclear Engineering. 2nd Edition, Addison-Wesley, USA (1983).

[3] T. Goorley, et al., "Initial MCNP6 Release Overview", Nuclear Technology, 180, pp 298-315 (Dec 2012).

[4] SCALE Code System, Version 6.2.1, B. T. Rearden and M. A. Jessee, Eds., ORNL/TM-2005/39, Oak Ridge National Laboratory, Oak Ridge, Tennessee. Available from Radiation Safety Information Computational Center as CCC-834, 2016.

[5] S.W. Mosher et al.: ADVANTG--An Automated Variance Reduction Parameter Generator, ORNL/TM 2013/416 Rev. 1, Oak Ridge National Laboratory (2015).

[6] ICRP Publication 116. Conversion Coefficients for Radiological Protection Quantities for External Radiation Exposures. ICRP Publication 116, Ann. ICRP 40(2–5), 2010.

DESIGN PERFORMANCE OF RMB REACTOR

P. CAMUSSO, D. HERGENREDER, F. BOSCHETTI, I. FERRARI, H. SARABIA, E. VILLARINO, S. KOROCHINSKY

Nuclear Engineering Department, INVAP S.E.
Cmte Luis Piedrabuena 4950, 8403 Bariloche – Rio Negro – Argentina

A. SANTOS, A. SOARES, J. PERROTTA
Comissão Nacional de Energia Nuclear CNEN
Av. Prof. Lineu Prestes 2242, Cidade Universitária, São Pablo, Brasil

ABSTRACT

The Brazilian Multipurpose Reactor (RMB) is a 30 MW multi-purpose open-pool research reactor designed by INVAP S.E. (Argentina) and CNEN (Brazil).
The reactor is cooled and moderated by light water and reflected by heavy water and Beryllium. The heavy water reflector makes possible to create large irradiation volumes where many irradiation positions are located. The Beryllium reflector adds irradiation volume with size and geometry flexibility, since the Beryllium blocks can be easily changed to accommodate the reactor to future irradiation requirements.
The reactor utilization covers a wide range of applications: material testing, fuel testing, radioisotope production and neutron beam utilizations.
The material testing irradiations can be performed at the in-core irradiations positions where there are large irradiation volumes with high fast flux levels.
The fuel testing irradiations are located at the Beryllium grid where the reflector flexibility can accommodate facilities for testing in steady state conditions and ramping tests.

1. Introduction

The Brazilian Multipurpose Reactor (RMB) is a 30 MW multi-purpose open-pool research reactor designed by INVAP S.E. (Argentina) and CNEN (Brazil). The RMB is called to become a high performance multifunctional international facility.

The reactor is cooled and moderated by light water and reflected by heavy water and Beryllium. The heavy water reflector makes possible to create large irradiation volumes where many irradiation positions are located. The Beryllium reflector adds irradiation volume with size and geometry flexibility, since the Beryllium blocks can be easily changed to accommodate the reactor to future irradiation requirements.

The reactor utilization covers a wide range of applications: material testing, fuel testing, radioisotope production and neutron beam utilizations.

The material testing irradiations can be performed at the in-core irradiations positions where there are large irradiation volumes with high fast flux levels.

The fuel testing irradiations are located at the Beryllium grid where the reflector flexibility can accommodate facilities for testing in steady state conditions and facilities to perform ramping tests.

The radioisotope production requirements are covered with many irradiation positions located at the heavy water reflector. Considering the irradiation requirements for the different radioisotopes, the irradiation positions are classified by the thermal flux level into high flux, medium flux and low flux.

Five irradiations positions are assigned to perform NTD for different sizes of Silicon ingots.

Several pneumatic irradiation facilities enhance the irradiation capabilities of the RMB for other radioisotope production, as well as NAA, DNAA and CNAA.

To provide services on neutron beam utilization, the reactor has a neutron beam for neutron imaging, two neutron beams with thermal spectrum and two neutron beams with cold neutrons. The cold neutrons are provided by a high-performance liquid deuterium Cold Neutron Source. At a certain distance from the core, the neutrons are transported by super-mirror guides to the experiment location.

The paper will describe the RMB reactor and will present the reactor performance in terms flux values at the irradiation positions, cycle length and safety related parameters.

2. RMB description

Table 1 shows the main data of RMB (Multipurpose Brazilian Reactor).

Thermal Power	30 MW
^{99}Mo irradiation positions	11
Ir irradiation positions	3
Other Radio Isotopes irradiation positions	5 (TeO_2)
In Core Surveillance program irradiation position (ageing)	2 (neutron fast flux)
Out Core Surveillance program irradiation position (ageing)	1 (neutron thermal flux)
Pneumatics rigs	14 (37 cans)
Neutron Transmutation Doping (NTD) irradiation positions	5
In-Core Irradiation Facilities (ICIF)	2
Thermal Neutron Beams	2
Cold Neutron Beams	2
Cold Neutron Source (CNS)	1
Neutrongraphy	1
Coolant	Light Water (H2O)
Reflector	Heavy Water (D2O)
Fuel Irradiation Facility (FIF)	1
Safety Shutdown Systems	2

Table 1: RMB main data

Figure 1 shows the global arrangement of the RMB and its facilities.

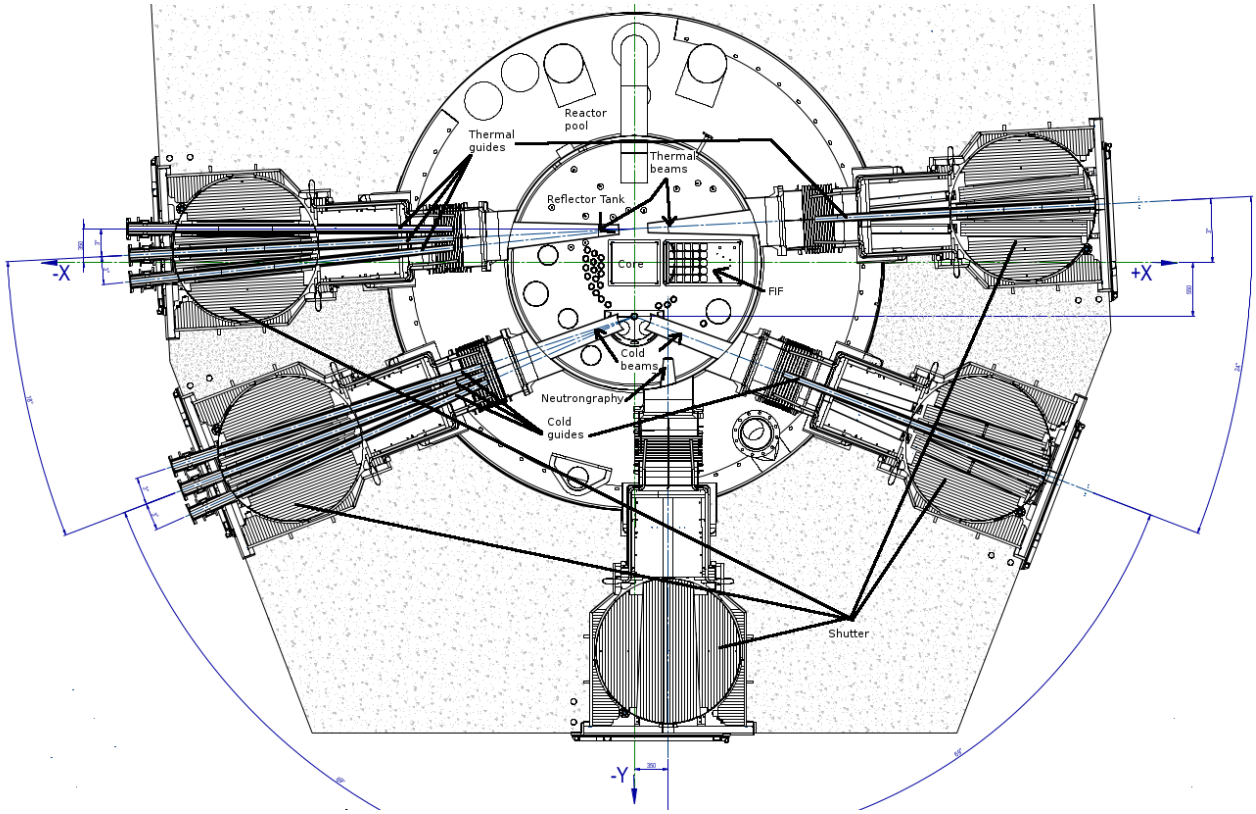

Figure 1: Global arrangement of RMB

Figure 2 shows the reactor and its facilities.

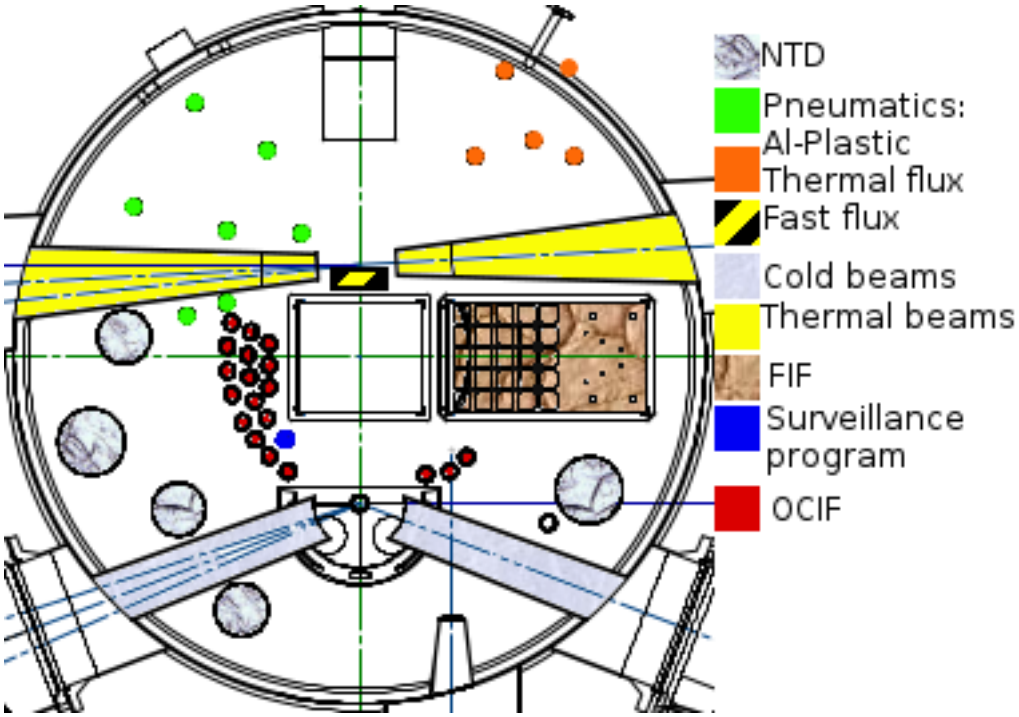

Figure 2: RMB facilities

3. Core

Figure 3 shows the core layout.

The core is made up 23 fuel elements, 6 control rods and 2 ICIF.

The First Shutdown System (FSS) are the control rods insertion; the Second Shutdown System

(SSS) is the draining of the reflector.
Table 2 shows the main data of the Fuel Assembly (FA).
Table 3 shows the performance core.

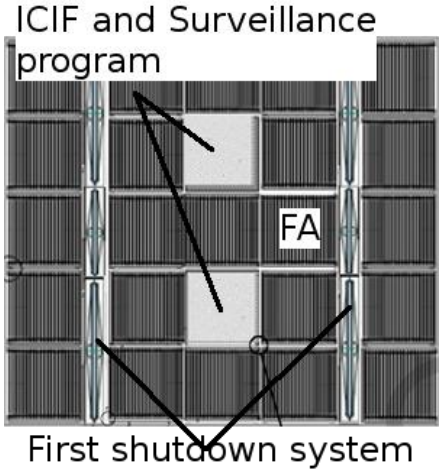

Figure 3: RMB core layout [mm]

FA type	MTR – meat U_3Si_2
Enrichment ^{235}U (average)	19.75 wt %
Uranium density in meat	3.7 gU/cm^3
^{235}U mass per FA	374.2 g
Fuel plate geometry	Flat plate
Burnable poisons material (wires)	Cadmium

Table 2: FA main data

Cycle length	33 Full Power Days (FPD)
Number of FA removed by refueling	6 (4 in the future)
Average discharge burnup [10^{21} fission/cm^3] / [%at^{235}U]	0.94 / 56
Shutdown margin of FSS	5930 pcm (8.4 $)
Shutdown margin of FSS with Single Failure	2650 pcm (3.7 $)
Shutdown margin of SSS (fully drained)	18250 pcm (25.7 $)

Table 3: Core performance

The discharge burnup of RMB is going to increase because CNEN is going to increase the U density to 4.8 g/cm^3. Thus, the number of removed FA is going to decrease to 4.

4. Radioisotope production

Figure 4 shows the irradiation positions and their aims, which is the reference condition.
The reference condition is the one in which all the OCIF (^{99}Mo, Ir and ORI) irradiation positions are used at their maximum capacity.
The Study case 1 is expected to happen at the beginning of the RMB life; it has 4 ^{99}Mo positions loaded and the other OCIF fully load. The remaining 7 ^{99}Mo positions are loaded with dummies.
Table 4 shows the target masses per position.

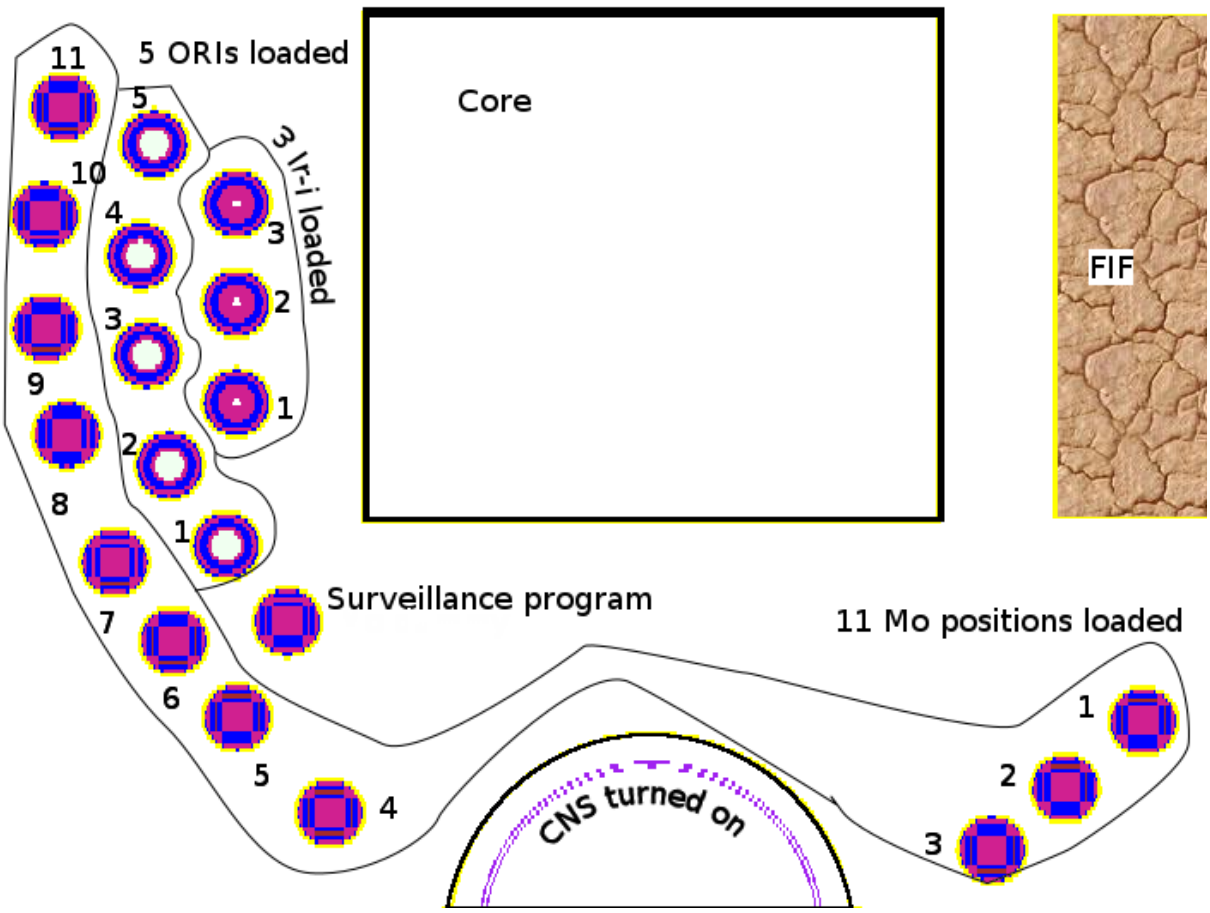

Figure 4: RMB reference conditions

Target	Target mass [g] per position
^{191}Ir	6.932
^{130}Te	53.62
^{235}U	21.24

Table 4: Target mass per position

Table 5 shows the activity of ^{99}Mo at EOI (End Of Irradiation).

Mo position	Reference condition	Study case 1
1	3200	3200
2	3200	3200
3	3200	3100
4	3400	3100
5	3200	0
6	2900	0
7	2600	0
8	2500	0
9	2500	0
10	2600	0

11	3000	0
Total	32300	12600

Table 5: ^{99}Mo activity after irradiation of 7 FPD [Ci]

Table 6 shows the activity of ^{192}Ir.

Case	^{192}Ir Activity [Ci]			
	Ir-i 1	Ir-i 2	Ir-i 3	Total
Reference condition.	1165	1248	1270	3683
Study case 1	1103	1185	1225	3513

Table 6: ^{192}Ir activity [Ci] after 33 FPD irradiation

Table 7 shows the activity of ^{131}I.

Case	^{131}I activity [Ci]					
	ORI-1	ORI-2	ORI-3	ORI-4	ORI-5	Total
Reference condition.	260	230	230	235	260	1215
Study case 1	240	210	210	220	250	1130

Table 7: ^{131}I activity after irradiation of 11 FPD

5. Shutdown Systems

RMB will have two independent and redundant shutdown systems.
FSS consists of 6 control rods which are inserted by gravity. It works by absorbing neutrons.
Even though the most important control rod failed (single failure), the FSS shutdown margin fulfills the requirement of 1000 pcm (single failure criterion).
SSS consists of the heavy water in the reflector tank and it is also drained by gravity when several parallel valves are opened. It works by increasing the neutron leakage.

6. Reactivity feedback coefficients

All the reactivity feedback coefficients are negative.

7. Thermal Neutron Beams

Table 8 shows the expected fluxes of the thermal neutron beams.

Thermal Neutron Beams to Guide hall	> 1.0 10^9 n/ cm^2 s
Thermal Neutron Beams to Reactor Face	> 1.0 10^{10} n/ cm^2 s

Table 8: Thermal neutrón beams fluxes

8. Cold Neutron Source and Cold Neutron Beams

RMB will have a Cold Neutron Source (CNS). It provides neutrons with energy smaller than 0.01 eV which are called cold neutrons.
They are produced in a 18 litres tank filled by liquid deuterium (^{2}H) at about 20 K.
CNS has two beams coupled to extract the cold neutrons from the reflector and transport them to the guides.
Table 9 shows the expected cold neutron fluxes.

Cold Neutron Beams to Guide hall	> 1.0 10^9 n/ cm^2 s
Cold Neutron Beams to Reactor Face	> 4.0 10^9 n/ cm^2 s

Table 9: Cold neutrón beams fluxes

9. Pneumatics

Pneumatics is a system that allows sending and bringing capsules (Aluminum or Plastic) to/from a position in the pneumatic rig in the reflector by air pulses. It is useful for neutron activation analysis.

RMB has three types of pneumatics rigs used for different fluxes.

For high fast and thermal flux there are two rigs with room for 3 capsules each one. It uses Aluminum capsules.

For high to medium thermal flux there are seven rigs with room for 3 capsules each one. It uses Aluminum capsules.

For low thermal flux there are five rigs with room for 2 capsules each one. It uses Plastic capsules.

Table 10 shows the neutron flux ranges of each type of rig.

Rig type	Total number of capsules	Thermal flux (E<0.625 eV) [n/cm^{2}s]	Fast flux (E>0.1 MeV) [n/cm^{2}s]
Fast/Thermal flux	6	$1.9\ 10^{14}$– $2.3\ 10^{14}$	$1.6\ 10^{13}$– $2.1\ 10^{13}$
High/medium thermal flux	21	$1.3\ 10^{13}$ – $1.8\ 10^{14}$	$3.1\ 10^{12}$ – $9.4\ 10^{12}$
Low thermal flux	10	$7.9\ 10^{11}$ – $1.1\ 10^{12}$	-

Table 10: Neutron fluxes in pneumatics

10. ICIF and in core surveillance program

RMB has two positions in core to irradiate structural materials. They are used to produce radiation damage by fast flux.

The surveillance program is to measure the ageing of in core materials (Zyrcalloy).

The detailed engineering stage has not finished by the time of writing this report, so no results are available.

11. Neutron Transmutation Doping (NTD)

RMB has five positions for NTD. Silicon ingots are irradiated to produce semiconductors for power electronics industry.

Table 11 shows the characteristic of the Silicon ingots.

Ingot diameter [mm]	Height [cm]	Number
154	60	3
205	60	2

Table 11: Silicon ingots characteristics

The detailed engineering stage has not finished by the time of writing this report, so no results are available.

The axial thermal flux uniformity is lower than 8%.

12. Fuel Irradiation Facility (FIF)

The FIF is used to test power ramps of Pressurized Water Reactors (PWR) fuels. It will have one or two high pressure tubes where the fuel rods are located. It will be able to test two PWR fuels simultaneously.

FIF is a pool with a grid where Be blocks can be arranged according to the needs.

For example one FA can be irradiated to get high burnup whereas other FA can be in a power ramp test (Figure 5).

The FAs in the FIF can move between a thermal flux of $5\ 10^{13}$ to $2\ 10^{14}$ n/cm^{2}s and a epithermal plus fast flux of $1\ 10^{13}$ to $4\ 10^{13}$ n/cm^{2}s for ramp power tests

Figure 5: Example use of FIF

FIRST SHIPMENT OF ISOTOPIC GENERATORS FROM FRANCE TO THE US: THE TN®MTR SOLUTION COUPLED WITH CEA'S MANON PACKAGE

N. BAUMET, N. GAMMELLA
CEA Cadarache
13108 St Paul lez Durance Cedex – France

L. DE ARAUJO
Orano TN
1 rue des Hérons, 78180 Montigny-le-Bretonneux – France

P. JACOT
Orano TN PALOMA
30204 Bagnols sur Ceze – France

V. VO VAN
Orano Cycle
Tour AREVA, 1 Place Jean Millier, 92400 Courbevoie – France

ABSTRACT

In terms of research reactor material management, operators are interested by flexible and universal transportation solutions which benefit from cooperative development and licensing efforts and also bring efficient and simple on-site operations.

Both TN®MTR and MANON packages have been developed to safely transport Material Testing Reactor (MTR) fuel (mostly irradiated fuel) and also a large variety of contents handled by research reactors such as sources, U3O8…

These casks will be used to transport isotopic generators from CEA in France to DOE site in the US for disposal. Both casks safety analysis reports are to be validated in France and in the US. The licensing process involving CEA, Orano TN French and US teams has started in 2017. Specific internal arrangements will be put in place for transportation, both packages have the authorization for US and French road transportation as well as maritime transportation. For such transport, the vessel will need to be selected on basis of several sensitive criteria such as the classification by a well-known classification Company or the checking of the Port State Controls for the last three years.

The TN®MTR packaging developed by Orano TN in the end of the 1990's is safely operated since nearly two decades on worldwide research facilities. It is used for shipments performed on routine basis from Australia, Belgium and French research sites to the Orano La Hague reprocessing plant. In addition, it has already been used for shipments from Indonesia and Portugal to the US DOE Savannah River Site.
The MANON system is used by the CEA to transport nuclear materials in France since 2017. This Transport Package is mainly made up of a casing, and, according to the types and sizes of contents to be transported, enclosing various cages or an External Enclosure Assembly with internal shimming system.

The purpose of the paper is to present the transportation solution coupling the CEA's MANON package and the Orano TN TN®MTR package, thus showing the benefit of cooperation for valuable transportation solution for research reactor fuels

and other types of research nuclear materials in terms of flexibility, universality and robustness.

1. Introduction

While working on evacuating from their site different types of nuclear materials, research operators are interested by flexible and universal transportation solutions which benefit from cooperative development and licensing efforts and also bring efficient and simple on-site operations.

The French CEA [1] is currently preparing to send Sr90 isotopic generators from CEA research facility in France to DOE site in the US for disposal (see Fig. 1). For organizing this shipment, the CEA is working with his logistics partner Orano TN [2].

Fig. 1: Shipment of isotopic generators from France to the US

The content to be transported comprises of four isotopic generators which will be transported in one cask each:

- One will be transported in one MANON unit
- The other three will be transported in three TN®MTR units.

The transportation project is composed of two parts:

- Obtaining of the required French license extensions and US transport license validations for both CEA 'MANON' and Orano TN 'TN®MTR' packages; the process started around end 2017 and licenses are expected to be obtained by Q2 2019;
- Organizing of the road and maritime shipment which should occur Q4 2019.

The CEA – Orano TN collaboration on this project is a successful example of implementation of cooperative licensing expertise as well as preparation of international shipment of nuclear materials.

2. MANON and TN®MTR designs

The MANON system is used by the CEA to transport nuclear materials in France since 2017 (see Fig. 2). The MANON system is a mechanical protection composed of two half shells, higher and lower, with cylindrical form and made of stainless steel sheets. The higher shell strip is attached to lower shell strip with screws. Higher and lower ends of this system are equipped with shock absorber.

MANON system cavity is designed to host an External Enclosure Assembly (EEA) composed of two half shells with cylindrical form and made of stainless steel. Both shells are attached with each other via their strips assembled with 12.9 class screws. In addition the higher end strip is designed to received two toric elastomer gaskets.

For transportation purpose, the Sr90 isotopic generators encaged in preliminary conditioning ensuring radiological protection are to be placed within the EEA with shimming system depending on the dimensions of the content.

Fig. 2: MANON system under radiological control prior to shipment between two French sites

The TN®MTR packaging developed by Orano TN in the end of the 1990's is safely operated since nearly two decades on worldwide research facilities (see Fig. 3 and 4). It is mainly composed of a body with a thick shell of lead as a gamma shielding and with resin for thermal protection and as a neutron shielding. Externally, the cask is covered by fins in order to allow the heat transfer of the radioactive material during the transport. Two trunnions, bolted on the body, allow to easily handle the cask in vertical position (without tilting) inside the facilities. The cavity is made of stainless steel.

The closure system is composed of a lid with gamma (lead) shielding. Two orifices are placed in the lid for the control of the cavity during the loading and unloading operation (water filling and draining, air injection and vacuum, control the cavity atmosphere). The leaktightness is obtained with elastomer gaskets which can be separately controlled. The shock absorber is mainly made of wood covered by stainless steel plates.

Fig. 3 and 4: TN®MTR cask loaded in a 20 feet ISO container for transport

This cask is used for shipments of Material Testing Reactor (MTR) fuel performed on routine basis from Australian, Belgian and French research sites to the Orano La Hague reprocessing plant in France. In addition, it has already been used for shipments from Indonesia, Portugal [3] and Denmark [4] to the US DOE Savannah River Site (SRS). After five months review by US Nuclear Regulatory Commission (NRC) and US Department of Transport (DOT), Orano TN just obtained TN®MTR new US license for transporting irradiated MTR fuel. The cask is now ready for shipments to SRS and can be used for instance for foreign fuel return shipments.

3. MANON and TN®MTR: on-going licensing process

Being already licensed in France for the road transport of Sr90 isotopic generators, the MANON cask design needs to obtain the French license extension for maritime transport. Being already licensed in France and in the US for road and maritime transport of other contents (MTR fuel), the TN®MTR cask design needs to obtain the French license extension for the Sr90 isotopic generators to be transported. Once the French license has been granted, the CEA and Orano TN apply for the US validation for the MANON and TN®MTR packages respectively (see Tab. 1).

	MANON	TN®MTR
Licensed in France for Sr90 isotopic generators	Yes	
Licensed in France for road transport	Yes	Yes
Licensed in France for maritime shipment		Yes
French license requested	**Maritime shipment**	**Sr90 isotopic generators**
Licensed in the US (for any content)		Yes
US license requested	**Road and maritime transport of Sr90 isotopic generators**	**Road and maritime transport of Sr90 isotopic generators**

Tab. 1: Summary of MANON and TN®MTR licensing status at the beginning of the project

Specific internal arrangements are expected to be put in place for transportation. The licensing process involving the CEA and both Orano TN French and US teams has started around Q2 2018:

- The MANON system obtained the French license in November 2017 and is expected to obtain the US license by mid-2019
- The TN®MTR cask obtained the French license in December 2018 and is expected to obtain the US license by mid-2019.

The project thus takes benefit from a smooth licensing process based on robust CEA and Orano TN licensing expertise and also on synergies from collaborative efforts. The newly obtained US and French licenses come in addition to existing licenses for other similar contents and demonstrate how robust and flexible these cask designs are.

4. Preparation for shipment

As for the shipment expected to occur by end 2019, the CEA intent is to have Orano TN performing it.

Mobilizing three transportation companies (French road, maritime, US road) and including two transshipments, the shipment from French CEA site to US DOE site is a challenge that Orano TN is fully ready to take up based on multiple successful similar experiences.

Orano TN is an authorized transport company which carries out nuclear materials maritime shipments on a regular basis. The 2019 shipment for the CEA will be organized in a similar way to the 2018 shipment arranged by Orano TN from Port Kembla in Australia to Cherbourg in France for transporting four TN®MTR cask units loaded with ANSTO [5] spent fuel elements [6]. According to the activity level of the nuclear materials, an INF 2 [7] ship was required.

Several criteria have been used for the selection of the ship:

- Classification of the ship by a well-known classification company
- No significant Port State Controls deficiency within the last three years
- No restriction of use of the ship of any kind in any place in the world
- Flag of the chosen ship within the Paris memorandum list which is the top flags list

All these criteria, plus other specific criteria related to Orano TN have been written down in a specific technical condition specification, which has been transmitted to several potential maritime companies for an international call for bid. Tender result was selection of the BBC company [8] which proposed the BBC Austria ship (flag Antigua Barbuda - within the Paris memorandum list, see Fig. 5).

Fig. 5: The BBC Austria vessel recently used for shipment of nuclear research materials (BBC picture)

Orano TN unique nuclear logistics experience (maritime shipment, real time tracking, 24/7 assistance, licensing expertise, project management, knowledge of competent authorities requirements in multiple countries, management of public acceptance) is a valuable asset for CEA project of shipping isotopic generators to the USA.

5. Conclusion

The transportation solution coupling the MANON package and the TN®MTR package being jointly prepared and organized by the CEA and Orano TN, shows the benefit of cooperation for valuable transportation solution for research reactor fuels and other types of research nuclear materials in terms of flexibility, universality and robustness.

For shipping of nuclear materials, the CEA can especially rely on Orano TN fifty years nuclear logistics experience providing unique cask design and licensing expertise in addition to safe and optimized international shipment performed according to international standards.

6. References

[1] http://www.cea.fr/english

[2] https://www.orano.group/en/expertise/facilities/service-and-engineering-activities/nuclear-packages-and-services-sites

[3] Return of HEU fuel from the Portuguese research reactor – RERTR 2008 – JG MARQUES, NP BARRADAS, A. KLING, AR RAMOS, C. ANNE, V. GARCIA

[4] Shipment of 255 DIDO Fuel Elements to the Savannah River Site to Empty the Storage and Reactor Pools at Risoe National Laboratory – RERTR 2002 – M. BAGGER HANSEN, JL MONDANEL, C. ANNE

[5] https://www.ansto.gov.au/

[6] Maritime Back End transport: Overview of a successful operation for transport of OPAL Spent Fuel from Australia to France – PATRAM 2019 – M. HEAKY, P. JACOT

[7] Code for the Safe Carriage of Packaged Irradiated Nuclear Fuel, Plutonium and High-Level Radioactive Wastes in Flasks on Board Ships (INF Code) and Guidelines for Developing Shipboard Emergency Plans for Ships Carrying Materials Subject to the INF Code – International Maritime Organization

[8] https://www.bbc-chartering.com/

RESEARCH REACTOR BACK-END OPERATIONS: GROWING NEEDS AND AVAILABLE SERVICES

J.F. VALERY, A. TALBI, V. VO VAN
Back-End Sales, Orano Cycle
Tour AREVA, 1 Place Jean Millier, 92400 Courbevoie – France

J.M. CHABEUF
International Operations, Orano DS
La Hague BP716, 50447 Beaumont Hague CEDEX – France

P. JACOT, R. LE BLEVENNEC
Transportation Business Line, Orano TN PALOMA
30204 Bagnols sur Cèze – France

ABSTRACT

In terms of back-end operations, research reactor operators are dealing today with two major challenges:

- Identifying sustainable used (or spent) fuel and waste management solutions
- Defining and implementing the best fitted dismantling strategy.

Considering international and national regulations' request for clarification of used fuel and radioactive waste management strategy, organizations in charge of Research Reactor Spent Fuel (RRSF) management face increasing need for identification of sustainable nuclear material management solutions. Treatment of RRSF, being performed at industrial scale since decades and allowing to remove fissile material and IAEA safeguards from final waste to be disposed of, is an answer when sustainable spent fuel management solution is being looked for.
Reprocessing of Uranium-Aluminum (UAl) and Uranium-Aluminum-Silicium (USi also called Silicide) spent fuel at La Hague and all related activities have been performed since decades by Orano on behalf of international operators. Range of spent fuels that can be reprocessed has been extended; new types of casks are being developed; a new facility is to be implemented in the existing plant, thus opening additional reprocessing capacities for special fuel like RRSF.

When moving to final shutdown, research reactor owners confront the challenge of establishing and deploying the most adapted decommissioning programme. Orano brings research reactors its strong experience in defining efficient and cost-effective strategies for several types of nuclear facilities. In addition, Orano 40 years' nuclear operating experience and continuous R&D efforts allow providing operators with integrated waste management solutions including characterization, treatment, logistics...

Hence, Orano keeps supporting research reactors in their back-end operations through robust and valuable solutions. The purpose of the paper is to present the industrial existing and innovative solutions for management of RRSF, as well as the D&D and waste management support proposed by Orano based on strong experience in own and international context.

1. Sustainable used fuel management

Identification of sustainable spent fuel management solutions is a major challenge faced today by research reactor operators. In terms of Research Reactor Spent Fuel (RRSF) management up to disposal, two strategies are available (see Fig 1.):

- RRSF conditioning followed by disposal of spent fuel
- RRSF reprocessing and final waste conditioning followed by disposal of non-fissile waste.

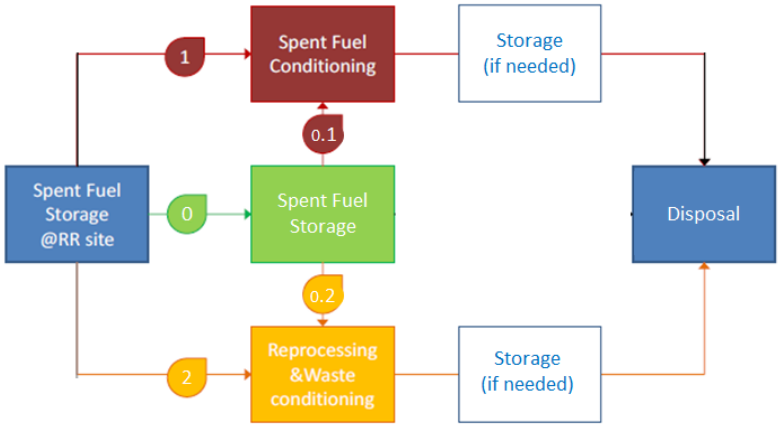

Fig 1. Two available RRSF management strategies

Whereas technologies for conditioning of RRSF are currently under development, reprocessing of RRSF is today a mature technology implemented since years by several RR operators with Orano support. In reprocessing their RRSF the nuclear operators benefit from:

- Reduced volume and radiotoxicity of final waste as compared with unprocessed used fuel
- Waste packaged in form designed for stability for thousands of years
- Final waste exempted of IAEA safeguards.

These combined advantages lead to clear predictability on the RRSF management cost, to reductions of risks with regard to long-term management of nuclear materials and to optimized disposal in terms of design and operations.

1.1 Transportation of RRSF

Since early 1990's, around 150 MTR-type RRSF transportation casks have been transported to the Orano 'La Hague' used fuel reprocessing plant. As of today, the 'TN®-MTR' cask (see Fig 2.) is used for shipments of MTR used fuel performed on routine basis from Australian, Belgian and French research sites to the La Hague plant in France. In addition, it has already been used for shipments from Indonesia, Portugal [1] and Denmark [2] to the US DOE Savannah River Site (SRS). After five months review by US Nuclear Regulatory Commission and US Department of Transport, Orano TN just obtained TN®-MTR new US license for transporting irradiated MTR fuel [3]. The cask is now ready for shipments to SRS and can be used for instance for foreign fuel return shipments.

Its main features are as follows:

- Several types of basket, generic or specialized according to the RRSF design
- The highest RRSF transportation capacity worldwide, with a 68-positions basket
- Wet or dry loading at RR site.

Fig 2. TN®-MTR cask

A new package, the 'TN®-LC' cask, can also be proposed for transportation of used fuel from RR (NRU/NRX, TRIGA, MTR…), full-length commercial irradiated fuel assemblies, irradiated pins. The TN®-LC is licensed in the USA with several foreign validations underway.

In 2017, the RRSF transportation service offer was extended: transport (for reprocessing purpose) of non-intact aluminum-cladded fuel is now authorized by the French Safety Authority, based on the use of aluminum cans designed by SCK•CEN [4] with Orano support.

1.2 RRSF reprocessing

Through conditioning of final waste under strongly optimized and stable form, reprocessing of RRSF allows to:

- Obtain clear predictability on the RRSF management cost,
- Reduce the risks with regard to long-term management of nuclear materials and
- In the end move to an optimized disposal in terms of design and operations.

Reprocessing of RRSF is industrially performed in France since decades (see Fig 3.) with more than 30 tons of UAl-type RRSF treated in both Marcoule and La Hague plants.

Marcoule	Up to the 90's: 18 tons of UAl-type RRSF from 21 reactors in 11 countries
La Hague	From 2005: > 10 tons of UAl-type RRSF Since 2017: Silicide type RRSF reprocessed

Fig 3. Industrial RRSF reprocessing experience in France

More specifically, the Orano La Hague plant initially designed for reprocessing of LWR used fuel (over 30,000 tHM reprocessed since end of the 70's) has reprocessed more than 10 tons of UAl-type RRSF since 2005. Since obtaining of Competent Authority authorization for reprocessing of Silicide fuel in 2017, additional quantities of such type of RRSF have been reprocessed.

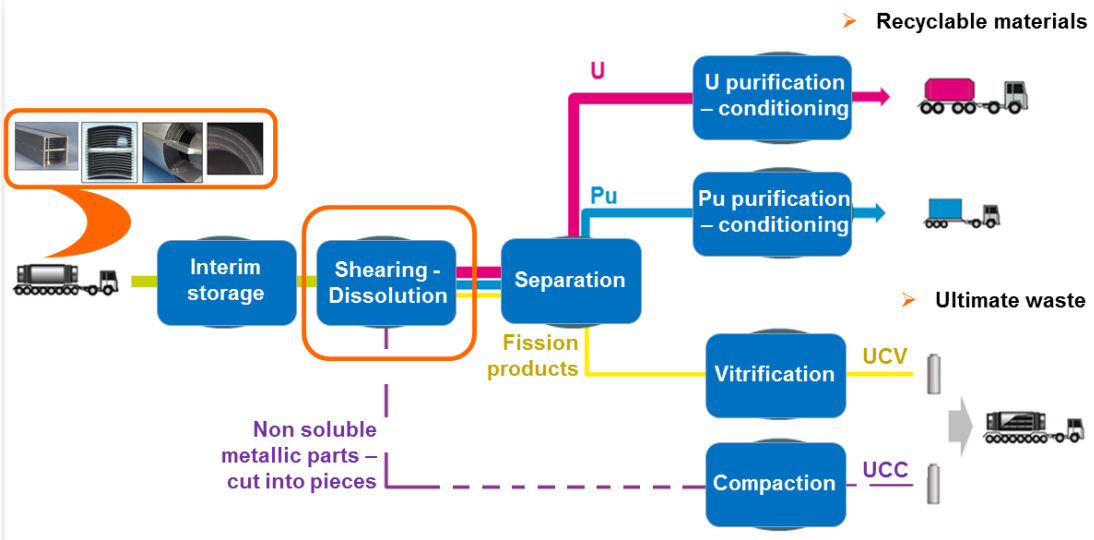

Fig 4. Process diagram for RRSF reprocessing on La Hague site

The reprocessing operations on La Hague site are summarized in Fig 4. The UAl RRSF specific reprocessing operations mainly take place at the dissolution step.

From wet storage pool to the dissolution facility, the RRSF is transferred with a shuttle basket with operations performed by operators with dedicated cranes and tele-manipulators. The RRSF are then loaded in the dissolution pit one by one by directly dropping them in the boiling nitric acid. The dissolution process is monitored thanks to a dedicated camera placed on the top of the dissolution pit. Once the RRSF batch is completely dissolved, the solution is mixed with LWR dissolution solution coming from the other dissolution lines.

The first industrial Silicide fuel reprocessing campaign was performed at La Hague plant in 2017 [5]. The process is the same as for UAl RRSF except for one additional operation performed prior to the mix with the LWR dissolution solution: separation of Silicon from the dissolution solution. The Silicide RRSF reprocessing capacity is similar to the UAl RRSF reprocessing capacity in terms of tons of alloy/year.

In 2017 also, reprocessing of non-intact aluminium-cladded fuel was authorized and performed based on the use of aluminium cans designed by SCK•CEN with Orano support.

In order to meet with expanding needs in terms of RRSF management, a new Special Fuel Treatment facility is to be implemented in the existing La Hague reprocessing plant opening thus additional reprocessing capacities for special fuel like RRSF and allowing also to extend even more the range of special fuel which can be reprocessed. This future facility, called 'TCP' (see Fig 5.), will benefit from Orano's industrial spent fuel reprocessing feedback while taking part in the next steps towards a fast reactor fuel cycle development using innovative treatment solutions.

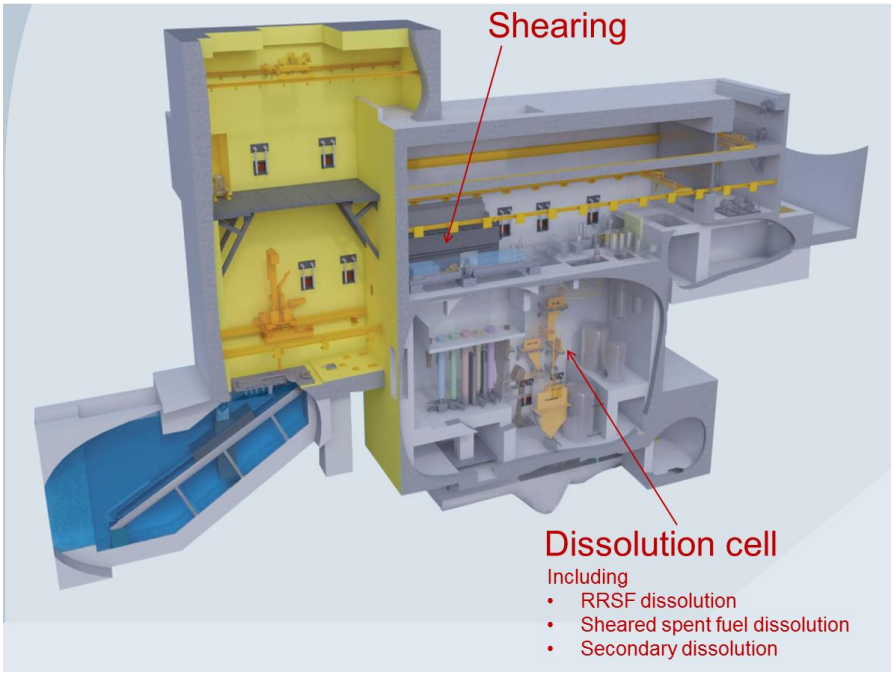

Fig 5. Overview of main TCP facility operations

1.3 Managemenf of final waste produced from reprocessing

As per French law [6], any introduction of spent fuel or radioactive waste from abroad onto the French territory shall only be authorized pursuant to intergovernmental agreements and provided that no residual radioactive waste resulting from the processing of such substances shall be stored in France beyond the term prescribed by such agreements.

Compliant with the French law, the Orano La Hague EXPER waste accountancy system is used to determine the equivalence of final waste that needs to be sent out of France after reprocessing of materials coming from abroad.

The equivalence is determined with two units being the residue activity unit (UAR) based on neodymium content (in dg, because it is a representative indicator that can be effectively measured), and the residue mass unit (UMR) based on weight of non-soluble metallic structural components of the spent fuel (in kg). UAR and UMR are sent out of France under the form of Universal vitrified residues Canister and Universal compacted residues Canister respectively (see Fig 6.):

- Vitrified residues. The fission products and minors actinides are vitrified in a homogeneous glass matrix and conditioned in Universal Canister. This type of conditioning is very stable and ensures containment over thousands of years.
- Compacted residues. Structural waste coming from non-soluble-metallic parts of fuels are compacted and conditioned in Universal Canister - with the same external geometry as vitrified residues canister.

Fig 6. Mock-up - Vitrified and Compacted residues Universal Canisters with height 1.3 m

Conditioning of final waste into Universal Canisters (UC) leads to multiple benefits:

- Simplified transport and on-site handling conditions thanks to standardization,
- Volume saving in storage/disposal facilities,
- High stability of the residues demonstrated for the very long term,
- Exemption of IAEA safeguards and
- Rationalization of the ultimate waste policy through standardized type of waste.

UCs are managed today in Australia, Belgium, France, Germany, Japan, the Netherlands, Switzerland and the UK. Casks for large quantities of UCs (up to 28 UCs, vitrified type or up to 20 UCs, compacted type) are operated today on routine basis:

- The 'TN®28' cask (transport) licensed in Belgium, France, Japan, the Netherlands and the UK,
- The 'TN®81' cask (transport and storage), licensed in Australia, France, Spain, Switzerland, and the UK.

The hereabove casks may not be adapted to the return or storage of small quantities of radioactive residues.

The ‘TN®MW’ cask design having been licensed by the French and Belgian Safety Authorities for transport of nuclear waste [7], an adaptation of this cask for accommodating one UC is being developed (see Fig 7.).

Fig 7. Future TN®MW cask design (~1.9 m high) for one UC

1.4 RRSF dry storage

Decision can be made for putting in place an intermediary step before implementation of one or the other available RRSF management strategies. In such a case, RR operators may need modular dry storage solutions.

Orano will be able to propose in the near future a cask for transport and storage of radioactive material with fissile content such as RRSF (see Fig 8.). This cask will be based on existing TN®MW cask design [7]:

- It has been licensed in 2017 by the French and Belgian Safety Authorities for transport of material resulting from production of Molybdenum 99
- Two units have been successfully delivered and loaded on client’s site in 2017 and two additional units have been delivered in 2018.

Such solution presents following advantages in terms of support to RR operations:

- Modularity
- Flexibility keeping door open to both RRSF management strategies
- Support to management of spent fuel storage facility (pool, vault…) capacity.

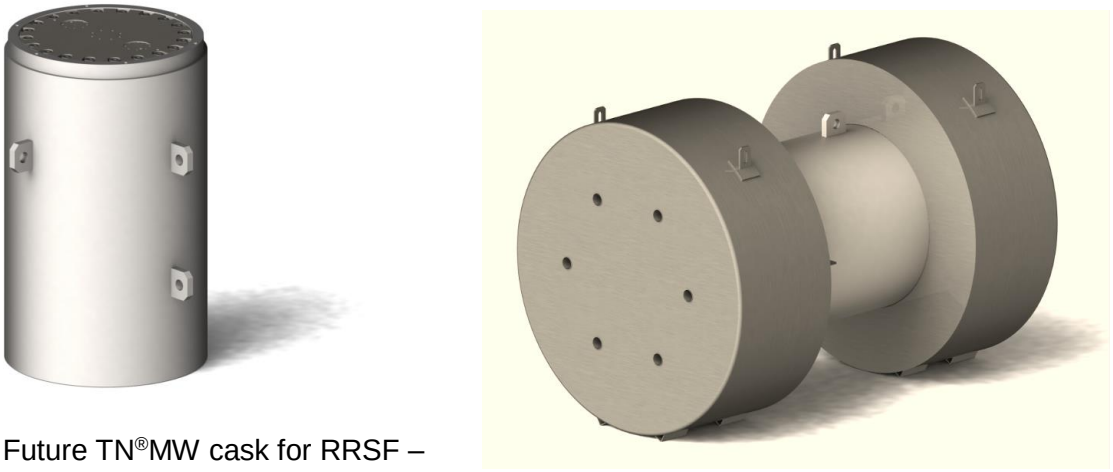

Fig 8. Future TN®MW cask for RRSF – storage (l) and transport (r) configuration

2. Decommissioning, dismantling and waste management

When approaching the RR’s end of life, the challenge faced by operators resides in conducting a safe and efficient plant rundown to reduce the radiological inventory and prepare the reactor for future works, while at the same time establishing the most adapted and economically viable decommissioning and waste management program. Operators also

have to manage major issues such as budgeting and financing, relations with regulatory authorities and defining a resource management strategy.

As an owner-operator and service provider, Orano has accumulated extensive experience in D&D of nuclear facilities over the last decades [8]. Orano is indeed in charge of the decommissioning of its own facilities such as UP2-400 treatment facility on La Hague site or the GB1 enrichment plant. Being involved in several major decommissioning programs in France, the UK, Japan, and in the US, Orano has delivered several RR decommissioning projects such as SVAFO in Sweden (see Fig 9.), Phebus in Cadarache, Phenix in Marcoule, Ulysse in Saclay, as well as TRITON, EL3, PEGASE, MELUSINE, SCARABE.

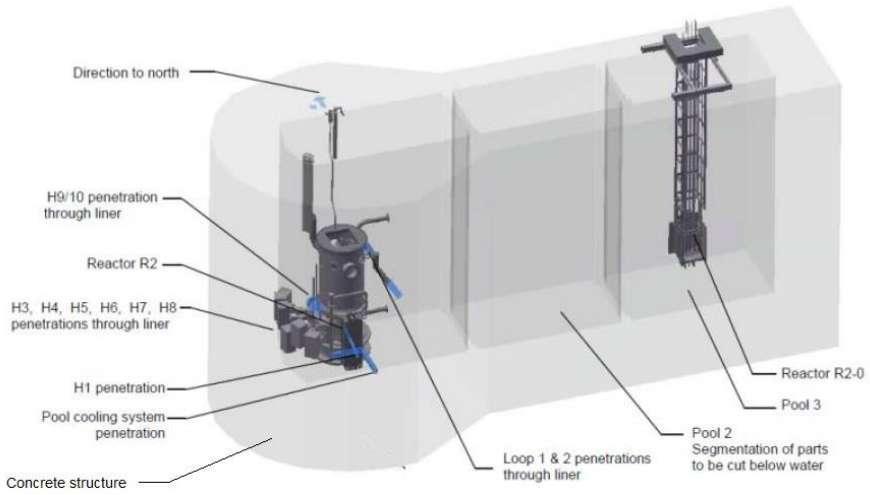

Fig 9. SVAFO reactors dismantling scope of work

Based on its experiences from these worldwide D&D projects, Orano provides the RR operators community with optimized and comprehensive D&D services as well as efficient waste management solutions.

2.1 D&D planning and operations

Sufficient planning and preparation are central in the success of a decommissioning project. Making use of its extensive D&D experience, Orano supports operators during the transition period from operations to the decommissioning project, and also for performance of decommissioning activities.
The objectives of the decommissioning planning are to:

- Establish a robust hazard reduction, waste driven technical scenario
- Organize the resource transition from operations to decommissioning
- Develop a stakeholder/regulator engagement process to secure the deployment of the scenario
- Establish a baseline cost and schedule to secure funding and endorsement by funding and regulatory authorities.

The decommissioning plan is defined and implemented taking into account the human and financial resources as well as the local regulatory and safety requirements, with the objective to define the best fitted strategy in terms of costs, planning and technologies. The final plant rundown and the first 3 years after final shutdown are also critical transition periods that can create opportunities or risks for the future of the decommissioning program. Orano offers RR operators to take benefit of its robust know-how in all disciplines of the D&D, from planning (studies, concepts development, engineering and licensing) to the realization of the D&D (sampling, characterization, decontamination and components dismantling).

2.2 Waste management

Waste management is the backbone of the decommissioning program: identification and successful implementation of the best fitted management strategy are known to be the crucial points to manage the total cost of dismantling. Based on its 40 years' experience in waste management, Orano proposes a unique integrated range of management solutions for legacy, operational and dismantling waste.

Characterization is the first step towards a rigorous strategy definition therefore Orano has been developing innovative waste characterization tools such as Nanopix (developed in collaboration with the CEA [9]), CartoOnline, Collecte, Riana™ and Manuela™ (see Fig 10.) to provide operators with standard, simple and adaptable tools. Once thoroughly characterized, the waste can be oriented in the best stream in terms of costs, disposal approach and future environmental protection.

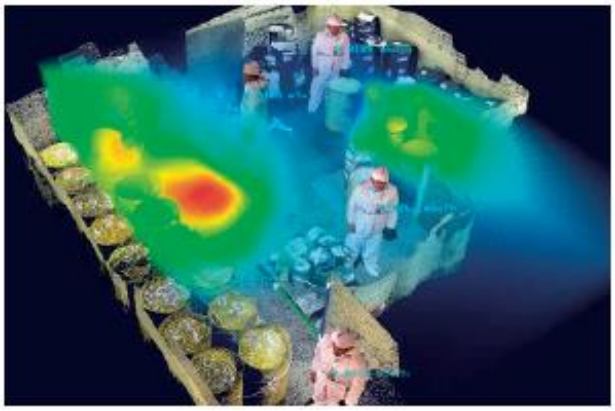

Fig 10. Example of 3D radiological mapping with MANUELA™

As regards to waste conditioning, the objective is to safely and durably stabilize the waste into a solid waste form. Operating more than 80% of the waste conditioning units in France and Orano is bringing RR operators its expertise in radiolysis, corrosion, lixiviation and long-term behavior to managing waste routes in a sustainable, innovative and cost effective manner. Having conditioned and transported ~300,000+ m3 of VLL-SL-LL French radioactive waste, Orano is also able to support RR operators with their own Safety Authorities in regards to packaging acceptance.

Such global approach aims to minimize the costs, the volume and toxicity of the final waste as well as the incremental investments, while achieving environmental, safety, political and legal requirements.

3. Conclusions

Considering the evolution of international and national regulations, and their request for clarification of used fuel and radioactive waste management, the identification of a used fuel management sustainable strategy is one of the major challenges RR operators are facing today.
Upon entering end of life phase of the reactor, the operators face additional challenge relating to definition and implementation of best fitted dismantling strategy.
Based on its long-term and international experience on RRSF management in addition to successful implementation of decommissioning programs on its own and other operators' facilities, Orano is able to offer the RR operators up-to-date and adapted back-end services. Continuously meeting the evolving market needs, Orano is ready to set up sustainable partnerships with its RR customers in order to robustly manage their back-end operations.

4. Acronyms

D&D	Decommissioning and Dismantling
LL	Long Lived (waste)
LWR	Light Water power Reactor
MTR	Material Testing Reactor
RR	Research Reactor
RRSF	Research Reactor Spent Fuel
SL	Short Lived (waste)
TRIGA	“Training, Research, Isotopes, General Atomics” type RR
UAR	Residue Activity Unit
UC	Universal Canister (packaging for post-reprocessing residues)
UMR	Residue Mass Unit
VLL	Very Low Level (waste)

5. References

[1] Return of HEU fuel from the Portuguese research reactor – RERTR 2008 – JG Marques, NP Barradas, A. Kling, AR Ramos, C. Anne, V. Garcia

[2] Shipment of 255 DIDO Fuel Elements to the Savannah River Site to Empty the Storage and Reactor Pools at Risoe National Laboratory – RERTR 2002 – M. Bagger Hansen, JL Mondanel, C. Anne

[3] First shipment of isotopic generators from France to the US: the TN®MTR Solution coupled with CEA’s MANON package – RRFM 2019 – N. Baumet, N. Gammella, P. Jacot, L. De Araujo, V. Vo Van

[4] https://www.sckcen.be/en

[5] Research Reactor silicide fuel reprocessing at La Hague plant – RERTR 2017 – C. Lavalette, JF Valery, V. Vo Van, A. Talbi, L. Halle, C. Pechard, X. Renault

[6] Act No.2006-739, dated 28 June 2006, on the Sustainable Management of Radioactive Materials and Waste and Decree 2008-209, dated 3 March 2008

[7] The TN®MW, a new optimized cask for research reactor’s waste management – RRFM 2018 – A. Boogaerts, A. Talbi, JF Valery, V. Vo Van, M. Ghobrini, C. Lamouroux, C. Grandhomme, B. Kerr, C. Herve

[8] Orano decommissioning and waste management services for research reactors – RRFM 2019 – A. Talbi, JF Valery, V. Vo Van, JM Chabeuf

[9] http://www.cea.fr/english